

**Diverse Aspects of the Sorting and Assembly Machinery
in Human Mitochondria**



DISSERTATION

zur Erlangung des akademischen Grades

doctor rerum naturalium

(Dr. rer. nat.)

im Fach Biologie

eingereicht an der Fakultät für Biologie

der Julius-Maximilians-Universität Würzburg

vorgelegt von

Dipl. Biol.

Christine Kornelia Ott

geboren am 12.11.1983 in Würzburg

Würzburg, Juni 2013

Eingereicht am:

Mitglieder der Prüfungskommission:

Vorsitzender:

Erstgutachter: PD Dr. Vera Kozjak-Pavlovic

Zweitgutachter: Prof. Dr. Georg Krohne

Tag des Promotionskolloquiums:

Doktorurkunde ausgehändigt am:

CONTENTS

ABSTRACT	7
ZUSAMMENFASSUNG.....	8
1 INTRODUCTION	10
1.1 Mitochondria.....	10
1.2 Mitochondrial import systems	10
1.2.1 The translocase of the outer membrane (TOM)	10
1.2.2 The TIM23 pathway.....	12
1.2.3 The TIM22 pathway.....	13
1.2.4 The MIA pathway	13
1.2.5 Insertion of proteins into the OMM.....	14
1.3 Conservation of the transport and membrane insertion of β -barrel proteins	17
1.4 The IMM: respiratory chain and membrane structure	19
1.4.1 The respiratory chain.....	19
1.4.2 IMM structure and maintenance	22
1.5 Aims of the work	26
2 MATERIAL AND METHODS	27
2.1 Material	27
2.1.1 Cell lines.....	27
2.1.2 Bacterial strains	28
2.1.3 Plasmids.....	28
2.1.4 Oligonucleotides.....	31
2.1.5 Antibodies.....	34
2.1.6 Kits	35
2.1.7 Markers	35
2.1.8 Buffers, solutions and media.....	35

2.1.9 Enzymes.....	38
2.1.10 Chemicals.....	38
2.1.11 Technical equipment.....	39
2.1.12 Software.....	39
2.2 Methods.....	40
2.2.1 DNA methods.....	40
2.2.2 Gel electrophoresis and western blotting.....	41
2.2.3 Bacterial culture methods.....	42
2.2.4 Cloning of DNA fragments into vectors.....	44
2.2.5 Cell culture methods.....	45
2.2.6 Transfection of cells.....	45
2.2.7 Trichloroacetic acid (TCA) precipitation.....	46
2.2.8 MitoTracker® Orange staining and immunofluorescence staining.....	46
2.2.9 Transmission electron microscopy (TEM).....	47
2.2.10 Isolation of mitochondria and of the cytosolic fraction.....	47
2.2.11 Submitochondrial localization of mitochondrial proteins.....	48
2.2.12 Membrane extractability of proteins.....	49
2.2.13 Co-Immunoprecipitation.....	49
2.2.14 <i>In vitro</i> import of radio-labeled proteins into isolated mitochondria.....	49
2.2.15 Production of inducible shRNA-mediated knockdown cell lines.....	50
2.2.16 Stable isotope labeling of amino acids in cell culture (SILAC).....	51
3 RESULTS.....	52
3.1 Targeting of β -barrel proteins to human mitochondria.....	52
3.1.1 Neisserial β -barrel proteins are imported into human mitochondria.....	52
3.1.2 Neisserial Omp85 can assemble PorB of <i>Neisseria</i> sp. into the OMM.....	54
3.1.3 Targeting of Omp85 _{Ng0} to mitochondria depends on its C-terminal half, whereas the last quarter of the protein is not sufficient.....	55

3.1.4 Amino acids of the ultimate β -strand are involved in the mitochondrial targeting of Omp85	59
3.1.5 The C-terminal quarter of PorB is important for its mitochondrial targeting.....	62
3.1.6 The last β -strand is not involved in mitochondrial targeting of PorB	65
3.1.7 The β -signal of Omp85 cannot mediate OMM integration of PorB.....	65
3.1.8 At least two POTRA domains are required for Omp85 integration and function	66
3.2 The Mitochondrial Intermembrane space Bridging (MIB) complex.....	68
3.2.1 Loss of CHCHD3 influences Sam50 and mitofilin protein levels.....	68
3.2.2 Sam50, mitofilin and CHCHD3 are present in one complex.....	69
3.2.3 CHCHD6 and DnaJC11 are peripheral components of the MIB complex.....	72
3.3 Sam50 influences the assembly of the respiratory chain	78
3.4 The MIB complex is connected to the tetratricopeptide 19 protein (TTC19).....	82
3.4.1 TTC19 is localized to mitochondria in HeLa cells.....	82
3.4.2 TTC19 is reduced in mitochondria of Sam50- and mitofilin-depleted cells	83
3.4.3 <i>In vitro</i> import studies confirm a connection between Sam50 and TTC19.....	85
3.4.4 TTC19 depletion does not have an effect on MIB complex components	87
3.4.5 TTC19 and MIB complex components are not present in one complex	88
3.5 TTC19 is involved in the assembly of respiratory chain complexes	90
3.5.1 SILAC analysis of TTC19-depleted cells shows an effect of TTC19 on respiratory chain complexes.....	90
3.5.2 TTC19 influences protein levels of respiratory complex subunits	91
3.5.3 TTC19 plays a role in respiratory complex assembly	94
4 DISCUSSION	97
4.1 Human mitochondria exhibit high specificity regarding import and assembly of bacterial β -barrel proteins	97
4.2 β -barrel proteins do not possess a linear signal which targets them to mitochondria	99
4.3 Two POTRA domains are required for OMM integration and function of Omp85.....	100
4.4 The β -sorting signal is not sufficient for membrane integration of Omp85 and PorB.....	101

4.5 The MIB complex is a crucial organizer of cristae structure	101
4.6 Mitofilin complexes as organizers of cristae structure are evolutionary conserved	105
4.7 The MIB complex influences respiratory complex assembly	109
4.8 The MIB complex influences TTC19	112
4.9 TTC19 plays a role in respiratory complex assembly	113
4.10 Perspectives.....	114
5 REFERENCES	116
6 APPENDIX	132
6.1 List of abbreviations	132
6.2 Publications and presentations	135
6.3 Danksagung	136
6.4 Selbständigkeitserklärung	137

ABSTRACT

Mitochondria are organelles of endosymbiotic origin, which play many important roles in eukaryotic cells. Mitochondria are surrounded by two membranes and, considering that most of the mitochondrial proteins are produced in the cytosol, possess import machineries, which transport mitochondria-targeted proteins to their designated location. A special class of outer mitochondrial membrane (OMM) proteins, the β -barrel proteins, require the sorting and assembly machinery (SAM) for their OMM integration. Both mitochondrial β -barrel proteins and the central component of the SAM complex, Sam50, have homologs in gram-negative bacteria. In yeast mitochondria, bacterial β -barrel proteins can be imported and assembled into the OMM. Our group demonstrated that this, however, is not the case for human mitochondria, which import only neisserial β -barrel proteins, but not those of *Escherichia coli* and *Salmonella enterica*. As a part of this study, I could demonstrate that β -barrel proteins such as Omp85 and PorB of different *Neisseria* species are targeted to human mitochondria. Interestingly, only proteins belonging to the neisserial Omp85 family were integrated into the OMM, whereas PorB was imported into mitochondria but not assembled. By exchanging parts of homologous neisserial Omp85 and *E. coli* BamA and, similarly, of neisserial PorB and *E. coli* OmpC, it could be demonstrated in this work that the mitochondrial import signal of bacterial β -barrel proteins cannot be limited to one short linear sequence, but rather secondary structure and protein charge seem to play an important role, as well as specific residues in the last β -strand of Omp85. Omp85 possesses five conserved POTRA domains in its amino-terminal part. This work additionally demonstrated that in human mitochondria, at least two POTRA domains of Omp85 are necessary for membrane integration and functionality of Omp85.

In the second part of this work, the influence of Sam50 on the mitochondrial cristae structure was investigated. This work contributed to a study performed by our group in which it was confirmed that Sam50 is present in a high molecular weight complex together with mitofilin, CHCHD3, CHCHD6, DnaJC11, metaxin 1 and metaxin 2. This connection between the inner and outer mitochondrial membrane was shown to be crucial for the maintenance of the mitochondrial cristae structure. In addition, a role of Sam50 in respiratory complex assembly, suggested by a SILAC experiment conducted in our group, could be confirmed by *in vitro* import studies. An influence of Sam50 not only on respiratory complexes but also on the recently described respiratory complex assembly factor TTC19 was demonstrated. It was shown that TTC19 not only plays a role in complex III assembly as published, but also influences the assembly of respiratory complex IV. Thus, in this part of the work a connection between the OMM protein Sam50 and maintenance of cristae structure, respiratory complex assembly and an assembly factor could be established.

ZUSAMMENFASSUNG

Mitochondrien sind Zellorganellen endosymbiotischen Ursprungs, die viele wichtige Funktionen in eukaryotischen Zellen haben. Mitochondrien sind von zwei Membranen umgeben, und da die meisten Mitochondrienproteine im Cytosol hergestellt werden, besitzen sie Importmaschinerien, die die für die Mitochondrien bestimmten Proteine zu ihrem jeweiligen Zielort transportieren. Eine besondere Klasse von Proteinen der äußeren Mitochondrienmembran (ÄMM), die β -Fassproteine, benötigen die Sortierungs- und Assemblierungsmaschinerie (SAM) für ihre Integration in die ÄMM. Sowohl mitochondriale β -Fassproteine als auch die zentrale Komponente des SAM-Komplexes, Sam50, haben Homologe in gramnegativen Bakterien. In Hefemitochondrien können bakterielle β -Fassproteine importiert und in der ÄMM assembliert werden. Unsere Gruppe hat gezeigt, dass dies jedoch nicht auf humane Mitochondrien zutrifft, die nur neisserielle β -Fassproteine importieren, nicht aber diejenigen von *Escherichia coli* und *Salmonella enterica*. Im Rahmen dieser Studie konnte ich zeigen, dass β -Fassproteine verschiedener Neisserienarten, wie Omp85 und PorB, in humane Mitochondrien aufgenommen werden. Interessanterweise wurden nur Proteine der neisseriellen Omp85-Familie in die ÄMM eingebaut, während PorB zwar importiert, jedoch nicht assembliert wurde. Durch das Austauschen von Teilen von homologem neisseriellen Omp85 und *E.coli* BamA und ebenso von neisseriellem PorB und *E. coli* OmpC konnte in dieser Arbeit gezeigt werden, dass das mitochondriale Importsignal bakterieller β -Fassproteine nicht auf eine kurze lineare Sequenz eingegrenzt werden kann, sondern dass die Sekundärstruktur und die Ladung des Proteins eine wichtige Rolle zu spielen scheinen, sowie im Fall von Omp85 einige bestimmte Aminosäurereste des letzten β -Stranges. Omp85 besitzt fünf konservierte POTRA-Domänen in seiner aminoterminalen Hälfte. In dieser Arbeit wurde zudem demonstriert, dass in humanen Mitochondrien mindestens zwei POTRA-Domänen von Omp85 für die Membranintegration und Funktionalität von Omp85 vorhanden sein müssen.

Im zweiten Teil dieser Arbeit wurde der Einfluss von Sam50 auf die mitochondriale Cristastruktur untersucht. Diese Arbeit hat zu einer von unserer Gruppe durchgeführten Studie beigetragen, in der bestätigt werden konnte, dass Sam50 in einem hochmolekularen Komplex mit Mitofilin, CHCHD3, CHCHD6, DnaJC11, Metaxin 1 und Metaxin 2 vorliegt. Es wurde gezeigt, dass diese Verbindung zwischen der inneren und äußeren Mitochondrienmembran unverzichtbar für die Aufrechterhaltung der mitochondrialen Cristastruktur ist. Zudem konnte eine Rolle von Sam50 bei der Assemblierung von Atmungskettenkomplexen, die durch ein in unserem Labor durchgeführtes SILAC-Experiment nahegelegt worden war, durch *in-vitro*-Importstudien bestätigt werden. Weiterhin wurde ein Einfluss von Sam50 nicht nur auf Atmungskettenkomplexe, sondern auch auf einen vor

kurzem beschriebenen Assemblierungsfaktor der Atmungskette, TTC19, demonstriert. Es wurde gezeigt, dass TTC19 nicht nur, wie veröffentlicht, eine Rolle bei der Assemblierung des Atmungskettenkomplexes III spielt, sondern auch die Assemblierung des Atmungskettenkomplexes IV beeinflusst. In diesem Teil der Arbeit konnte folglich eine Verbindung zwischen dem ÄMM-Protein Sam50 und der Organisation der Cristastruktur, der Atmungskettenassemblierung und einem Assemblierungsfaktor nachgewiesen werden.

1 INTRODUCTION

1.1 Mitochondria

Mitochondria take a special position among cell organelles as they are the result of an endosymbiotic event between an α -proteobacterium and a host cell that took place 1.5 – 2 billion years ago (Sicheritz-Ponten et al., 1998). In contrast to the way they are often depicted, mitochondria are not simply single rod-shaped structures but form a highly dynamic network throughout the cytosol, constantly fusing and dividing (Hoppins et al., 2007). Their number, form and size depend strongly on the cell type and its respective tasks (Detmer and Chan, 2007). Mitochondria possess about 1000 (yeast) to 1500 (mammals) proteins (Meisinger et al., 2008; Pagliarini et al., 2008; Reinders et al., 2006). Although most of the mitochondrial genes have been shifted to the cellular nucleus or have been lost during the course of evolution (Gabaldon and Huynen, 2003), mitochondria have retained their own small genome encoding 36 genes in mammalian mitochondria, among them 13 for subunits of respiratory complexes (Anderson et al., 1981). As in bacteria, the human mitochondrial DNA (mtDNA) is present in the form of a circular double-stranded molecule and is organized in nucleoids that are tethered to the inner mitochondrial membrane (IMM) (Chen and Butow, 2005).

Mitochondria possess two membranes which divide them into four compartments: the outer mitochondrial membrane (OMM), the inner mitochondrial membrane (IMM), the intermembrane space (IMS) and the matrix. The IMM forms multiple invaginations called cristae and harbors the respiratory chain complexes, which produce most of the cell's energy (Mannella et al., 2001). Apart from their role in energy production, mitochondria play a crucial role in various other cellular processes, such as cell signaling, apoptosis and fatty acid metabolism (Westermann, 2010).

1.2 Mitochondrial import systems

1.2.1 The translocase of the outer membrane (TOM)

As the genetic information of nearly all mitochondrial proteins has been shifted from the mitochondrial matrix to the nucleus during evolution, eukaryotic cells had to develop highly regulated mitochondrial import systems to transport the cytosolically produced proteins to their designated mitochondrial compartment. At the same time, mitochondrial proteins had to acquire specific mitochondrial targeting signals (Dolezal et al., 2006). In the past fifteen years, mitochondrial import systems have extensively been investigated. They were first described in yeast but many components could meanwhile be identified in human cells.

Virtually all mitochondrial proteins enter the mitochondria through the translocase of the outer membrane (TOM) complex (Figure 3-1), which translocates them across the OMM into the IMS (Chacinska et al., 2009). The TOM machinery is composed of the channel forming central β -barrel protein Tom40 (Hill et al., 1998), the receptors Tom20, Tom22 and Tom70 (Alvarez-Dolado et al., 1999; Goping et al., 1995; Saeki et al., 2000), and the small TOM proteins Tom5, Tom6 and Tom7 (Johnston et al., 2002; Kato and Mihara, 2008). In order to be recognized by the Tom receptors, proteins have to contain a mitochondrial targeting signal. This signal can either be an amino-terminal (N-terminal) presequence consisting of 15 – 55 amino acids which form an amphipathic α -helix with a net positive charge (Vögtle et al., 2009), or an internal targeting signal (Neupert and Herrmann, 2007). Mitochondrial proteins with an N-terminal targeting signal are recognized by Tom20 and then transferred to the central Tom22 receptor (Bohnert et al., 2007; Brix et al., 1999). Subsequently, they are transferred presequence first to Tom40 with the assistance of Tom5, and then to Tom7 and the IMS domain of Tom22, where their release is induced (Chacinska et al., 2009; Dietmeier et al., 1997; Endo et al., 2003). Mitochondrial proteins with an internal targeting signal are delivered to the TOM complex by an Hsp70/Hsp90 chaperone complex (Young et al., 2003) and recognized by the Tom70 receptor (Brix et al., 1999), or, in the case of β -barrel proteins, by Tom20 (Krimmer et al., 2001; Model et al., 2001). The small Tom proteins Tom6 and 7 play a role in the regulation of the TOM complex assembly (Alconada et al., 1995; Honlinger et al., 1996). Tom22 is also involved in stabilizing the TOM complex in addition to its receptor function (van Wilpe et al., 1999). Recently, phosphorylation of Tom receptors was shown to play an important role in regulation of protein translocation through the TOM complex (Schmidt et al., 2011).

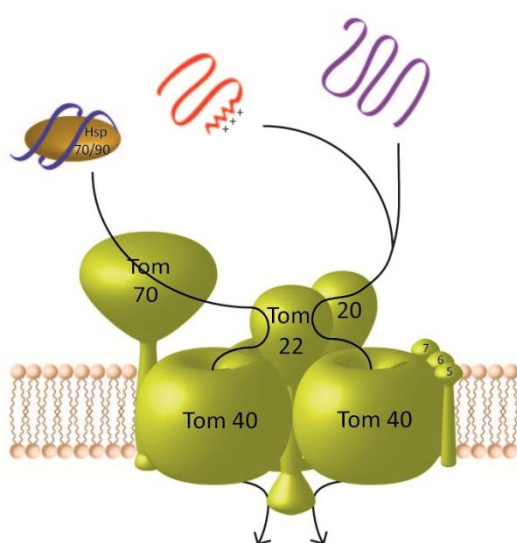


Figure 1-1 The Translocase of the Outer Membrane (TOM). Virtually all nuclear-encoded mitochondrial proteins are translocated across the OMM via the TOM complex. Proteins can either possess a positively charged N-terminal presequence or an internal targeting signal. Depending on the signal, they are recognized by the receptors Tom20 or Tom70, transferred to the central receptor Tom22, and translocated through the Tom40 pore to the IMS domain of Tom22 with the help of Tim7. In the IMS, the import ways of mitochondrial proteins divide, depending on their signals and designated compartment.

1.2.2 The TIM23 pathway

After translocation of the proteins into the IMS via the TOM complex, there are different routes that they can take depending on their final destination and on their signals. Preproteins with an N-terminal targeting sequence are translocated from the IMS into the matrix or the IMM by the translocase of the inner membrane 23 (TIM23) complex, whose core consists of the channel-forming protein Tim23 and two other inner membrane proteins, Tim50 and Tim17 (Dekker et al., 1993; Maarse et al., 1994; Yamamoto et al., 2002). Proteins imported via this route are passed directly from the IMS domain of Tom22 to the TIM23 machinery where they bind to a receptor region formed by Tim50 and Tim23 (Geissler et al., 2002; Yamamoto et al., 2002). Binding of a preprotein to Tim50 leads to the opening of the Tim23 pore (Meinecke et al., 2006), which is facilitated by the interaction of Tim21, the fourth subunit of the TIM23 complex (Chacinska et al., 2005), with respiratory supercomplexes (van der Laan et al., 2006). The membrane potential ($\Delta\Psi$) is then required for driving the positively-charged presequence into the IMM (Chacinska et al., 2009). To completely translocate the proteins into the matrix, the presequence translocase-associated import motor (PAM) using energy in the form of ATP is required in addition (Pfanner and Meijer, 1995). It is recruited to the TIM23 complex by Tim17 (Chacinska et al., 2005). Its central component is the molecular chaperone heat shock protein 70 (mtHsp70), which binds to the polypeptide and moves it into the matrix, using energy derived from ATP hydrolysis (Schneider et al., 1994; Ungermann et al., 1994). After translocation of the preprotein into the matrix, the mitochondrial processing peptidase (MPP) removes the presequence (Taylor et al., 2001). The PAM complex furthermore comprises the four membrane-bound co-chaperones Tim44, Pam18, Pam16, and Pam17, which play a role in organizing the TIM23-PAM interaction and stimulating the ATP activity of mtHsp70 (Chacinska et al., 2009).

The TIM23 machinery not only imports matrix proteins but also proteins destined for the IMM. These proteins possess a hydrophobic sorting signal behind their N-terminal targeting signal which arrests them in the IMM (Gärtner et al., 1995). The proteins are then laterally released from the TIM23 complex with the help of Tim17 (Chacinska et al., 2005). This translocation only requires energy in the form of $\Delta\Psi$, whereas the PAM is not needed (Voos et al., 1993). Additionally, it is possible that the protein is then cleaved behind the hydrophobic signal by the inner membrane peptidase (IMP), releasing the protein into the IMS (Glick et al., 1992; Nunnari et al., 1993).

1.2.3 The TIM22 pathway

Inner membrane carrier proteins and some components of the TIM23 and TIM22 complexes are imported via the TIM22 pathway (Jensen and Dunn, 2002). These proteins do not possess an N-terminal presequence but contain internal targeting signals that can be located all over the protein, with each element comprising about ten amino acid residues (Chacinska et al., 2009).

After translocation via the TOM machinery, the Tim9-Tim10 chaperone complex or in case of some proteins the Tim8-Tim13 chaperone complex bind to the protein and guide it through the IMS to the TIM22 machinery (Endres et al., 1999; Leuenberger et al., 1999; Paschen et al., 2000; Sirrenberg et al., 1998). Then, Tim9 and Tim10 assemble with Tim12 at the TIM22 machinery forming the Tim9-Tim10-Tim12 complex (Adam et al., 1999; Sirrenberg et al., 1998). The TIM22 complex consists of three integral membrane subunits, the central channel forming component Tim22, Tim54, and Tim18 (Kerscher et al., 1997; Kerscher et al., 2000; Sirrenberg et al., 1996). The TIM22 machinery is a twin-translocase consisting of two channels and requires energy only in form of $\Delta\Psi$ (Rehling et al., 2003). After insertion of the proteins into the Tim22 channel, they are laterally released in a mechanism still not deciphered (Chacinska et al., 2009).

1.2.4 The MIA pathway

As small molecules can diffuse freely between the cytosol and the IMS, it was assumed for a long time that the IMS, like the cytosol, constitutes a reducing environment (Chacinska et al., 2009; Lu et al., 2004). Surprisingly, however, it was found that many IMS proteins possess cysteine motifs and form intramolecular disulfide bonds (Allen et al., 2003). Many of these proteins are of low molecular weight below 20 kDa, e.g. small Tim proteins (Lutz et al., 2003).

These IMS proteins are assembled via the Mitochondrial IMS import and assembly (MIA) pathway which consists of the central component Mia40 and the sulfhydryl oxidase Erv1 (essential for respiratory growth and viability 1) in yeast or ALR (augmenter of liver regeneration) in humans (Chacinska et al., 2004; Hofmann et al., 2005; Mesecke et al., 2005). The central component Mia40 contains a characteristic motif consisting of six invariant cysteines and possesses a hydrophobic binding cleft (Milenkovic et al., 2007; Naoe et al., 2004; Sideris and Tokatlidis, 2007). IMS proteins exhibit a mitochondrial intermembrane space signal (MISS), including a cysteine residue that can form a mixed disulfide bond with the cysteine motif of Mia40 (Milenkovic et al., 2009; Sideris et al., 2009). Directly after or during translocation across the OMM in the reduced form, IMS proteins are bound by Mia40 via mixed disulfide bonds (Milenkovic et al., 2007; Muller et al., 2008; Sideris and Tokatlidis, 2007). Mia40 then promotes the formation of intramolecular disulfide bonds in the

substrate protein by oxidizing it (Mesecke et al., 2005). Thereby, the cysteine residues of Mia40 are reduced and have to be reoxidized by Erv1. This protein transfers the electrons from Mia40 to the respiratory chain via cytochrome c (cyt c), allowing a new redox-cycle of Mia40 (Bihlmaier et al., 2007; Dabir et al., 2007). Interestingly, fungal Mia40 is membrane-bound (Naoe et al., 2004), whereas its human homolog is significantly smaller and soluble, lacking the N-terminal mitochondrial targeting signal and the transmembrane domain (Hofmann et al., 2005).

1.2.5 Insertion of proteins into the OMM

OMM proteins of mitochondria belong to two classes – β -barrel proteins, which traverse membranes with β -plated sheets, and α -helical proteins, which are anchored in the OMM through one or more α -helices (Chacinska et al., 2009). β -barrel proteins are only present in the outer membranes (OM) of gram-negative bacteria, mitochondria and chloroplasts, pointing to the bacterial origin of these two cell organelles (Tamm et al., 2004). Proteins of β -barrel topology are integrated into the OMM by the evolutionary conserved sorting and assembly machinery (SAM) (Wiedemann et al., 2003), also known as topogenesis of mitochondrial outer membrane β -barrel proteins (TOB) (Paschen et al., 2003).

Eukaryotic cells only possess a limited number of β -barrel proteins. In yeast, they include the central component of the SAM/TOB machinery, Sam50/Tob55, mitochondrial distribution and morphology protein Mdm10, Mmm2/Mdm34 and two isoforms of porin (Paschen et al., 2005). In mammalian cells, only the yeast porin homolog, the voltage dependent anion-sensitive channel (VDAC), was found besides Tom40 and Sam50. VDAC forms a pore in the OMM that allows the diffusion of small metabolites between the IMS and the cytosol, thereby enabling communication between these two compartments (Colombini, 1979). It is present in three different isoforms (Rahmani et al., 1998). VDAC1 is the only eukaryotic β -barrel protein whose structure could be solved. In contrast to many bacterial β -barrel proteins, it does not have 16 but 19 β -strands, thereby being the first β -barrel identified with an odd number of β -strands (Bayrhuber et al., 2008; Ujwal et al., 2008). Tom40 exhibits sequence and predicted secondary structure homology to VDAC1, and therefore probably also contains 19 β -strands (Bayrhuber et al., 2008).

After translocation through the TOM, β -barrel proteins are bound by a chaperone complex consisting either of the small Tim proteins Tim9/Tim10 or Tim8/Tim13 (Habib et al., 2005; Wiedemann et al., 2004). The Tim9-Tim10 or Tim8-Tim13 complex forms a hexameric ring structure and guides the β -barrel proteins to the SAM complex (Habib et al., 2005; Wiedemann et al., 2004). In yeast, where this complex was first described, its core complex consists of the central component Sam50/Tob55 (Kozjak et al., 2003; Paschen et al., 2003), the essential protein Sam35 (Tob38/Tom38) (Ishikawa et al., 2004; Milenkovic et al., 2004; Waizenegger et al., 2004), which behaves as a

peripheral membrane protein but seems to be embedded into the OMM via its association with Sam50 (Kutik et al., 2008), and the integral membrane protein Sam37 (Mas37/Tom37), which is dispensable for growth (Wiedemann et al., 2003). Sam50 itself is a β -barrel protein and possesses a polypeptide transport-associated (POTRA) domain facing the IMS at its N-terminus (Kozjak et al., 2003; Paschen et al., 2003) and a carboxy-terminal (C-terminal) β -barrel consisting of 16 β -strands (Gentle et al., 2005). Sequence comparisons between the components of the β -barrel assembly machinery in bacteria and eukaryotes show that the central import component Sam50 is homologous to Omp85/BamA, which integrates β -barrel proteins into the OM of gram-negative bacteria (Kozjak et al., 2003; Paschen et al., 2003).

β -barrel proteins exhibit a β -sorting signal within their last β -strand which comprises a large polar amino acid, an invariant glycine and two large hydrophobic amino acids (Kutik et al., 2008). This β -signal is recognized by Sam35 and its binding induces a change in the properties of the SAM channel leading to its opening and increased conductance. Several β -strands are inserted and the protein is then laterally released from the SAM complex into the OMM (Kutik et al., 2008). Alternatively, it could be possible that β -barrel proteins are not inserted into the Sam50 pore but use this protein as a scaffold to be integrated at the protein-lipid interface (Gentle et al., 2004; Habib et al., 2005). The POTRA domain of Sam50 was first thought to play a role in protein binding (Habib et al., 2007) but a more recent study showed that it is not essential for this step (Kutik et al., 2008). Recently, it was demonstrated that this domain and Sam37 play a role in the release of β -barrel proteins from the SAM complex (Chan and Lithgow, 2008; Stroud et al., 2011).

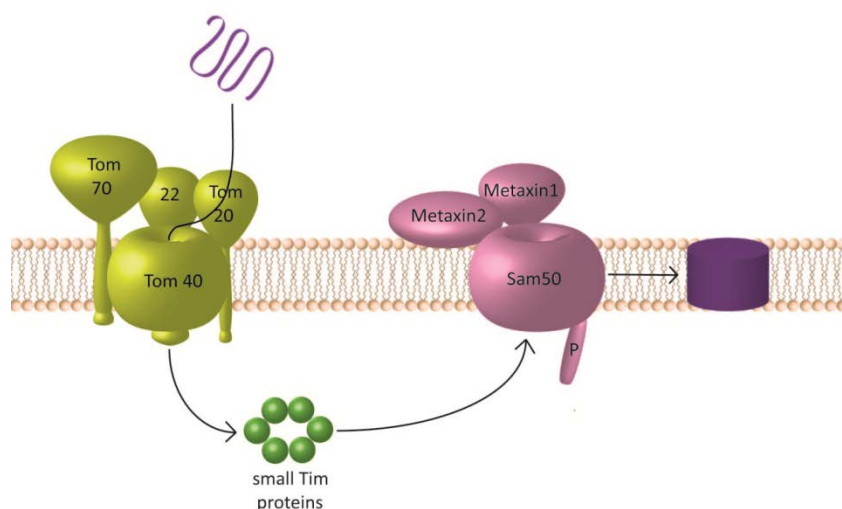


Figure 1-2 Assembly of β -barrel proteins in mammalian mitochondria. β -barrel proteins are recognized by the Tom20 receptor and translocated across the outer mitochondrial membrane (OMM) via the TOM complex. In the intermembrane space, they are bound by the small Tim chaperone complexes Tim9-Tim10 or Tim8-Tim13 and guided to the sorting and assembly machinery (SAM), which integrates the β -barrel proteins into the OMM.

The mammalian SAM complex (Figure 3-2) consists of Sam50, which is similar to its yeast counterpart (Humphries et al., 2005), and two additional proteins, metaxins 1 and 2 (Armstrong et al., 1997; Armstrong et al., 1999; Kozjak-Pavlovic et al., 2007). The integral membrane protein metaxin 1 exhibits sequence homology to yeast Sam37 in its N-terminal region (Armstrong et al., 1997). It is anchored to the OMM with its C-terminal domain, and tethers metaxin 2, which seems to be the equivalent of Sam35 although the proteins share very remote sequence similarity, to the cytosolic surface of the OMM (Armstrong et al., 1997; Armstrong et al., 1999). Both proteins are present in a complex with Sam50 (Xie et al., 2007) and were shown to play a role in the import of β -barrel proteins (Kozjak-Pavlovic et al., 2007).

Whereas β -barrel proteins are all integrated into the OMM by the SAM complex, many different ways for the integration of α -helical proteins into the OMM seem to exist. The signals of α -helical OMM proteins can be present at both termini or in the middle of the protein and normally consist of an α -helical transmembrane segment often flanked by positively charged residues (Beilharz et al., 2003; Kemper et al., 2008; Setoguchi et al., 2006). It could be shown that the SAM complex can play a role in the OMM integration for some α -helical proteins (Stojanovski et al., 2007). The SAM core complex consisting of Sam50, Sam35 and Sam37 can associate with Mdm10 or Tom5/Tom40 for this task depending on which proteins have to be integrated (Thornton et al., 2010). Assembly of Mdm10 with a subfraction of the core SAM complex, for instance, is required for the integration of Tom22 (Meisinger et al., 2004; Thornton et al., 2010).

Most α -helical proteins, however, do not depend on the SAM complex for OMM integration. Mim1 (mitochondria import 1), for instance, cooperates with Tom70 to import α -helical outer membrane proteins with multiple transmembrane segments (Becker et al., 2011). In addition, it is required for the membrane insertion and assembly of the signal-anchored Tom receptors (Becker et al., 2008). Some signal-anchored proteins were shown to depend on Tom40 for their import but not on the other TOM components (Ahting et al., 2005). Additionally, it was recently demonstrated that proteins can be released laterally from the TOM complex into the OMM (Harner et al., 2011b), although this had been considered to be energetically unfavorable (Chacinska et al., 2009). The import of the signal-anchored protein Mcr1, on the other hand, does not involve the TOM complex at all (Meineke et al., 2008). The tail-anchored protein Fis1 was also shown not to use any known import route, and rather the lipid composition of the OMM might play an important role in its integration (Kemper et al., 2008; Setoguchi et al., 2006).

Most studies about the integration of α -helical proteins into the OMM were conducted in yeast. Little is known about the situation in mammalian cells, and for important yeast components such as Mdm10 and Mim1 no homologs could be identified (Hulett et al., 2008; Zeth, 2010).

1.3 Conservation of the transport and membrane insertion of β -barrel proteins

Most bacterial OM proteins are of β -barrel topology (Koebnik et al., 2000), and all known bacterial β -barrel proteins form a cylindrical closed barrel with an even number of 8 - 22 amphipathic β -strands (Tamm et al., 2004). A common feature of β -barrel proteins is their β -signal at the C-terminus (Kutik et al., 2008; Struyve et al., 1991). In bacteria, it comprises a highly conserved phenylalanine (or tryptophan) at the ultimate C-terminal position, and hydrophobic residues at positions three (mostly tyrosine), five, seven, and nine from the C-terminus (Struyve et al., 1991). Despite the conservation of this signal among gram-negative bacteria, species-specific features can be observed (Walther et al., 2009b). In most neisserial OM proteins, for instance, a positively charged residue is present at the penultimate position (Robert et al., 2006; Walther et al., 2009b). When compared to the β -sorting signal of eukaryotic β -barrel proteins, the composition of this signal is not completely conserved. As mentioned, the eukaryotic β -signal sequence contains a terminal large polar amino acid instead of the phenylalanine in bacteria and an invariant glycine and two large hydrophobic amino acids instead of alternating hydrophobic residues as seen in bacteria (Kutik et al., 2008). Additionally, studies with human VDAC1 demonstrated that not only the β -signal but various other amino acids all over the protein are crucial for OMM integration (Kozjak-Pavlovic et al., 2010).

In contrast to the OMM, the bacterial OM does not constitute a symmetric phospholipid bilayer but an asymmetric membrane, with one leaflet consisting of phospholipids and the other of lipopolysaccharides (LPS) (Tamm et al., 2004). Bacterial β -barrel proteins are synthesized in the cytoplasm with an N-terminal signal sequence. The signal is recognized by cytosolic chaperones which deliver the β -barrel protein to the Sec machinery in the inner membrane (Walther et al., 2009b). This machinery subsequently translocates the protein across the plasma membrane into the periplasm (de Keyser et al., 2003). During or directly after translocation, the N-terminal signal is removed by the signal peptidase (Mogensen and Otzen, 2005). In the periplasm, chaperones bind to the polypeptide and guide it to the β -barrel assembly machinery (BAM) (Walther et al., 2009b). In *E. coli*, the BAM consists of the essential central component BamA/Omp85 (outer membrane protein)/YaeT (Werner and Misra, 2005), and the accessory membrane-associated lipoproteins BamB (YfgL), BamC (NlpB), BamD (YfiO) and BamE (SmpA) (Sklar et al., 2007; Wu et al., 2005). The number of accessory lipoproteins in the BAM complex depends on the bacterial species. In *N. meningitidis*,

for instance, the BAM complex includes Omp85, homologs of BamD (ComL), BamC and BamE, and the additional component RmpM, whereas no BamB homolog exists (Volokhina et al., 2009; Voulhoux et al., 2003). BamA/Omp85 consists of a C-terminal β -barrel comprising 16 β -strands, and an N-terminal periplasmic domain (Gentle et al., 2005; Voulhoux et al., 2003). The periplasmic domain possesses five POTRA domains (Sanchez-Pulido et al., 2003). As mentioned, eukaryotic Sam50 also possesses 16 β -strands in its C-terminal domain (Gentle et al., 2005), but only one POTRA domain in its N-terminal part (Habib et al., 2007). Whereas in *N. meningitidis* one POTRA domain is sufficient for the function of the protein (Bos et al., 2007), only the first or second POTRA domain can be deleted in *E. coli* (Kim et al., 2007). As the fifth POTRA domain of *E. coli* was demonstrated to weakly bind one of the BAM substrates, PhoE, it was suggested that the POTRA domains are involved in guiding β -barrel proteins to the core of the BAM complex (Knowles et al., 2008; Walther et al., 2009b). Of all four lipoproteins, only BamD/ComL is essential in both *E. coli* and *N. meningitidis* (Malinverni et al., 2006; Volokhina et al., 2009). As gonococcal BamD/ComL is covalently linked to peptidoglycan and some bacteria exhibit BamE homologs with a peptidoglycan binding domain, it was suggested that the accessory Bam proteins might be involved in anchoring the BAM complex to peptidoglycan, and possibly in modulating peptidoglycan to allow access of outer membrane proteins to the BAM complex (Walther et al., 2009b). When compared to the eukaryotic SAM complex, the four accessory lipoproteins of the BAM complex have no homologs in eukaryotes and *vice versa* – the other proteins of the SAM complex cannot be traced to bacterial ancestors.

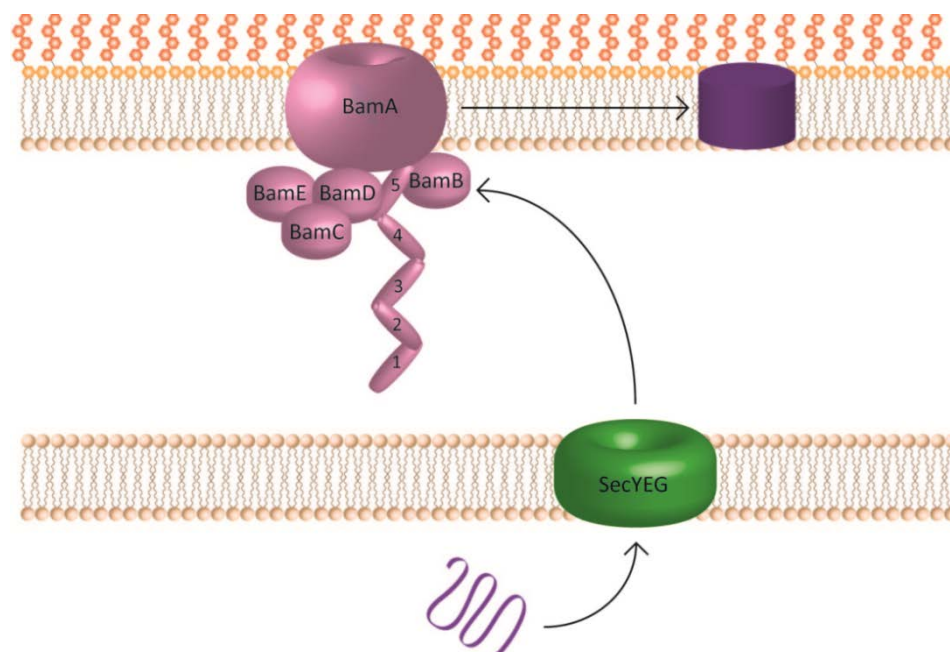


Figure 1-3 The β -barrel assembly machinery (BAM) of *E. coli*. β -barrel proteins are synthesized in the cytosol and translocated across the inner membrane via the Sec machinery. Subsequently, periplasmic chaperones guide the proteins to the BAM complex whose core component BamA mediates their outer membrane integration.

Despite these differences in the sorting signal and the assembly machineries, bacteria were shown to integrate eukaryotic VDAC into their OM (Walther et al., 2010), and yeast cells can equally translocate β -barrel proteins of bacterial origin (Walther et al., 2009a). The ability of mitochondria to import bacterial β -barrel proteins might play a role in infection. An interesting example is the neisserial porin PorB. Studies of *N. meningitidis* PorB revealed that it possesses 16 β -strands and integrates into the OM as a trimer (Derrick et al., 1999; Minetti et al., 1997). Upon infection, meningococcal PorB is targeted to mitochondria and protects cells from apoptosis (Massari et al., 2000; Massari et al., 2003). Gonococcal PorB is also translocated to human mitochondria, but accompanied by cytochrome c release and apoptosis (Müller et al., 2000). Experiments with overexpressed PorB_{NgO} in human cell lines demonstrated that PorB is imported into mitochondria but not integrated into the OMM, accumulating in the IMS/IMM compartment and thereby leading to the loss of $\Delta\Psi$ and damage of the mitochondria (Kozjak-Pavlovic et al., 2009; Müller et al., 2002).

1.4 The IMM: respiratory chain and membrane structure

The IMM is crucial for cellular function. It contains multiple invaginations into the matrix called cristae. These harbor the respiratory chain complexes, which are required for the energy production of the cell. Cristae are highly organized structures and their morphology is maintained by protein complexes. As a connection between the maintenance of cristae and respiratory function exists, the next paragraphs will introduce both cristae structure and respiratory complexes in more detail.

1.4.1 The respiratory chain

One major task of mitochondria is providing energy in the form of adenosine triphosphate (ATP) to the cell. Most of the ATP is produced by the respiratory chain which resides in the cristae membrane (CM) of the IMM (Gilkerson et al., 2003). The respiratory chain consists of four protein complexes, which pump protons out of the matrix and generate a protonmotive force, and the ATP synthase, which couples the influx of protons back into the matrix to oxidative phosphorylation of ADP (Rich and Marechal, 2010).

Complex I (or NADH:ubiquinone oxidoreductase) is the major entry point for electrons. It catalyzes the electron transfer from NADH, which is produced during glycolysis and in the tricarboxylic acid cycle by reduction of nicotinamide adenine dinucleotide (NAD⁺), to ubiquinone (Rich and Marechal, 2010). Research of the bovine respiratory complexes demonstrated that complex I comprises 45 subunits, of which seven are mtDNA-encoded (Carroll et al., 2006). It has a size of around 980 kDa and possesses eight iron-sulfur centers and flavin mononucleotide (FMN) as

cofactors (Carroll et al., 2003; Carroll et al., 2006). Complex I is shaped L-like with a hydrophobic arm in the IMM and a hydrophilic peripheral arm extended to the matrix side (Grigorieff, 1998). Based on the respective task, it can be subdivided into three modules: the dehydrogenase module comprising the NDUFV2, NDUFV1 and NDUFS1 subunits, the hydrogenase module, which consists of NDUFS2, NDUFS3, NDUFS7 and NDUFS8, and the proton translocation module, which includes the seven mtDNA-encoded subunits (Vogel et al., 2007). Studies in the fungus *N. crassa* demonstrated that the two arms are assembled independently (Tuschen et al., 1990). In mammalian cells, assembly of complex I occurs by formation of several intermediates which are then combined to the mature complex (Lazarou et al., 2007). Different models exist, but they all assume that assembly starts with the peripheral arm components NDUFS2 and NDUFS3 being anchored to a membrane part that includes MT-ND1, followed by the addition of the other subunits, thereby forming distinct intermediates of around 450 kDa and 830 kDa (McKenzie and Ryan, 2010; Vogel et al., 2007). Known assembly factors of complex I are NDUFAP1 and NDUFAL2L (Ogilvie et al., 2005; Vogel et al., 2005). NDUFAP1 transiently interacts with complex I intermediates and its loss leads to reduced levels of complex I (Dunning et al., 2007; Vogel et al., 2005). NDUFAL2L probably stabilizes intermediates of complex I and helps to incorporate specific subunits, as mutations in the gene encoding it result in the accumulation of a complex I subcomplex but do not completely prevent mature complex assembly (Barghuti et al., 2008; Ogilvie et al., 2005).

Complex II (or succinate dehydrogenase) is an additional entry point for electrons into the respiratory chain. It catalyzes the transfer of electrons from succinate, an intermediate of the tricarboxylic acid cycle, via flavin adenine dinucleotide (FAD) to ubiquinone (Hägerhäll, 1997). In this step, no protons are pumped across the IMM, making complex I an energetically more favorable entry point for electrons into the respiratory chain (Rich and Marechal, 2010). Complex II is present as a monomer of about 125 kDa (Sun et al., 2005). It consists of a soluble heterodimer in the matrix and a heterodimer in the IMM. The matrix part comprises the subunits SDHA with a covalently bound FAD, and SDHB, which harbors three Fe-S clusters (Hägerhäll, 1997). The IMM part of complex II consists of subunits SDHC, SDHD and a single heme (Sun et al., 2005). All complex II subunits are nuclear-encoded. Only recently, two assembly factors for complex II could be identified. Loss of SDHAF1 results in a reduced complex II activity and this factor may be involved in the insertion of Fe-S clusters into the complex (Ghezzi et al., 2009). The second factor, SDHAF2, plays a role in adding the FAD prosthetic group to the SDHA flavoprotein (Hao et al., 2009).

Complex III (or ubiquinol:cytochrome c oxidoreductase) catalyzes the electron transfer from ubiquinol to cytochrome c (cyt c) in the IMS (Mitchell, 1976). Complex III forms a homodimer in the

IMM, with each monomer consisting of eleven subunits (Schagger et al., 1986). Cytochrome b (MT-CYB) is the only mtDNA-encoded component. MT-CYB, cytochrome c-1 (CYC1) and Rieske Fe-S polypeptide 1 (RISP, UQCRFS1) contain the metal centers of the complex which are necessary for the electron transfer (Iwata et al., 1998). Studies in yeast demonstrated that complex III is first assembled in the three subcomplexes MT-CYB/UQCRB (Qcr7)/UQCRQ (Qcr8), CYC1/UQCRHQ (Qcr6)/UQCR10 (Qcr9) and Core1 (UQCRC1)/Core2 (UQCRC2), which then assemble into the cytochrome *bc1* precomplex (Zara et al., 2004). Eventually, RISP and UQCR11 (Qcr10) are incorporated (Cruciat et al., 1999). A well-established complex III assembly factor is Bcs1p (called BCS1L in mammalian cells), which is involved in the ATP-dependent addition of RISP and UQCR11 (Cruciat et al., 1999; Fernandez-Vizarra et al., 2007). Recently, tetratricopeptide repeat 19 (TTC19) was described as a novel complex III assembly factor (Ghezzi et al., 2011). Clinical isolates of patients with mutations in the *ttc19* gene showed reduced complex III activity, and it could be demonstrated that TTC19 physically interacts with complex III components in mouse cells (Ghezzi et al., 2011).

Complex IV (or cytochrome c oxidase) transfers electrons from cyt c to oxygen, thereby reducing it to H₂O (Fernandez-Vizarra et al., 2009). Complex IV is composed of 13 subunits and has a size of about 200 kDa (Kadenbach et al., 1983; Schagger and Pfeiffer, 2000). Its catalytic core is formed by the mtDNA-encoded subunits MTCO1 and MTCO2, and contains two copper centers and two heme A moieties (Tsukihara et al., 1996). The third mtDNA-encoded subunit (MTCO3) is also part of the core but does not bind any cofactors. The other subunits probably have stabilizing and regulatory functions (Arnold and Kadenbach, 1997; Fernandez-Vizarra et al., 2009). Complex IV assembly starts with the insertion of MTCO1 into the IMM, followed by COX4 and COX5A together with heme A, forming the S2 assembly intermediate (Antonicka et al., 2003b; Williams et al., 2004). Next, integration of MTCO2 takes place, probably preceded by Cu_B, heme a₃ and Cu_A insertion (Stiburek et al., 2005; Williams et al., 2004). Subsequently, MTCO3 is incorporated, followed by the integration of most other components (S3 intermediate) and eventually by the insertion of the remaining subunits (S4 intermediate) (Nijtmans et al., 1998; Williams et al., 2004). Finally, the complex dimerizes (Nijtmans et al., 1998). In yeast, around 30 assembly factors for complex IV were reported and at least 10 homologs are known in humans (Stiburek and Zeman, 2010). Deficiency of SURF1, for instance, results in the accumulation of assembly intermediates (Tiranti et al., 1999), whereas COX10 and COX15 are involved in the biosynthesis of the heme A of the catalytic center (Antonicka et al., 2003a; Barros et al., 2001). The assembly factor Leucine-rich pentatricopeptide repeat cassette (LRPPRC) is required for the stability of MTCO1 and MTCO3 mRNAs (Xu et al., 2004).

Complex V (or ATP synthase) couples the influx of protons back into the matrix to the phosphorylation of ADP to ATP (Engelbrecht and Junge, 1997). It consists of the hydrophobic membrane-integrated F_0 motor and the hydrophilic F_1 module, which faces the matrix (Abrahams et al., 1994; Collinson et al., 1994). The F_1 module is formed by five different subunits and contains the ATP synthase domain (Abrahams et al., 1994). The F_0 module comprises eight subunits, including two subunits encoded by the mitochondrial genes MT-ATP6 (subunit α) and MT-ATP8 (subunit A6L) (Collinson et al., 1994). Formation of the F_1 module occurs independently (Kucharczyk et al., 2009). F_0 assembly starts with the c subunits, followed by binding of the F_1 part, and subsequently of all other subunits. Eventually, the two mtDNA-encoded subunits are integrated (Wittig et al., 2010). Complex V monomers can assemble into dimers or even oligomers (Arnold et al., 1998; Krause et al., 2005; Schagger and Pfeiffer, 2000). In humans, only ATP11 and ATP12 could be identified as complex V assembly factors, with both probably being involved in F_1 synthesis (De Meirleir et al., 2004; Wang et al., 2001).

Respiratory complexes I, III and IV associate to form supercomplexes called respirasomes (Cruciat et al., 2000; Schagger and Pfeiffer, 2000). These supercomplexes consist of one complex I, two complex III and up to four complex IV molecules (Schagger and Pfeiffer, 2000). Cardiolipin, a characteristic mitochondrial phospholipid, has an important function in stabilizing supercomplexes (Pfeiffer et al., 2003; Zhang et al., 2002). Loss of phosphatidylethanolamine (PE), another major phospholipid of the IMM, on the other hand leads to formation of larger supercomplexes, indicating that this phospholipid destabilizes respiratory supercomplexes and functions antagonistic to cardiolipin (Böttlinger et al., 2012). Depletion of cardiolipin and of PE both result in decreased membrane potential, underlining the importance of correct supercomplex formation (Böttlinger et al., 2012; Jiang et al., 2000). Interestingly, cardiolipin was recently demonstrated to be required for complex II stability and activity as well (Schwall et al., 2012).

As respiration is a crucial cellular process, deficiencies in each respiratory complex lead to various diseases. They can be caused by mutations in both nuclear and mtDNA encoded subunits, or in genes encoding assembly factors (Fernandez-Vizarra et al., 2009).

1.4.2 IMM structure and maintenance

In recent years, it has become clear that the IMM is not one continuous membrane but can be subdivided into the inner boundary membrane (IBM), running parallel to the OMM, and the cristae membrane (CM) (Mannella et al., 1994; Perkins et al., 1997). This view is supported by the finding that both membranes differ significantly in their protein composition (Vogel et al., 2006; Wurm and

Jakobs, 2006). The IBM harbors proteins involved in protein translocation and mitochondrial fusion and fission. The CM, on the other hand, mainly possesses proteins required for oxidative phosphorylation, mitochondrial protein biosynthesis and transport of mtDNA-encoded proteins (Gilkerson et al., 2003; Vogel et al., 2006; Wurm and Jakobs, 2006). Cristae are tubular compartments which are connected to the IBM via crista junctions (CJ) (Frey and Mannella, 2000; Perkins et al., 1997). Often, several cristae merge to form a lamellar compartment (Perkins et al., 1997). CJs are narrow, tubular or slot-like openings with a diameter between 12 – 40 nm and a length of 30 – 50 nm (Perkins et al., 1997; Perkins et al., 2001; Zick et al., 2009). It was suggested that CJs are not permanent structures but that their formation is a dynamic process (Zick et al., 2009). The exact role of CJs remains unclear. It is assumed, however, that they constitute a barrier between IBM and CM and between IMS and intracristal space (ICS), allowing mitochondria to regulate diffusion of metabolites between these compartments (Mannella et al., 2001; Perkins et al., 1997; Zick et al., 2009).

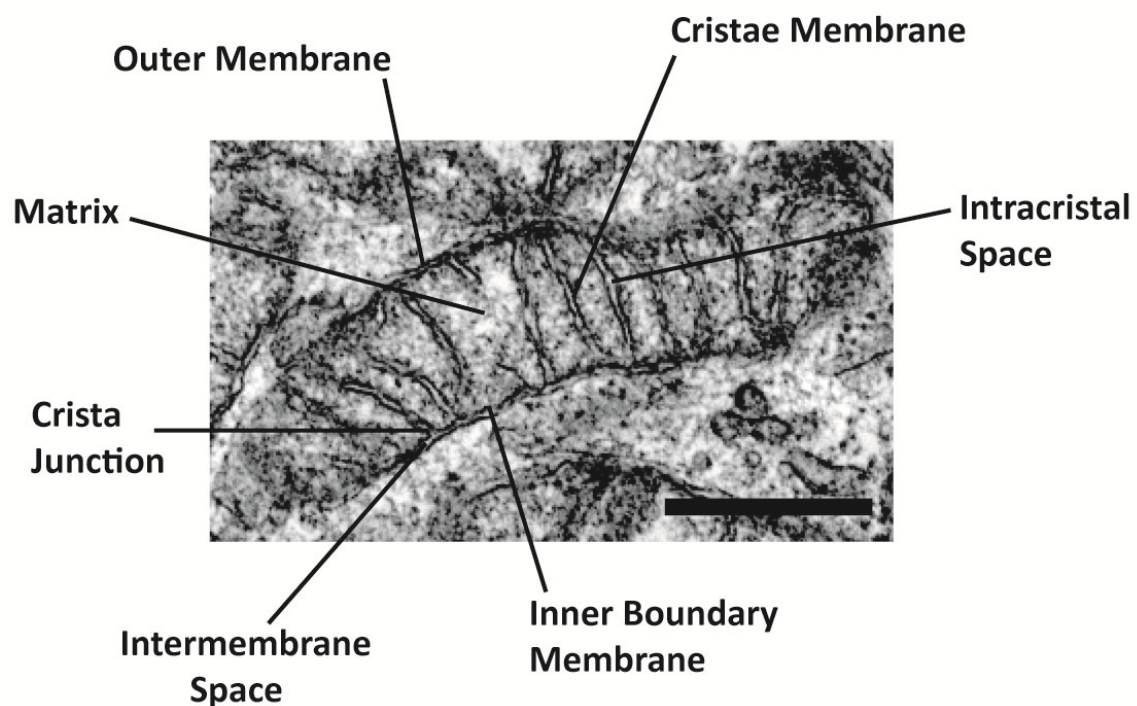


Figure 1-4 The mitochondrial ultrastructures. The different mitochondrial structures are highlighted in a TEM image of a HeLa cell mitochondrion. The scale bar represents 1 μm .

Little is known about the formation, maintenance and remodeling of cristae and CJs, although different proteins were shown to possibly be involved in these processes. Studies in yeast cells demonstrated that the dimerization of the ATP synthase is required for maintaining the cristae structure (Giraud et al., 2002; Paumard et al., 2002; Rak et al., 2007). When subunits e and g are

absent, the dimerization of the complex is prevented and the cristae are arranged in concentric circles (Giraud et al., 2002; Paumard et al., 2002). Furthermore, reduction in PTEN-induced putative kinase 1 (PINK1) results in altered cristae structures (Exner, 2007).

For the formation of CJs, different proteins were suggested to play a role as well. The large dynamin-like GTPase optic atrophy 1 (Opa1) is a key protein of mitochondrial fusion together with the mitofusins (Cipolat et al., 2004; Griparic et al., 2004; Misaka et al., 2002). In addition, Opa1 has been shown to play a role in cristae-remodeling during apoptosis (Frezza et al., 2006; Olichon et al., 2003). Depletion of Opa1 leads to alterations in cristae morphology and cyt c release from mitochondria (Olichon et al., 2003), whereas Opa1 overexpression delays cyt c release and induces CJ tightening (Frezza et al., 2006; Zick et al., 2009). Additionally, prohibitins were suggested to be involved in CJ formation, as they form large ring-like structures with diameters similar to that of CJs (Tatsuta et al., 2005). Reduction in prohibitin levels results in loss of long Opa1 isoforms and aberrant cristae formation (Merkwirth et al., 2008). Recently, prohibitins were shown to regulate Opa1 processing, linking these two proteins hypothesized to be involved in cristae remodeling (Merkwirth et al., 2008).

Another protein shown to control cristae structure is mitofilin (John et al., 2005). Mitofilin is an IMM protein and exists in two isoforms of 88 and 90 kDa (Giefers 1997). When mitofilin is reduced, cristae do not form tubular compartments but stacks of membrane sheets, and CJs are absent (John et al., 2005). Several diseases have been linked to decreased mitofilin levels, e.g. Parkinson's disease, diabetic cardiomyopathy, and Down syndrome (Baseler et al., 2011; Myung et al., 2003; Van Laar et al., 2008). In yeast, mitofilin (also called Formation of Crista Junction protein 1, Fcj1 in this organism) is also required for CJ formation, and it was demonstrated that this protein and ATP synthase subunits e and g genetically interact, suggesting that mitofilin might influence the oligomeric state of the ATP synthase and thereby membrane curvature of cristae (Rabl et al., 2009). Recently, mammalian mitofilin was found in a complex with Sam50, CHCHD3, CHCHD6, DnaJC11, and the metaxins, but no further investigations into the role of this complex were performed (Xie et al., 2007). Furthermore, interactions of mitofilin with PARP-1 and DISC1 were reported (Park et al., 2010; Rossi et al., 2009). It was suggested that the interaction with PARP-1 is required for mitochondrial PARP-1 uptake, and that mitochondrial PARP-1 localization is important for the maintenance of mtDNA (Rossi et al., 2009). DISC1, on the other hand, seems to play an important role in mitofilin stability, as its deficiency results in mitofilin ubiquitination (Park et al., 2010).

Apart from proteins, mitochondrial lipid composition was suggested to play a role in cristae formation as well. Patients with Barth syndrome have a mutation in the gene encoding Tafazzin, a

protein involved in the biosynthesis of the mitochondrial-specific phospholipid cardiolipin (Bione et al., 1996; Xu et al., 2003). Their cardiolipin levels are strongly reduced and they exhibit alterations in their cristae morphology (Acehan et al., 2007). As cardiolipin also stabilizes respiratory supercomplexes (Pfeiffer et al., 2003), it remains unclear whether the effects of cardiolipin on the cristae structure are direct by influencing IMM curvature or indirect by affecting supercomplex formation (Zick et al., 2009).

The IBM is not only connected to cristae membranes, but additionally remains in contact with the OMM at specific regions termed contact sites, even when the matrix contracts (Hackenbrock, 1966; Hackenbrock, 1968). Contact sites are about 14 nm in width and, depending on cell type and fixation method used, each mitochondrion exhibits between 80 – 270 contact sites (Perkins et al., 1997; Reichert and Neupert, 2002). This connection between IMM and OMM is thought to be important for protein and metabolite transport, lipid translocation, formation of the permeability transition pore during apoptosis, and mitochondrial fusion and fission (Crompton, 2000; Epand et al., 2007; Reichert and Neupert, 2002). Several proteins in the inner and outer membrane were demonstrated to interact at contact sites, e.g. VDAC and adenine nucleotide translocase (ANT), and subunits of the TIM23 and TOM complexes; however, these seem to be only transient interactions and not morphologically defined contact site structures (Reichert and Neupert, 2002). It was suggested that contact sites are close to CJs (van der Klei et al., 1994) but electron tomography studies demonstrated that these two structures are not associated (Perkins et al., 1997).

The fact that the ATP synthase was demonstrated to be involved in cristae formation and in addition that protein import complexes are present at contact sites, led to speculations that the maintenance of cristae structure, protein import and respiratory complex assembly are linked (Reichert 2002). However, despite efforts to investigate this connection, protein complexes which form cristae junctions and contact sites could not be determined yet and many questions about the nature of this connection remain open.

1.5 Aims of the work

A study by Walther and co-workers demonstrated that yeast mitochondria can import and assemble all tested bacterial β -barrel proteins (Walther et al., 2009a). Work by our group, on the other hand, has shown that this finding cannot be generalized to all eukaryotic mitochondria as β -barrel proteins of *E. coli* and *Salmonella enterica* were not imported into mitochondria when expressed in human cells (Kozjak-Pavlovic et al., 2011). As earlier studies had demonstrated that PorB of *N. gonorrhoeae* and *N. meningitidis* can be imported into human mitochondria (Massari et al., 2000; Müller et al., 2000), I aimed to examine the import behavior of β -barrel proteins of other *Neisseria* species.

Whereas the signal for SAM complex recognition of β -barrel proteins is well established, it is not known how they are recognized by the TOM complex. Therefore, I aimed to elucidate the nature of the signal that targets β -barrel proteins to human mitochondria by exchanging domains of neisserial β -barrel proteins which are taken up into mitochondria with those of homologous *E. coli* proteins which are not imported.

Work in our group has demonstrated that depleting the central component of the SAM complex, Sam50, leads to a loss of cristae morphology (Ott et al., 2012). In the second part of my work, I therefore aimed to investigate the role of Sam50 in the maintenance of the mitochondrial cristae structure. As this protein was reported to be present in a complex with the CJ organizer mitofilin and CHCHD3, CHCHD6, DnaJC11 and the metaxins (Xie et al., 2007), I wanted to confirm the presence of this protein complex and establish the connection to cristae morphology.

In addition to the loss of cristae structure, a stable isotope labeling with amino acids in cell culture (SILAC) experiment performed by our group showed an influence of Sam50 on respiratory complex components and putative assembly factors (Ott et al., 2012). Therefore, I wanted to confirm the role of Sam50 in respiratory complex assembly. Besides, I aimed to establish the connection between Sam50 and the recently described respiratory complex factor TTC19 (Ghezzi et al., 2011). Finally, I wanted to investigate the influence of TTC19 on the respiratory complexes.

2 MATERIAL AND METHODS

2.1 Material

2.1.1 Cell lines

Table 2.1 Cell lines

Cell line	Properties	Source
HeLa	human epithelial cervical carcinoma cells	ATCC CCL-227
HEK 293T	human embryonic kidney epithelial cells	ATCC CRL-11268
HeLa KRAB	HeLa cells with the gene encoding the KRAB-tTR repressor integrated into the chromosomal DNA	Kozjak-Pavlovic et al., 2007; Alexander Karlas
<i>sam50kd-2</i>	HeLa KRAB cells with inducible shRNA-mediated knockdown of Sam50	Kozjak-Pavlovic et al., 2007
<i>tom40kd-2</i>	HeLa KRAB cells with inducible shRNA-mediated knockdown of Tom40	Kozjak-Pavlovic et al., 2007
<i>mtx2kd-2</i>	HeLa KRAB cells with inducible shRNA-mediated knockdown of Mtx2	Kozjak-Pavlovic et al., 2007
<i>chchd3kd-2</i>	HeLa KRAB cells with inducible shRNA-mediated knockdown of CHCHD3	Ott et al., 2012; own work
<i>ndufs1kd-1</i>	HeLa KRAB cells with inducible shRNA-mediated knockdown of NDUFS1	Ott et al., 2012; own work
<i>cox5akd-2</i>	HeLa KRAB cells with inducible shRNA-mediated knockdown of CoxVa	Ott et al., 2012; Sebastian Straub
<i>core1kd-1</i>	HeLa KRAB cells with inducible shRNA-mediated knockdown of Core1	this study; own work
<i>chchd6kd-3</i>	HeLa KRAB cells with inducible shRNA-mediated knockdown of CHCHD6	this stud;; own work
<i>dnajc11kd-3</i>	HeLa KRAB cells with inducible shRNA-mediated knockdown of DnaJC11	this study; own work
<i>ttc19kd-2</i>	HeLa KRAB cells with inducible shRNA-mediated knockdown of TTC19; siRNA sequence: GCATGAAGCAGGAGGACAATG	this study; from Monika Götz
<i>PLVTHM</i>	HeLa KRAB cells with empty pLVTHM plasmid; control cell line	Kozjak-Pavlovic et al., 2007

HEK 293T cells were cultured in DMEM supplemented with 10 % FCS and 1 % Penicillin/Streptomycin. All other cells were cultured in RPMI 1640 supplemented with 10 % FCS and 1 % Penicillin/Streptomycin.

2.1.2 Bacterial strains

Table 2.2 Bacterial strains

Bacterial strain	Source
<i>E. coli</i> DH5 α	Hanahan, 1983
<i>N. lactamica</i> 2358	N78, Max-Planck-Institut für Infektionsbiologie
<i>N. sicca</i> 2182	N79, Max-Planck-Institut für Infektionsbiologie
<i>N. cinerea</i> 194	N87, Max-Planck-Institut für Infektionsbiologie

E. coli were grown on LB agar plates or in LB medium, neisserial strains were grown on GC agar plates.

2.1.3 Plasmids

All plasmids used are listed in table 2.3. Oligonucleotides and restriction sites used are specified for all plasmids I cloned during the course of this work.

Table 2.3 Plasmids

Plasmid	Vector	Comment	Source
PorB _{<i>Ngo</i>}	pcDNA3-FLAGM	from Vera Kozjak-Pavlovic	Kozjak-Pavlovic et al., 2007
Myc-PorB _{<i>Ngo</i>}	pcDNA3-MycM	amplified from <i>N. gonorrhoeae</i> genomic DNA	Ott et al., 2013
Omp85 _{<i>Ngo</i>}	pcDNA3-FLAGM	from Monika Götz	Kozjak-Pavlovic et al., 2011
OmpC _{<i>E.coli</i>}	pcDNA3-FLAGM	from Monika Götz	Kozjak-Pavlovic et al., 2011
BamA _{<i>E.coli</i>}	pcDNA3-FLAGM	from Monika Götz	Kozjak-Pavlovic et al., 2011
PorB _{<i>Nla</i>}	pcDNA3-FLAGM	amplified with Nla_PorB-f/Nla_PorB-r from <i>N. lactamica</i> 2358 whole cell DNA (EcoI/XhoI)	Kozjak-Pavlovic et al., 2011
PorB _{<i>Nsi</i>}	pcDNA3-FLAGM	amplified with Nsi_PorB-f/Nsi_PorB-r from <i>N. sicca</i> 2182 whole cell DNA (EcoI/XhoI)	Kozjak-Pavlovic et al., 2011
PorB _{<i>Nci</i>}	pcDNA3-FLAGM	amplified with Nla_PorB-f/Nla_PorB-r from <i>N. cinerea</i> 194 whole cell DNA (EcoI/XhoI)	Kozjak-Pavlovic et al., 2011
Omp85 _{<i>Nci</i>}	pcDNA3-FLAGM	amplified with Nci_Omp85-f/Nci_Omp85-r from <i>N. cinerea</i> 194 whole cell DNA (EcoI/XbaI)	Ott et al., 2013
Omp85 $\frac{1}{2}$ BamA $\frac{1}{2}$	pcDNA3-FLAGM	amplified with T7/Omp85_1089-r from Omp85 _{<i>Ngo</i>} and BamA_1096-f/SP6 from BamA _{<i>E.coli</i>} (EcoRI/XbaI)	Ott et al., 2013

BamA $\frac{1}{2}$ Omp85 $\frac{1}{2}$	pcDNA3-FLAGM	amplified with T7/BamA_1085-r from BamA _{E.coli} and Omp85_1080-f/SP6 from Omp85 _{Ngo} (EcoI/XbaI)	Ott et al., 2013
Omp85 $\frac{1}{2}$ BamA $\frac{1}{4}$ Omp85 $\frac{1}{4}$	pcDNA3-FLAGM	amplified with T7/Omp85_1089-f + Omp85_1680/ SP6 from Omp85 _{Ngo} and BamA_1096-f/ BamA_1686-f from BamA _{E.coli} (BamHI/XbaI)	Ott et al., 2013
BamA $\frac{1}{2}$ Omp85 $\frac{1}{4}$ BamA $\frac{1}{4}$	pcDNA3-FLAGM	amplified with T7/BamA_1085-r + BamA_1686/ SP6 from BamA _{E.coli} and Omp85_1080-f/ Omp85_1679-r from Omp85 _{Ngo} (BamHI/XbaI)	Ott et al., 2013
Omp85 $\frac{1}{4}$ BamA $\frac{1}{4}$	pcDNA3-FLAGM	amplified with T7/Omp85_1679-r from Omp85 _{Ngo} and BamA_1686-f/SP6 from BamA _{E.coli} (BamHI/XbaI)	Ott et al., 2013
BamA $\frac{1}{4}$ Omp85 $\frac{1}{4}$	pcDNA3-FLAGM	amplified with T7/BamA_1685-r from BamA _{E.coli} and with Omp85_1680-f/SP6 from Omp85 _{Ngo} (BamHI/XbaI)	Ott et al., 2013
PorB $\frac{1}{2}$ OmpC $\frac{1}{2}$	pcDNA3-FLAGM	amplified with T7/PorB_467-r from PorB _{Ngo} and OmpC_634-f/SP6 from OmpC _{E.coli} (BamHI/XbaI)	Ott et al., 2013
OmpC $\frac{1}{2}$ PorB $\frac{1}{2}$	pcDNA3-FLAGM	amplified with T7/OmpC_633-r from OmpC _{E.coli} and PorB_468-f/SP6 from PorB _{Ngo} (BamHI/XbaI)	Ott et al., 2013
PorB $\frac{1}{2}$ OmpC $\frac{1}{4}$ PorB $\frac{1}{4}$	pcDNA3-FLAGM	amplified with T7/PorB_467-f and PorB_709-f/ SP6 from PorB _{Ngo} and OmpC_634-f/ OmpC_900r from OmpC _{E.coli} (BamHI/XbaI)	Ott et al., 2013
PorB $\frac{1}{4}$ OmpC $\frac{1}{4}$	pcDNA3-FLAGM	amplified with T7/PorB_708-r from PorB _{Ngo} and OmpC_901-f/SP6 from OmpC _{E.coli} (BamHI/XbaI)	Ott et al., 2013
OmpC $\frac{1}{4}$ PorB $\frac{1}{4}$	pcDNA3-FLAGM	amplified with T7/OmpC_900-r from OmpC _{E.coli} and PorB_709-f/SP6 from PorB _{Ngo} (BamHI/XbaI)	Ott et al., 2013
PorB-12aaOmp85	pcDNA3-FLAGM	amplified with T7/PorB_12aa-r from PorB _{Ngo} and Omp85_12aa-f/SP6 from Omp85 _{Ngo}	Ott et al., 2013
Omp85-12aaPorB	pcDNA3-FLAGM	amplified with T7/Omp85_12aa-r from Omp85 _{Ngo} and PorB_12aa-f/SP6 from PorB _{Ngo}	Ott et al., 2013
PorB-12aaOmpC	pcDNA3-FLAGM	amplified with T7/PorB-12aaOmpC-r from PorB _{Ngo} and OmpC-12aaPorB-f/SP6 from OmpC _{E.coli}	Ott et al., 2013
OmpC-12aaPorB	pcDNA3-FLAGM	amplified with T7/OmpC-12aaPorB-r from OmpC _{E.coli} and PorB-12aaOmpC-f/SP6 from PorB _{Ngo} pcDNA3	Ott et al., 2013
Omp85-R783E	pcDNA3-FLAGM	amplified with T7/Omp85-R783E-r and Omp85-R783E-f/SP6 from Omp85 _{Ngo} (BamHI/XbaI)	Ott et al., 2013

Omp85-Q787G	pcDNA3-FLAGM	amplified with T7/Omp85-RQ87G-r and Omp85-Q787G-f/SP6 from Omp85 _{NgO} (BamHI/XbaI)	Ott et al., 2013
Omp85-Q787E	pcDNA3-FLAGM	amplified with T7/Omp85-Q787E-r from Omp85 _{NgO} (BamHI/XbaI)	Ott et al., 2013
Omp85-Q787N	pcDNA3-FLAGM	amplified with T7/Omp85-Q787N-r from Omp85 _{NgO} (BamHI/XbaI)	Ott et al., 2013
Omp85-T790K	pcDNA3-FLAGM	amplified with T7/Omp85-T790K-r and Omp85-T790K-f/SP6 from Omp85 _{NgO} (BamHI/XbaI)	Ott et al., 2013
Omp85-6aa	pcDNA3-FLAGM	amplified with T7/Omp85-6aa-r from Omp85 _{NgO} (BamHI/XbaI)	Ott et al., 2013
Omp85-5aa	pcDNA3-FLAGM	amplified with T7/Omp85-5aa-r from Omp85 _{NgO} (BamHI/XbaI)	Ott et al., 2013
Omp85-4aa	pcDNA3-FLAGM	amplified with T7/Omp85-4aa-r from Omp85 _{NgO} (BamHI/XbaI)	Ott et al., 2013
Omp85-3aa	pcDNA3-FLAGM	amplified with T7/Omp85-3aa-r from Omp85 _{NgO} (BamHI/XbaI)	Ott et al., 2013
Omp85-2aa	pcDNA3-FLAGM	amplified with T7/Omp85-2aa-r from Omp85 _{NgO} (BamHI/XbaI)	Ott et al., 2013
Omp85-1aa	pcDNA3-FLAGM	amplified with T7/Omp85-1aa-r from Omp85 _{NgO} (BamHI/XbaI)	Ott et al., 2013
TTC19	pcDNA3-FLAGS	from Monika Götz	this study
TTC19 isoform2	pcDNA3-FLAGS	amplified with TTC19-iso2-f and TTC19-iso2-r from TTC19 pcDNA3-FLAGS	this study
NDUFS1	pGEM-4Z	amplified with NDUFS1-f/NDUFSS1-r from HeLa whole cell cDNA (KpnI/BamHI)	Ott et al., 2012
Core1	pGEM-4Z	amplified with Core1-f/Core1-r from cDNA clone 4096628 (ThermoScientific)(KpnI/HindIII)	this study
SDHA	pGEM-4Z	amplified with SDHA-f/SDHA-r from cDNA clone 3051442 (ThermoScientific)(KpnI/HindIII)	this study
COX6A	pGEM-4Z	amplified with Cox6a-f/Cox6a-r from HeLa cell cDNA (EcoRI/HindIII)	Ott et al., 2012
CHCHD3	pGEM-4Z	amplified with CHCHD3-f/CHCHD3-r cDNA clone 2901125 (EcoRI/HindIII)	Ott et al., 2012
TTC19-TNT	pCMV-TNT	from Monika Götz	this study
COX6A-TNT	pCMV-TNT	amplified with Cox6a-f/Cox6a-r_KpnI from Cox6a pGem-4Z (EcoRI/KpnI)	this study
NDUFS1-1	pLVTHM	inserted: annealed NDUFS1-1f and NDUFS1-1r (ClaI/MluI)	Ott et al., 2012
CHCHD3-2	pLVTHM	inserted: annealed CHCHD3-2f and CHCHD3-2r (ClaI/MluI)	Ott et al., 2012
Core1-1	pLVTHM	inserted: annealed Core1-1f and Core1-1r (ClaI/MluI)	this study

CHCHD6-3	pLVTHM	inserted: annealed CHCHD6-3f and CHCHD6-3r (Clal/Mlul)	this study
DnaJC11-3	pLVTHM	inserted: annealed DnaJC11-3f and DnaJC11-3r (Clal/Mlul)	this study
pcDNA3-FLAGM		pcDNA3 expression vector for introducing an N-terminal FLAG-tag	Kozjak-Pavlovic et al., 2010
pcDNA3-MycM		pcDNA3 expression vector for introducing an N-terminal Myc-tag	Kozjak-Pavlovic et al., 2010
pcDNA3-FLAGS		pcDNA3 expression vector for introducing a C-terminal FLAG-tag	Kozjak-Pavlovic et al., 2010
pGEM [®] -4Z		expression vector with SP6 promoter	Promega P2161
PCMV-TNT [™]		expression vector with SP6 and T7 promoter	Promega L5620
pLVTHM		shRNA expression vector; Addgene plasmid 12247	Wiznerowicz and Trono, 2003
psPAX		viral packaging vector; Addgene plasmid 12260	Wiznerowicz and Trono, 2003
pCMV-VSV-G		viral envelope vector; Addgene plasmid 8454	(Stewart et al., 2003)

2.1.4 Oligonucleotides

Table 2.4 Oligonucleotides for PCR

Name	Sequence (5' → 3')	Comment
pLVTHM-f	ACAGGGGAGTGGCGCCCTGC	for screening clones and sequencing
pLVTHM-r	GTTAGCCAGAGAGCTCCCAGG	for screening clones and sequencing
Nla_PorB-f	TTTTTGAATTCGATGTTACCCTGTACGG	EcoI site
Nla_PorB-r	AAAAACTCGAGTTAGAATTTGTGGCGCA	XhoI site
Nsi_PorB-f	TTTTTGAATTCGACGTGACTCTGTACGG	EcoI site
Nsi_PorB-r	AAAAACTCGAGTTAGAATTTGTGACGCAG	XhoI site
Nci_Omp85-f	TTTTTGAATTCCTTACCATCCAAGACATC	EcoI site
Nci_Omp85-r	AAAAATCTAGATTAGAACGTCGTACCGAG	XbaI site
Omp85_Nci-1000r	GCCGGTAATGTTGATTC	for screening clones and sequencing
NDUFS1-f	TTTTTGGTACCATGTTAAGGATACCTGTA	KpnI site, with ATG ^{Start}
NDUFS1-r	AAAAAGGATCCTCAGCATATGGATGGTTC	BamHI site
NDUFS1_1000-r	CAATTGCTGCCACATCTTTGC	for sequencing NDUFS1
Omp85_1089-r	CAGACGCTCCTTGGAGCGTTGCAG	with 12 bp BamA overhang
BamA_1096-f	CTGCAACGCTCCAAGGAGCGTCTG	with 12 bp Omp85 overhang
BamA_1085-r	GGAGCGTTGCAGCAGATCGCTCCC	with 12 bp Omp85 overhang
Omp85_1080-f	GGGAGCGATCTGCTGCAACGCTCC	with 12bp BamA overhang

Omp85_1680-f	AACAAGCTTGACAGCGCGTTATGG	with 12 bp BamA overhang
Omp85_1679-r	GAAGTAACCACGGTTCGGTTTTGTTGCG	with 12 bp BamA overhang
BamA_1686-f	AACAAAACCGACCGTGGTTACTTC	with 12 bp Omp85 overhang
BamA_1685-r	CCATAACGCGCTGTCAAGCTTGTT	with 12 bp Omp85 overhang
PorB_468-f	CAAAACGGCGACTCTTACCATGCA	with 12 bp OmpC overhang
PorB_467-r	ACCGCCGACGCCTTCGCTGCGATT	with 12 bp OmpC overhang
OmpC_634-f	AATCGCAGCGAAGGCGTCGGCGGT	with 12 bp PorB overhang
OmpC_633-r	TGCATGGTAAGAGTCGCCGTTTTG	with 12 bp PorB overhang
Cox6a-f	AAAAAGAATTCATGGCGGTAGTT	EcoRI site, with ATG ^{Start}
Cox6a-r	TTTTTAAGCTTTTATTCATCTTC	HindIII site
CHCHD3-f	AAAAAGAATTCATGGGTGGGACC	EcoRI site, with ATG ^{Start}
CHCHD3-r	TTTTTAAGCTTTTATCCCTCCCTT	HindIII site
OmpC_901-f	GCATACCGCTTCGACTTCGGTCTG	with 12 bp PorB overhang
OmpC_900-r	CGTTACGTTGCC GAACTGGTACTG	with 12 bp PorB overhang
PorB_709-f	CAGTACCAGTTCGGCAACGTAACG	with 12 bp OmpC overhang
PorB_708-r	CAGACCGAAGTCGAAGCGGTATGC	with 12 bp OmpC overhang
SDHA-f	AAAAAGGTACCATGTCGGGGGTC	KpnI site, with ATG ^{Start}
SDHA-r	TTTTTAAGCTTTCACTAGGAGCG	HindIII site
SDHA_630-r	TCGCAGAGACCTCCATATA	for screening clones and sequencing
SDHA-650f	GGAGTATTTGCCTTGGATCT	for sequencing
Core1-f	AAAAAGGTACCATGGCGGCGTCC	KpnI site, with ATG ^{Start}
Core1-r	TTTTTAAGCTTCTAGAAGCGCAG	HindIII site
Core1_770-r	TATGTCCATGGGATGCCACC	for screening clones and sequencing
TTC19-iso2-f	TTTTTAAGCTTATGAAAGATGAG	HindIII site
TTC19-iso2-r	AAAAAGGATCCGAGCTTGACAGA	BamHI site
Omp85_12aa-f	GAAAAATTCGTAATCCAACGCTTC	with 12 bp PorB overhang
PorB_12aa-r	GAAGCGTTGGATTACGAATTTTTTC	with 12 bp Omp85 overhang
PorB_12aa-f	CCGGAAGACGAAGCGACTGTCCGG	with 12 bp Omp85 overhang
Omp85_12aa-r	GCCGACAGTCGCTTCGTCTCCGG	with 12 bp PorB overhang
OmpC-12aaPorB-f	GAAAAATTCGTAGATAACATCGTA	with 12 bp PorB overhang
PorB-12aaOmpC-r	TACGATGTTATCTACGAATTTTTTC	with 12 bp OmpC overhang
PorB-12aaOmpC-f	GGCATCAACACTGCGACTGTCCGG	with 12 bp OmpC overhang
OmpC-12aaPorB-r	GCCGACAGTCGAGTGTGATGCC	with 12 bp PorB overhang
Cox6a-r_Kpn	TTTTTGGTACCTTATTCATCTTC	KpnI site
Omp85-R783E-f	GAAATCCAAGAATTCCAATTC	
Omp85-R783E-r	GAATTGGAATTCTTGGATTTTC	
Omp85-Q787G-f	TTCCAATTCGGACTCGGCACG	
Omp85-Q787G-r	CGTGCCGAGTCCGAATTGGAA	
Omp85-T790K-f	CAACTCGGCAAGACGTTCTAA	
Omp85-T790K-r	TTAGAACGTCTTGCCGAGTTG	
Omp85-Q787N-r	AAAAATCTAGATTAGAACGTGCGGAGGTTGA	XbaI site
	ATTG	

Omp85-Q787E-r	AAAAATCTAGATTAGAACGTCGTGCCGAGTTCGA ATTG	Xbal site
Omp85-6aa-r	AAAAATCTAGATTAGAATTGGAAGCG	Xbal site
Omp85-5aa-r	AAAAATCTAGATTATTGGAATTGGAA	Xbal site
Omp85-4aa-r	AAAAATCTAGATTAGAGTTGGAATTG	Xbal site
Omp85-3aa-r	AAAAATCTAGATTAGCCGAGTTGGAA	Xbal site
Omp85-2aa-r	AAAAATCTAGATTACGTGCCGAGTTG	Xbal site
Omp85-1aa-r	AAAAATCTAGATTACGTCGTGCCGAG	Xbal site
T7	TAATACGACTCACTATAGGG	binds to T7 promoter region
SP6	ATTTAGGTGACACTATAGAA	binds to SP6 promoter region

Table 2.5 Oligonucleotides for shRNAs

Name	Sequence (5'→3')
NDUFS1-1f	CGCGTCCCCGCATGCAGATCCCTCGATTCTTTCAAGAGAAGAATCGAGGGATCTGCATGCTTTT TGAAAT
NDUFS1-1r	CGATTTCCAAAAGCATGCAGATCCCTCGATTCTTCTCTTGAAGAATCGAGGGATCTGCATGC GGGA
CHCHD3-2f	CGCGTCCCCTATCAGAAAGCTGCTGAAGAGGTGGAAGCTTCAAGAGAGCTTCCACCTCTTCAG CAGCTTTCTGATATTTTTGGAAAT
CHCHD3-2r	CGATTTCCAAAATATCAGAAAGCTGCTGAAGAGGTGGAAGCTCTTGAAGCTTCCACCTCTT CAGCAGCTTTCTGATAGGGGA
Core1-1f	CGCGTCCCCGGTCTTTAACTACCTGCATGCTTCAAGAGAGCATGCAGGTAGTTAAAGACCTTTT TGAAAT
Core1-1r	CGATTTCCAAAAGGTCTTTAACTACCTGCATGCTCTTGAAGCATGCAGGTAGTTAAAGACC GGGA
CHCHD6-3f	CGCGTCCCCGGGTGTCAAGAGGTATGAACATTCAAGAGATGTTTCATACCTCTTGACACCTTTT TGAAAT
CHCHD6-3r	CGATTTCCAAAAGGGTGTCAAGAGGTATGAACATCTTGAATGTTTCATACCTCTTGACACCC GGGA
DnaJC11-3f	CGCGTCCCCGCACCGTCTGATCATCAAACCTTCAAGAGAGGTTTGATGATCAGACGGTGCTTTT TGAAAT
DnaJC11-3r	CGATTTCCAAAAGCACCGTCTGATCATCAAACCTCTTGAAGGTTTGATGATCAGACGGTGC GGGA

2.1.5 Antibodies

Table 2.6 Primary antibodies (WB: western blot; IF: immunofluorescence staining)

Antibody	Origin	Dilution	Company
6xHis	Mouse monoclonal	1:1000 WB	GeneTex GTX18184
CHCHD3	Rabbit polyclonal	1:500 WB	Abcam ab98975
CHCHD6	Rabbit polyclonal	1:200 WB	Abcam ab111502
c-myc	Rabbit	1:500 WB	Gramsch laboratories, CM-100
COX1	Mouse monoclonal	1:1000 WB	Molecular Probes (Invitrogen) 459600
COX2	Rabbit monoclonal	1:500 WB	GeneTex GTX62145
COX5A	Rabbit polyclonal	1:500 WB	Novus Biologicals NBPI-32550
DnaJC11	Mouse polyclonal	1:200 WB	Abnova (Biozol) H00055735-B01P
FLAG	Rabbit	1:500 WB, 1:300 IF	SIGMA F7425
Hsp60	Mouse polyclonal	1:2000 WB,	Enzo life sciences ADI-SPA-806
ICDH	Rabbit polyclonal	1:500 WB	Biogenesis 0200-0498
Metaxin 1	Rabbit polyclonal	1:100 WB	Raised against the full length protein with a N-terminal 6xHis tag, Gramsch laboratories
Mitofilin	Rabbit polyclonal	1:2000 WB	Abcam ab48139
NDUFA9	Mouse monoclonal	1:1000 WB	Molecular Probes (Invitrogen) 459100
NDUFS1	Rabbit polyclonal	1:500 WB	Santa Cruz sc-99232
NDUFS2	Rabbit polyclonal	WB 1:1000	GeneTex GTX114924
Sam50	Rabbit polyclonal	1:100 WB	Raised against the full length protein with a N-terminal 6xHis tag; Gramsch laboratories
SDHA	Mouse monoclonal	1:200 - 1:500 WB	Molecular Probes (Invitrogen) 459200
Tim23	Mouse monoclonal	1:1000 WB	Transduction Laboratories 611222
Tom20	Mouse monoclonal	1:1000 WB, 1:500 IF	BD Transduction Laboratories 612278
Tom40	Rabbit polyclonal	1:200 WB	Santa Cruz sc-11414
TTC19	Rabbit	1:250 WB	SIGMA HPA023010
UQCRC1 (Core1)	Mouse monoclonal	1:1000 WB	Invitrogen (Molecular Probes) 459140
UQCRC1 (RISP)	Rabbit polyclonal	1:500 WB	GeneTex102150
UQCRC1 (subunit 8)	Rabbit polyclonal	1:500 WB	Ab136679

Table 2.7 Secondary antibodies

Antibody	Origin	Dilution	Company
ECLTM anti-rabbit IgG HRP-linked	Goat	1:3000	Santa Cruz sc2004
ECLTM anti-mouse IgG HRP-linked	Goat	1:3000	Santa Cruz sc2005
Anti-rabbit IgG Cy2-linked	Goat	1:150	Dianova
Anti-rabbit IgG Cy5-linked	Goat	1:150	Dianova

2.1.6 Kits

Table 2.8 Kits

Kit	Manufacturer
GeneJet™ Gel Extraction Kit	Fermentas
Wizard® SV Gel and PCR Clean-Up System	Promega
PureYield™ Plasmid Midiprep System	Promega
AxyPrep™ Plasmid Miniprep Kit	Axygen
RNeasy® Mini Kit	Qiagen
RevertAid First Strand cDNA Synthesis Kit	Fermentas
TNT® T7 Quick Coupled Transcription/Translation System	Promega
TNT® SP6 Quick Coupled Transcription/Translation System	Promega

2.1.7 Markers

DNA and protein markers used in this work were GeneRuler™ 1kb DNA ladder (Fermentas), Prestained protein weight marker (Fermentas), PageRuler™ Prestained Protein Ladder (Fermentas) and HMW native marker (GE Healthcare).

2.1.8 Buffers, solutions and media

Table 2.9 Media and solutions for cell culture

Medium/Chemical	Supplier
RPMI 1640	GIBCO
DMEM	Sigma Aldrich
Opti-MEM® I Reduced Serum Medium	GIBCO
DPBS	GIBCO or Sigma Aldrich
TrypLE™ Express	GIBCO
Fetal calf serum (FCS)	PAA
Penicillin/Streptomycin	Sigma Aldrich

Table 2.10 Bacterial culture media and neisserial DNA isolation buffer

Medium/Buffer	Ingredients
LB Medium	10 g tryptone, 5 g yeast extract, 10 g NaCl (ad 1l dH ₂ O)
LB Agar	11 g tryptone, 5 g yeast extract, 10 g NaCl, 15 g agar (ad 1l dH ₂ O)
Vitamin Mix Solution I	200 g D(+)-glucose, 20 g L-glutamine, 52 g L-cysteine-hydrochloride-monohydrate, 0.2 g cocarboxylase, 0.04 g iron-(III)-nitrate-nonahydrate, 0.006 g thiamine hydrochloride (vitamin B1), 0.026 g 4-aminobenzoic acid, 0.5 g NAD, 0.02 g vitamin B12; add 1 l dH ₂ O
Vitamin Mix Solution II	2.2 g L-cystine, 2 g adenine-hemisulfate, 0.06 g guanine-hydrochloride, 0.3 g L-arginine-monohydrochloride, 1 g uracil, add 600 ml dH ₂ O, 30 ml 32 % HCl
Vitamin Mix	combine Vitamin Mix Solution I and II (ad 2 l dH ₂ O)
GC Agar	36.23 g GC Agar base (Oxoid) in 1 l ddH ₂ O; after autoclaving add 1 % vitamin mix
Stocking solution	50 % glycerol, 2.9 % NaCl
Proteose Peptone Medium (PPM)	15 g proteose peptone, 5 g NaCl, 0.5 g soluble starch, 1 g KH ₂ PO ₄ , 4 g KH ₂ PO ₄ . Adjust to pH 7.2. Sterilize by sterile filtration
GTE buffer	50 mM glucose, 25 mM Tris/HCl pH 8.0, 10 mM EDTA

Table 2.11 Buffers for agarose gel electrophoresis, SDS-PAGE, BN-PAGE and western blotting

Buffer	Ingredients
1 x TAE buffer	2 M Tris, 0.05 M EDTA, 1 M acetic acid (pH 8.5)
2 x Laemmli buffer	4 % SDS, 20 % glycerol, 120 mM Tris pH 6.8, 0.4 - 2 % β-mercaptoethanol, 0.02 bromphenolblue
14 % SDS gel solution	7.9 ml Acrylamid/bis (30/0.8), 3.5 ml 1.875 M Tris pH 8.8, 0.1 % (w/v) SDS, 6.3 ml dH ₂ O, 100 μl 10 % (w/v) APS, 10 μl TEMED
SDS stacking gel solution	0.83 ml Acrylamid/bis (30/0.8), 0.5 ml 0.8 M Tris pH 6.8, 50 μl 10 % (w/v) SDS, 3.55 ml dH ₂ O, 50 μl 10 % w/v APS, 10 μl TEMED
SDS running buffer	25 mM Tris, 0.191 M glycine, 1 % (w/v) SDS
Coomassie staining solution	40 % ethanol, 7 % acetic acid, 0.2 % (w/v) coomassie R-250
Coomassie destaining solution	30 % ethanol, 10 % acetic acid
BN Acrylamide	49.5 % acrylamide (96 g), 3 % bis-acrylamide (3 g), ad 200 ml dH ₂ O
1 x digitonin buffer	20 mM Tris/HCl pH 7.4, 0.1 mM EDTA, 50 mM NaCl, 10 % glycerol
3 x BN gel buffer	200 mM ζ-amino n-caproic acid, 150 mM Bis-Tris pH 7.0
4 % BN gel solution	12 ml 3 x BN gel buffer, 2.92 ml BN acrylamide, 152 μl 10 % APS, 15 μl TEMED, 20.9 ml dH ₂ O
10 % BN gel solution	12 ml 3 x BN gel buffer, 7.28 ml BN acrylamide, 7.2 ml glycerol, 120 μl 10 % APS, 12 μl TEMED, 9.39 ml dH ₂ O

13 % BN gel solution	12 ml 3 x BN gel buffer, 9.4 ml BN acrylamide, 7.2 ml glycerol, 120 µl 10 % APS, 12 µl TEMED, 7.27 ml dH ₂ O
BN stacking gel solution	10 ml 3 x BN gel buffer, 2.4 ml BN Acrylamide, 120 µl 10 % APS, 12 µl TEMED, 17.5 ml dH ₂ O
1 X BN cathode buffer	50 mM Tricin, 15 mM Bis-Tris pH 7.0, +/- 0.02 % (w/v) Commassie blue G-250
1 X BN anode buffer	50 mM Bis-Tris pH 7.0
10 x BN loading dye	5 % (w/v) Coomassie blue G-250, 500 mM ζ-amino n-caproic acid, 100 mM Bis-Tris pH 7.0
3 x Tris-Tricine gel buffer	0.3 % (w/v) SDS, 3 M Tris pH 8.45
16.5 % Tris-Tricine gel solution	10 ml BN Acrylamide, 10 ml 3 x Tris-Tricine gel buffer, 4 ml glycerol, 6 ml dH ₂ O, 150 µl 10 % APS, 15 µl TEMED
Tris-Tricine stacking gel solution	2.5 ml BN Acrylamide, 7.5 ml 3 x Tris-Tricine gel buffer, 20 ml dH ₂ O, 250 µl 10 % APS, 25 µl TEMED
Tris-Tricine cathode buffer	1 M Tris, 1 M Tricine, 1 % (w/v) SDS
Tris-Tricine anode buffer	2 M Tris pH 8.9
1 x transfer buffer	2 mM Tris, 15 mM Glycin, 0.02 % SDS, 20 % methanol
1 x TBS buffer	0.15 M NaCl, 20 mM Tris/HCl pH 7.5
ECL solution 1	2.5 mM Luminol, 0.4 mM p-coumaric acid
ECL solution 2	100 mM Tris HCl pH 8.5, 0.02 % H ₂ O ₂

Table 2.12 Buffers for transfection of cells, immunofluorescence staining and transmission electron microscopy (TEM)

Buffer	Ingredients
2 x HBS	50 mM Hepes pH 7.00, 280 mM NaCl, 1.5 mM Na ₂ HPO ₄
Blocking solution	10 % goat serum, 0.2 % Triton X-100 in 1 x PBS
Antibody dilution solution	3 % goat serum, 0.05 % Tween 20 in 1 x PBS
Mowiol	35 g glycerol, 12 g Mowiol, 30 ml dH ₂ O, 60 ml 0.2 M Tris/HCl pH 8.5
TEM fixing solution	2.5 % glutaraldehyde, 50 mM cacodylate pH 7.2, 50 mM KCl, 2.5 mM MgCl ₂

Table 2.13 Buffers for experiments with isolated mitochondria

Buffer	Ingredients
1 x PBS	137 mM NaCl, 2.7 mM KCl, 8 mM Na ₂ HPO ₄ , 1.5 mM KH ₂ PO ₄
Buffer A	Buffer B containing 2 mg/ml BSA
Buffer B	20 mM Hepes pH 7.6, 220 mM mannitol, 70 mM sucrose, 1 mM EDTA, 0.5 mM PMSF
SET buffer	250 mM sucrose, 10 mM Tris/HCl pH 7.6, 1 mM EDTA
ET buffer	10 mM Tris/HCl pH 7.6, 1 mM EDTA
BSA import buffer	250 mM sucrose, 20 mM Hepes pH 7.4, 80 mM KCl, 5 mM MgCl ₂ , 3 % BSA (w/v), 2 mM KH ₂ PO ₄ , 5 mM methionine, 2 mM ATP, 10 mM Na-succinate

KAc import buffer	250 mM sucrose, 5 mM Mg-acetate, 80 mM K-acetate, 20 mM Hepes pH 7.4, 10 mM Na-succinate, 2 mM ATP, 1 mM DTT
Lysis buffer	10 mM Tris/HCl pH 7.4, 2 mM EDTA, 50 mM NaCl, 1 mM PMSF, 0.5 - 1 % digitonin

Table 2.14 Annealing buffer for shRNA oligonucleotides

Buffer	Ingredients
Annealing buffer	100 mM K-acetate, 30 mM Hepes KOH pH 7.4, 2 mM Mg-acetate

2.1.9 Enzymes

Enzymes used in this work were iProof™ High-Fidelity DNA Polymerase (BIO-RAD), MolTaq DNA polymerase (Molzym), T4 DNA ligase (Fermentas) and FastAP Thermosensitive Alkaline Phosphatase (Thermo Scientific). Additionally, all restriction enzymes were purchased from Fermentas.

2.1.10 Chemicals

Table 2.15 Inhibitors, inductors and fine chemicals

Chemical	Supplier
Acrylamide, 2 x cryst.	Roth
Albumin Fraktion V (BSA)	Roth
Ammonium persulfate (APS)	Merck
Adenosine triphosphate (ATP)	Roth
Coomassie G250	Roth
Coomassie R250	Roth
Digitonin	Sigma
Dithiothreitol	Roth
Doxycycline (Dox)	Sigma
Lipofectamine® 2000	Invitrogen
MitoTracker® Orange	Invitrogen
N,N'-Methylene bisacrylamide	Roth
Na-succinate	Fluka Analytical
Phenylmethylsulfonyl fluoride (PMSF)	Roth
Polyethylenimine (PEI)	Sigma
Protein A Sepharose™ CL-4B	GE Healthcare
Proteinase K	Roth
Restore™ Plus Western Blot Stripping buffer	Thermo Scientific
RotiphoreseR acrylamide	Roth
Tetramethylethylenediamine (TEMED)	Fluka Analytical

All other chemicals were obtained from Roth, Sigma Aldrich, Serva or Merck Chemicals if not stated otherwise.

2.1.11 Technical equipment

Table 2.16

Equipment	Manufacturer
OPTIMA Max-XP ultracentrifuge	Beckham Coulter
Avanti™ J-25T centrifuge	Beckham Coulter
Chemiluminescence camera system	Intas
Cold centrifuge 5417R	Eppendorf
Douncer RW16basic	IKA Labortechnik
Electric balance ABS 80-4	Kern
Electric balance EW 1500-2M	Kern
Hera Cell 240i incubator	Thermo
Hera Safe sterile hood	Thermo
Hoefer SE 600 Chroma™ gel system	Hoefer
Laboratory vacuum pump	Welch
Labtherm ET1311	Liebisch
Magnetic stirrer RMO	Gerhardt
Megafuge 1.0R	Heraeus
Mini Rocker-Shaker MR-1	Biosan
NanoDrop 1000 spectrophotometer	Peqlab Biotechnology
PerfectBlue™ Semi-Dry Elektrobloetter	Peqlab Biotechnology
PerfectBlue™ Vertical Double Gel Systems	Peqlab Biotechnology
Peristaltic pump P-1	Pharmacia Biotech
pH electrode SenTix	WTW
Scanjet G4010	HP
Spectrophotometer Ultrospec 3100 pro	Amersham Bioscience
Systec VX-150 autoclave	Systec GmbH
TCS SPE confocal microscope	Leica
Thermal cycler 2720	Applied Biosystems
Thermal cycler GS1	G-STORM
Thermo mixer comfort	Eppendorf
Vortex shaker Reax 2000	Heidolph
XCell SureLock™ Mini-Cell electrophoresis system	Invitrogen

2.1.12 Software

MS Office2010, Adobe Photoshop, Adobe Illustrator, NCBI blast, ClustalW2, NEBcutter V2.0, ExPASy – Translate Tool, LAS AF confocal microscopy software, ChemoStar Imager software (Intas), Typhoon Scanner Control software, ImageQuant, NanoDrop ND-1000.

2.2 Methods

2.2.1 DNA methods

Polymerase chain reaction (PCR)

PCR was used for amplifying DNA fragments, either to clone them into a vector or to screen for successfully transformed bacterial colonies.

For cloning, iProofTM polymerase (BIO-RAD) was used with the following reaction mix:

x µg	Template DNA
0.5 µl	Primer-f (100 mM)
0.5 µl	Primer-r (100 mM)
0.5 µl	dNTPs (100 mM)
2 µl	MgCl ₂
10 µl	5 x iProof TM buffer
0.5 µl	iProof TM polymerase
add 50 µl	dH ₂ O

After an initial denaturation at 98°C for 30s, 30 cycles of 10 s denaturation at 98°C, 10 s annealing at 50 – 60°C (depending on the melting temperature of the oligonucleotide primers), and elongation (30 s per 1 kb) at 72°C followed. After a final elongation step at 72°C for 5 min, the PCR reaction was gradually cooled down to 4°C. To assess the success of the PCR, 2 µl of the reaction were mixed with 2 µl of 6x loading dye (Fermentas) and 8 µl of dH₂O, and separated on a 1.5 % agarose gel containing ethidium bromide (Roth) or Intas HD Green (Intas). DNA bands were visualized using UV light.

In order to screen for *E. coli* DH5α clones transformed with the desired plasmid, MolTaq polymerase (Molzym) was used. For that purpose, bacterial material was resuspended in 50 µl of dH₂O, incubated 10 min at 95°C and then centrifuged for 2 min at 10000 g. 5 µl of the supernatant were used as a template in the following reaction mix:

5 µl	Template
0.5 µl	Primer-f (100 mM)
0.5 µl	Primer-r (100 mM)
0.5 µl	dNTPs (100 mM)
1 µl	Enhancer
5 µl	10 x Buffer
0.25 µl	MolTaq Polymerase
add 50 µl	dH ₂ O

Initial denaturation was performed at 94°C for 5 min, followed by 30 cycles at 94°C for 30 s, at 50°C for 30 s, and at 72°C depending on the size of the amplified DNA fragment (45 s per 1 kb). After a final elongation step for 5 min at 72°C, the PCR was gradually cooled down to 4°C.

DNA purification

To remove salts, primers and PCR buffers after PCR amplification and DNA restriction, the GeneJet™ Gel Extraction Kit (Fermentas) was used.

Gel extraction

In order to ensure that only the desired DNA fragment was cloned into the vector after PCR amplification, the PCR sample was separated on a 1.5 % agarose gel. The respective band was excised under UV light and the DNA was extracted using the Wizard® SV Gel and PCR Clean-Up System (Promega).

Restriction of insert and vector DNA

Amplified DNA and vector were restricted with suitable restriction enzymes (Fermentas). If the two restriction enzymes did not share the same optimal buffer, one enzyme after the other was applied. The reaction mix was purified after each restriction using the GeneJet™ Gel Extraction Kit (Fermentas). The vector was dephosphorylated after restriction using FastAP Thermosensitive Alkaline Phosphatase (Fermentas) (exception: the pLVTHM vector, which was not dephosphorylated).

Ligation of a DNA fragment into the target vector

T4 DNA ligase (Fermentas) was used to ligate the insert and the vector. The DNA fragments were added in an insert:vector ratio of 3:1 or 4:1 in a total volume of 10 – 15 µl, and incubated overnight at 16°C.

DNA precipitation

To precipitate DNA, 0.1 volumes of NaAc (pH 4.8) and 2.5 volumes of 96 % EtOH were added, and the sample was centrifuged for 30 min at 14000 rpm and 4°C. The precipitated DNA was washed with 70 % EtOH (15 min, 14000 rpm, 4°C) and subsequently resuspended in dH₂O.

2.2.2 Gel electrophoresis and western blotting

Agarose gel electrophoresis

DNA samples were mixed with 6 x loading dye (Fermentas) and dH₂O, and separated on a 1.5 % agarose gel (in TAE buffer) by applying 160 V for 35 – 40 min.

SDS-PAGE

All samples subjected to SDS-PAGE were resuspended in 2 x Laemmli buffer, shaken for 5 min and incubated at 95°C for 5 min to denature the proteins (exception: protein which were precipitated by TCA precipitation were shaken at 65°C and 650 rpm for 15 min). Proteins were separated by electrophoresis either on 14 % SDS gels (200V, 25mA), on 4 -12 % NuPAGE® Novex® 4-12% Bis-Tris Gels (200V, 125mA), or on Tris-Tricine gels (80V).

BN-PAGE

BN-PAGE was utilized to separate protein complexes under non-denaturizing conditions. To prepare the samples for electrophoresis, 50 – 75 µg of mitochondria were resuspended in 45 – 50 µl of 1 % digitonin buffer. The samples were incubated for 15 min on ice and subsequently centrifuged for 10 min at 14000 rpm and 4°C. 10 x BN loading dye was added to a final concentration of 10 % and the samples were loaded on 4 – 13 % or 4 – 10 % BN gels. 100 V was applied until the samples entered into the stacking gel, after which the voltage was increased to 200 V (NuPAGE system) or 600 V (Hoeffer gel system).

Western blotting and immunodetection

Gels were blotted on PVDF membranes using a semi-dry blotting chamber for 90 – 120 min (1 mA per cm²). The membrane was then stained with Coomassie staining solution and subsequently destained with Coomassie detaining solution to allow assessment of protein transfer and sample loading. Subsequently, the membrane was completely destained with methanol and blocked for 1 h in 5 % milk in 1 x TBS. The membrane was incubated in the diluted primary antibody (usually in 1 x TBS) overnight at 4°C, washed twice for 10 min in 1 x TBS, and incubated in the diluted secondary antibody (1:3000 in 5% milk in 1 x TBS) for at least 1 h at room temperature. The membrane was then washed three times for 5 min in 1 x TBS, and the ECL solutions 1 and 2 were added in a 1:1 ratio. The signal was subsequently detected using an IntasImager digital system.

2.2.3 Bacterial culture methods**Culturing of *E. coli* DH5α**

E. coli were cultured overnight on LB agar plates at 37°C and 5% CO₂ or in LB medium at 37°C and 190 rpm. If the bacteria carried an antibiotic resistance, the respective antibiotic was added to the medium or antibiotic-supplemented LB agar plates were used.

Culturing of *Neisseria*

Neisseria sp. were cultured overnight on GC agar plates at 37°C and 5 % CO₂.

Production of chemo-competent *E. coli* DH5 α

100 ml of LB medium were inoculated with an *E. coli* overnight culture, and bacteria were grown to an OD₆₀₀ = 0.6. Bacteria were then incubated for 15 min on ice and subsequently centrifuged for 10 min at 4000 rpm and 4°C. The pellet was resuspended in 20 ml of 0.1M CaCl₂, and again centrifuged (10 min, 4000 rpm, 4°C). Then, the pellet was resuspended in 10 ml of 0.1M CaCl₂/20 % glycerol and stored at -80°C in aliquots of 200 – 300 μ l.

Transformation of chemo-competent *E. coli* DH5 α

An aliquot of chemo-competent *E. coli* DH5 α was thawed on ice and 100 μ l were added to one ligation sample. The sample was incubated for 30 min on ice, then heat-shocked for 90 s at 42°C, and again incubated 2 min on ice. 1 ml of LB medium was added and the sample was incubated for 30 - 60 min at 37°C and 850 rpm. The sample was then centrifuged for 3 min at 4000 rpm and the supernatant was removed. The pellet was resuspended in 100 μ l of LB medium and plated on antibiotic-supplemented LB agar plates.

Bacterial stocks

500 – 750 μ l of an *E. coli* overnight culture were mixed with the same volume of stocking medium and stored at -80°C.

Isolation of neisserial DNA

Neisserial colonies were collected with cotton swabs from a GC agar plate and resuspended in PPM medium. After 1 min centrifugation at maximum speed, the pellet was resuspended in GTE buffer. RNAseA to a final concentration of 0.2 mg/ml and subsequently SDS to a final concentration of 0.1 % was added, and the sample was mixed. Then the sample was incubated at 42°C for at least 10 min until it became clear. Subsequently, one volume of Roti®Phenol/Chloroform/Isoamylalcohol was added and the sample was thoroughly mixed. The sample was then centrifuged for 5 min at maximum speed and the upper phase was transferred into a new Eppendorf Cup. The same volume of Roti®Phenol/Chloroform/Isoamylalcohol was added and the sample was again centrifuged for 5 min at maximum speed. This step was repeated twice, and subsequently, the DNA was precipitated. For this, 0.1 volume of 3 M NaAc and 2 volumes of 100 % EtOH were added, and the sample was mixed. Then it was centrifuged for 5 min at maximum speed, and the pellet was washed with ice-cold 70 % EtOH. The supernatant was removed, and the pellet was air dried and then dissolved in dH₂O.

Isolation of plasmids from bacterial liquid cultures

Plasmids were isolated from bacterial overnight cultures using the PureYield™ Plasmid Midiprep System (Promega) (yield: 100 – 200 µg of plasmid DNA from a 50 ml *E. coli* culture) or the AxyPrep™ Plasmid Miniprep Kit (Axygen) (yield: 10 – 20 µg of plasmid DNA from 2 ml of an *E. coli* culture).

2.2.4 Cloning of DNA fragments into vectors

As templates for cloning, either plasmid DNA, chromosomal DNA, or cDNA obtained by reverse transcription of cellular RNA were used. Template DNA was amplified using PCR. To clone chimeric constructs, each part of the construct was amplified from its respective template plasmid using primers f1 and r1 and primers f2 and r2 (Figure 2-1). Primers r1 and f2 had 12 nucleotides attached of the sequence to which the respective fragment should be fused, so that both fragments overlapped 24 nucleotides in sequence after amplification. The two fragments were either purified using a PCR purification kit or by extraction from a 1.5 % agarose gel, and fused by a second PCR using primers f1 and r2.

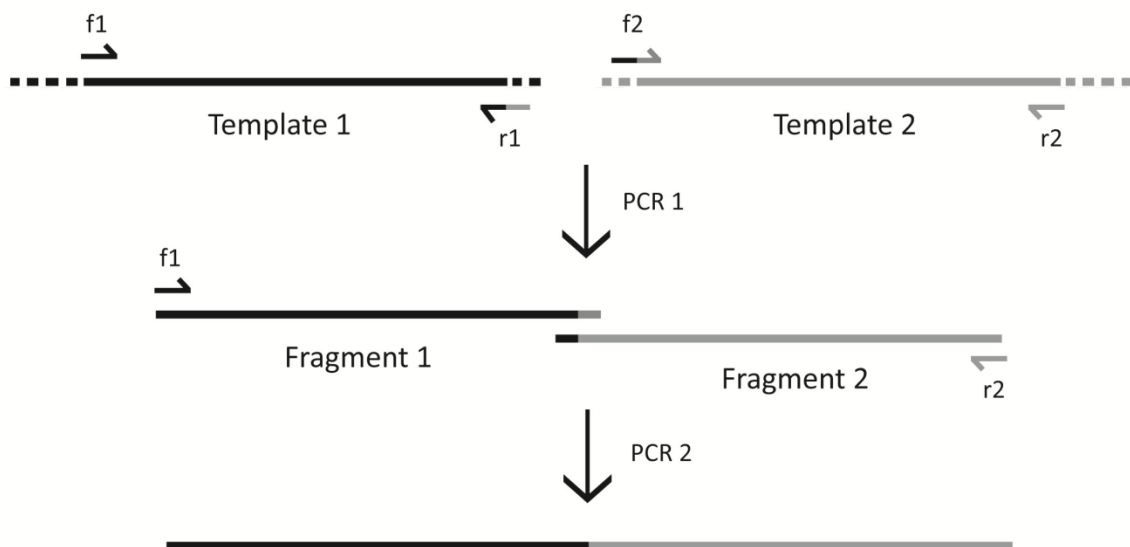


Figure 2-1 Fusing two DNA fragments by overlapping PCR. DNA fragments 1 and 2 were amplified in a first PCR step from templates 1 and 2 with primers f1 and r1 and primers f2 and r2, respectively. Primers r1 and f2 had 12 nucleotides attached of the sequence to which the fragment was to be fused. In a second PCR step, fragments 1 and 2 were fused using primers f1 and r2.

Amplified DNA fragments and their target vector were restricted with the respective restriction enzymes (Table 2.3) and ligated overnight at 16°C. Chemo-competent *E. coli* DH5α were transformed with the ligation mix and bacterial clones were screened by PCR (MolTaq) for clones carrying the plasmid. The plasmid was then isolated and the inserted DNA fragment was verified by sequencing (Seqlab).

2.2.5 Cell culture methods

Culturing of cells

Cells were cultured in 75 cm² culture flasks at 37°C and 5 % CO₂, and passaged every two to three days. For passaging, the cells were washed with DPBS, 1 ml Trypsin was added, and the cells were incubated at 37°C until they detached. Subsequently, fresh cell culture medium was added and a part of the cells was transferred to a fresh 75 cm² culture flask for further culturing or seeded in multi-well plates for experiments. If bigger amounts of cells were needed, they were grown in 175 cm² flasks and for the isolation of mitochondria cells were seeded in 145 cm² cell culture dishes.

Preparation of cell culture stocks

To obtain cell stocks, cells from a confluent 75 cm² culture flask were detached by the addition of 1 ml Trypsin, after which 4 ml of the cell culture medium was added for trypsin inactivation. The cells were transferred to a 15 ml falcon tube and pelleted (800 g, 5 min). In the meantime, 400 µl FCS and 100 µl DMSO were added to 2 – 3 cell culture cryo tubes. The pelleted cells were resuspended in 1 - 1.5 ml FCS, and 500 µl were transferred to each cryo tube. The cryo tubes were placed in a styropor box at -80°C, so that the stocks were cooled down gradually. For longer storage, the tubes were transferred to a liquid nitrogen tank and stored at -180°C.

Isolation of cellular RNA and generation of cDNA

Cellular RNA was isolated using the RNeasy® Mini Kit (Qiagen). cDNA was obtained from the RNA using the RevertAid First Strand cDNA Synthesis Kit (Fermentas).

2.2.6 Transfection of cells

Lipofectamin transfection and PEI transfection were applied to transfect HeLa cells seeded in 12 well plates. If the transfected cells were subsequently prepared for confocal microscopy, they were seeded on cover slips one day before transfection. Calcium phosphate transfection was used to transfect HEK 293T cells grown in 145 cm² dishes.

Lipofectamin transfection

Lipofectamin transfection was performed according to the manufacturer's protocol. For transfection of HeLa cells grown in one well of a 12 well plate, 0.75 –1 µg DNA were mixed with 50 µl of OPTIMEM medium and 1.5 µl of Lipofectamin were mixed with 50 µl of OPTIMEM medium, and both samples were incubated for 5 min at room temperature. Subsequently, the samples were mixed together and incubated for 20 min at room temperature. In the meantime, the cells were washed with DPBS and 400 µl of OPTI-MEM® medium were added. After the 20 min incubation, the transfection mix was

added to the well and the plate was incubated at 37°C. After 4 – 6 h, the medium was exchanged with fresh RPMI medium, and 36 – 48 h post transfection, cells were stained with MitoTracker® Orange and fixed with 3 % PFA, or resuspended in 2 x Laemmli buffer.

Polyethylenimine (PEI) transfection

PEI was solubilized in dH₂O to a concentration of 1 mg/ml. For transfection of HeLa cells grown in one well of a 12 well plate, 8 µl of PEI were mixed with 2 µg of plasmid DNA in 100 µl of OPTI-MEM® medium, and incubated 10 min at room temperature. In the meantime, old medium was removed from the well and 400 µl of fresh RPMI medium was added. After the 10 min incubation, the DNA-PEI mixture was added to the well and the plate was incubated at 37°C. After 4 – 6 h, medium was exchanged with fresh RPMI medium, and 36 – 48 h post transfection, cells were stained with MitoTracker® Orange and fixed with 3 % PFA, or resuspended in 2 x Laemmli buffer.

CaPhosphate transfection

One day before transfection, 293T cells were seeded on a 145cm² plate in 20 ml of DMEM medium in such a way that they reached about 70 % confluency on the day of transfection. For transfecting the cells, 25 – 40 µg of plasmid DNA were mixed with 1.7 ml of dH₂O and 200 µl of M CaCl₂. 2 ml of 2 x HBS were added dropwise while bubbling using a pipet boy with a Pasteur pipette. The mixture was incubated 15 – 20 min at room temperature. In the meantime, 4 ml of medium of the 145 cm² plate was removed and chloroquine was added to a final concentration of 25 µM. After incubation, the mixture was added dropwise to the plate while gently shaking it.

2.2.7 Trichloroacetic acid (TCA) precipitation

In order to precipitate proteins, TCA was added to a final concentration of 14.4 % and sodiumdeoxycholate was added to a final concentration of 0.0125 %, and the sample was incubated 30 min on ice. Then, it was centrifuged for 30 min at 14000 rpm and 4°C, washed with ice-cold acetone, and again centrifuged (10 min, 14000 rpm, 4°C). The pellet was resuspended in an appropriate amount of 2 x Laemmli buffer and shaken for 15 min at 65°C and 800 rpm.

2.2.8 MitoTracker® Orange staining and immunofluorescence staining

One vial of lyophilized MitoTracker® Orange (Invitrogen) was resuspended in DMSO to a final concentration of 1 mM. For Mitotracker staining, MitoTracker® Orange was added to a final concentration of 150 – 200 nM to fresh RPMI medium. Cells grown in 12 well plate on coverslips were washed once with sterile DPBS and the RPMI medium supplemented with MitoTracker® Orange

was added. The plate was incubated for 30 min at 37°C and 5 % CO₂, and subsequently, the cells were washed twice with PBS and 3 % PFA was added to fix the cells. After 1 h incubation at room temperature in the dark, the cells were washed three times with PBS. Cells were then kept in PBS at 4°C until further treatment.

For immunofluorescence staining, PBS was removed and blocking solution was added, followed by 30 min incubation. As in all following incubation steps, cells were kept in the dark at room temperature. Then, cells were washed once with PBS and primary antibody diluted in antibody dilution solution was added. After 1 h incubation, cells were washed twice with PBS and incubated in blocking solution for 10 min. Subsequently, cells were again washed once with PBS and secondary antibody diluted in antibody dilution solution was added. After 1 h incubation, cells were washed twice with PBS and once with dH₂O, and the cover slips were mounted on microscope slides with Mowiol. Samples were analyzed using a TCS SPE confocal microscope (Leica).

2.2.9 Transmission electron microscopy (TEM)

Cells were grown on coverslips in a 12 well plate and, if required, knockdown was induced by addition of 1 µg/ml Dox for 7 d. Cells were washed with PBS and fixed with TEM fixing solution for 1 h at room temperature. Then, cacodylate (pH7.2) was added and the samples were transferred to the electron microscopy department (group of Prof. Dr. Georg Krohne) for further preparation. There, the cells were fixed for 2 h at 4°C with 2 % OsO₄ buffered with 50 mM cacodylate (pH 7.2). They were subsequently washed with H₂O, and incubated overnight at 4°C with 0.5% uranyl acetate in H₂O. Then, the cells were dehydrated, embedded in Epon 812 and stained with uranyl acetate and lead citrate. The sections were analyzed with a Zeiss EM10 or EM900 electron microscope (Zeiss, Oberkochen, Germany).

2.2.10 Isolation of mitochondria and of the cytosolic fraction

145 cm² cell culture plates were washed with PBS and cells were collected using a cell scraper. Cells were pelleted (7 min, 800 g, 4°C) and the pellet was resuspended in 4 ml of Buffer A per plate. After 20 min incubation on ice, cells were homogenized with 20 strokes using a drill-fitted Dounce homogenizer. Cells were centrifuged for 5 min at 800 g and 4°C, and the supernatant was transferred to Eppendorf Cups. The crude mitochondrial fraction was pelleted (10 min, 10000 g, 4°C). If also isolating cytosolic proteins, the supernatant was preserved for further analysis. The pellet was resuspended in 1 ml of Buffer B and centrifuged for 10 min at 10000 g and 4°C. The supernatant was discarded and the pellet resuspended in an appropriate amount of Buffer B. To determine

mitochondrial protein concentration, 2 μ l of protein were resuspended in 100 μ l of 0.1 % SDS. Absorption at 280 nm and 310 nm was measured at the NanoDrop and mitochondrial protein concentration was calculated using the following formula (Clarke, 1976):

$$c(\text{protein}) = \frac{A_{280\text{nm}} - A_{310\text{nm}}}{1.05} \times \frac{100 \mu\text{l}}{2 \mu\text{l}} \mu\text{g}/\mu\text{l}$$

To isolate cytosolic proteins, the supernatant obtained after pelleting the crude mitochondrial fraction was centrifuged for 1 h at 100000 g and 4°C, and the supernatant was subjected to TCA precipitation.

2.2.11 Submitochondrial localization of mitochondrial proteins

Freshly isolated mitochondria were resuspended in SET buffer (two samples) and ET buffer (two samples) by pipetting up and down 20 times. The samples were incubated for 30 min on ice with pipetting 20 times up and down after 15 min. Subsequently, they were centrifuged for 5 min at 12000 g and 4°C. The supernatant was discarded and one SET buffer and one ET buffer sample were resuspended in 2 x Laemmli buffer. The two remaining samples were resuspended in SET buffer, and PK to a final concentration of 50 μ g/ml. After 15 min incubation on ice, PMSF to a final concentration of 2 mM was added, followed by 10 min incubation on ice. Then, the samples were centrifuged for 5 min at 12000 g and 4°C, and the pellet was washed with SET buffer containing 0.1 mM PMSF (5 min, 12000 g, 4°C). The supernatant was discarded and the pellet was resuspended in 2 x Laemmli buffer. Additionally, freshly isolated mitochondria were resuspended in 1 % Triton X-100 in digitonin buffer by pipetting ten times up and down, and incubated for 10 min on ice. The sample was centrifuged for 10 min at 14000 rpm and 4°C, and the supernatant was transferred to a fresh Eppendorf cup. PK was added to a final concentration of 50 μ g/ml was added, followed by 15 min incubation on ice. After the addition of PMSF to a final concentration of 4 mM and 10 min incubation on ice, TCA to a final concentration of 14 % was added to precipitate the proteins. The sample was incubated for 30 min on ice and subsequently centrifuged for 30 min at 14000 rpm and 4°C. The supernatant was discarded and the pellet was washed with ice-cold acetone (10 min, 14000 rpm, 4°C). Then, the pellet was air dried, resuspended in 2 x Laemmli buffer and shaken for 15 min at 650 rpm and 65°C.

2.2.12 Membrane extractability of proteins

50 – 75 µg of mitochondria were resuspended in 0.1 M Na₂CO₃ (pH 10.8) and 0.1 M Na₂CO₃ (pH 11.5), respectively, by pipetting up and down 10 times. The samples were incubated for 20 min on ice with pipetting 10 times up and down after 10 min. Subsequently, they were centrifuged for 1 h at 100000 g and 4°C. The pellet was resuspended in 2 x Laemmli, shaken for 5 min and incubated at 95°C for 5 min. The supernatant was transferred into a fresh Eppendorf cup and proteins were precipitated by TCA precipitation (2.2.7) adding sodiumdeoxycholate to a final concentration of 0.0125 % and TCA to a final concentration of 14 %. After centrifugation and washing with ice-cold acetone, the pellet was resuspended in 2 x Laemmli buffer, and the samples were shaken for 15 min at 65°C and 650 rpm.

2.2.13 Co-Immunoprecipitation

To prepare the Protein-A-Sepharose slurry, Protein-A-Sepharose CL-4B powder was washed with dH₂O (10 ml dH₂O per 50 mg powder; centrifugation for washing was performed for 30 s at 400 g) and resuspended in the same volume of 1 x PBS. For one experiment, 30 µl of sepharose beads were pelleted in an Eppendorf cup for 30 s at 400 g and washed twice with lysis buffer for 30 s at 400 g. Then 5 - 10 µl of antibody and PBS to a final volume of 30 µl were added, and the sample was incubated for 30 min at room temperature with gentle shaking. In the meantime, 60 - 70 µg of mitochondria were solubilized in 250 µl of lysis buffer and incubated for 15 min on ice. Then, the sample was centrifuged for 10 min at 14000 rpm and 4°C. The beads were washed three times with lysis buffer (30 s at 400 g) and the mitochondrial supernatant was added. The sample was incubated for 1 - 3 h at 4°C with inversion to allow binding of the protein complex to the antibody. Subsequently, the sepharose beads were washed twice with lysis buffer and once with Tris/HCl pH 7.4, and resuspended in 2 x Laemmli buffer.

2.2.14 *In vitro* import of radio-labeled proteins into isolated mitochondria

³⁵S-labeled proteins were obtained using the TNT[®] SP6 Quick Coupled Transcription/Translation System or TNT[®] T7 Quick Coupled Transcription/Translation System (Promega). For *in vitro* import experiments, 50 µg of freshly isolated mitochondria per sample were resuspended in 100 µl of import buffer freshly supplemented with 10 mM sodium succinate, 2 – 5 mM ATP and 1 mM DTT, and ³⁵S-labeled protein lysate to a final concentration of 5 % was added. For controls with dissipated ΔΨ, 10 mM CCCP and 10 mM valinomycin were added. The samples were incubated at 37°C for different time points, and then centrifuged for 5 min at 12000 g and 4°C. The pellet was washed with

SET buffer (5 min, 12000 g, 4°C) and stored at -80°C until subjected to BN-PAGE, or resuspended in 2 x Laemmli buffer and analyzed by SDS-PAGE. If samples were to be subjected to PK treatment after incubation at 37°C, PK to a final concentration of 50 µg/ml was added and samples were incubated for 15 min on ice. Subsequently, 2 mM PMSF was added, followed by 10 min incubation on ice. Mitochondria were pelleted by centrifugation for 5 min at 12000 g and 4°C, washed with SET buffer containing 0.1 mM PMSF, and resuspended in 2 x Laemmli buffer.

2.2.15 Production of inducible shRNA-mediated knockdown cell lines

For the creation of inducible shRNA-mediated knockdown cell lines, the Tronolab system, which utilizes human immunodeficiency virus type 1-derived lentiviral vectors, was used (Wiznerowicz and Trono, 2003). In this system, the desired shRNA sequence is cloned into the pLVTHM vector under the control of the PolIII promoter H1. As a marker, the plasmid contains a gene coding for green fluorescent protein (GFP) under the control of the polII promoter EF-1a. In order to render the system inducible, the pLV-tTR-KRAB-red plasmid is required in addition (Wiznerowicz and Trono, 2003). This vector encodes tTR-KRAB, a fusion of the *E. coli* tetracycline repressor (tTR) to the KRAB domain of human Kox1, and the marker DsRed under the constitutively active EF-1a promoter. The KRAB domain can trigger heterochromatin formation, thereby inhibiting both polII and polIII promoters (Deuschle et al., 1995; Wiznerowicz et al., 2006). Fused to tTR, KRAB binds to the *tet* operator (*tetO*) and suppresses promoters in vicinity, thus inhibiting the transcription of the shRNA and of the GFP marker gene (Wiznerowicz and Trono, 2003). This repression can be blocked by the addition of doxycycline (Dox) as this substance sequesters tTR-KRAB and prevents its binding to *tetO* (Figure 2-2) (Deuschle et al., 1995). Both the pLVTHM and the pLV-tTR-KRAB-red plasmid are introduced into the target cell line via lentiviruses (Wiznerowicz and Trono, 2003).

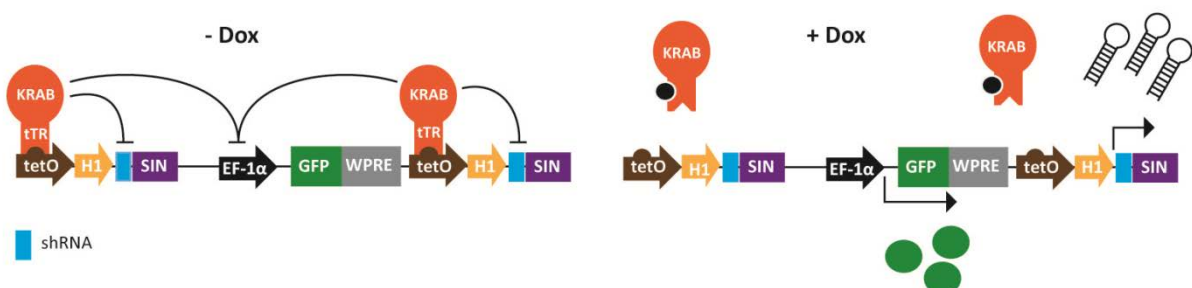


Figure 2-2 Mode of action of the Tronolab inducible shRNA-mediated knockdown system (adapted from Wiznerowicz and Trono, 2003). The plasmids pLVTHM and pLV-tTR-KRAB-Red are introduced into the target cells via lentiviruses. The gene cassettes of both plasmids are integrated into the nuclear genome by reverse transcription. After genomic integration of the proviruses, the constantly expressed tTR-KRAB repressor can bind to the *tet* operator (*tetO*), thereby inhibiting transcription of the GFP marker and the shRNA gene. Upon doxycycline (Dox) addition, this molecule sequesters the repressor, thus enabling shRNA and GFP production.

Oligonucleotides for suitable shRNAs were designed using the BLOCK-iT™ RNAi Designer (Invitrogen) and adapting them to the requirements of the pLVTHM system. Oligonucleotides were dissolved to a concentration of 1 M, and 1 µl of the forward and 1 µl of the reverse oligonucleotide strand were added to 48 µl of annealing buffer. The sample was incubated at 96°C for 4 min and at 70°C for 10 min and then gradually cooled down by incubation at room temperature to obtain a double stranded DNA fragment with ClaI and MluI restriction sites. This fragment was ligated into the pLVTHM vector restricted with ClaI/MluI. The construct was introduced into chemo-competent *E. coli* DH5α by transformation, and then isolated by the PureYield™ Plasmid Midiprep System (Promega) from a positive bacterial clone. Subsequently, HEK 293T cells were transfected with 20 µg of pLVTHM plasmid together with 10 µg of psPAX plasmid and 10 µg of pCMV-VSV-G plasmid via CaPhosphate transfection. After 4 – 6 h, fresh medium was added, and after 48 h the supernatant was collected and sterile filtered using a 0.45 µm filter. 10 µg/ml polybrene was added and the supernatant was added to HeLa KRAB cells. This cell line already had the gene encoding the KRAB-tTR repressor required for suppression of the shRNA expression introduced into its chromosomal DNA by lentiviral transduction (Kozjak-Pavlovic et al., 2007). The next day, cells were split into a fresh 75 cm² cell culture flask and a part of the cells was transferred to two wells of a 12 well plate. 1 µg/ml Dox was added to one of the wells to induce the protein knockdown. The cells were harvested after 7 d, resuspended in 2 x Laemmli buffer and subjected to SDS-PAGE followed by western blotting to assess the efficiency of the knockdown. If a sufficient knockdown of the target protein in the cell pool was present, single cell clones were isolated.

2.2.16 Stable isotope labeling of amino acids in cell culture (SILAC)

ttc19-kd2 cells were grown either in heavy ¹³C₆ L-lysine/L-arginine-containing RPMI medium (Invitrogen) or in RPMI medium containing light ¹²C₆ L-lysine/L-arginine. After 3 passages, knockdown of TTC19 was induced in the unlabeled cells by addition of 1 µg/ml Dox. After 9 d of knockdown induction, mitochondria of induced and non-induced cells were isolated. The same protein amount of both samples was mixed and sent for mass spectrometry analysis (Bernd Thiede, Oslo).

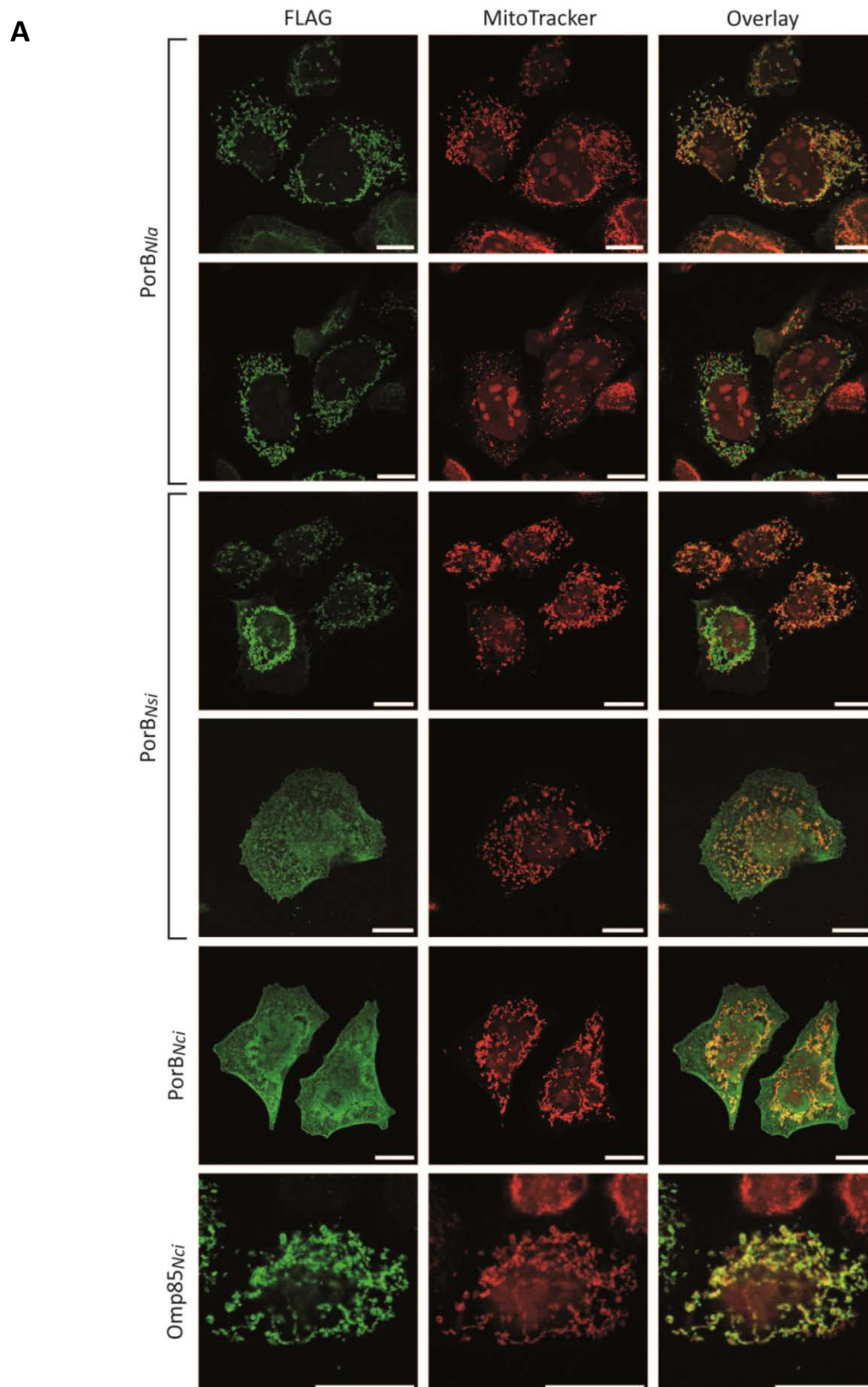
3 RESULTS

3.1 Targeting of β -barrel proteins to human mitochondria

3.1.1 Neisserial β -barrel proteins are imported into human mitochondria

The central component of the mammalian β -barrel assembly machinery, Sam50, is conserved from gram-negative bacteria to eukaryotes. Although the remaining components of the sorting and assembly machinery (SAM) show no homology, it could be demonstrated that the eukaryotic β -barrel protein VDAC can be assembled into the OM of gram-negative bacteria (Walther et al., 2010). Likewise, reports appeared showing that yeast mitochondria are able to import and integrate β -barrel proteins of bacterial origin (Walther et al., 2009a). Our previous work demonstrated that the β -barrel protein PorB of *N. gonorrhoeae* (PorB_{Ngo}) is imported into human mitochondria both in infection and upon expression (Kozjak-Pavlovic et al., 2009; Müller et al., 2000; Müller et al., 2002). However, OmpC, a β -barrel protein from *E. coli*, remained cytosolic upon expression (Müller et al., 2002). Therefore, our previous results contradicted the data published for yeast mitochondria and we aimed to clarify how mammalian mitochondria behave in regard to bacterial β -barrel proteins. When we expressed the β -barrel proteins OmpA, OmpC, PhoE and BamA of *E. coli* and YaeT of *Salmonella enterica* in human cells, we observed no mitochondrial localization. YaeT and BamA are homologs of Omp85 of *N. gonorrhoeae* (Omp85_{Ngo}), which, on the other hand, was imported, and, in contrast to PorB_{Ngo}, also integrated into the outer mitochondrial membrane (OMM) (Kozjak-Pavlovic et al., 2011). As previous studies showed that PorB of the commensal *N. mucosa* is not targeted to human mitochondria, raising the interesting hypothesis that this ability is linked to neisserial pathogenicity (Müller et al., 2002), I investigated the behavior of β -barrel proteins of other commensal *Neisseria* strains. For that purpose, chromosomal DNA of *N. lactamica*, *N. sicca* and *N. cinerea* was isolated, and the genes encoding their PorB and Omp85 proteins were cloned without their bacterial N-terminal signal sequence into the expression vector pcDNA3 introducing an N-terminal FLAG-tag, thus creating the constructs PorB_{Nla}, PorB_{Nsi}, PorB_{Nci} and Omp85_{Nci}. The genes encoding Omp85 of *N. lactamica* and *N. sicca* could not be amplified by PCR. To determine whether these β -barrel proteins are targeted to mitochondria, the constructs were expressed in HeLa cells grown on coverslips by Lipofectamin transfection. Subsequently, the cells were stained with the $\Delta\Psi$ -sensitive dye MitoTracker and with an antibody against the FLAG-tag. Analysis by confocal microscopy revealed that PorB_{Nci} was not targeted to human mitochondria (Figure 3-1). PorB_{Nla} and PorB_{Nsi} could be imported into mitochondria, but some of the protein could also be detected in the cytosol. Interestingly, when targeted to mitochondria, $\Delta\Psi$ was only lost when a strong signal for PorB was observed. This is in contrast to the previous findings of our lab for PorB_{Ngo} whose expression

always resulted in the loss of $\Delta\Psi$ (Kozjak-Pavlovic et al., 2009). Omp85_{Nci} like Omp85_{Ngo}, was exclusively targeted to mitochondria and $\Delta\Psi$ was retained, indicating that this protein was correctly assembled in the OMM.



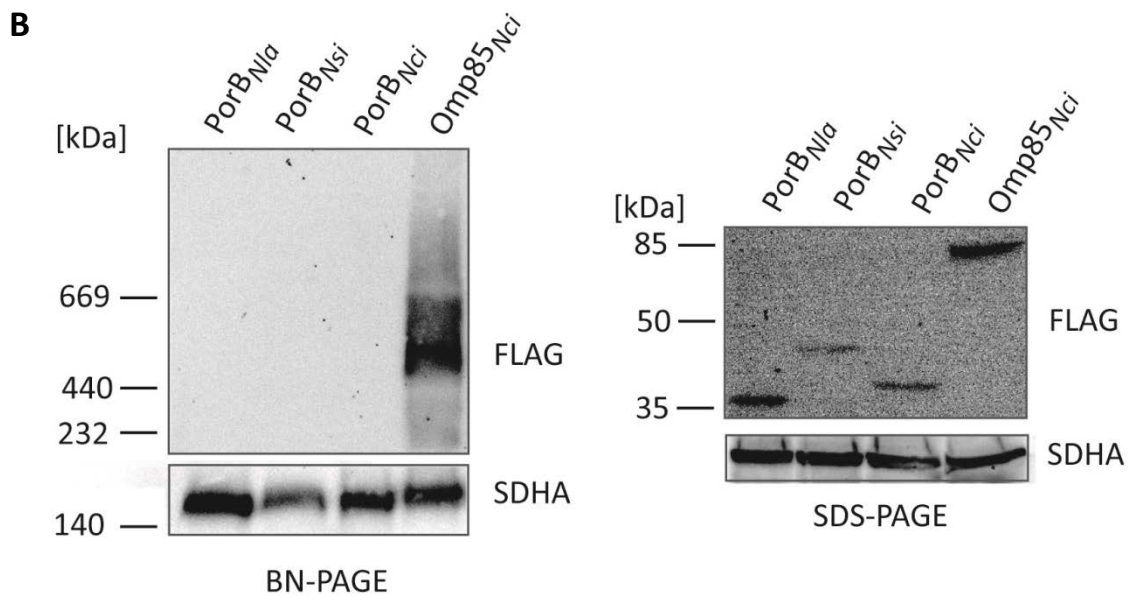


Figure 3-1 β -barrel proteins of *Neisseria* sp. can be imported into human mitochondria. Chromosomal DNA from *N. lactamica* (*Nla*), *N. sicca* (*Nsi*), and *N. cinerea* (*Nci*) was isolated and genes encoding their PorB and Omp85 proteins were cloned into a pcDNA3 vector introducing an amino-terminal FLAG-tag. (A) HeLa cells seeded on coverslips were transfected with the plasmids coding for PorB_{Nla}, PorB_{Nsi}, PorB_{Nci} or Omp85_{Nci} by Lipofectamin transfection. Cells were stained with MitoTracker, fixed with 3 % PFA and immunostained with an antibody against the FLAG-tag. Samples were analyzed by confocal microscopy. Scale bars represent 100 μ m. (B) The constructs from (A) were expressed in HEK293T cells and 50 μ g of isolated mitochondria were analyzed on SDS-PAGE or BN-PAGE followed by western blotting. SDHA: subunit A flavoprotein of complex II.

To further examine whether the proteins were integrated into the OMM, the constructs were expressed in HEK293T cells. Mitochondria were isolated and analyzed by BN-PAGE followed by western blotting. Detection with an antibody against the FLAG-tag revealed that only Omp85_{Nci} formed protein complexes in the OMM. Overexpression of the FLAG-tagged constructs was confirmed by separation of mitochondria on SDS-PAGE followed by western blotting and immunodecoration with an antibody against the FLAG-tag (Figure 3-1B). Of note, we observed in our group that a signal is detected in the mitochondrial fraction also for proteins which are exclusively localized to the cytosol. Therefore, SDS-PAGE followed by western blotting is not entirely suitable for proving the mitochondrial localization of a protein. It can, however, be utilized to confirm protein expression in transfected cells.

3.1.2 Neisserial Omp85 can assemble PorB of *Neisseria* sp. into the OMM

Previous work of our group showed that expressed Omp85_{Ngo} can exercise its natural function when integrated into the OMM, namely to assemble PorB_{Ngo} (Kozjak-Pavlovic et al., 2011). Therefore, I

aimed to elucidate whether this function of Omp85_{NgO} is specific for the OMM integration of PorB_{NgO} or whether it can also assemble the PorB proteins of *N. lactamica*, *N. sicca*, and *N. cinerea*. FLAG-tagged Omp85_{NgO} was overexpressed in HEK293T cells together with FLAG-tagged PorB_{Nla}, PorB_{Nsi} or PorB_{Nci} by calcium phosphate transfection. 48 h after transfection, mitochondria were isolated and subsequently analyzed by BN-PAGE followed by western blotting, or, as a control for protein expression, separated by SDS-PAGE followed by western blotting. Likewise, Omp85_{Nci} was overexpressed together with PorB_{Nla}, PorB_{Nsi}, or PorB_{Nci}. The experiments demonstrated that Omp85_{NgO} could assemble PorB_{Nla} and, to a lesser extent, PorB_{Nci} into the OMM (Figure 3-2A and Kozjak-Pavlovic et al., 2011). Omp85_{Nci} was also able to integrate PorB of *N. lactamica* (Figure 3-2B). Interestingly, PorB_{Nci} could be integrated into the OMM although it seemed to be localized exclusively in the cytosol when examined by confocal microscopy.

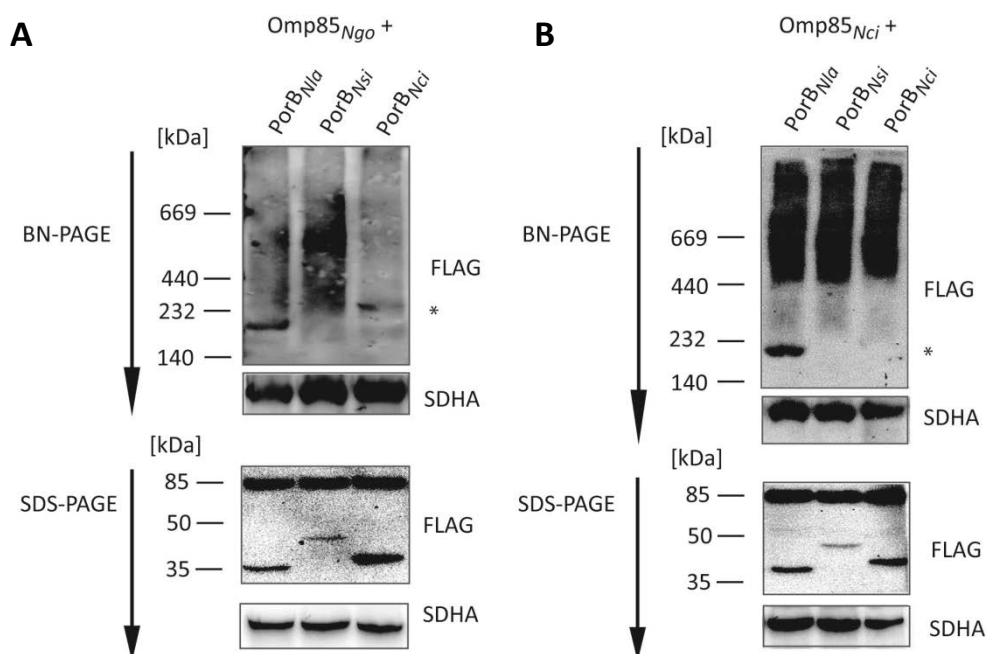


Figure 3-2 Omp85 can assemble PorB proteins of other neisserial origin. Omp85_{NgO} was expressed together with PorB_{Nla}, PorB_{Nsi} and PorB_{Nci} (A), and Omp85_{Nci} was expressed simultaneously with PorB_{Nla}, PorB_{Nsi} and PorB_{Nci} (B) in HEK293T cells. Mitochondria were isolated and separated by BN-PAGE or, as a control for protein expression, on SDS-PAGE followed by western blotting. The PorB protein complexes are marked with an asterisk. SDHA: subunit A flavoprotein of complex II.

3.1.3 Targeting of Omp85_{NgO} to mitochondria depends on its C-terminal half, whereas the last quarter of the protein is not sufficient

Omp85_{NgO} and Bama_{Ecoli} are homologous proteins (Werner and Misra, 2005). They constitute the central component of the bacterial β -barrel assembly machinery (Voulhoux et al., 2003). Both consist of an N-terminal periplasmic domain comprising five POTRA domains (Sanchez-Pulido et al., 2003)

and of an OM-integrated C-terminal β -barrel part with 16 β -strands (Gentle et al., 2005) (Figure 3-3). Expression of both proteins in HeLa cells, however, demonstrated that, despite their similarity, only Omp85_{Ngo} is targeted to human mitochondria and assembled into the OMM (Kozjak-Pavlovic et al., 2011). Therefore, I aimed to identify the signal in Omp85_{Ngo} that leads to the observed difference in targeting between this protein and BamA_{Ecoli}.

		POTRA1	
Omp85 <i>Ngo</i>	-MKLKQIASALMMLGISPLAFAD	FTIQDIRVEGLQRTEPSTVFNYLPVKVGDYNDTHGS	59
BamA <i>Eco</i>	MAMKKLLIASLLFSSATVYGAG	EVVKDIHFEGLRVAVGAALLSMPVRTGDTVNDEDIS	60
	* : : : * : : : * : : : * : : : * : : : * : : : * : : : * : : : * : : : * : : : * : : : * : : : *		
Omp85 <i>Ngo</i>	AIKSLYATGFFDDVRVETADGQLLLTVIER	PTIGSLNITGAKMLQNDIAIKKNLESFGLA	119
BamA <i>Eco</i>	NTIRALFATGNFEDVRVLRDGD	TLVQVKEPTIASITFSGNKSVKDDMLKQNL	120
	* : : : * : : : * : : : * : : : * : : : * : : : * : : : * : : : * : : : * : : : * : : : *		
		POTRA2	
Omp85 <i>Ngo</i>	QSQYFNQATLNQAVAGLKEEYLGRGKLN	IQITPKVTKLARNRVDIDITIDEGKSAKITDI	179
BamA <i>Eco</i>	VGESLDRTTIADIEKGLDFYYSVGKYSAS	VKAVVTPLPNRVLDLKLVFQEGVSAEIQQI	180
	. : : : * : : : * : : : * : : : * : : : * : : : * : : : * : : : * : : : * : : : * : : : *		
		POTRA3	
Omp85 <i>Ngo</i>	EFEQNQVYSDRKLMRQMSLTEGGIWTW	LRSDRFDQKFAQDMEKVTDFYQNGYDFDRI	239
BamA <i>Eco</i>	NIVGNHAF	TTDELISHFQLRDEVPWNVVGD	240
	. : : : * : : : * : : : * : : : * : : : * : : : * : : : * : : : * : : : * : : : * : : : *		
		POTRA4	
Omp85 <i>Ngo</i>	LTDIQTNEDKTRQTIKIVHEGSR	FRWGKVSIEGDTNEVPKAELEKLLTMKPGK	299
BamA <i>Eco</i>	DSTQVSLTPDKKIYVTVNI	TEGDDQYKLSGVEVSGN-LAGHSAEIEQLTKIE	299
	. * : : . * . : : : * : : : * : : : * : : : * : : : * : : : * : : : * : : : * : : : *		
Omp85 <i>Ngo</i>	QMTAVLGEIQNRMG	SAGYAYSEISVQPLPNAGTKTVDFVLHIEPGRK	359
BamA <i>Eco</i>	KVTKMEDDIKLLGRYGYAYPRVQSMPE	INDADKTVKLRVNDAGNRIFYVRKIRFEGNDT	359
	. : * : : : : * : : : * : : : * : : : * : : : * : : : * : : : * : : : * : : : *		
		POTRA5	
Omp85 <i>Ngo</i>	TRDEVVRELRQMESAPYDTSKLQ	RSKERVELLGYFDNVQF	419
BamA <i>Eco</i>	SKDAVLRREM	QMEGAWLGS	419
	. : * : : * : : : * : : : * : : : * : : : * : : : * : : : * : : : * : : : * : : : *		
Omp85 <i>Ngo</i>	ERSTGSLDLSAGWVQDTGLVMSAGV	QDNLFGTGKSAALRASRSKTTLNGLSL	479
BamA <i>Eco</i>	ERN	TGSFNFYIGYGTESGVSFQAGVQDN	479
	** . * : : : * : : : * : : : * : : : * : : : * : : : * : : : * : : : * : : : * : : : *		
Omp85 <i>Ngo</i>	ADGVS	LDIYKAFDPRKASTSVKQYKTTTAGGGV	539
BamA <i>Eco</i>	VDGVS	LDGRLFYNDFQADDAD--LSDYTNKSYG	537
	. * : : * : : * : : * : : * : : * : : * : : * : : * : : * : : * : : * : : * : : *		
Omp85 <i>Ngo</i>	TYN--KAPKRYADFIKQYKTDGADG	SFKGLLYKGTVWGWRNKTD	597
BamA <i>Eco</i>	NMQPQVAMWRYLSMGEHPSTSDQ	NSFKTDDFTFNYGWTYNKLD	597
	. : * : : * : : * : : * : : * : : * : : * : : * : : * : : * : : * : : * : : *		
Omp85 <i>Ngo</i>	EIALPGSKLQYYSATHNQ	TWFFPLSKFTTLM	656
BamA <i>Eco</i>	KVTIPGSDNEYKVTLD	TATYVPIDDHKWVVLGRTRWGYDGLGK	657
	. : : : * : : : * : : : * : : : * : : : * : : : * : : : * : : : * : : : * : : : *		
Omp85 <i>Ngo</i>	GSVRGYESGTLGPKVYDEYGEKISYG	-----GNKKANVSAE	692
BamA <i>Eco</i>	STVRGFSNTIGPKAVYFPHQASNYD	PDYDYECATQDGAKDLCKSDDAV	717
	. : * : : * : : * : : * : : * : : * : : * : : * : : * : : * : : * : : * : : *		
Omp85 <i>Ngo</i>	LLFPMP--GAKDARTVRLSLFADAGS	VWDGRTYTAENGNNKSVYSENAHKSTFT	750
BamA <i>Eco</i>	FITPTPFISDKYANSVRTSFFWDMG	TVWDTNWDSSQYSG----YPDYSDPS	768
	. : * : : * : : * : : * : : * : : * : : * : : * : : * : : * : : * : : * : : *		
Omp85 <i>Ngo</i>	SAGGAVTWLSPLGPMKFSYAYPLKKK	PEDEIQRFFQLGTTF	792
BamA <i>Eco</i>	SAGIALQWMSPLGPLVFSYAQPFKKY	DGDKAEQFQFNIGKTW	810
	** * : : * : : * : : * : : * : : * : : * : : * : : * : : * : : * : : * : : *		

Figure 3-3 Sequence comparison of Omp85_{Ngo} and BamA_{Ecoli}. Sequences were aligned using the ClustalW2 program. Predicted POTRA domains were marked with boxes according to Bos et. al, 2007. The N-terminal bacterial signal peptide sequences, which were not cloned into the pcDNA3 vector, are marked in gray. This figure was first published in Ott et al., 2013.

To address this question, I first exchanged domains between $Omp85_{Ngo}$ and $BamA_{Ecoli}$. Genes for the chimerical proteins comprising the N-terminal part of $Omp85_{Ngo}$ and the C-terminal part of $BamA_{Ecoli}$, and vice versa, were cloned into a pcDNA3 vector introducing an N-terminal FLAG-tag, obtaining the constructs $Omp85\frac{1}{2}BamA\frac{1}{2}$ and $BamA\frac{1}{2}Omp85\frac{1}{2}$. The constructs were expressed in HeLa cells, stained with MitoTracker and subsequently with an antibody against the FLAG-tag. Analysis by confocal microscopy showed that only the construct $BamA\frac{1}{2}Omp85\frac{1}{2}$ with the C-terminal half of $Omp85_{Ngo}$ could be targeted to mitochondria (Figure 3-4A). Mitochondria retained their $\Delta\Psi$, indicating that the chimerical protein was correctly assembled into the OMM. Next, the functionality of $BamA\frac{1}{2}Omp85\frac{1}{2}$ was tested by expressing it together with Myc-tagged $PorB_{Ngo}$ in HEK293T cells. The isolated mitochondria were analyzed by BN-PAGE followed by western blotting, or by SDS-PAGE followed by western blotting as a control for protein expression (Figure 3-4B). Detection of $PorB_{Ngo}$ with an antibody against its Myc-tag revealed that it was forming complexes in the OMM, thereby indicating that the chimerical protein $BamA\frac{1}{2}Omp85\frac{1}{2}$ is functional in β -barrel protein assembly.

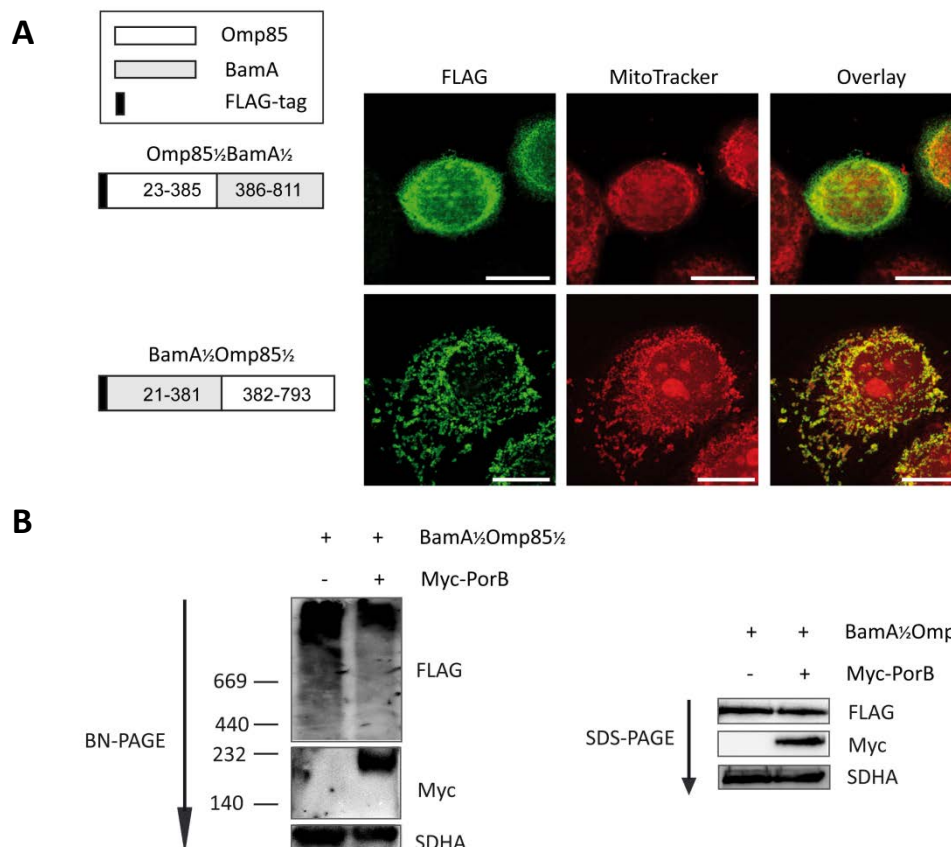


Figure 3-4 The C-terminal half of $Omp85$ mediates its mitochondrial targeting. **(A)** Genes encoding chimerical proteins with the N-terminal half of $Omp85_{Ngo}$ and the C-terminal half of $BamA_{Ecoli}$ ($Omp85\frac{1}{2}BamA\frac{1}{2}$) and vice versa ($BamA\frac{1}{2}Omp85\frac{1}{2}$) were cloned in the pcDNA3 vector introducing an N-terminal FLAG-tag and the constructs were expressed in HeLa cells. Scale bars represent 100 μ m. **(B)** N-terminally FLAG-tagged $BamA\frac{1}{2}Omp85\frac{1}{2}$ was expressed together with or without N-terminally Myc-tagged $PorB_{Ngo}$ in HEK293T cells. Mitochondria were isolated and subjected to BN-PAGE and SDS-PAGE followed by western blotting. Parts of this figure were first published in Ott et al., 2013.

In order to further pinpoint the domain of Omp85_{Ngo} responsible for mitochondrial targeting, I exchanged the last quarters of Omp85_{Ngo}, BamA_{Ecoli}, and of the chimerical constructs (Ott et al., 2013). Subsequently, the N-terminally FLAG-tagged constructs Omp85^{3/4}BamA^{1/4}, BamA^{3/4}Omp85^{1/4}, Omp85^{1/2}BamA^{1/4}Omp85^{1/4} and BamA^{1/2}Omp85^{1/4}BamA^{1/4} were expressed in HeLa cells seeded on coverslips, and stained with MitoTracker and an antibody against the FLAG-tag. Analysis of the samples by confocal microscopy revealed that none of the proteins could be targeted to mitochondria anymore (Figure 3-5). These results show that although the signal mediating mitochondrial import of Omp85_{Ngo} is contained within its C-terminal membrane-integrated part, it cannot be assigned to a short linear sequence. Rather, the secondary structure seems to play an important role as even the constructs Omp85^{3/4}BamA^{1/4} and Omp85^{3/4}BamA^{1/4}Omp85^{1/4}, possessing three quarters of Omp85_{Ngo}, could not be targeted to mitochondria.

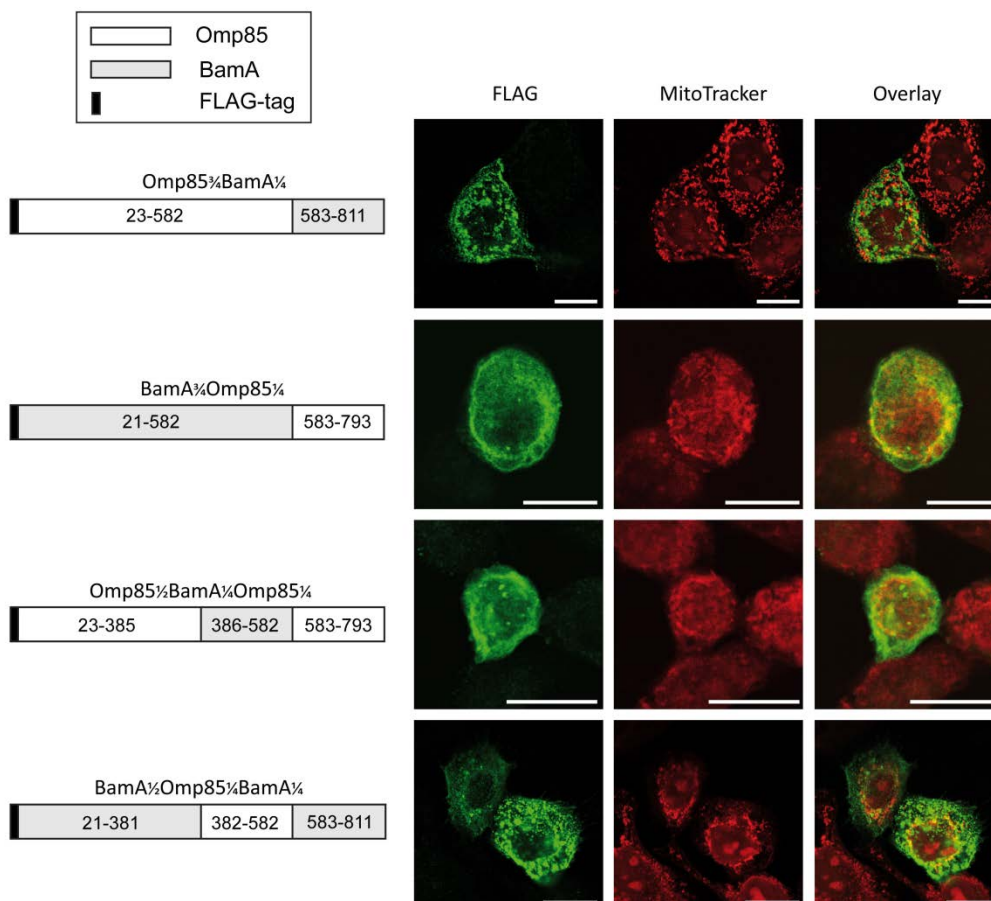


Figure 3-5 A quarter of Omp85_{Ngo} is not sufficient for mediating its mitochondrial import of Omp85_{Ngo}. The schemes on the left-hand side show the exchanges performed between Omp85_{Ngo} and BamA_{Ecoli}. Plasmids encoding the N-terminally FLAG-tagged constructs Omp85^{3/4}BamA^{1/4}, BamA^{3/4}Omp85^{1/4}, Omp85^{1/2}BamA^{1/4}Omp85^{1/4} and BamA^{1/2}Omp85^{1/4}-BamA^{1/4} were expressed in HeLa cells. Cells were stained with MitoTracker and an antibody against the FLAG-tag, and analyzed by confocal microscopy. Scale bars represent 100 μ m. This figure was first published in Ott et al., 2013.

3.1.4 Amino acids of the ultimate β -strand are involved in the mitochondrial targeting of Omp85

Recently, we could observe that removal of the β -sorting signal of Omp85_{NgO} not only prevents its OMM integration but also its import into mitochondria (Kozjak-Pavlovic et al., 2011). Therefore, I took a closer look at the importance of the β -signal of Omp85_{NgO} for mitochondrial import and mutated amino acids R783, Q787, and T790, obtaining the N-terminally FLAG-tagged constructs Omp85-R783E, Omp85-Q787G and Omp85-T790K. The constructs were expressed in HeLa cells grown on cover slips, and stained with MitoTracker and an antibody against the FLAG-tag. Analysis by confocal microscopy demonstrated that only Omp85-R783E and Omp85-T790K were imported into mitochondria, whereas Omp85-Q787G remained cytosolic (Figure 3–6A). To confirm the importance of the properties of this amino acid residue, the constructs Omp85-Q787E, where the polar residue was exchanged with a negatively charged one, and Omp85-Q787N, which should behave as the wild type, were cloned and subsequently expressed in HeLa cells. After decoration of the cells with MitoTracker and an antibody against the FLAG-tag, analysis with confocal microscopy showed that, as expected, Omp85-Q787E remained cytosolic, whereas Omp85-Q787N was imported into mitochondria (Figure 3-6A). To further confirm the confocal microscopy results, HEK293T cells were transfected with the constructs and mitochondria were isolated. BN-PAGE with mitochondria followed by western blotting and immunodecoration with an antibody against the FLAG-tag demonstrated that no protein complex formation could be detected for Omp85-Q787G and Omp85Q787E (Figure 3-6B), supporting the finding of the microscopy analysis that these constructs could not be imported into mitochondria. Taken together, the data demonstrate the importance of the polar property of glutamine at position 787 for mitochondrial targeting of Omp85_{NgO}.

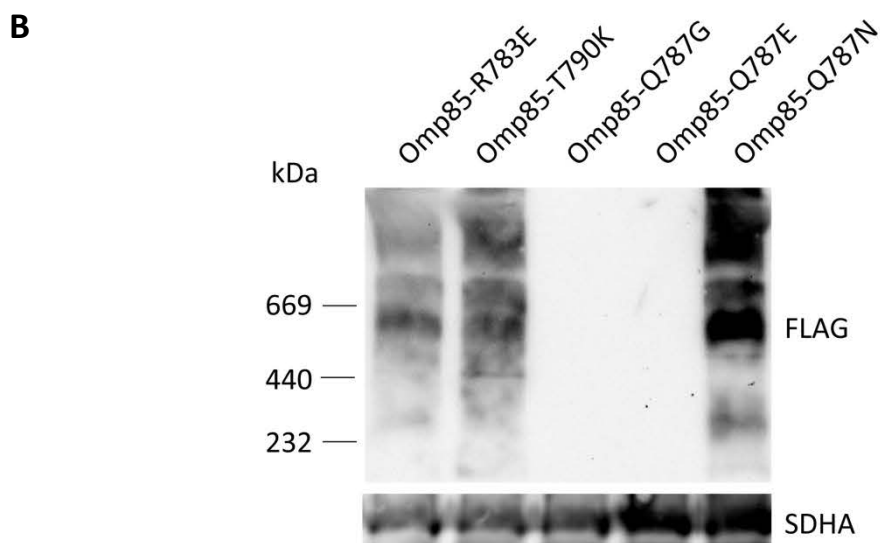
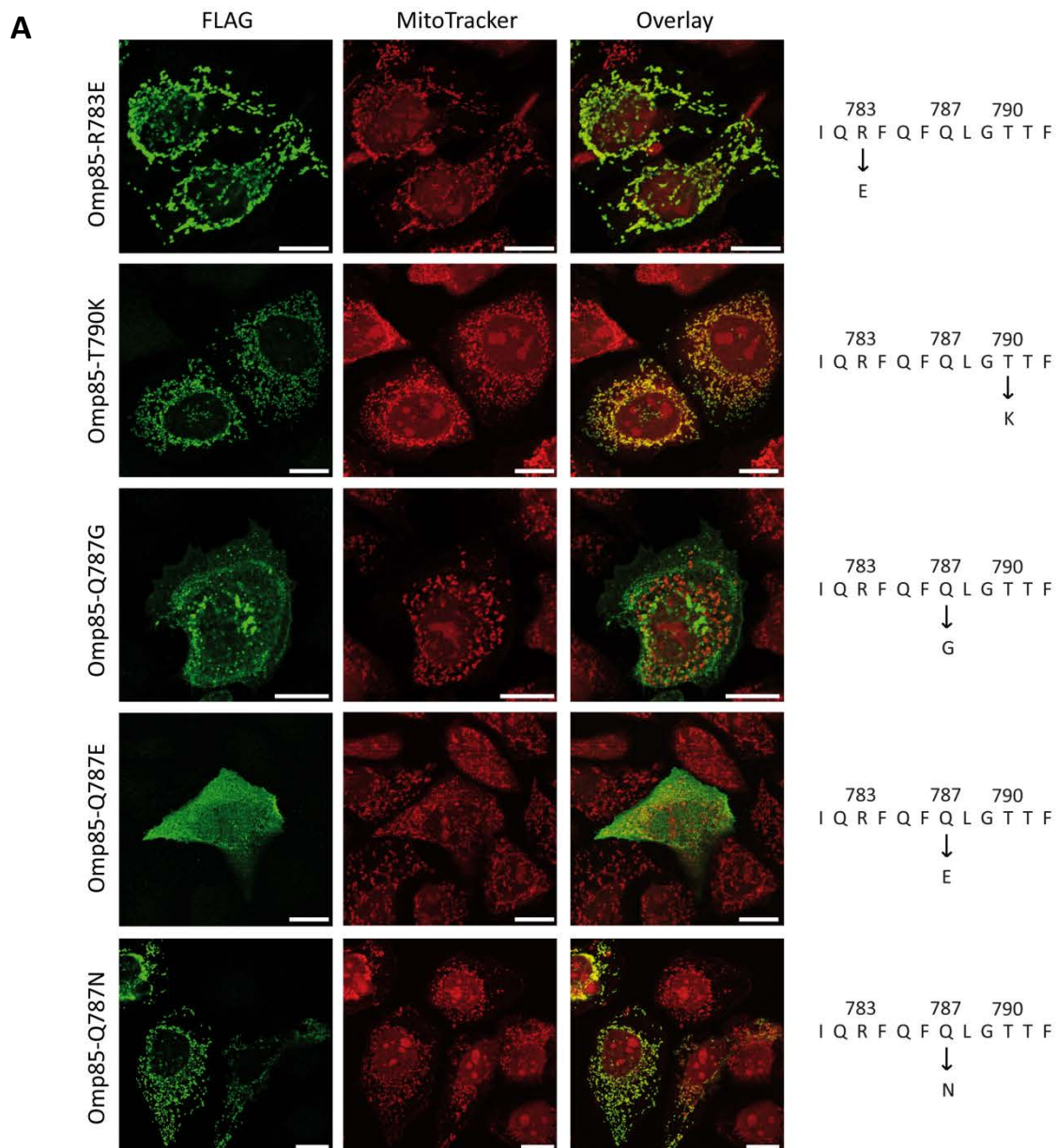


Figure 3-6 Glutamine at position 787 is required for mitochondrial import of Omp85. (A) Plasmids coding for the N-terminally FLAG-tagged constructs Omp85-R783E, Omp85-T790K, Omp85-Q787G, Omp85-Q787E and Omp85-Q787N were expressed in HeLa cells seeded on coverslips. Cells were stained with the $\Delta\Psi$ -sensitive dye MitoTracker and an antibody against the FLAG-tag, and analyzed by confocal microscopy. Scale bars represent 100 μ m. (B) The constructs from A were expressed in HEK293T cells, and mitochondria were isolated and analyzed by BN-PAGE followed by western blotting. SDHA: subunit A flavoprotein of complex II. This figure was first published in Ott et al., 2013.

In order to elucidate whether Q787 is the only crucial amino acid residue in the β -sorting signal of Omp85_{NgO}, I shortened the protein for one to six residues from the C-terminus (Ott et al., 2013). The N-terminally FLAG-tagged constructs Omp85-1aa, Omp85-2aa, Omp85-3aa, Omp85-4aa, Omp85-5aa, and Omp85-6aa were expressed in HeLa cells, and the cells were subsequently stained with MitoTracker and an antibody against the FLAG-tag. Confocal microscopy revealed that the removal of the phenylalanine at the ultimate position already impaired the mitochondrial import of Omp85_{NgO} (Figure 3-7 and not shown). Interestingly, when removing the last two amino acids, mitochondrial targeting could be observed in about 40 % of the cells. No mitochondrial localization was observed when three or more amino acid residues were removed.

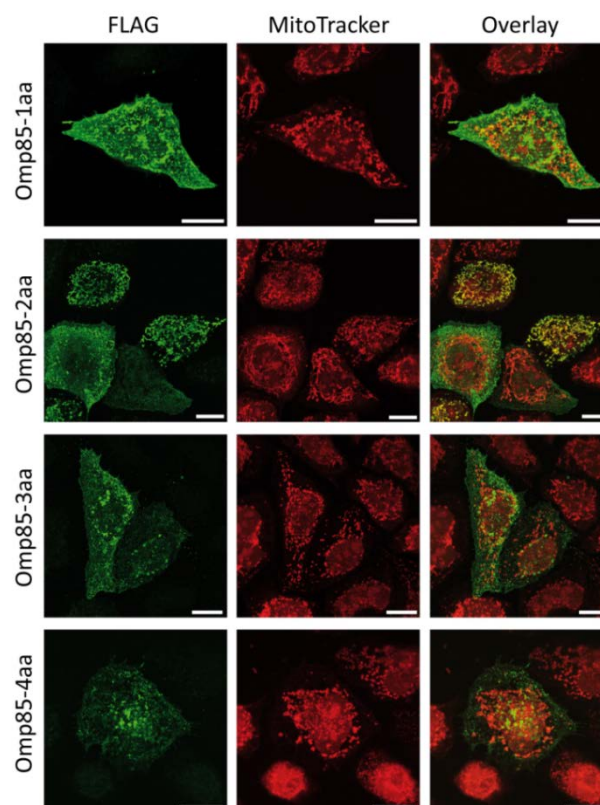


Figure 3-7 The ultimate phenylalanine plays an important role in mitochondrial targeting of Omp85_{NgO}. Omp85_{NgO} was shortened for one to four amino acid residues and plasmids encoding N-terminally FLAG-tagged Omp85-1aa, Omp85-2aa, Omp85-3aa and Omp85-4aa were expressed in HeLa cells seeded on coverslips. Cells were stained with the $\Delta\Psi$ -sensitive dye MitoTracker and an antibody against the FLAG-tag and analyzed by confocal microscopy. Scale bars represent 100 μ m. Parts of this figure were first published in Ott et al., 2013.

3.1.5 The C-terminal quarter of PorB is important for its mitochondrial targeting

Similar to Omp85_{NgO} and BamA_{Ecoli}, the β -barrel proteins PorB_{NgO} and OmpC_{Ecoli} are homologs (Figure 3-8), and only the neisserial protein can be imported into mitochondria. In contrast to Omp85_{NgO}, however, expression of PorB_{NgO} results in the loss of $\Delta\Psi$. This indicates that PorB_{NgO} cannot be assembled into the OMM but accumulates in the IMS, leading to damage of mitochondria (Kozjak-Pavlovic et al., 2009). In order to determine the signal of PorB_{NgO} which mediates its mitochondrial targeting, I exchanged domains of this protein for those of OmpC_{Ecoli} (Ott et al., 2013). Firstly, halves of the proteins were exchanged, cloning the genes encoding the constructs PorB $\frac{1}{2}$ OmpC $\frac{1}{2}$ and OmpC $\frac{1}{2}$ PorB $\frac{1}{2}$ into the pcDNA3 vector introducing an N-terminal FLAG-tag. The constructs were expressed in HeLa cells, which were subsequently stained with MitoTracker and an antibody against the FLAG-tag. Analysis by confocal microscopy revealed that only OmpC $\frac{1}{2}$ PorB $\frac{1}{2}$ could be imported into mitochondria (Figure 3-9), demonstrating that, as for Omp85_{NgO}, the C-terminal half of PorB_{NgO} contains the mitochondrial targeting information. PorB $\frac{1}{2}$ OmpC $\frac{1}{2}$ expression, like PorB_{NgO}, led to the loss of $\Delta\Psi$, indicating that the construct could not be assembled into the OMM.

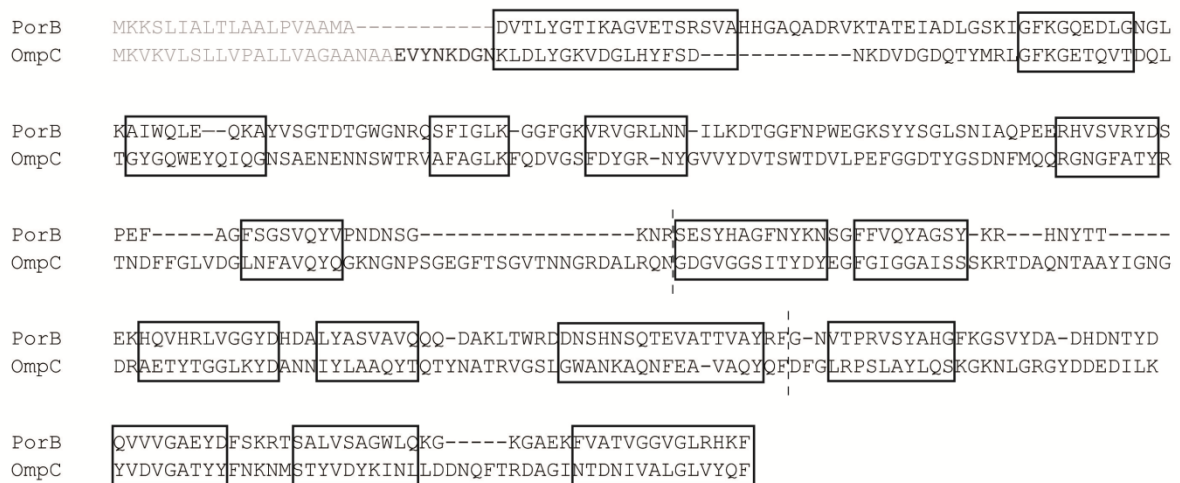


Figure 3-8 Sequence comparison of the homologous proteins PorB_{NgO} and OmpC_{Ecoli}. Predicted transmembrane domains are marked with boxes according to Tanabe and co-workers (Tanabe and Iverson, 2009). Marked with dotted lines are the sites where exchanges of halves and quarters were performed. The N-terminal bacterial signal peptide sequences, which were not cloned into the expression vector, are marked in gray.

Next, the C-terminal quarters of PorB_{NgO}, OmpC_{Ecoli} and PorB $\frac{1}{2}$ OmpC $\frac{1}{2}$ were exchanged, creating the N-terminally FLAG-tagged constructs PorB $\frac{3}{4}$ OmpC $\frac{1}{4}$, OmpC $\frac{3}{4}$ PorB $\frac{1}{4}$ and PorB $\frac{1}{2}$ OmpC $\frac{1}{4}$ PorB $\frac{1}{4}$. The constructs were expressed in HeLa cells, followed by staining with MitoTracker and an antibody against the FLAG-tag (Figure 3-9). Confocal microscopy analysis

demonstrated that PorB^{1/2}OmpC^{1/4}PorB^{1/4} was exclusively mitochondrial, whereas OmpC^{3/4}PorB^{1/4} was targeted to mitochondria in most of the cases with some of the protein remaining in the cytosol. PorB^{3/4}OmpC^{1/4} was predominantly cytosolic, but a small fraction could be detected in mitochondria. These results indicate that the C-terminal quarter of PorB_{NgO} is sufficient for mitochondrial targeting but not an absolute requirement. Besides, this demonstrates that PorB_{NgO} probably does not contain a short linear sequence mediating targeting but rather its secondary structure or charge seem to play an important role.

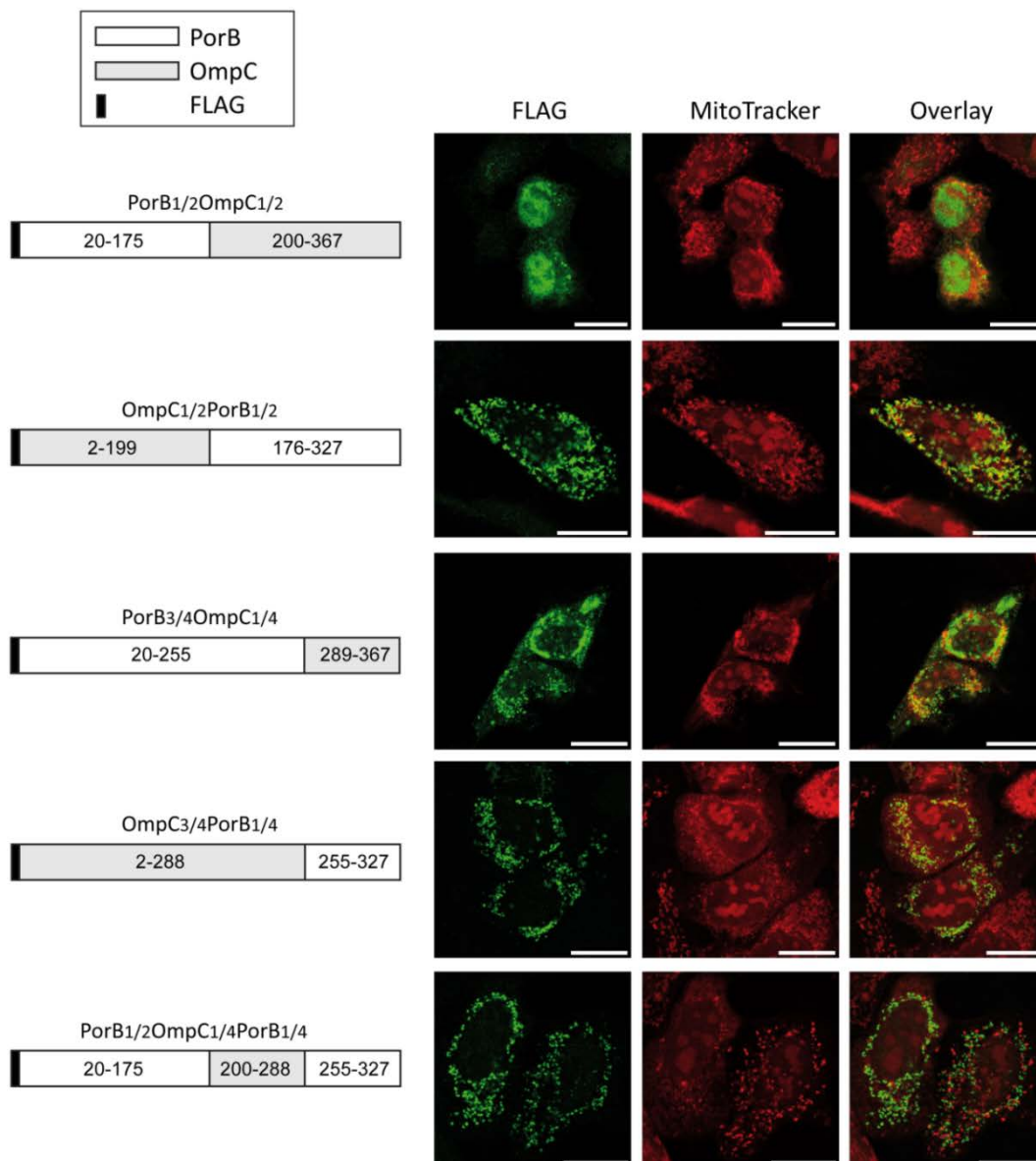


Figure 3-9 The C-terminal quarter of PorB_{NgO} is sufficient for mediating mitochondrial import. The constructs PorB^{1/2}OmpC^{1/2}, OmpC^{1/2}PorB^{1/2}, PorB^{3/4}OmpC^{1/4}, OmpC^{3/4}PorB^{1/4} and PorB^{1/2}OmpC^{1/4}PorB^{1/4} were cloned into the pcDNA3 vector introducing an N-terminal FLAG-tag and expressed in HeLa cells. Cells were stained with MitoTracker and an antibody against the FLAG-tag, and analyzed by confocal microscopy. The scheme on the left-hand side shows the composition of the constructs. Scale bars represent 100 μm. This figure was first published in Ott et al., 2013.

In order to examine whether an even shorter part of PorB_{NgO} could mediate mitochondrial targeting, the C-terminal eights of PorB_{NgO} and OmpC_{Ecoli} were exchanged. Therefore, 22 amino acid residues from the C-terminus of PorB_{NgO} were replaced by the 27 C-terminal amino acid residues of OmpC_{Ecoli}, and vice versa, creating the N-terminally FLAG-tagged constructs PorB-OmpC₃₄₁₋₃₆₇ and OmpC-PorB₃₀₆₋₃₂₇. After expression of the constructs in HeLa cells and staining with MitoTracker and an antibody against the FLAG-tag, cells were analyzed by confocal microscopy (Figure 3-10). For OmpC-PorB₃₁₆₋₃₂₇, both mitochondrial and cytosolic localization could be observed, which demonstrates that the 22 C-terminal amino acid residues of PorB are sufficient to mediate mitochondrial import. Interestingly, PorB-OmpC₃₄₁₋₃₆₇, which lacked only 22 amino acid residues of PorB_{NgO}, was exclusively cytosolic, whereas before, mitochondrial localization of PorB $\frac{3}{4}$ -OmpC $\frac{1}{4}$, which contained a bigger portion of OmpC_{Ecoli} in the C-terminal part, could be observed in some cases.

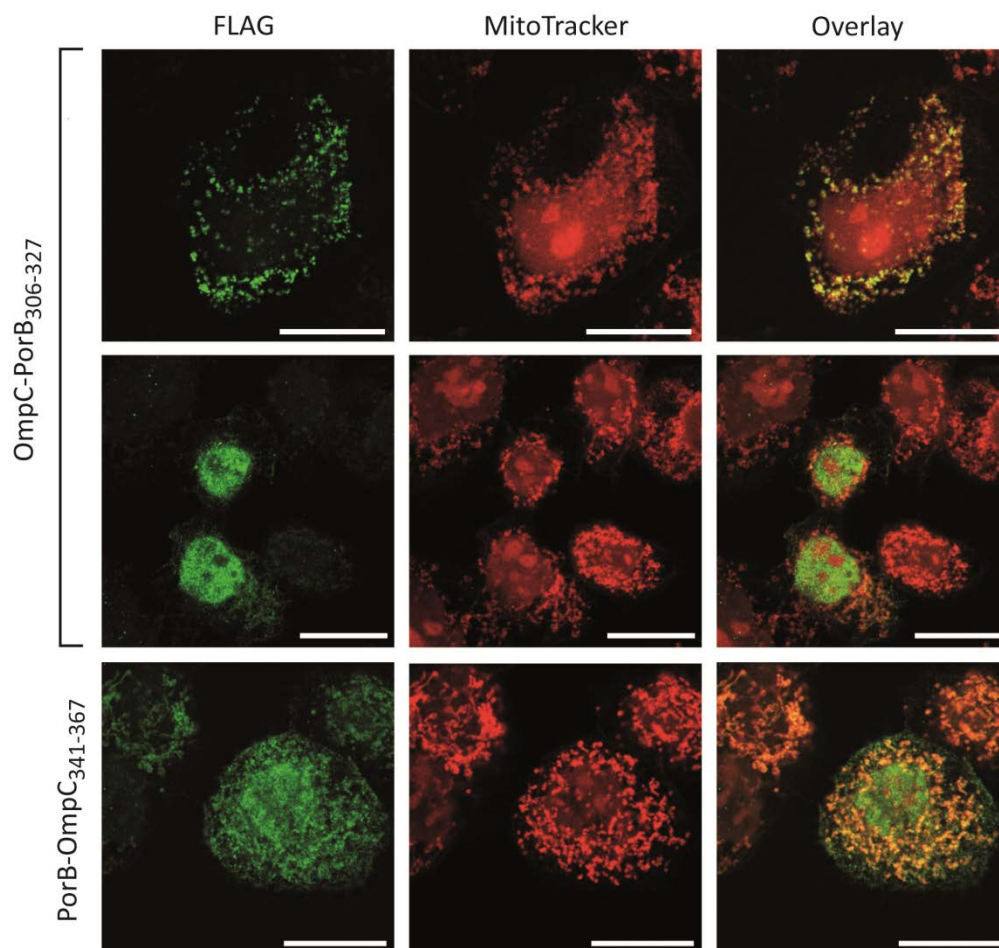


Figure 3-10 The ultimate 22 amino acid residues of PorB_{NgO} can mediate mitochondrial import. The 22 C-terminal amino acid residues of PorB_{NgO} were replaced with the 27 C-terminal amino acid residues of OmpC_{Ecoli}, and vice versa. The constructs were cloned into the pcDNA3 vector introducing an N-terminal FLAG-tag. Constructs were overexpressed in HeLa cells, and cells were stained with MitoTracker and an antibody against the FLAG-tag. Samples were analyzed by confocal microscopy. Scale bars represent 100 μ m.

3.1.6 The last β -strand is not involved in mitochondrial targeting of PorB

As exchanging the β -signal of Omp85_{Ngo} with the one of BamA_{Ecoli} prevented mitochondrial targeting of Omp85_{Ngo}, I examined whether the same applies to PorB_{Ngo} (Ott et al., 2013). For that purpose, the twelve C-terminal amino acid residues of PorB_{Ngo} and OmpC_{Ecoli} were exchanged, and the constructs PorB-12aaOmpC and OmpC-12aaPorB were expressed in HeLa cells, followed by staining with MitoTracker and antibodies against the FLAG-tag and the OMM protein Tom20. Confocal microscopy analysis demonstrated that PorB-12aaOmpC was still imported into mitochondria, indicating that, in contrast to Omp85_{Ngo}, amino acids of the ultimate β -strand of PorB_{Ngo} are not involved in its mitochondrial targeting (Figure 3-11).

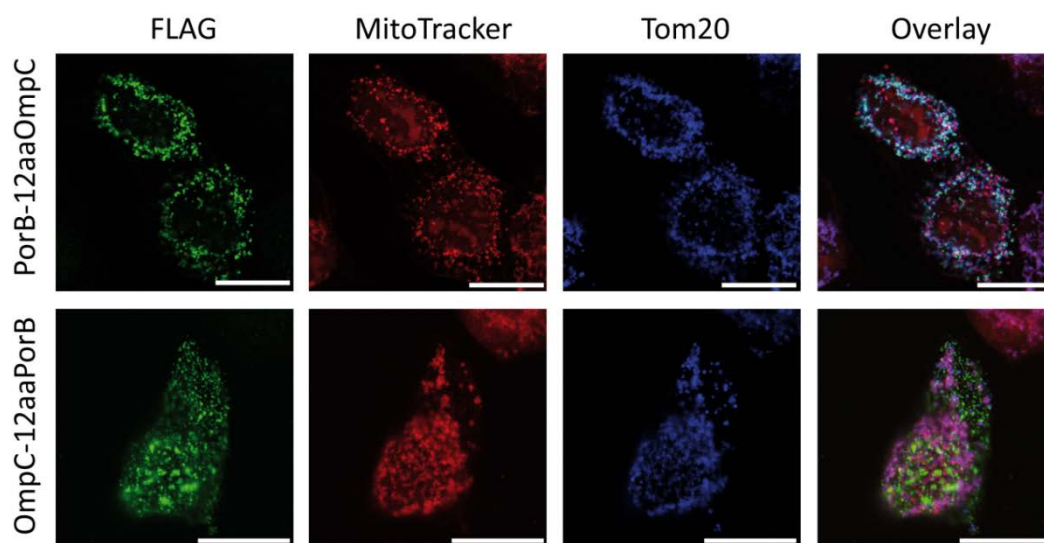


Figure 3-11 The ultimate β -strand of PorB is not involved in mitochondrial targeting. The last 12 amino acid residues of PorB_{Ngo} and OmpC_{Ecoli} were exchanged, and the N-terminally FLAG-tagged constructs PorB-12aaOmpC and OmpC-12aaPorB were cloned into the pcDNA3 vector. The constructs were expressed in HeLa cells seeded on coverslips, and cells were stained with MitoTracker and antibodies against the FLAG-tag and Tom20. Samples were analyzed by confocal microscopy. Scale bars represent 100 μ m. Tom20: subunit of the Translocase of the Outer Membrane. This figure was first published in Ott et al., 2013.

3.1.7 The β -signal of Omp85 cannot mediate OMM integration of PorB

As Omp85_{Ngo} is correctly assembled into the OMM whereas PorB is not recognized by the SAM complex and accumulates in the IMS, I wondered whether the β -signal of Omp85_{Ngo} could mediate PorB_{Ngo} OMM integration. The 12 C-terminal amino acid residues of PorB_{Ngo} were exchanged for those of Omp85_{Ngo}, creating the N-terminally FLAG-tagged construct PorB-12aaOmp85. The plasmid was expressed in HeLa cells, followed by staining with MitoTracker and antibodies against the FLAG-tag and Tom20 (Figure 3-12). Analysis by confocal microscopy showed that mitochondria lost their $\Delta\Psi$, demonstrating that the β -signal of Omp85_{Ngo} cannot mediate OMM integration of PorB_{Ngo}.

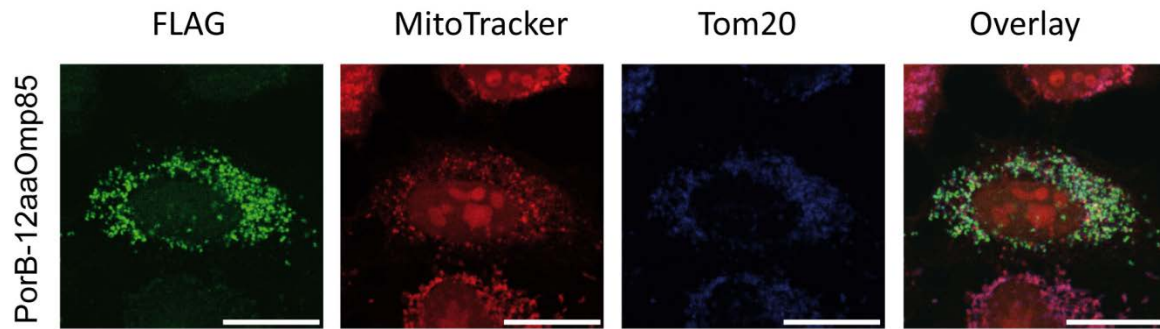


Figure 3-12 The β -sorting signal of Omp85_{NgO} cannot mediate OMM integration of PorB_{NgO}. The plasmid encoding PorB-12aaOmp85, where the last 12 amino acid residues of PorB_{NgO} are substituted by the last 12 amino acid residues of Omp85_{NgO}, was expressed in HeLa cells grown on coverslips, and cells were stained with MitoTracker and antibodies against the FLAG-tag and Tom20. Samples were analyzed by confocal microscopy. Scale bars represent 100 μ m. Tom20: subunit of the translocase of the outer membrane. This figure was first published in Ott et al. 2013.

3.1.8 At least two POTRA domains are required for Omp85 integration and function

A study of Bos and co-workers demonstrated that in *N. meningitidis* only the fifth POTRA domain of Omp85 is required for its function. In order to examine whether the same applied to Omp85_{NgO} when expressed in human cells, constructs of Omp85_{NgO} lacking one to five POTRA domains were created (Figure 3-13A). The constructs were overexpressed in HeLa cells, followed by staining with MitoTracker and an antibody against the FLAG-tag. Confocal microscopy analysis revealed that all constructs could be imported into mitochondria. $\Delta\Psi$, however, was only retained upon expression of Omp85-POTRA1, Omp85-POTRA2 and Omp85-POTRA3, whereas the removal of four or all five POTRA domains resulted in loss of $\Delta\Psi$, indicating that these two proteins could not be integrated into the OMM anymore and accumulated in the IMS (Figure 3-13B and not shown). In order to examine the functionality of the POTRA mutants, they were expressed in HEK293T cells together with or without Myc-tagged PorB_{NgO}. Mitochondria were isolated and analyzed by BN-PAGE, or, as a control for protein expression, on SDS-PAGE, followed by western blotting (Figure 3-13C). When testing for OMM integration of PorB_{NgO} with an antibody against its Myc-tag, complexes could be detected when it was expressed together with Omp85-POTRA1, Omp85-POTRA2 and Omp85-POTRA3. Immunodetection of the Omp85 complexes with an antibody against the FLAG-tag showed a signal only for Omp85-POTRA1 and Omp85-POTRA2. These results support the finding of the microscopy analysis that Omp85-POTRA4 and Omp85-POTRA5 cannot be integrated into the OMM and therefore are not functional. The fact that no complex formation of Omp85-POTRA3 is detectable although it does not lead to the loss of $\Delta\Psi$ and is functional could indicate that this protein is not able to oligomerize anymore but is present as a monomer, or that the oligomers are so instable that they are disrupted upon solubilization in digitonin.

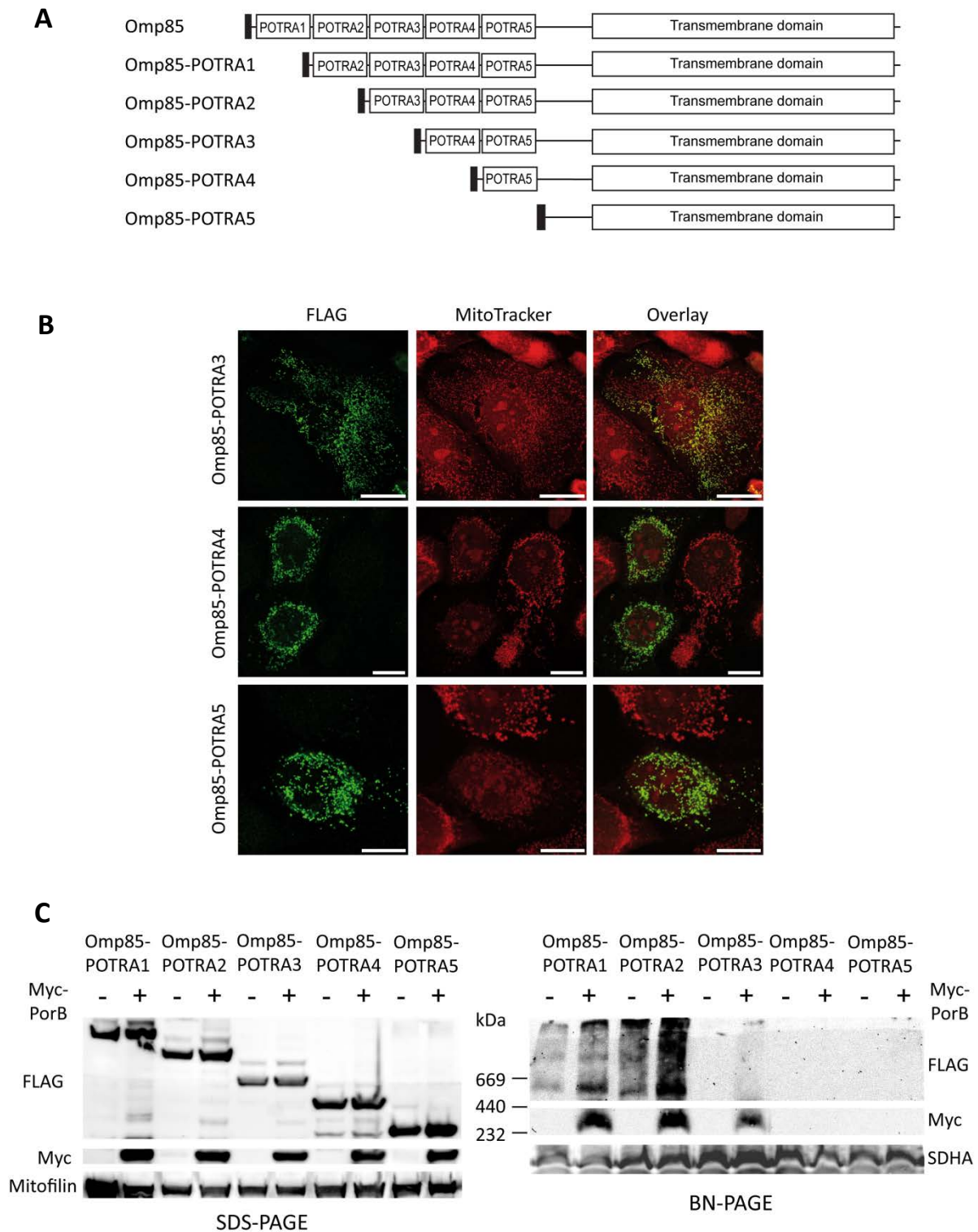


Figure 3-13 At least two POTRA domains are necessary for membrane integration and function of Omp85. (A) Scheme of the POTRA mutants. Omp85_{NgO} was shortened for one to five POTRA domains and genes encoding the mutants were cloned in the pcDNA3 vector introducing an N-terminal FLAG-tag. (B) Omp85-POTRA3, Omp85-POTRA4 and Omp85-POTRA5 were overexpressed in HeLa cells seeded on coverslips. Cells were stained with MitoTracker and an antibody against the FLAG-tag, and analyzed by confocal microscopy. Scale bars represent 100 μ m. (C) The constructs from (A) were overexpressed in HEK293T cells. Mitochondria were isolated and analyzed by SDS-PAGE or BN-PAGE followed by western blotting. SDHA: subunit A flavoprotein of complex II. This figure was published first in Ott et al., 2013.

3.2 The Mitochondrial Intermembrane space Bridging (MIB) complex

Sam50 is the central channel-forming component of the SAM complex, which integrates β -barrel proteins into the OMM. To allow profoundly studying the import route of β -barrel proteins, shRNA-mediated inducible Sam50 knockdown (*sam50kd-2*) cells were produced in our lab recently (Kozjak-Pavlovic et al., 2007). Interestingly, when Sam50 knockdown was induced, fragmentation of mitochondria and complete loss of cristae structure could be observed as a consequence (Ott et al., 2012). Xie and co-workers found Sam50 to be present in a complex with mitofilin, coiled-coil-helix-coiled-coil-helix domain containing 3 (CHCHD3), coiled-coil-helix-coiled-coil-helix domain-containing 6 (CHCHD6), DnaJC11, and metaxins 1 and 2, when they raised an antibody against mitofilin (Xie et al., 2007). The metaxins are part of the SAM complex and involved in the assembly of β -barrel proteins (Kozjak-Pavlovic et al., 2007). CHCHD3 and CHCHD6 are IMM-integrated or IMM-associated proteins and both possess a myristoylation site at position 2 and CX₉C motifs, which are typical for proteins imported via the MIA pathway (An et al., 2012; Darshi et al., 2011). Mitofilin is an integral inner membrane protein and was shown to be required for the maintenance of mitochondrial cristae morphology. Upon mitofilin depletion, cristae membranes are present in concentric circles and crista junctions are absent (John et al., 2005). Our own data, in addition to the work of Darshi and colleagues and Xie and colleagues (Darshi et al., 2011; Xie et al., 2007), indicated that the components of the SAM complex are present in the same protein complex as mitofilin and CHCHD3. Considering that this complex spans both membranes, we termed it mitochondrial intermembrane space bridging complex (MIB). My aim was to establish what kind of connection exists between Sam50 and IMM proteins and whether this connection is necessary for the maintenance of the cristae structure.

3.2.1 Loss of CHCHD3 influences Sam50 and mitofilin protein levels

In order to be able to investigate the function of the different proteins from the inner membrane which seemed to be connected to Sam50 and forming the MIB complex, an inducible shRNA-mediated knockdown cell line of CHCHD3 (*chchd3kd-2*; own work; Ott et al., 2012), and of mitofilin (*mflkd-2*; Sebastian Straub, diploma thesis; Ott et al., 2012) were produced. For that purpose, the Tronolab inducible knockdown system was used, where transcription of the shRNA sequence is inhibited by the constitutively expressed KRAB-tTR repressor (Wiznerowicz and Trono, 2003). This repression can be relieved by the addition of doxycycline (Dox), as this molecule sequesters the KRAB-tTR repressor, thereby preventing its inhibitory effect. When protein knockdown was induced by the addition of Dox for seven days, both cell lines showed a clear reduction in the protein level of the respective protein (Figure 3-14 and Ott et al., 2012). These two cell lines and the *sam50kd-2* cell

line, which has previously been produced (Kozjak-Pavlovic et al., 2007), were used to assess the connection between Sam50, mitofilin and CHCHD3. Knockdown of the respective protein was induced for 5, 7 and 14 days by Dox addition. Then, mitochondria were isolated, separated on SDS-PAGE followed by western blotting, and immunodecorated with antibodies against Sam50, mitofilin and CHCHD3 (Figure 3-14 and Ott et al., 2012). Knockdown of CHCHD3 and mitofilin resulted in reduced levels of the other two proteins, whereas Sam50 depletion led to decreased CHCHD3 levels but did not affect mitofilin levels. Therefore, the cristae loss observed upon Sam50 knockdown cannot be attributed to loss of mitofilin. As a recent study by Darshi and co-workers demonstrated a crucial role for CHCHD3 in the maintenance of cristae morphology, protein levels in mitochondria of *sam50kd-2* cells were also tested after five days of knockdown induction as cristae were already lost at this time point (Ott et al., 2011). Analysis by SDS-PAGE followed by western blotting showed that CHCHD3 levels at this point were only mildly reduced, indicating that the impaired cristae structure was indeed caused by Sam50 depletion and not a secondary effect due to CHCHD3 reduction upon loss of Sam50 (Ott et al., 2012).

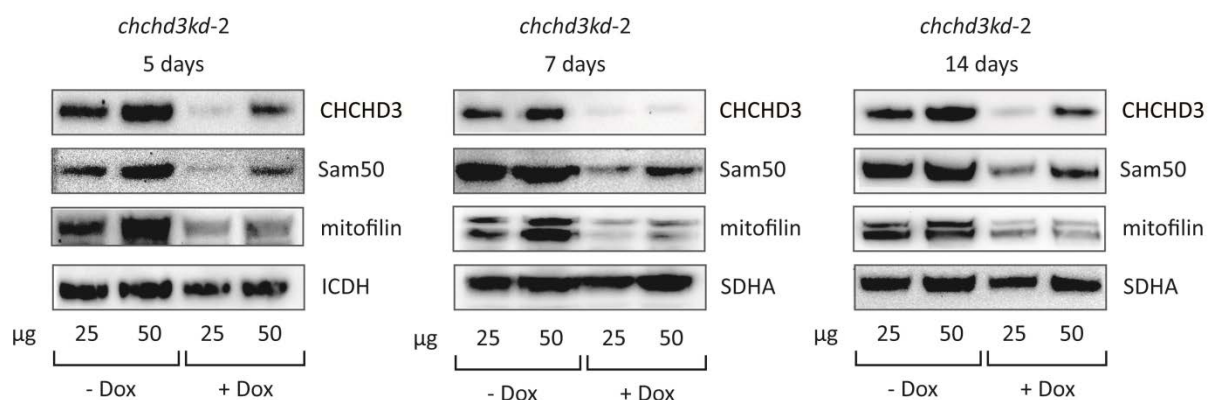


Figure 3-14 CHCHD3 influences protein levels of Sam50 and mitofilin. Knockdown of CHCHD3 was induced in *chchd3kd-2* cells for 5, 7 or 14 days by the addition of doxycycline (Dox). Mitochondria of Dox-treated (+ Dox) and untreated (- Dox) cells were isolated, and 25 µg and 50 µg of mitochondrial protein were analyzed by SDS-PAGE and western blotting. SDHA: subunit A flavoprotein of complex II; ICDH: isocitrate dehydrogenase.

3.2.2 Sam50, mitofilin and CHCHD3 are present in one complex

Next, I aimed to examine how loss of Sam50, mitofilin or CHCHD3 influenced complex formation of the other two proteins. Therefore, mitochondria isolated from Dox-induced and non-induced *chchd3kd-2*, *mflkd-2* and *sam50kd-2* cells were separated by BN-PAGE followed by western blotting, and the membranes were decorated with antibodies against CHCHD3, mitofilin and Sam50 (Figure 3-15). All three proteins appeared to migrate in a high molecular weight complex of a similar size of > 1 MDa, which we termed holo-MIB complex. In addition, CHCHD3 was detected in a smaller complex of about 700 – 800 kDa (Figure 3-15A). Upon mitofilin depletion, both CHCHD3-containing

complexes were nearly completely absent, consistent with the fact that the CHCHD3 level is strongly reduced when mitofilin is not present. Sam50 depletion resulted in a complete loss of the holo-MIB complex, whereas the levels of the lower complex were only slightly reduced. Mitofilin formed complexes of similar size as CHCHD3 (Figure 3-15B). However, knockdown of CHCHD3 did not lead to a decrease of all mitofilin containing complexes, but both CHCHD3 and Sam50 depletion resulted in a reduction of the holo-MIB complex but not in the amount of the lower mitofilin-containing complex. This shows that mitofilin stability in the lower complex does not depend on the presence of CHCHD3 in this complex. For mitofilin stability in the holo-MIB complex, on the other hand, CHCHD3 and Sam50 are required. Sam50 was only present in one or two high molecular weight complexes of > 1 MDa (Figure 3-15C). Detection of Sam50 in mitofilin- and CHCHD3-depleted cells showed that Sam50 complexes were completely lost after mitofilin depletion and strongly reduced in CHCHD3-knockdown mitochondria, consistent with the SDS-PAGE and western blot analysis which demonstrated an almost complete loss of Sam50 upon loss of mitofilin and a strong reduction upon CHCHD3 depletion (Figure 3-14 and Ott et al., 2012).

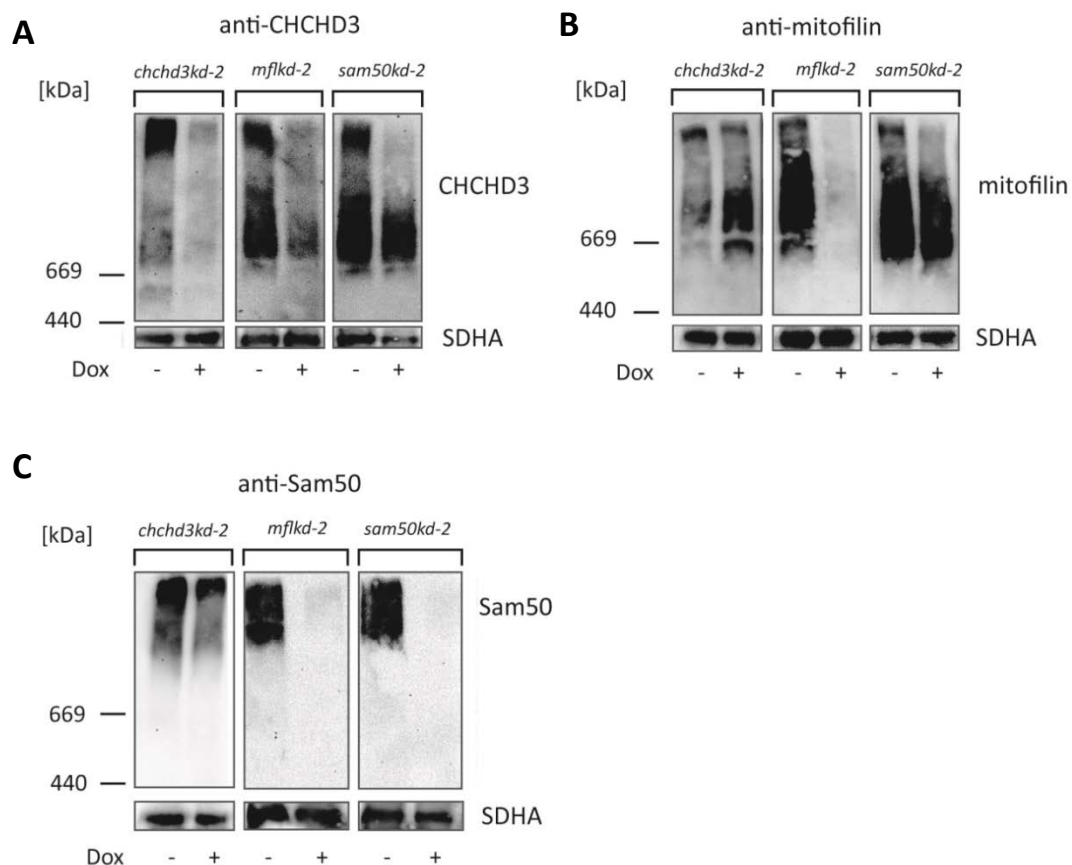


Figure 3-15 CHCHD3, Sam50 and mitofilin are present in one complex. Knockdown was induced in *chchd3kd-2*, *mflkd-2* and *sam50kd-2* cells for 7 days by the addition of doxycycline (Dox). Mitochondria of Dox-treated (+ Dox) and untreated (- Dox) cells were isolated and analyzed by BN-PAGE and western blotting. Complex formation was studied by immunodecoration with antibodies against CHCHD3 (A), mitofilin (B) and Sam50 (C), and SDHA as a control. SDHA: subunit A flavoprotein of complex II.

To confirm that Sam50 and mitofilin are present in a complex with CHCHD3 and therefore influence CHCHD3 complex assembly, ³⁵S-labeled CHCHD3 was *in vitro* imported into mitochondria of Dox-induced and non-induced *sam50kd-2* and *mflkd-2* cells (Figure 3-16A, B). Both in Sam50- and mitofilin-depleted mitochondria, assembly of CHCHD3 into the holo-MIB complex was significantly reduced, confirming that indeed a connection between CHCHD3 and the other two proteins exists. Next, *in vitro* import of ³⁵S-labeled CHCHD3 into mitochondria of Dox-induced and non-induced metaxin 2 knockdown (*mtx2kd-2*) cells was performed to elucidate whether the reduced CHCHD3-containing complex assembly in Sam50-depleted cells can be attributed to a defect of the SAM complex function. Metaxin 2 (Mtx2) is a component of the SAM complex (Kozjak-Pavlovic et al., 2007). The experiments, however, demonstrated that Mtx2 is not required for assembly of CHCHD3 into the complex (Figure 3-16C). This indicates that Sam50 influences CHCHD3 assembly independently of its role in the SAM complex. In addition, ³⁵S-labeled CHCHD3 was *in vitro* imported into mitochondria of Tom40-depleted cells to exclude that the reduced CHCHD3 assembly in Sam50-depleted cells was a consequence of decreased Tom40 levels, and therefore of reduced CHCHD3 import. The experiment showed that assembly of ³⁵S-labeled CHCHD3 was not affected in mitochondria with decreased Tom40 levels (Figure 2-16D). Thus, CHCHD3 assembly is specifically connected to Sam50 and mitofilin levels, supporting the assumption that these three proteins are present in one complex.

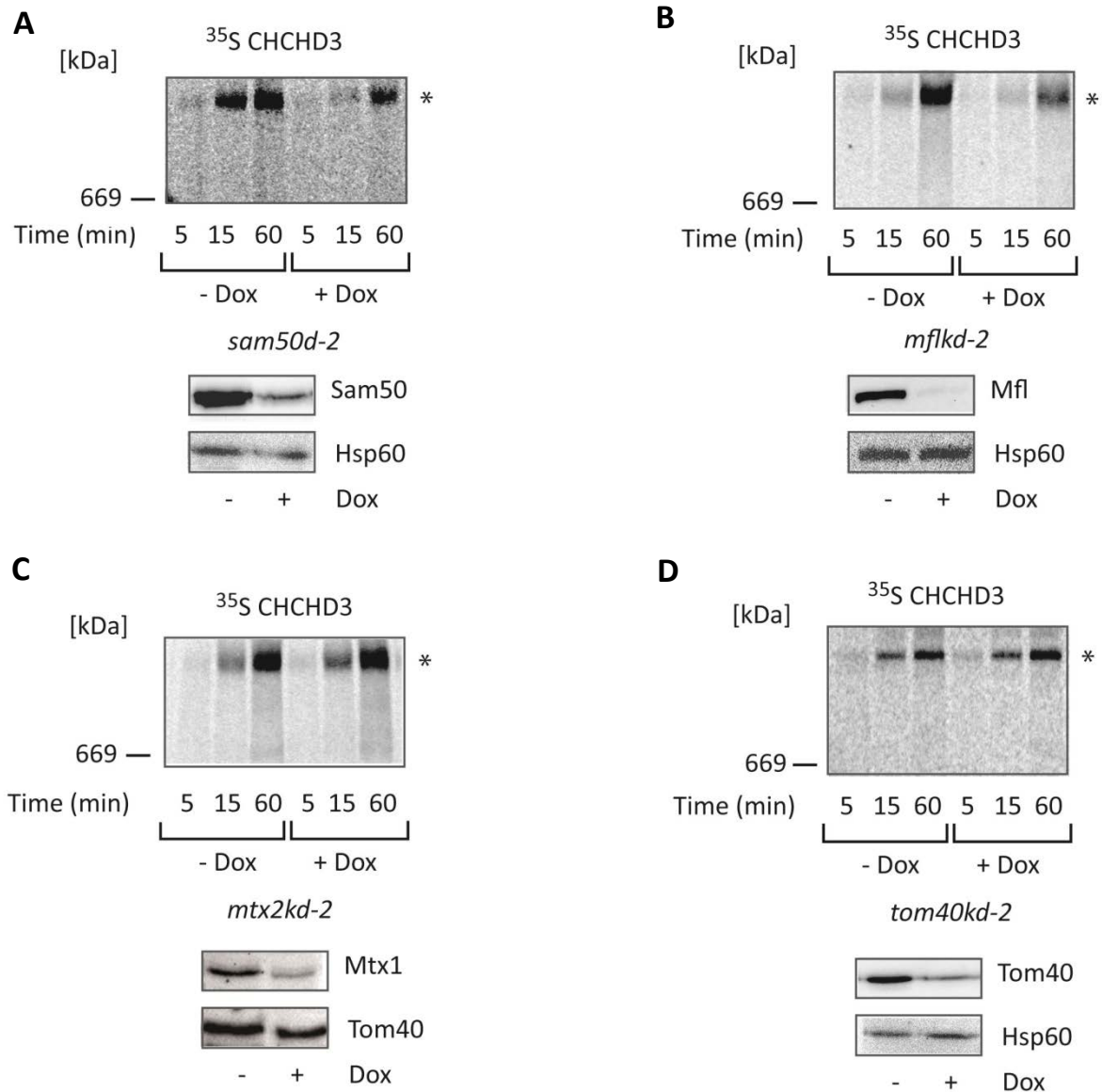


Figure 3-16 CHCHD3 assembly depends on Sam50 and mitofilin levels. CHCHD3 was labeled by transcription/translation *in vitro* in the presence of [^{35}S]methionine/[^{35}S] cysteine. Mitochondria were isolated from *sam50kd-2* (A), *mflkd-2*(B) and *mtx2kd-2* (C) cells were grown for 7 days and *tom40kd-2* (D) cells were grown for 5 days in the absence (- Dox) or presence (+ Dox) of doxycycline, and mixed with ^{35}S -labeled CHCHD3 for the indicated time points. Mitochondria were solubilized in 1% digitonin and analyzed by BN-PAGE and autoradiography. The asterisk marks the holo-MIB complex. This figure was first published in Ott et al., 2012. Copyright © 2012, American Society for Microbiology.

3.2.3 CHCHD6 and DnaJC11 are peripheral components of the MIB complex

Apart from Sam50, CHCHD3, and the metaxins, Xie and co-workers reported CHCHD6 and DnaJC11 to be present in a complex with mitofilin (Xie et al., 2007). Therefore, I aimed to investigate the connection of these proteins to the MIB complex and their function in the maintenance of cristae structure.

CHCHD6, like CHCHD3, has a predicted myristoylation site at its N-terminus and a coiled-coil-helix-coiled-coil-helix domain with a twin CX₉C motif at its C-terminus (An et al, 2012). It has a predicted size of 26.5 kDa. DnaJC11 possesses a DnaJ domain in its N-terminal region and is present in three isoforms of around 64 kDa, 57 kDa and 35 kDa (Figure 3-17A). The sequences of isoforms 1 and 2 are identical except for isoform 2 lacking amino acids 367 to 418 of isoform 1. Interestingly, this region includes the only predicted transmembrane domain of DnaJC11 isoform 1. Isoform 3 lacks the 22 N-terminal amino acid residues of the other two isoforms. Its first 234 identical amino acids are identical to the sequence of the other isoforms, but it differs in its 84 C-terminal amino acids. Like isoform 2, it has no predicted transmembrane domain.

Whereas CHCHD6 is described to be an IMM-associated protein (An et al., 2012), nothing is known about the submitochondrial localization of DnaJC11. Therefore, I first tested the membrane extractability of DnaJC11 by carbonate extraction experiments to elucidate whether it is membrane-integrated or soluble. Analysis of the mitochondrial fractions by SDS-PAGE and western blotting demonstrated that the 64 kDa isoform of DnaJC11 was present in the supernatant fraction, whereas the 57 kDa isoform was found in the membrane fraction (Figure 3-17B). The 35 kDa isoform could not be detected with the antibody.

Next, I aimed to determine the submitochondrial localization of the DnaJC11 isoforms by swelling experiments. Mitochondria were incubated either in hypotonic buffer to induce swelling of mitochondria and rupturing of the OMM, or in isotonic buffer, in which mitochondria remained intact, with or without proteinase K (PK) treatment. Additionally, a portion of mitochondria was completely lysed by incubation in 1% triton and PK treatment. Analysis of the mitochondria by SDS-PAGE and western blotting demonstrated that the 64 kDa isoform of DnaJC11 could be degraded by PK even when mitochondria were intact, as the OMM protein Tom20, suggesting that the protein is localized in the OMM. The 35 kDa isoform of DnaJC11 remained protected from PK treatment when mitochondria were intact but could be degraded when the OMM was ruptured, like the IMM protein mitofilin (Figure 3-17C). This isoform is therefore localized in the IMS or IMM. The 57 kDa isoform could not be detected with the antibody against DnaJC11.

A

Isoform 1	MATALSEEELDNEDYYSLLNVRREASSEELKAAAYRRLCMLYHPDKHRDPELKSQAERLFN	60
Isoform 2	MATALSEEELDNEDYYSLLNVRREASSEELKAAAYRRLCMLYHPDKHRDPELKSQAERLFN	60
Isoform 3	-----MLYHPDKHRDPELKSQAERLFN	22
Isoform 1	LVHQAYEVLSDPQTRAIYDIYGKRGLEMEGWVVERRRTPAEIREEFERLQREEREERLQ	120
Isoform 2	LVHQAYEVLSDPQTRAIYDIYGKRGLEMEGWVVERRRTPAEIREEFERLQREEREERLQ	120
Isoform 3	LVHQAYEVLSDPQTRAIYDIYGKRGLEMEGWVVERRRTPAEIREEFERLQREEREERLQ	82
Isoform 1	QRTNPKGTISVGVDATDLFDYDEEYEDVSGSSFPQIEINKMHISQSIEAPLTATDTAIL	180
Isoform 2	QRTNPKGTISVGVDATDLFDYDEEYEDVSGSSFPQIEINKMHISQSIEAPLTATDTAIL	180
Isoform 3	QRTNPKGTISVGVDATDLFDYDEEYEDVSGSSFPQIEINKMHISQSIEAPLTATDTAIL	142
Isoform 1	SGSLSTQNGNGGGSINFALRRVTSAKGWGELEFGAGDLQGPFGLKLFRLNLTTPRCFVTTN	240
Isoform 2	SGSLSTQNGNGGGSINFALRRVTSAKGWGELEFGAGDLQGPFGLKLFRLNLTTPRCFVTTN	240
Isoform 3	SGSLSTQNGNGGGSINFALRRVTSAKGWGELEFGAGDLQGPFGLKLFRLNLTTPRCFVTTN	202
Isoform 1	CALQFSSRGIRPGLTTLVARNLDKNTVGYLQWRWGIQSAMNTSIVRDTKTSHFVALQLG	300
Isoform 2	CALQFSSRGIRPGLTTLVARNLDKNTVGYLQWRWGIQSAMNTSIVRDTKTSHFVALQLG	300
Isoform 3	CALQFSSRGIRPGLTTLVARNLDKNTVGYLQWRWGIQSAMNTSIVRDTKTSHFVALQLG -----HCSSPLLQVQRPHRNTRACAPEPSFRFF	262
Isoform 1	IPHSFALISYQHKFQDDQTRVKGSLKAGFFGTVVEYGAERKISRHSVLGAAVSVGVPPQ	360
Isoform 2	IPHSFALISYQHKFQDDQTRVKGSLKAGFFGTVVEYGAERKISRHSVLGAAVSVGVPPQ	360
Isoform 3	LHVPTWDAECSGARTPSTAWTSAAVKLREACLSGPGSGSHQLLLLTPRSKRRTGGG----	318
Isoform 1	VSLKVKLNRSQTYFFPIHLTDQLLPSAMFYATVGPLVVYFAMHRLI IKPYLRAQKEKEL	420
Isoform 2	VSLKVK-----EL	368
Isoform 3	-----	
Isoform 1	EKQRESAATDVLQKKQEAESAVRLMQESVRRRIEAEESRMGLIIVNAWYKGFVNDKSRKS	480
Isoform 2	EKQRESAATDVLQKKQEAESAVRLMQESVRRRIEAEESRMGLIIVNAWYKGFVNDKSRKS	428
Isoform 3	-----	
Isoform 1	EKVKVIDVTVPLQCLVKDSKLILTEASKAGLPGFYDPCVGEENLKVLYQFRGVLHQVMV	540
Isoform 2	EKVKVIDVTVPLQCLVKDSKLILTEASKAGLPGFYDPCVGEENLKVLYQFRGVLHQVMV	488
Isoform 3	-----	
Isoform 1	LDSEALRIPKQSHRIDTDG	559
Isoform 2	LDSEALRIPKQSHRIDTDG	507
Isoform 3	-----	

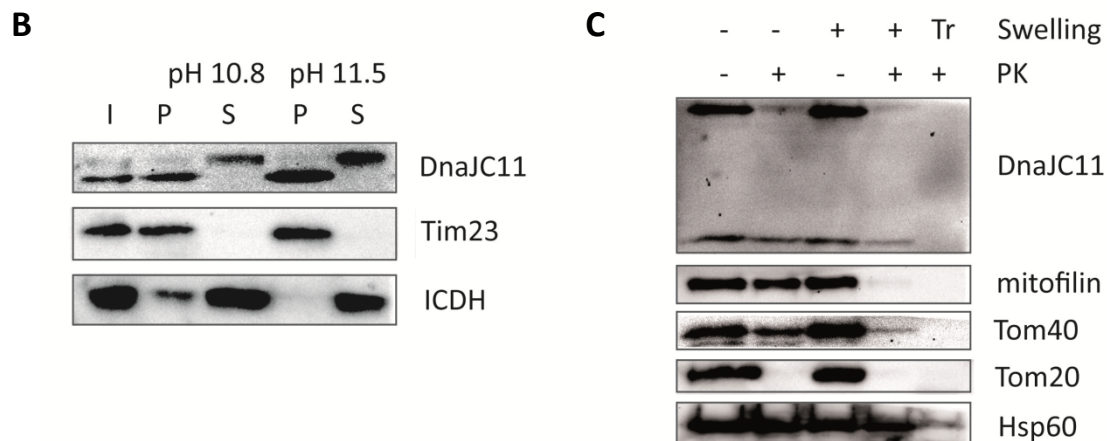


Figure 3-17 DnaJC11 isoforms are localized in the OMM and the IMS/IMM. (A) Sequence of DnaJC11 isoforms. The dotted line marks the point from where on isoform 3 differs from the other isoforms (B) Mitochondria were solubilized in 0.1 M Na_2CO_3 pH10.8 and 0.1 M Na_2CO_3 pH11.5, and membrane (P) and soluble (S) fraction were analyzed by SDS-PAGE and western blotting. (C) Mitochondria were incubated in isotonic (- Swelling) or hypotonic (+ Swelling) buffer, and treated with Proteinase K (+ PK) or left untreated (- PK). A portion of mitochondria was completely solubilized in 1 % triton (Tr) and subsequently treated with PK. Samples were analyzed by SDS-PAGE followed by western blotting. I: Protein input; ICDH: isocitrate dehydrogenase; Tim23: subunit of the Translocase of the Inner Membrane; Hsp60: mitochondrial heat shock protein.

In order to examine whether CHCHD6 and DnaJC11 are affected by the loss of MIB components, *sam50kd-2*, *mflkd-2* and *chchd3kd-2* cells were treated with Dox for 7 and 14 days to induce protein knockdown. Mitochondria of Dox-treated and untreated cells were isolated and analyzed by SDS-PAGE and western blotting (Figure 3-18). Immunodecoration with an antibody against CHCHD6 showed that this protein was lost almost completely in mitofilin-depleted cells, whereas CHCHD6 levels were not altered by Sam50 or CHCHD3 reduction. DnaJC11 levels, on the other hand, were only significantly affected in mitochondria lacking Sam50. Mitofilin loss led to a slight decrease in DnaJC11 levels, whereas CHCHD3 depletion did not affect DnaJC11 levels.

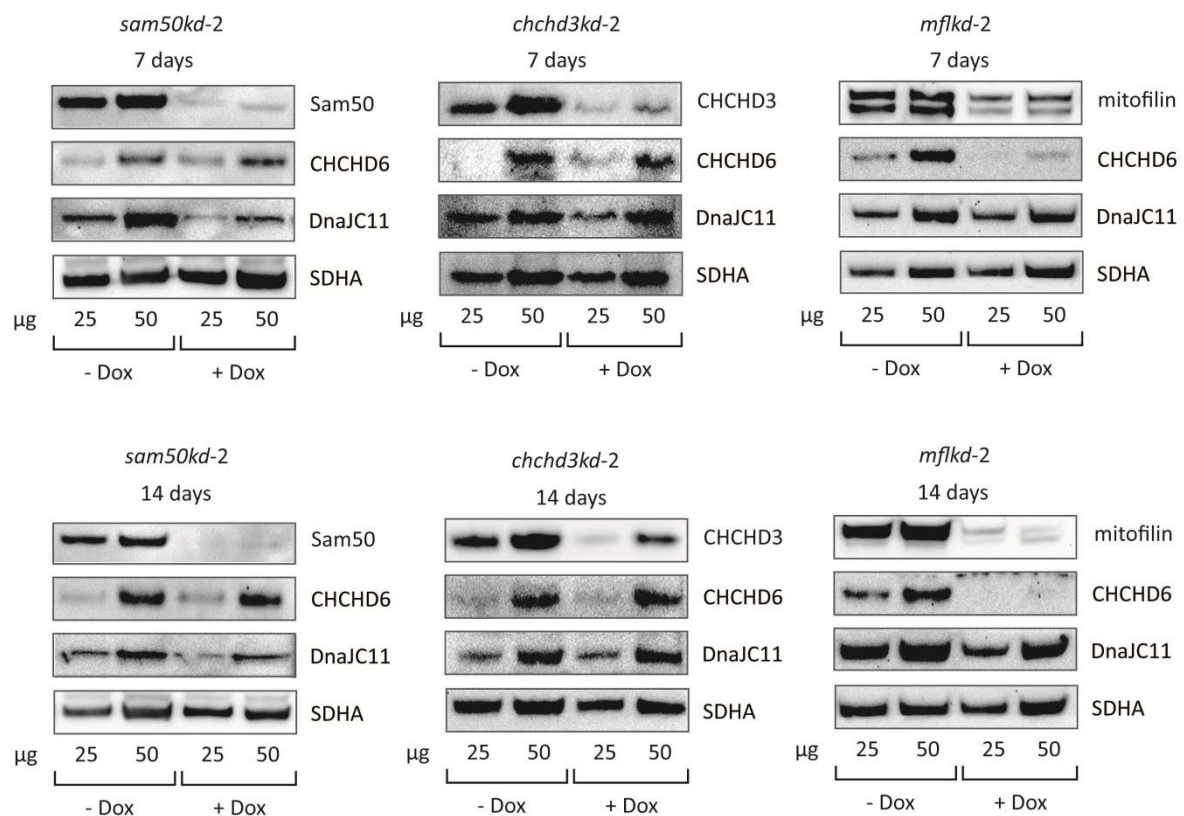


Figure 3-18 Knockdown of MIB components influences CHCHD6 and DnaJC11 levels. Knockdown was induced in *sam50kd-2*, *mflkd-2* and *chchd3kd-2* cells for 7 and 14 days by the addition of doxycycline (Dox). Mitochondria of Dox-induced and non-induced cells were isolated, and 25 µg and 50 µg of mitochondrial protein were analyzed by SDS-PAGE and western blotting.

In order to be able to study the function of CHCHD6 and DnaJC11, I produced the inducible shRNA-mediated knockdown cell lines *chchd6kd-3* and *dnajc11kd-3*. The siRNA utilized for DnaJC11 knockdown only targets the 64 kDa isoform of DnaJC11, which I predominantly found when I analyzed mitochondria by SDS-PAGE and western blotting. With the help of these knockdown cell lines, the influence of CHCHD6 and DnaJC11 on the other MIB components was examined. Knockdown of the respective protein was induced for 7 days by the addition of Dox, and

mitochondria of Dox-induced and non-induced cells were isolated. Subsequently, mitochondria were analyzed by SDS-PAGE followed by western blotting. Immunodecoration with antibodies against the MIB complex components Sam50, mitofilin, CHCHD3, CHCHD6 and DnaJC11 demonstrated that both CHCHD6 and DnaJC11 depletion did not affect the levels of other MIB complex components (Figure 3-19).

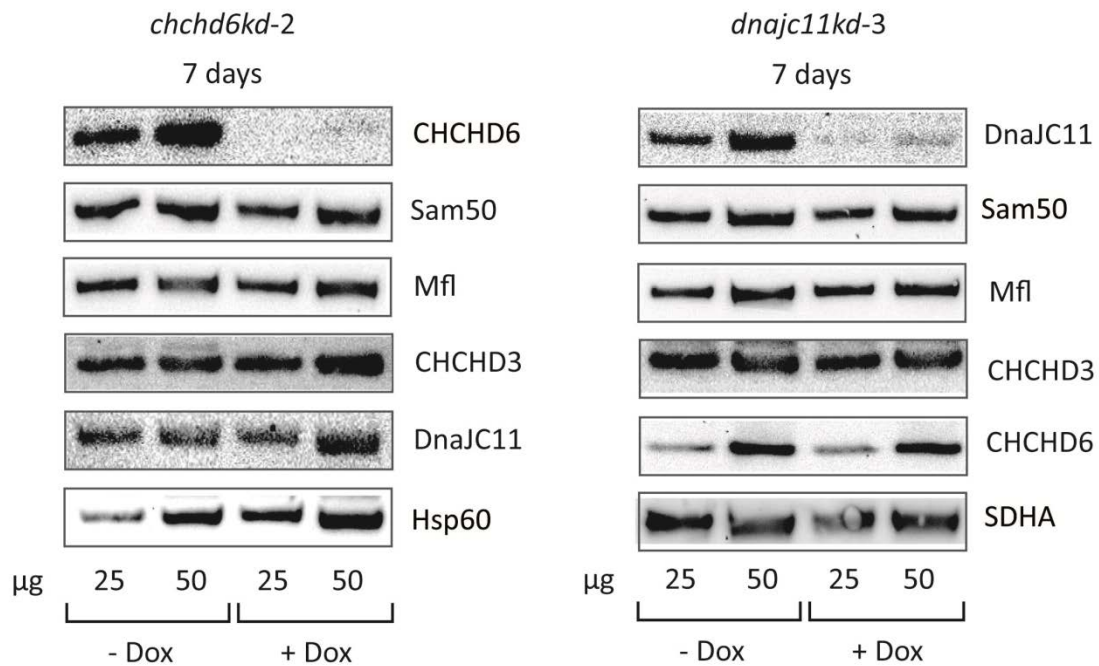


Figure 3-19 CHCHD6 and DnaJC11 do not affect the levels of other MIB components. Mitochondria of doxycycline-induced (+ Dox) and non-induced (- Dox) *chchd6kd-3* and *dnajc11kd-3* cells were isolated and analyzed by SDS-PAGE and western blotting. Hsp60: mitochondrial heat-shock protein, SDHA: subunit A flavoprotein of complex II.

As depletion of Sam50, mitofilin, and CHCHD3 resulted in loss of mitochondrial cristae structure, I aimed to elucidate whether CHCHD6 and DnaJC11 are also required for the maintenance of cristae morphology. Analysis of CHCHD6- and DnaJC11-depleted cells by transmission electron microscopy (TEM), however, showed that these two proteins do not exercise a pronounced effect on cristae morphology (Figure 3-20), suggesting that these two proteins probably are only peripheral components of the MIB complex.

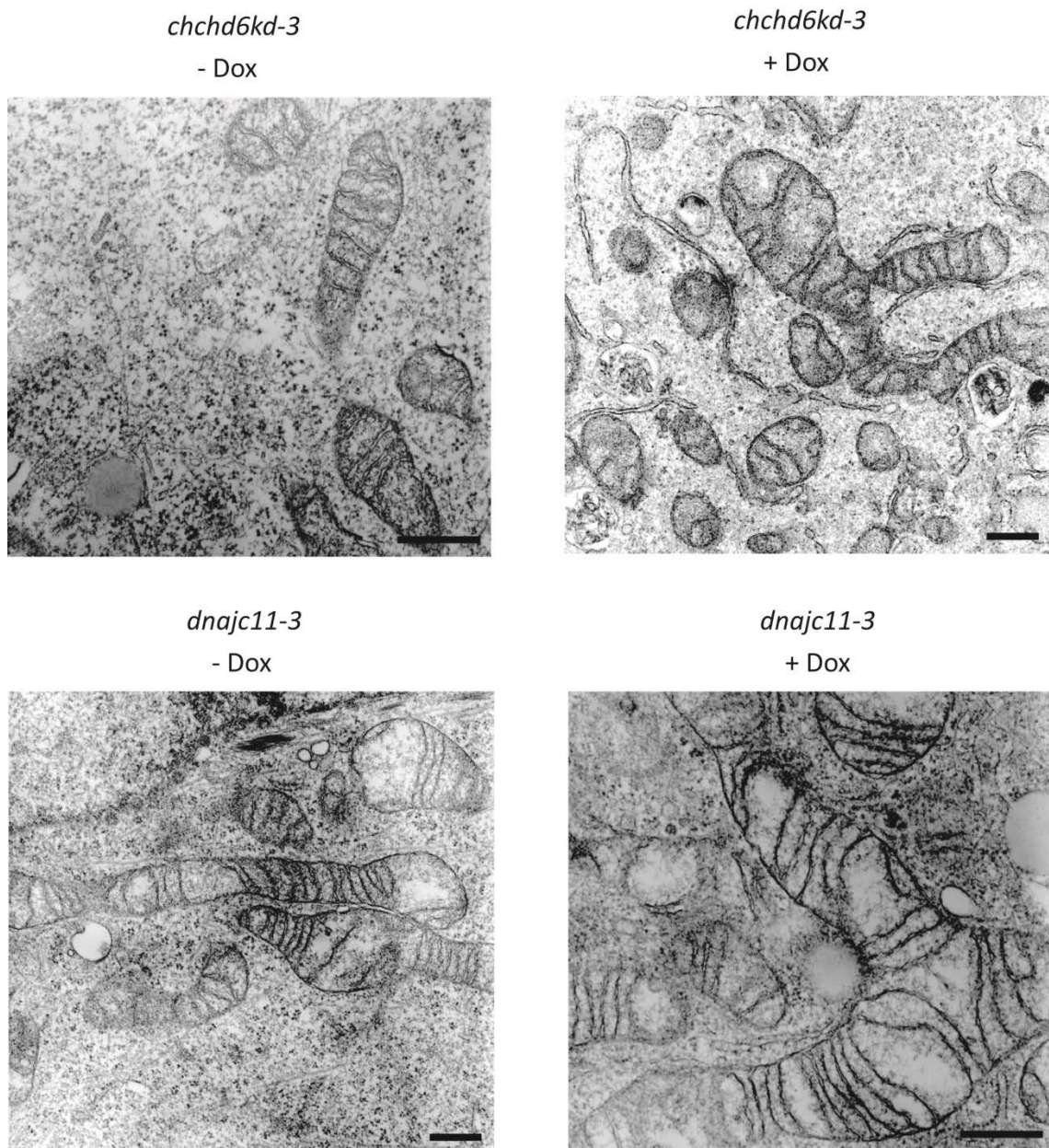


Figure 3-20 Knockdown of CHCHD6 or DnaJC11 does not influence cristae structure. Knockdown of CHCHD6 or DnaJC11 was induced in *chchd6kd-3* or *dnajc1kd1-3* cells for 7 days by the addition of doxycycline (Dox), and Dox-treated (+ Dox) and untreated (- Dox) cells were analyzed by TEM. Scale bars represent 1 μm.

3.3 Sam50 influences the assembly of the respiratory chain

In order to elucidate which proteins are affected by Sam50 reduction, a SILAC experiment with Sam50-depleted cells was previously performed (Ott et al., 2012). *sam50kd-2* cells were labeled by growth in $^{13}\text{C}_6$ L-lysine/L-arginine-containing medium, and knockdown was induced by Dox addition in the unlabeled cells. Quantitative mass spectrometry analysis showed that, apart from the Sam50 substrates Tom40 and VDAC and the SAM complex component metaxin 1, protein levels of subunits of respiratory chain complexes I and IV were reduced. Western blot analysis confirmed a reduction in the levels of respiratory complex I subunit NDUFS1 and respiratory complex IV subunit COX2 when Sam50 was depleted for 7 days, and additionally a reduction in respiratory complex III subunit Core1 level after 21 days of Sam50 knockdown induction. The levels of complex II subunit SDHA, complex III subunit cyt c, and complex V subunit F1 α were not altered (Ott et al., 2012). Depletion of mitofilin for 7 days only showed a reduction of NDUFS1, whereas after 21 days of knockdown induction also COX2 levels were strongly reduced (Ott et al., 2012). BN-PAGE analysis of Sam50-depleted mitochondria showed decreased complex I and IV levels (Ott et al., 2012).

To further study the effect of Sam50 and mitofilin depletion and to confirm the findings of the western blot analysis performed in our group, *in vitro* imported ^{35}S -labeled NDUFS1 and COX6A precursors into mitochondria isolated from Dox-induced and non-induced *sam50-kd2* and *mflkd-2* cells. In both Sam50- and mitofilin-depleted mitochondria, complex I and complex IV assembly were reduced (Figure 3-21A, B). Next, import experiments with mitochondria of Mtx2-depleted cells were performed. As the β -barrel assembly function of the SAM complex is impaired after depletion of Mtx2, whereas Sam50 and mitofilin levels are unaltered, these mitochondria were used to examine whether there is a connection between the assembly of β -barrel proteins by the SAM complex and the function of Sam50 in respiratory complex I and IV assembly. Mtx2 depletion exerted no effect on complex IV assembly and led only to a mild reduction in complex I assembly. (Figure 3-21C). As Tom40 levels are also reduced upon Sam50 depletion (Kozjak-Pavlovic et al., 2007; Ott et al., 2012), import experiments with mitochondria of *tom40kd-2* cells were performed additionally to exclude that the reduction in respiratory complex I and IV assembly is due to reduced protein import into mitochondria. Analysis of mitochondria by BN-PAGE and autoradiography, however, demonstrated that Tom40 depletion does not influence respiratory complex I and IV assembly (Figure 3-21D).

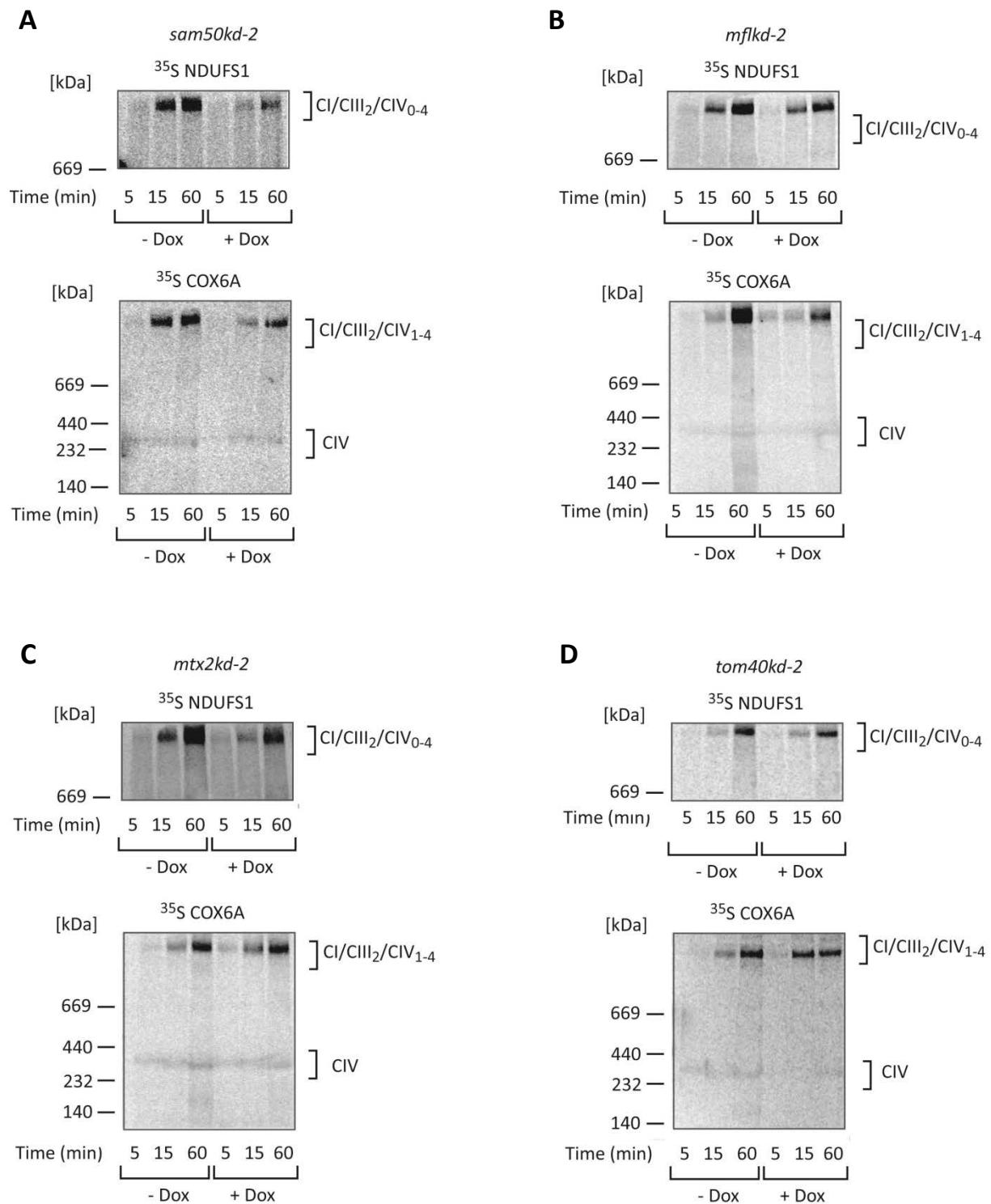


Figure 3-21 Assembly of respiratory complexes I and IV is impaired in Sam50- and mitofilin-depleted mitochondria. *sam50kd-2* (A), *mflkd-2* (B) and *mtx2kd-2* (C) cells were grown for 7 days and *tom40kd-2* cells (D) were grown for 5 days in the presence (+ Dox) or absence (- Dox) of doxycycline. Mitochondria were isolated and mixed with ³⁵S-labeled NDUFS1 or COX6A in BSA import buffer for the indicated time points. Mitochondria were solubilized in 1 % digitonin and analyzed by BN-PAGE and autoradiography. This figure was first published in Ott et al., 2012. Copyright © 2012, American Society for Microbiology.

Finally, ^{35}S -labeled ferredoxin and F1 β were *in vitro* imported into Sam50-depleted mitochondria to exclude that a reduction of Sam50 leads to a general import deficiency. Analysis of import samples by SDS-PAGE and autoradiography, however, showed that loss of Sam50 did not affect the import of ferredoxin and F1 β (Figure 3-22). Therefore, reduced complex I and IV assembly in Sam50-depleted mitochondria cannot be explained by a general impairment of protein import.

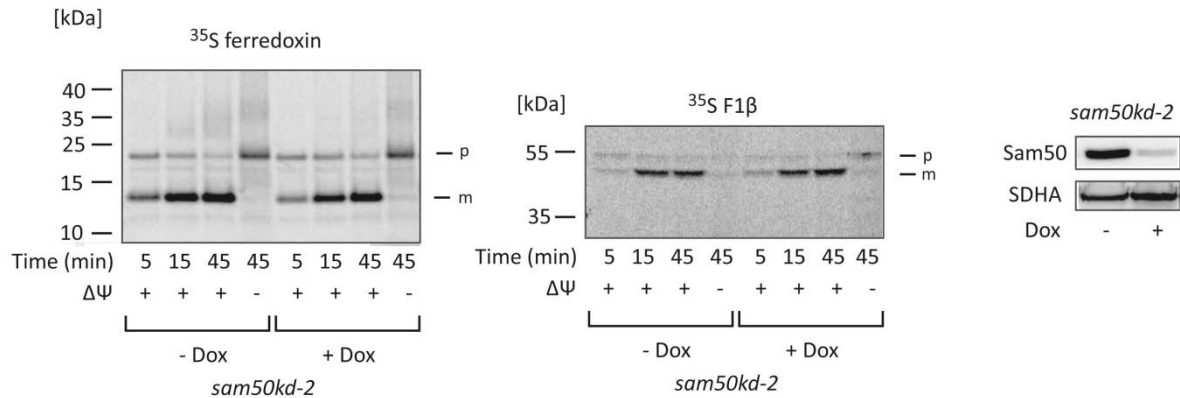


Figure 3-22 Import of ferredoxin and F1 β is not affected by Sam50 depletion. Ferredoxin and F1 β were labeled by transcription/translation *in vitro* in the presence of [^{35}S]methionine/[^{35}S] cysteine. ^{35}S -labeled proteins were imported into mitochondria of *sam50kd-2* cells grown in the absence (- Dox) or presence of doxycycline (+ Dox) for 7 days. Mitochondria were analyzed by SDS-PAGE and autoradiography. As a control for Sam50 knockdown, 50 μg of mitochondria were analyzed by SDS-PAGE and western blotting. This figure was first published in Ott et al., 2012. Copyright © 2012, American Society for Microbiology.

To test whether reduction in complex I and IV subunits was the result or the cause of the depletion of MIB components, I created the NDUFS1 knockdown cell line *ndufs1kd-1*. Additionally, the COX5A knockdown cell line *cox5akd-2* was created in our group (Ott et al., 2012). Western blot analysis showed that neither Sam50 nor mitofilin or CHCHD3 were reduced upon NDUFS1 or COX5A depletion (Figure 3-23 and Ott et al., 2012), and EM studies revealed no changes in cristae structure (Ott et al., 2012). These experiments confirmed that the reduction of respiratory chain complexes is a consequence and not the cause of Sam50 or mitofilin loss.

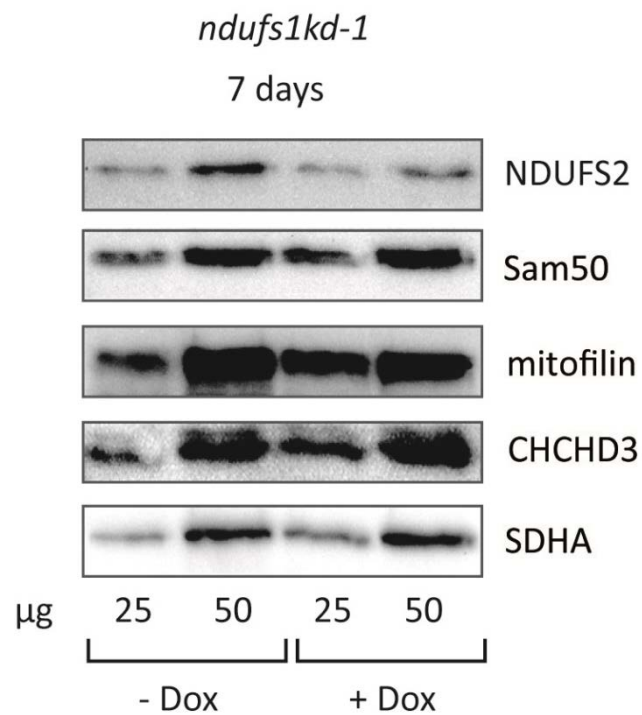


Figure 3-23 Sam50, mitofilin and CHCHD3 levels are not altered in NDUFS1-depleted mitochondria. Mitochondria of *ndufs1kd-1* cells were isolated after growth in the absence (- Dox) or presence (+ Dox) of doxycycline for 7 days, and analyzed by SDS-PAGE and western blotting.

3.4 The MIB complex is connected to the tetratricopeptide 19 protein (TTC19)

3.4.1 TTC19 is localized to mitochondria in HeLa cells

Our data of the SILAC experiment performed with mitochondria where Sam50 had been depleted revealed not only a reduction in the levels of respiratory complex subunits but also of TTC19 in the absence of Sam50. A similar SILAC analysis performed with mitofilin-depleted cells showed a downregulation of TTC19 as well after reduction of mitofilin levels (Vera Kozjak-Pavlovic, unpublished data). TTC19 is present in the cell in two isoforms (Figure 3-24A). Isoform 1 has a length of 380 amino acid residues and a predicted N-terminal mitochondrial targeting sequence of 69 amino acids. Isoform 2 comprises the 273 C-terminal amino acid residues of isoform 1 and does not have an N-terminal mitochondrial targeting signal.

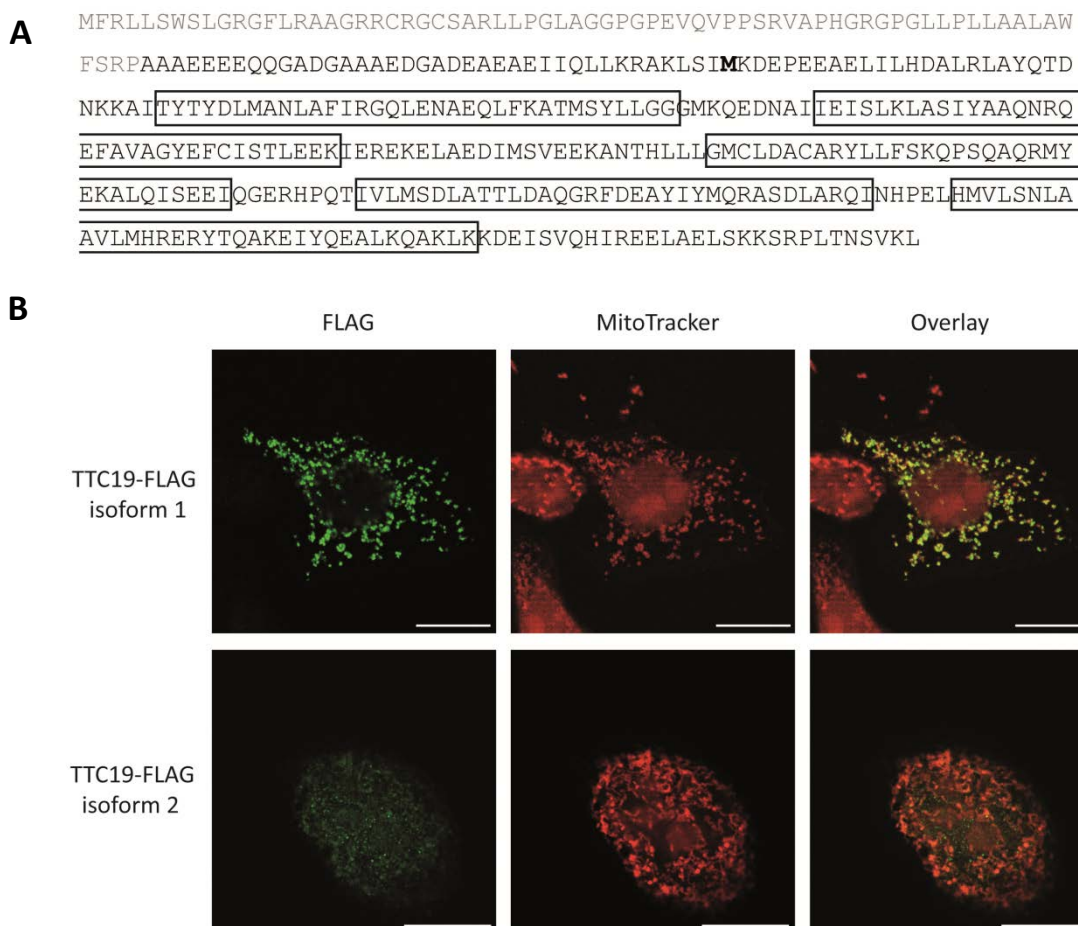


Figure 3-24 Isoform 1 of TTC19 is targeted to mitochondria. (A) Sequence of TTC19 isoform 1; the sequence of isoform 2 starts with the bold M. The predicted N-terminal mitochondrial targeting sequence of isoform 1 is marked in gray (Claros and Vincens, 1996) and the five predicted tetratricopeptide repeat domains are framed with boxes. (B) The genes for TTC19 isoform 1 and isoform 2 were cloned into the pcDNA3 vector introducing a C-terminal FLAG-tag. The protein constructs were expressed in HeLa cells, followed by staining with MitoTracker and an antibody against the FLAG-tag. Samples were analyzed by confocal microscopy. Scale bars represent 100 μ m.

Isoform 1 of TTC19 was recently demonstrated to be an IMM protein involved in respiratory complex III assembly (Ghezzi et al., 2011). As TTC19 was also shown to be localized to the nucleus, playing a role in regulation of cytokinesis (Sagona et al., 2010), I first aimed to confirm the mitochondrial localization of TTC19. Therefore, the genes encoding isoform 1 and isoform 2 of TTC19 were cloned into the pcDNA3 vector introducing a C-terminal FLAG-tag, and the constructs were expressed in HeLa cells. Subsequently, the cells were stained with MitoTracker and an antibody against the FLAG-tag. Analysis by confocal microscopy confirmed the mitochondrial localization of isoform 1 of TTC19 reported by Ghezzi and co-workers (Figure 3-24B). Isoform 2 of TTC19, on the other hand, was not imported into mitochondria.

3.4.2 TTC19 is reduced in mitochondria of Sam50- and mitofilin-depleted cells

After confirming the mitochondrial localization of TTC19 isoform 1, I next tested whether loss of Sam50 results in reduced TTC19 protein levels. Knockdown of Sam50 was induced in *sam50kd-2* cells by Dox addition. Mitochondria were isolated after 7 and 14 days of knockdown induction and analyzed by SDS-PAGE followed by western blotting (Figure 3-25A). Immunodecoration with an antibody against TTC19 confirmed a reduction in TTC19 levels in mitochondria of Sam50-depleted cells. Next, TTC19 levels were examined in mitochondria of Dox-treated or untreated *mflkd-2*, *chchd3kd-2*, *chchd6kd-3* and *dnajc11kd-3* cells. Western blot analysis demonstrated that in mitochondria of CHCHD3-, CHCHD6- and DnaJC11-depleted cells, the levels of TTC19 were not altered (Figure 3-25B). In the mitochondria of mitofilin-depleted cells, on the other hand, TTC19 levels were reduced (Figure 3-25B). This shows that reduction of TTC19 upon Sam50 knockdown cannot be explained as a consequence of impaired protein import due to Tom40 reduction, as mitochondria of mitofilin-depleted cells have reduced Sam50 but normal Tom40 levels (Ott et al., 2012). To additionally exclude that the reduction of TTC19 in mitochondria of Sam50-depleted cells was a consequence of reduced Tom40 levels, TTC19 levels were also examined in mitochondria of *tom40kd-2* cells, in which knockdown of Tom40 was induced by Dox addition for 5 days. Analysis of mitochondria by SDS-PAGE and western blotting demonstrated that Tom40 depletion did not affect TTC19 levels (Figure 3-25C). Finally, in order to exclude that TTC19 reduction was a side-effect of Dox treatment, *PLVTHM* cells, which possess the empty pLVTHM vector without a sequence coding for an shRNA, were treated with Dox for 7 days or left untreated as a control, and isolated mitochondria were analyzed by SDS-PAGE and western blotting (Figure 3-25D). TTC19 was present in equal amounts in mitochondria of Dox-treated and untreated *PLVTHM* cells, demonstrating that Dox treatment did not affect TTC19 levels.

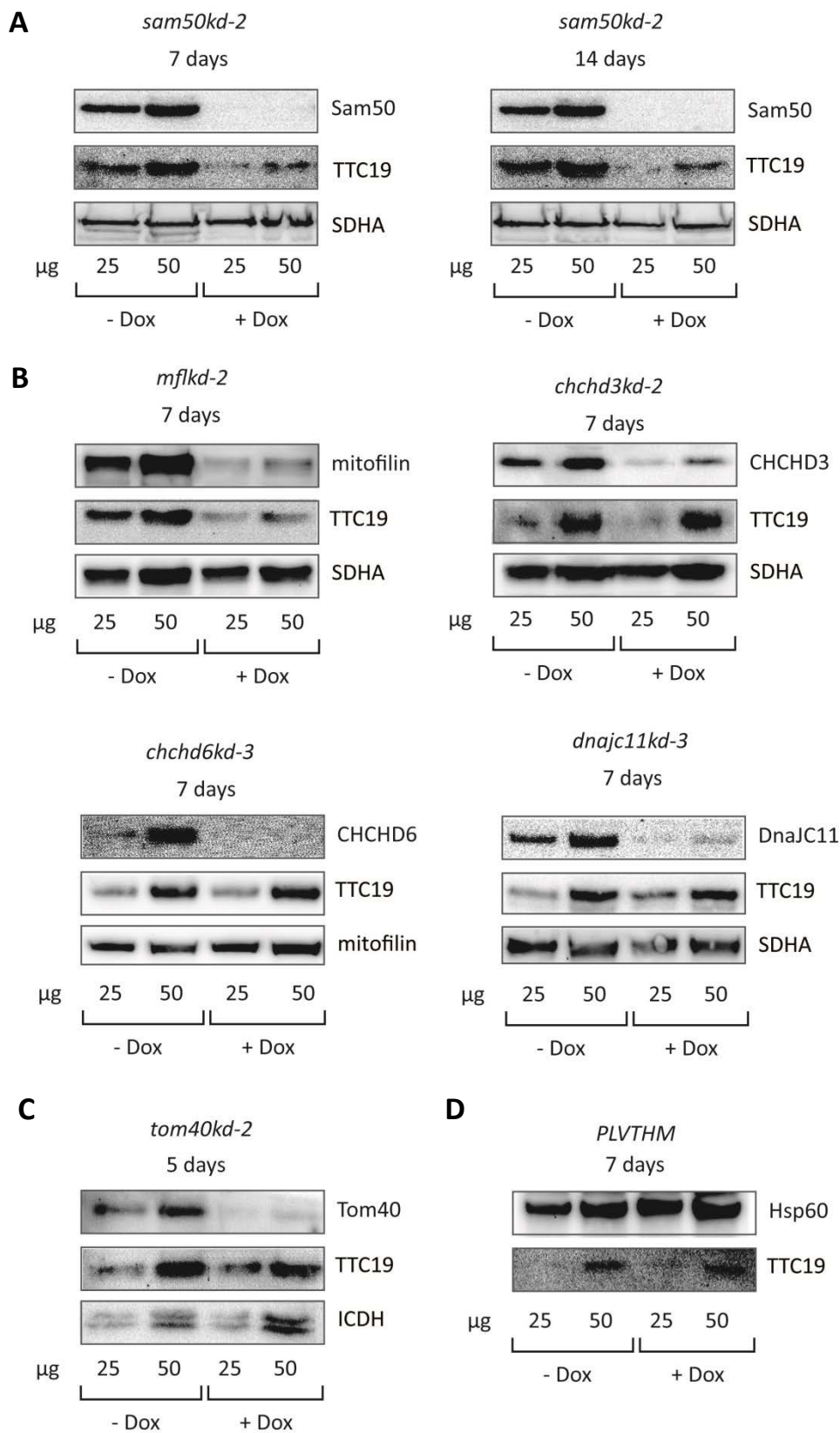


Figure 3-25 TTC19 levels are reduced in Sam50- and mitofilin-depleted cells. *sam50kd-2* (A), *mflkd-2*, *chchd3kd-2*, *chchd6kd-3*, *dnajc11kd-3* (B), *tom40kd-2* (C) and *PLVTHM* cells (D) were treated with doxycycline (Dox) for the indicated time periods. Mitochondria of non-induced (- Dox) and Dox-induced (+ Dox) cells were isolated and analyzed by SDS-PAGE and western blotting.

3.4.3 *In vitro* import studies confirm a connection between Sam50 and TTC19

To support the finding that Sam50 and mitofilin influence TTC19, *in vitro* import studies with ^{35}S -labeled TTC19 were performed. First, I tested whether isoform 1 of TTC19 can be *in vitro* imported into mitochondria of HeLa cells. For that purpose, mitochondria from HeLa cells were isolated and ^{35}S -labeled TTC19 was imported for different time points. Separation of mitochondria on SDS-PAGE followed by autoradiography showed that the precursor of TTC19 is about 45 kDa of size, and TTC19 is processed into a mature form of about 35 kDa upon import (Figure 3-26), confirming the findings of Ghezzi and colleagues (Ghezzi et al., 2011). As expected, import of ^{35}S -labeled TTC19 was not possible when $\Delta\Psi$ was disrupted, as TTC19 has an N-terminal mitochondrial targeting signal and therefore is most likely imported through the TIM23 pathway, which needs $\Delta\Psi$ to insert proteins into the IMM.

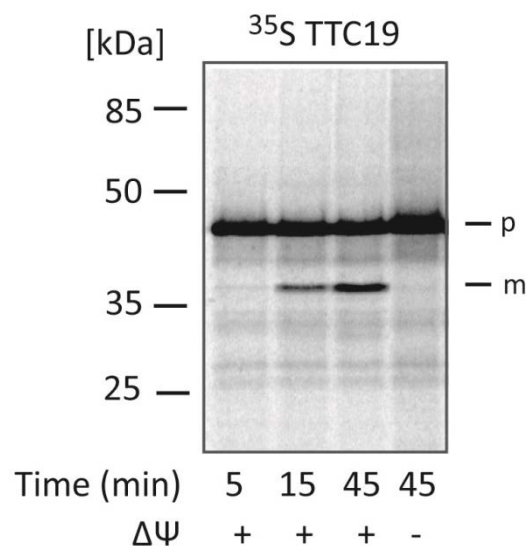


Figure 3-26 TTC19 is imported into mitochondria *in vitro*. Mitochondria isolated from HeLa cells were mixed with ^{35}S -labeled TTC19 in KAc import buffer and incubated at 37°C for the indicated time points. Membrane potential ($\Delta\Psi$) was dissipated by the addition of valinomycin and CCCP. Mitochondria were analyzed by SDS-PAGE followed by autoradiography. p: precursor; m: mature protein.

Next, I investigated the effect of Sam50 and mitofilin knockdown on the import of TTC19. I performed *in vitro* import experiments of ^{35}S -labeled TTC19 into mitochondria isolated from *sam50kd-2* and *mflkd-2* cells in which knockdown had been induced for 7 days or which had been left untreated as a control. SDS-PAGE analysis of mitochondria followed by autoradiography revealed that the import of TTC19 was reduced when Sam50 was depleted (Figure 3-27). Upon mitofilin loss, TTC19 import was also affected, but not as strongly as upon Sam50 depletion. Therefore, reduced TTC19 import upon mitofilin loss could be a consequence of decreased Sam50 levels. The fact that

TTC19 import is also reduced upon mitofilin depletion demonstrates that the impairment of TTC19 import into Sam50-depleted mitochondria cannot be explained by reduced Tom40 levels in these cells, as mitofilin knockdown for 7 days does not affect Tom40 levels (Ott et al., 2012). Besides, I could demonstrate before by *in vitro* import of ^{35}S -labeled ferredoxin and F1 β that import into Sam50-depleted mitochondria is not generally impaired (Figure 3-23). Finally, to exclude that the reduction in TTC19 import is a side-effect of Dox addition, ^{35}S -labeled TTC19 was also *in vitro* imported into mitochondria isolated from Dox-treated or untreated *PLVTHM* cells. Analysis by SDS-PAGE followed by western blotting demonstrated that import of TTC19 into mitochondria is not impaired by Dox treatment.

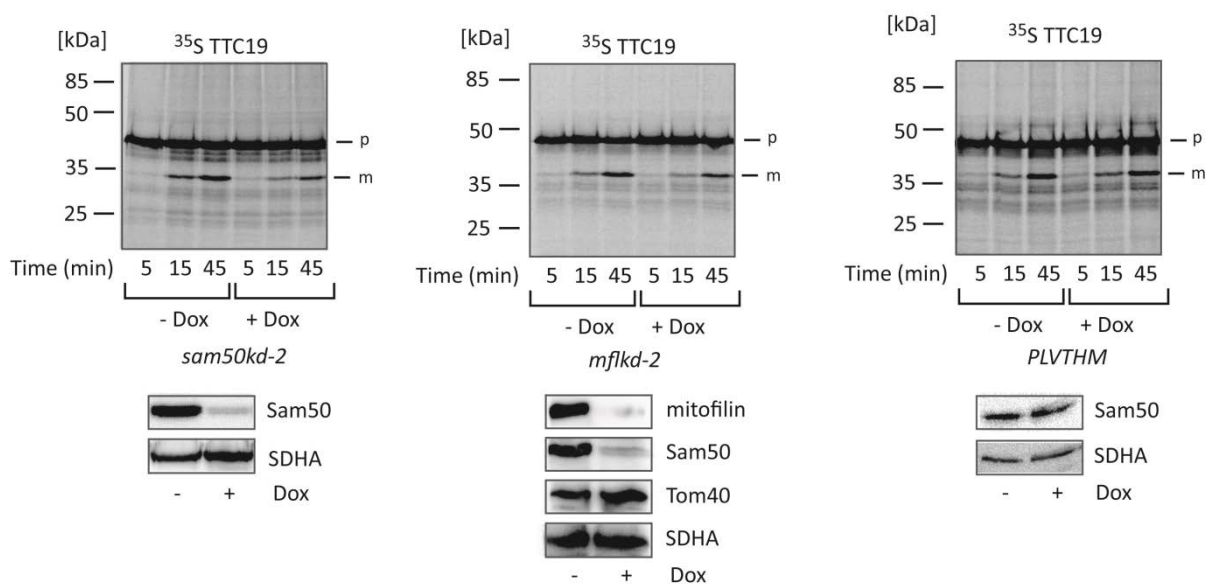


Figure 3-27 Import of TTC19 is reduced in Sam50- and mitofilin-depleted cells. ^{35}S -labeled TTC19 was mixed with mitochondria isolated from 7 days Dox-induced (+ Dox) and non-induced (- Dox) *sam50kd-2*, *mflkd-2* and *PLVTHM* cells in KAc import buffer and incubated at 37°C for the indicated time points. Mitochondria were separated by SDS-PAGE followed by autoradiography. 50 μg of mitochondria were analyzed by SDS-PAGE followed by western blotting and immunodecoration with antibodies against the downregulated protein and SDHA as a control. SDHA: subunit A flavoprotein of complex II; p: precursor; m: mature protein.

Next, complex formation of TTC19 in Sam50-depleted mitochondria was examined. ^{35}S -labeled TTC19 was imported into mitochondria of Dox-treated and untreated *sam50kd-2* cells. When analyzing the mitochondria by BN-PAGE followed by autoradiography, one TTC19 containing complex of approximately 550 – 600 kDa and two complexes of more than 1 MDa could be observed in mitochondria of non-induced *sam50kd-2* cells. Upon Sam50 depletion, the assembly of the two higher TTC19 complexes was strongly reduced, whereas the smallest complex became detectable at an earlier time point (Figure 3-28).

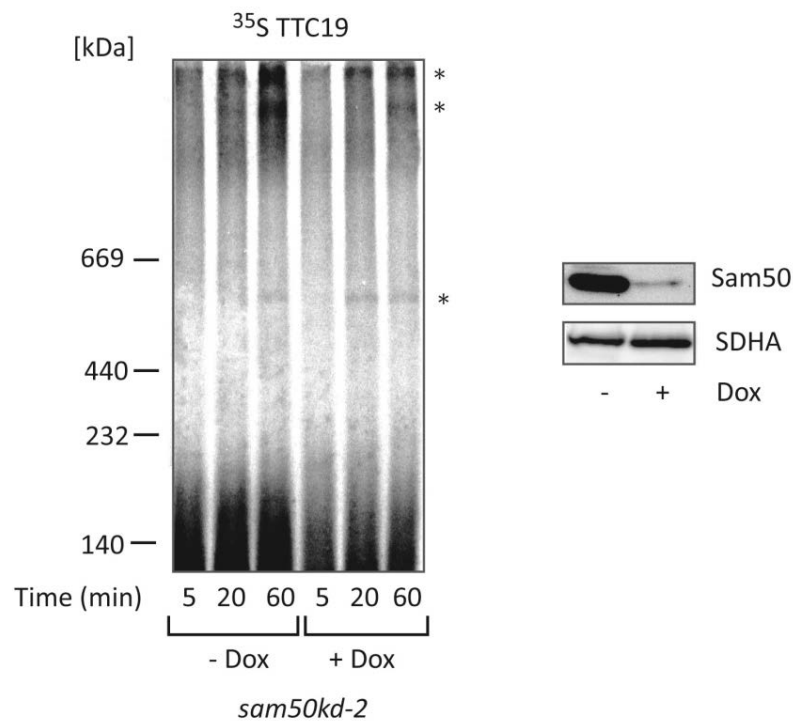


Figure 3-28 Formation of TTC19 protein complexes is altered in Sam50-depleted mitochondria. Mitochondria were isolated from *sam50kd-2* cells induced for 7 days by the addition of doxycycline (+ Dox) or left untreated (- Dox), and incubated with ^{35}S -labeled TTC19 in KAc import buffer at 37°C for the indicated time points. Mitochondria were separated by BN-PAGE followed by autoradiography. The observed complexes are marked with an asterisk. As a control for knockdown efficiency, $50\ \mu\text{g}$ of mitochondria were subjected to SDS-PAGE followed by western blotting and immunodecoration with antibodies against Sam50 and SDHA. SDHA: subunit A flavoprotein of complex II.

3.4.4 TTC19 depletion does not have an effect on MIB complex components

In order to examine whether depletion of TTC19 influences the protein levels of MIB complex components, a cell line with inducible shRNA-mediated knockdown of TTC19 (*ttc19kd-2*) was produced (by Monika Götz). Knockdown of TTC19 was induced by addition of Dox for 7 days, and mitochondria from Dox-treated and untreated cells were isolated and separated by SDS-PAGE followed by western blotting. Immunodetection using antibodies against Sam50, mitofilin, CHCHD3, CHCHD6 and DnaJC11 demonstrated that TTC19 does not influence the levels of MIB components (Figure 3-29). Therefore, TTC19 reduction is a consequence and not the cause of Sam50 or mitofilin depletion.

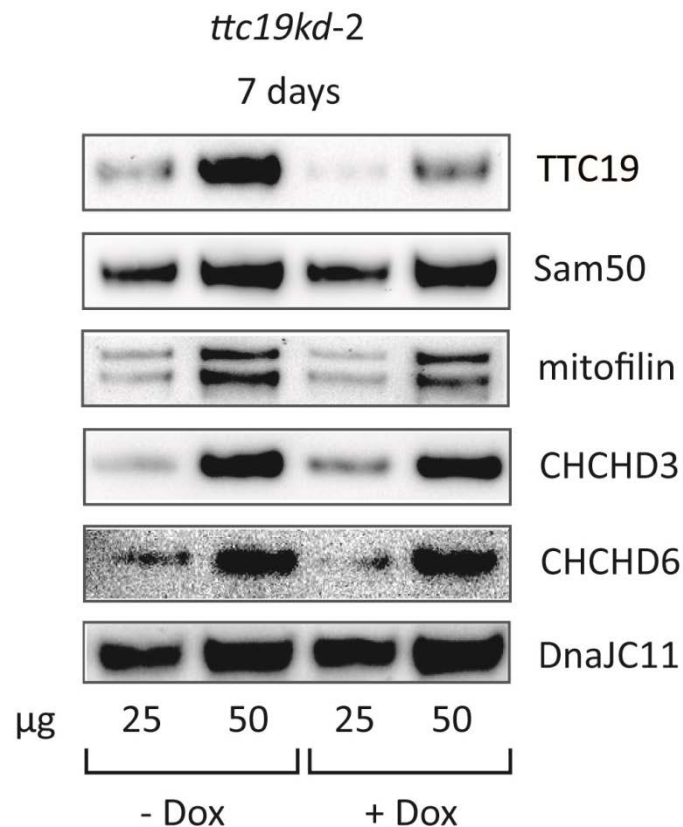


Figure 3-29 Levels of MIB components are not reduced in TTC19-depleted cells. Mitochondria of *ttc19kd-2* cells grown for 7 days in the absence (- Dox) or presence (+ Dox) of doxycycline were isolated, and analyzed by SDS-PAGE and western blotting.

3.4.5 TTC19 and MIB complex components are not present in one complex

Ghezzi and co-workers reported that TTC19 assembles into two complexes in mouse cells, one of about 500 kDa and a bigger one of more than 1 MDa. They showed that TTC19 interacts with Core1 and RISP, and therefore suggested that the smaller complex probably corresponds to respiratory complex III (Ghezzi et al., 2011). In HeLa cells, Ghezzi and co-workers could only detect the bigger more than 1 MDa complex. Interestingly, this complex was also present in 143B-derived ρ^0 cells which do not possess the four respiratory complexes that contain mitochondrially encoded (mtDNA-encoded) subunits, and therefore, they suggested that TTC19 has another function independent of its role in complex III assembly (Ghezzi et al., 2011). As I observed reduced formation of the bigger TTC19-containing complexes upon Sam50 depletion whereas the smaller complex was detectable at an earlier time point, it was intriguing to speculate that the bigger TTC19-containing complex corresponds to the MIB complex. To examine this hypothesis, co-immunoprecipitation experiments with antibodies against mitofilin, Sam50 and TTC19 were performed with mitochondria isolated from HeLa cells (Figure 3-30). However, while an interaction of Sam50 with mitofilin could be detected,

TTC19 was not immunoprecipitated with antibodies against Sam50 or mitofilin. Likewise, when precipitating TTC19-containing complexes, mitofilin could not be detected. Therefore, a direct interaction between TTC19 and Sam50 or mitofilin could not be confirmed. The presence of Sam50 could not be detected with an antibody against Sam50, as the immunoglobulin heavy chains of the antibodies migrated at a similar size as Sam50.

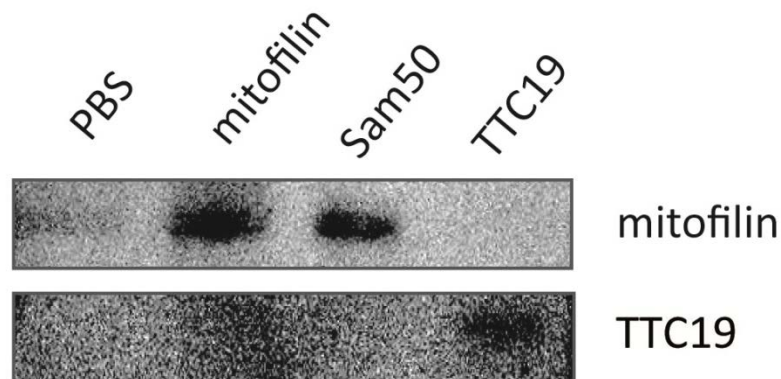


Figure 3-30 Mitofilin and Sam50 do not interact with TTC19. Mitochondria of HeLa2000 cells were solubilized in 0.75 % digitonin in lysis buffer and incubated with antibodies against mitofilin, Sam50 or TTC19 coupled to sepharose beads. The beads were subsequently analyzed by SDS-PAGE and western blotting for co-immunoprecipitated proteins.

3.5 TTC19 is involved in the assembly of respiratory chain complexes

3.5.1 SILAC analysis of TTC19-depleted cells shows an effect of TTC19 on respiratory chain complexes

In order to elucidate the consequence of TTC19 reduction, a SILAC analysis with the *ttc19kd-2* cell line was performed. *ttc19kd-2* cells were labeled by growth in $^{13}\text{C}_6$ L-lysine/ L-arginine containing medium, and knockdown was induced in unlabeled cells for nine days by Dox addition. Mitochondria of Dox-induced and non-induced cells were isolated and protein levels were analyzed by quantitative mass spectrometry (Bernd Thiede, Oslo). Table 3-1 lists the proteins which were significantly reduced upon TTC19 depletion.

Table 3-1: Proteins significantly downregulated upon TTC19 depletion

UniProt no.	Name	Mass (kDa)	Ratio (H/L)
Q6DKK2	Tetratricopeptide repeat protein 19 (TTC19)	55.80	2.6515
P03928	ATP synthase protein 8	7.99	1.8147
O95182	NADH dehydrogenase [ubiquinone] 1 alpha subcomplex subunit 7	12.55	1.6434
P17568	NADH dehydrogenase [ubiquinone] 1 beta subcomplex subunit 7	16.40	1.6329
Q9UI09	NADH dehydrogenase [ubiquinone] 1 alpha subcomplex subunit 12	17.21	1.6242
O95169	NADH dehydrogenase [ubiquinone] 1 beta subcomplex subunit 8	21.77	1.6046
P00403	Cytochrome c oxidase subunit 2	25.57	1.5474
O43181	NADH dehydrogenase [ubiquinone] iron-sulfur protein 4	20.11	1.5425
O94925-1	Glutaminase kidney isoform	73.46	1.4968
P56378	6.8 kDa mitochondrial proteolipid	8.62	1.4771
B4DJAO	NADH-ubiquinone oxidoreductase 75 kDa subunit (NDUFS1)	81.00	1.4768
B4DLZ8	cDNA FLJ55789	51.28	1.4658
P12074	Cytochrome c oxidase subunit 6A1	12.16	1.4585
O00483	NADH dehydrogenase [ubiquinone] 1 alpha subcomplex subunit 4	9.37	1.4493
O43678	NADH dehydrogenase [ubiquinone] 1 alpha subcomplex subunit 2	10.92	1.4441
P05161	Interferon-induced 15 kDa protein	17.89	1.4438
P55285-1	Cadherin-6	88.31	1.4378
P14406	Cytochrome c oxidase subunit 7A2	12.84	1.4337
P14927	Complex III subunit 7	13.53	1.4336
P09669	Cytochrome c oxidase subunit 6C	8.78	1.4247
P49821-1	NADH dehydrogenase [ubiquinone] flavoprotein 1	50.82	1.4190
B5MD66	Putative uncharacterized protein TMX2	42.47	1.4182
Q9Y6M9	NADH dehydrogenase [ubiquinone] 1 beta subcomplex subunit 9	21.83	1.4149
P02792	Ferritin light chain	20.02	1.4072
P10606	Cytochrome c oxidase subunit 5B	13.70	1.3573
P19404	NADH dehydrogenase [ubiquinone] flavoprotein 2	27.91	1.3558
P15954	Cytochrome c oxidase subunit 7C	7.25	1.3473
O43920	NADH dehydrogenase [ubiquinone] iron-sulfur protein 5	12.52	1.3320
Q8WU60	NADH dehydrogenase [ubiquinone] flavoprotein 3	50.98	1.3261

O95168	NADH dehydrogenase [ubiquinone] 1 beta subcomplex subunit 4	15.21	1.3205
O43677	NADH dehydrogenase [ubiquinone] 1 subunit C1	8.73	1.3201
O14949	Complex III subunit 8	9.91	1.3200
O95298	NADH dehydrogenase [ubiquinone] 1 subunit C2	14.19	1.3133

Knockdown was induced in *ttc19kd-2* cells by the addition of doxycycline for 9 days. Non-induced *ttc19kd-2* cells were labeled by growth in $^{13}\text{C}_6$ -lysine/L-arginine containing medium (H), whereas Dox-treated *ttc19kd-2* cells remained unlabeled (L). The higher the ratio H/L, the bigger the reduction of the protein in the knockdown mitochondria.

Interestingly, many proteins reduced upon TTC19 depletion were respiratory complex subunits, similar to what we have observed after the reduction of Sam50. Respiratory complex I was affected the most, followed by complex IV. Concerning complex V, only the mtDNA-encoded subunit ATP synthase protein 8 was reduced. Additionally, the levels of the 6.8 kDa mitochondrial proteolipid, which had been shown to be a protein associated with ATP synthase (Meyer et al., 2007), were affected. Besides, two subunits of respiratory complex III, subunit 7 (UQCRB) and subunit 8 (UQCRCQ), were reduced upon TTC19 depletion. Both components form a subcomplex with MT-CYB, the only mtDNA-encoded subunit of this respiratory complex, before being assembled into the cytochrome *bc1* precomplex. Interestingly, a reduction of Core1 or RISP was not observed, although these two proteins were shown to interact with TTC19 by Ghezzi and co-workers (Ghezzi et al., 2011). In addition to respiratory complex subunits, glutaminase (kidney isoform, K-glutaminase) and a protein of unknown function (cDNA FLJ55789) were reduced upon loss of TTC19.

3.5.2 TTC19 influences protein levels of respiratory complex subunits

In order to validate the findings of the SILAC analysis, I investigated the protein amounts of respiratory complex subunits in TTC19-depleted cells. For this purpose, knockdown of TTC19 was induced in *ttc19-kd2* cells for 7 and 14 days by addition of Dox. Mitochondria of non-induced and Dox-induced cells were isolated and analyzed by SDS-PAGE and western blotting. Protein levels of respiratory complex components were assessed by immunodecoration with antibodies against various proteins (Figure 3-31). NDUFS1 levels were mildly reduced upon TTC19 depletion for 7 and 14 days, but there was hardly any effect on the NDUFS2 and NDUF9 levels. Regarding complex III, a weak reduction in Core1 levels could be observed, whereas RISP and subunit 8 were more strongly affected. For complex IV, a mild reduction in COX2 levels after 14 days of TTC19 depletion but not in COX5a or COX1 levels could be detected. The levels of the complex II component SDHA were not altered. Besides, reduction of K-glutaminase in TTC19-depleted cells, as found in the SILAC experiment, could not be confirmed.

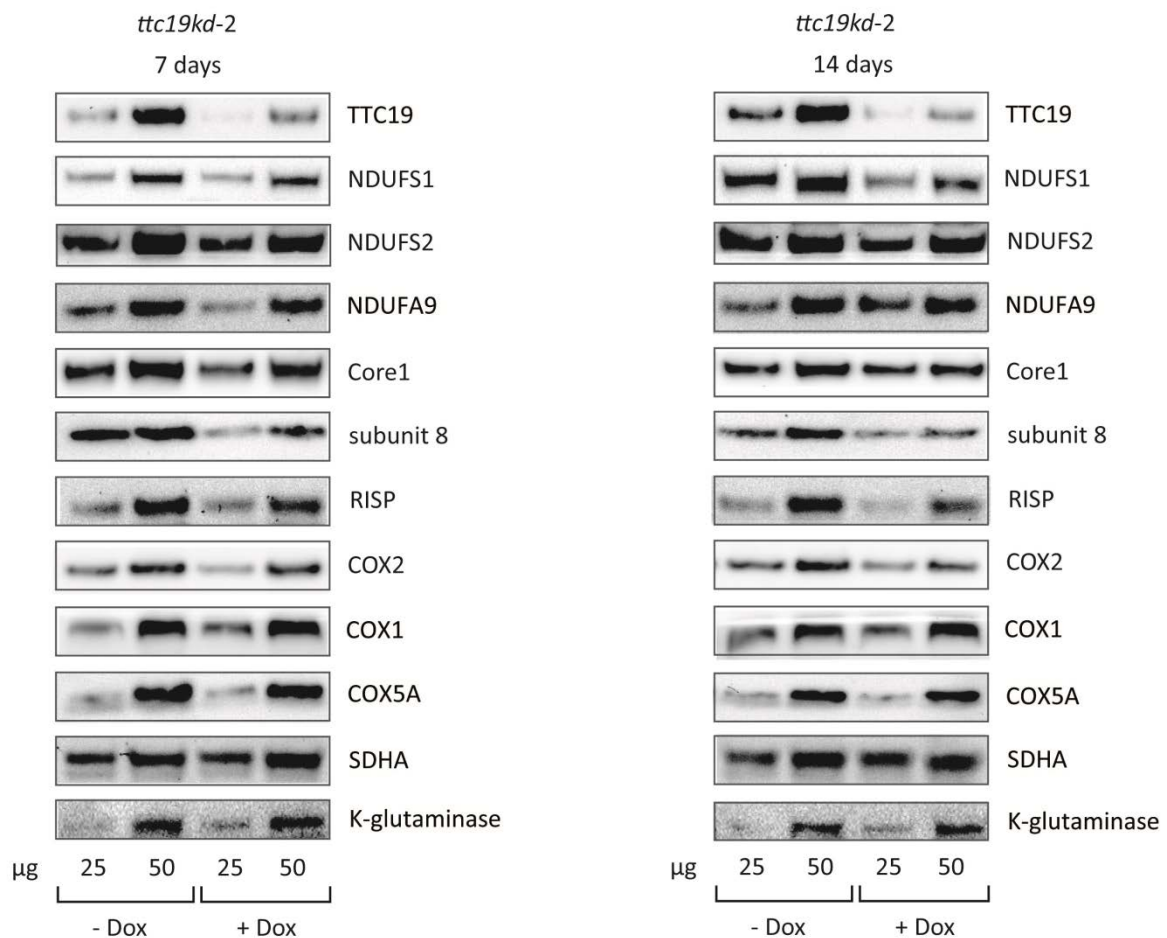


Figure 3-31 Several respiratory complex components are affected by TTC19 depletion. *ttc19kd-2* cells were grown in the presence (+ Dox) or absence (- Dox) of doxycycline for 7 or 14 days. Mitochondria were isolated, and 25 µg and 50 µg of mitochondrial protein were analyzed by SDS-PAGE and western blotting.

As TTC19 has been described to be involved in respiratory complex III assembly, I produced an inducible shRNA-mediated knockdown cell line of Core1, *core1kd-1*, to examine whether the observed effect of TTC19 depletion on complex I subunit NDUFS1 and complex IV subunit COX2 was not perhaps a side-effect of reduced complex III levels. After 7 days of Core1 knockdown induction by Dox addition, mitochondria of Dox-treated and untreated cells were isolated and analyzed by SDS-PAGE followed by western blotting. Immunodecoration with antibodies against RISP, NDUFS1, COX2 and SDHA showed that Core1 depletion only affected the stability of the complex III component RISP, whereas levels of subunits of the other complexes were unaltered (Figure 3-32). Therefore, the reduction in protein levels of complex I and complex IV components upon TTC19 depletion cannot be attributed to decreased complex III levels.

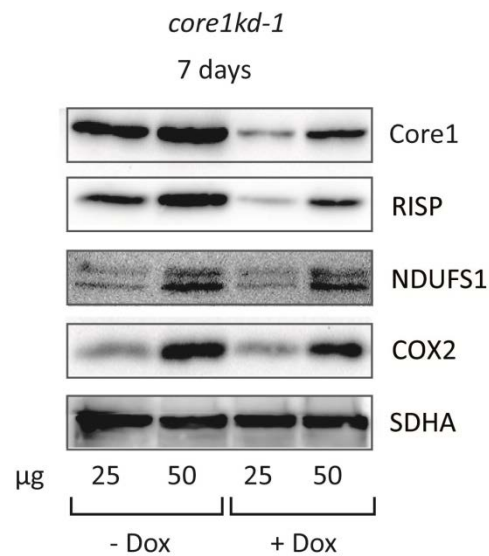


Figure 3-32 Protein levels of complex I, II and IV components are not altered in Core1-depleted cells. Mitochondria of *core1-kd1* cells grown for 7 days in the presence (+ Dox) or absence (- Dox) of doxycycline were isolated, and 25 µg and 50 µg of mitochondrial protein were analyzed by SDS-PAGE followed by western blotting.

Next, I aimed to elucidate whether only TTC19 depletion affected levels of respiratory complex components or whether respiratory complexes equally had an influence on the amount of TTC19 in mitochondria. Therefore, knockdown of the respective protein was induced in *ndufs1kd-1*, *core1kd-1* and *cox5akd-2* cells by Dox addition for 7 days, and mitochondria of Dox-treated and untreated cells were isolated. Subsequently, they were separated by SDS-PAGE followed by western blotting. Immunodecoration with an antibody against TTC19 showed that the levels of this protein were not altered when respiratory complex subunits were reduced (Figure 3-33). This demonstrated that reduced levels of respiratory complex components were the consequence and not the cause of TTC19 depletion.

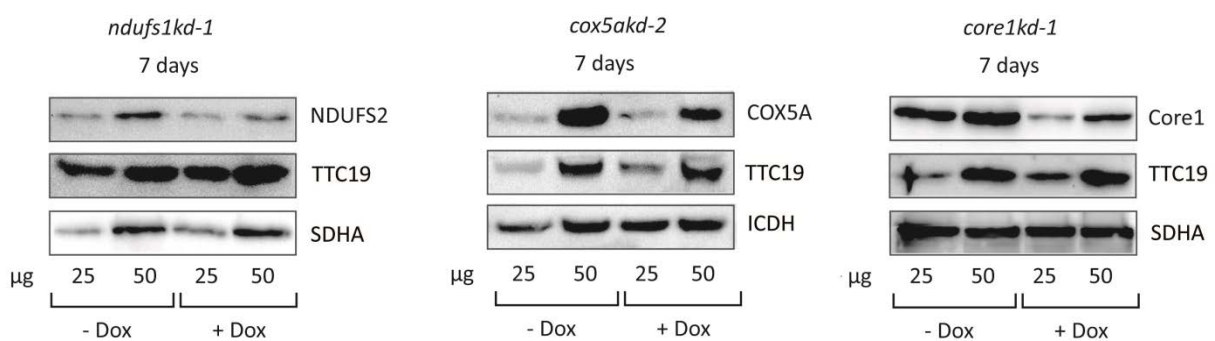


Figure 3-33 Respiratory complexes I, III and IV do not influence TTC19 levels. Knockdown of the respective protein was induced in *ndufs1kd-1*, *core1kd-1* and *cox5akd-2* cells for 7 days by the addition of doxycycline (Dox). Mitochondria were isolated and analyzed by SDS-PAGE and western blotting.

3.5.3 TTC19 plays a role in respiratory complex assembly

In order to examine whether TTC19 depletion affected respiratory complex formation, mitochondria of Dox-induced and non-induced *ttc19kd-2* cells were subjected to BN-PAGE and western blotting. Levels of each respiratory complex were assessed by immunodecoration with antibodies against NDUFA9, SDHA, Core1 and COX1. Whereas levels of respiratory complexes I and II were not altered, the complex III dimer was completely absent and a subcomplex of complex IV strongly reduced in TTC19-depleted mitochondria (Figure 3-34).

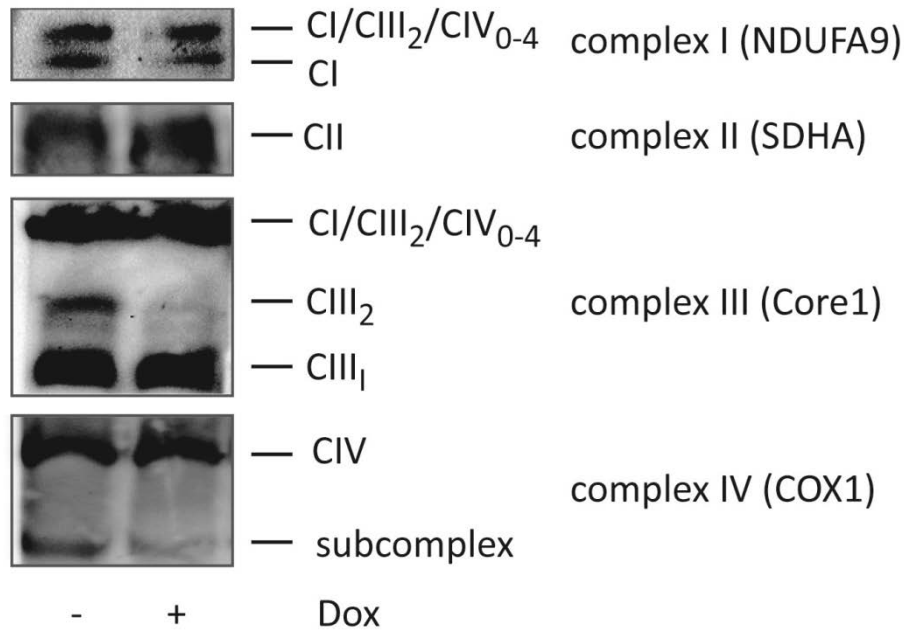


Figure 3-34 TTC19 influences respiratory complexes III and IV. *ttc19kd-2* cells were grown for 7 days in the presence (+ Dox) or absence (+ Dox) of doxycycline. Mitochondria were isolated, solubilized in 1 % digitonin and subjected to BN-PAGE and western blotting.

To further investigate the effect of TTC19 loss on respiratory complex assembly, *in vitro* import studies were performed. Mitochondria of *ttc19-kd2* cells treated with Dox for 7 days to induce knockdown and of untreated cells were isolated, and ³⁵S-labeled NDUFS1, Core1, subunit 7 and COX6A were *in vitro* imported. Analysis of mitochondria by BN-PAGE followed by autoradiography demonstrated that loss of TTC19 affected supercomplex formation of respiratory complexes I, III and IV (Figure 3-35). Besides, the amounts of the complex IV monomer were strongly reduced, whereas the effect on complex I subcomplexes was not as pronounced. Complex III was almost exclusively present in supercomplexes when ³⁵S-labeled Core1 was imported. An effect of TTC19 depletion on complex III dimer formation could not be observed. However, the dimer formation was difficult to assess as the signal for the complex III dimer was very weak. Therefore, I imported ³⁵S-labeled subunit 7 to be able to better visualize the complex III dimer and could observe that both the

amounts of the supercomplexes and the complex III dimer were strongly reduced upon TTC19 depletion, confirming the role of TTC19 in complex III assembly. The results of the *in vitro* experiments corroborate the idea that TTC19 is involved in respiratory complex assembly and might especially be important for supercomplex formation.

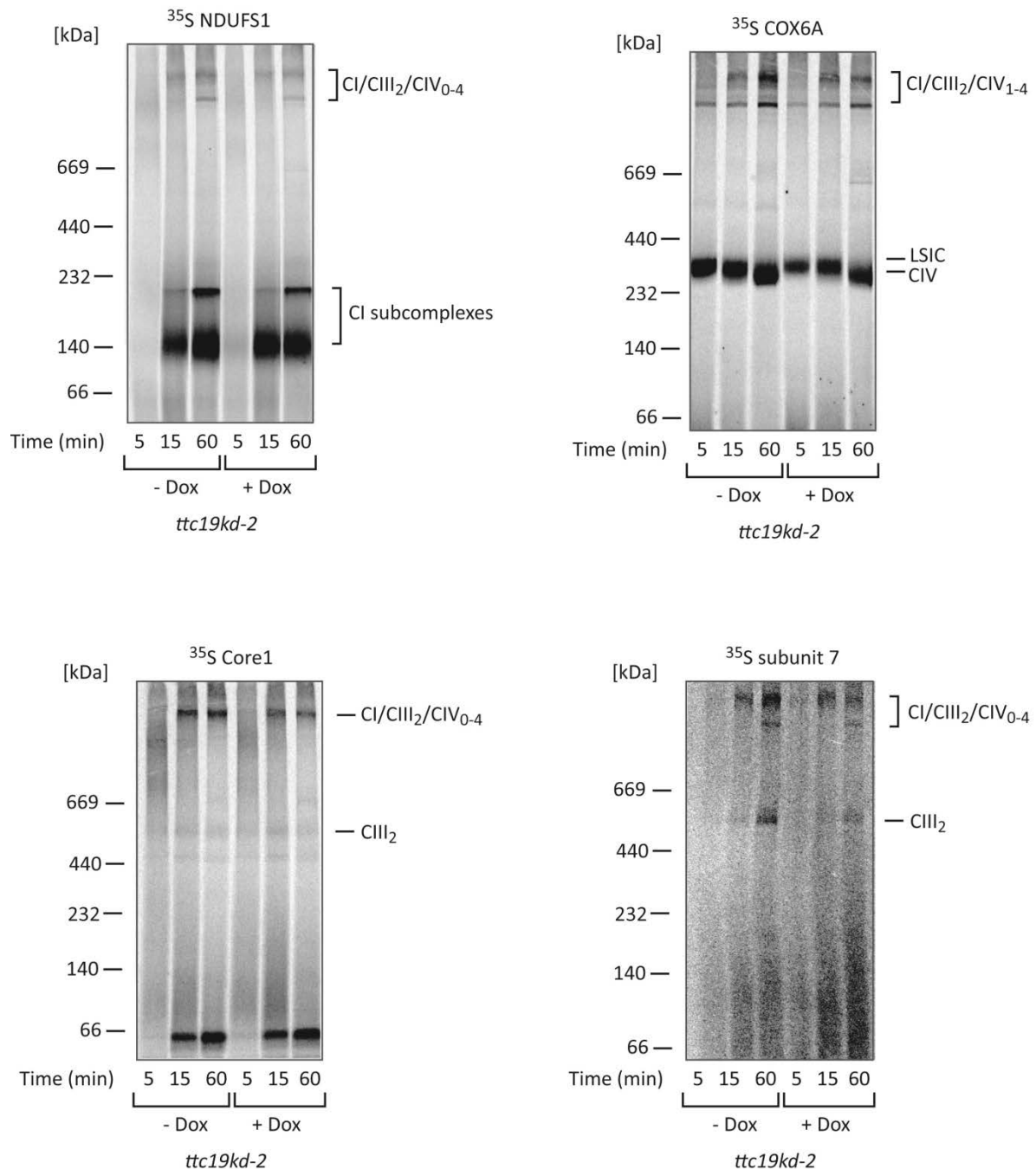


Figure 3-35 Respiratory complex formation is impaired in TTC19-depleted cells. NDUF51, COX6A, Core1 and subunit 7 were labeled by transcription/translation *in vitro* in the presence of [^{35}S] methionine/[^{35}S] cysteine. ^{35}S -labeled proteins were mixed in KAc buffer with mitochondria of *ttc19kd-2* cells grown for 7 days in the presence (+ Dox) or absence (- Dox) of doxycycline. Mitochondria were solubilized in 1% digitonin, and analyzed by BN-PAGE followed by autoradiography. LSIC: late-stage intermediate complex.

Finally, in order to exclude that loss of TTC19 results in a general impairment of protein import, ^{35}S -labeled ferredoxin was *in vitro* imported into mitochondria of TTC19-depleted mitochondria (Figure 3-36). Analysis by SDS-PAGE and autoradiography demonstrated that TTC19 depletion does not affect the import of ferredoxin, confirming that TTC19 specifically influences respiratory complex components.

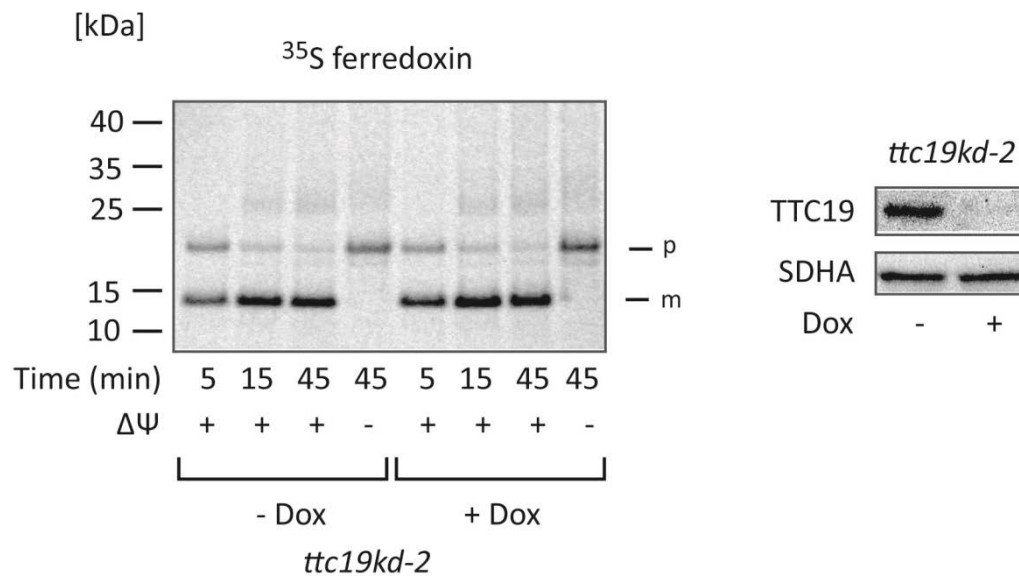


Figure 3-36 Import of ferredoxin is not affected by TTC19 depletion. *ttc19kd-2* cells were grown for 7 days in the presence (+ Dox) or absence (- Dox) of doxycycline. Mitochondria were isolated and mixed with ^{35}S -labeled ferredoxin in KAc buffer for the indicated time points. Mitochondria were analyzed by SDS-PAGE and autoradiography, or western blot as a control for knockdown efficiency (right hand panel). SDHA: subunit A flavoprotein of complex II.

4 DISCUSSION

4.1 Human mitochondria exhibit high specificity regarding import and assembly of bacterial β -barrel proteins

Sam50/Omp85, the central component of the mitochondrial sorting and assembly machinery (SAM), is evolutionary conserved from gram-negative bacteria to mammalian cells (Humphries et al., 2005; Kozjak et al., 2003; Paschen et al., 2003). The C-terminal part of Sam50/Omp85 consists of 16 β -strands which are integrated into the OM (Gentle et al., 2005). The N-terminal part is exposed to the intermembrane space in mitochondria or the periplasm in bacteria (Kozjak et al., 2003; Paschen et al., 2003; Voulhoux et al., 2003). In mitochondria, the N-terminus of Sam50 includes one polypeptide transport-associated (POTRA) domain, whereas bacterial Omp85 possesses five POTRA domains (Gentle et al., 2005; Sanchez-Pulido et al., 2003).

A study by Walther and colleagues demonstrated that the β -barrel protein VDAC of the fungus *Neurospora crassa* can be assembled into the OM of *E. coli* (Walther et al., 2010). Likewise, β -barrel proteins of *E. coli* and *N. gonorrhoeae* can be imported into mitochondria of the baker's yeast *Saccharomyces cerevisiae* and are integrated into their OMM (Walther et al., 2009a). Therefore, we aimed to elucidate whether the same applies to bacterial β -barrel proteins in human cells. All β -barrel proteins tested of *E. coli* and *S. enterica* were not targeted to human mitochondria. Only Omp85 of *N. gonorrhoeae* was imported (Kozjak-Pavlovic et al., 2011). Earlier studies have demonstrated that PorB of *N. gonorrhoeae* (PorB_{NgO}) and PorB of *N. meningitidis* (PorB_{Nme}) are imported into mitochondria (Massari et al., 2000; Müller et al., 2000), whereas PorB of the commensal strain *N. mucosa* remained cytosolic (Müller et al., 2002). This raised the interesting hypothesis that the ability to target PorB to mitochondria is linked to pathogenicity (Müller et al., 2002). When I tested whether human mitochondria can import PorB of *N. lactamica* (PorB_{Nla}), *N. sicca* (PorB_{Nsi}) and *N. cinerea* (PorB_{Nci}) within this study, I, however, could not confirm this link (Figure 3-1A). PorB_{Nla} and PorB_{Nsi} were both targeted to mitochondria, although not exclusively. PorB_{Nci}, on the other hand, appeared to be only cytosolic, but when I tested the ability of Omp85_{NgO} to integrate the PorB proteins, there was also a weak signal of a protein complex formed by PorB_{Nci} in mitochondria (Figure 3-2 and Kozjak-Pavlovic et al., 2011). Thus, probably a small fraction of this protein was imported into mitochondria as well. One interesting difference was observed between PorB_{NgO} and the other PorB proteins when assessing the loss of $\Delta\Psi$. Whereas PorB_{NgO} expression always resulted in the loss of $\Delta\Psi$, in the case of PorB_{Nla} and PorB_{Nsi} $\Delta\Psi$ was lost only when there was a strong signal and therefore probably a high concentration of these proteins in the mitochondria.

When only a weak signal was detected, which would correspond to less protein in the mitochondria, $\Delta\Psi$ was retained. When examined by BN-PAGE, however, no formation of complexes could be observed, indicating that PorB_{Nla} and PorB_{Nsi} were accumulating in the IMS similar to PorB_{Ngo} although they did not always affect $\Delta\Psi$. The fact that lower levels of PorB_{Nla} and PorB_{Nsi} do not cause loss of $\Delta\Psi$ could indicate that they are not as harmful to mitochondria as PorB_{Ngo}. This would support the hypothesis that the ability to target PorB_{Ngo} to mitochondria is linked to the pathogenicity of *N. gonorrhoeae* (Kozjak-Pavlovic et al., 2009; Müller et al., 2002). On the other hand, it could also be possible that PorB_{Nla} and PorB_{Nsi} are imported into mitochondria less efficiently than PorB_{Ngo} and therefore do not always reach an amount that can affect mitochondria. This explanation could be supported by the fact that PorB_{Nla} and PorB_{Nsi} were not exclusively localized to mitochondria, but a portion of these proteins remained cytosolic.

Apart from the PorB proteins of different neisserial strains, I also tested whether Omp85_{Nci} could be targeted to mitochondria. Overexpression experiments showed that Omp85_{Nci}, as Omp85_{Ngo}, is efficiently imported into mitochondria. Interestingly, PorB of the same strain appears to remain cytosolic. In contrast to the tested neisserial PorB proteins, Omp85_{Nci}, as Omp85_{Ngo}, never affected $\Delta\Psi$, and BN-PAGE analysis demonstrated that it was integrated into the OMM. This shows that although both PorB and Omp85 are recognized by the TOM complex, only Omp85 is recognized by the SAM complex. The difference in membrane integration between Omp85 and PorB might occur because the mammalian Sam50, who itself is assembled by the SAM complex, is homologous to bacterial Omp85, whereas PorB is not conserved in eukaryotes and shows no homology to eukaryotic porin/VDAC. Interestingly, when expressing the PorB proteins of different neisserial strains together with Omp85_{Ngo} and Omp85_{Nci}, PorB integration into the OMM could be observed (Figure 3-2 and Kozjak-Pavlovic et al., 2011). This demonstrates that Omp85 is not only integrated into the OMM but can also exercise its natural function in mitochondria, which is to assist membrane assembly of β -barrel proteins.

The results of my work and that of our group are in contrast to a study by Jiang and co-workers in which they show that the PorB proteins of *N. gonorrhoeae* and *N. meningitidis* are recognized by the SAM complex and integrated into the OMM in mouse cells, and generalize this finding to all mammalian cells (Jiang et al., 2011). In our work, however, we always observe a loss of $\Delta\Psi$ when PorB_{Ngo} is present in human mitochondria, indicating that it cannot be integrated into the OMM but accumulates in the IMS/IMM and causes damage to mitochondria (Kozjak-Pavlovic et al., 2009; Kozjak-Pavlovic et al., 2011). Even though the authors claim that only a small amount of PorB_{Ngo} is membrane integrated in mouse mitochondria, if that was indeed the case with human mitochondria

we would expect to be able to detect these small amounts of assembled PorB in the form of protein complexes in the human OMM. However, we have never observed any protein complexes formed by PorB after targeting to human mitochondria. This difference between the work of Jiang and co-workers on the one hand and our work on the other hand shows that they cannot generalize their findings in mouse cells to all mammalian cells.

Whereas Walther and co-workers suggest that no eukaryotic-specific mitochondrial import signal has evolved in β -barrel proteins upon their finding that bacterial β -barrel proteins can be imported into yeast mitochondria, and contemplate this as a prove for the strict conservation between the β -barrel assembly of bacteria and eukaryotes (Walther et al., 2009a), my work and the work of our group contradicts this hypothesis (Kozjak-Pavlovic et al., 2011). The fact that not all bacterial β -barrel proteins can be imported into mitochondria in mammalian cells and not all imported proteins can be integrated into the OMM demonstrates that although the TOM complex and Sam50 of the SAM complex are conserved among the organisms, they are not similar enough to recognize always the same proteins. The human import machinery, in contrast to the yeast one, seems to exhibit a certain selectivity regarding the import and membrane assembly of β -barrel proteins. This finding emphasizes that mechanisms found in model organisms like *S. cerevisiae* or *N. crassa* cannot necessarily be transferred to mammalian cells even though the proteins involved are conserved. Therefore, it is inevitable to carefully investigate the processes in mammalian cells even though it is more difficult and complex to conduct studies in the mammalian model system.

4.2 β -barrel proteins do not possess a linear signal which targets them to mitochondria

After expression of the *E. coli* β -barrel proteins BamA and OmpC in human cells, we found that they were not targeted to mitochondria (Ott et al., 2012). Therefore, I next aimed to answer the question why their import behavior differed from their neisseiral neisserial homologs, Omp85 and PorB. I tried to locate the signal that targets Omp85 and PorB to mitochondria by exchanging domains of these proteins with those of BamA and OmpC, respectively. For Omp85_{NgO}, I could show that the signal is localized in its C-terminal half, which includes its 16 β -strands (Figure 3-4A). However, it was not possible to further limit the targeting signal to a single quarter of the Omp85_{NgO} sequence, as I observed the loss of mitochondrial targeting in the chimeric proteins Omp85 $\frac{3}{4}$ BamA $\frac{1}{4}$ and Omp85 $\frac{1}{2}$ BamA $\frac{1}{2}$ Omp85 $\frac{1}{4}$, which still contained three quarters of Omp85_{NgO} (Figure 3-5). On the other hand, targeting of Omp85_{NgO} to human mitochondria could be impaired by mutating only single amino acids (Figures 3-6 and 3-7). This demonstrates that there probably are amino acids important for mitochondrial targeting spread throughout the C-terminal half of Omp85_{NgO}, indicating that the

secondary structure and charge of the protein, rather than a linear signal sequence, are very important for import into mitochondria.

In the case of PorB_{NgO}, its 22 C-terminal amino acid residues were sufficient to mediate mitochondrial import, as I could show by expressing the construct OmpC-PorB₃₁₆₋₃₂₇ (Figure 3-10). The construct PorB-OmpC₃₄₁₋₃₆₇, in which the 22 C-terminal amino acid residues were replaced with the 27 C-terminal amino acid residues of OmpC_{Ecoli}, was exclusively cytosolic, underlining the importance of these amino acids for the mitochondrial targeting of PorB_{NgO}. On the other hand, the construct PorB^{3/4}OmpC^{1/4}, which lacked the 71 C-terminal amino acid residues of PorB_{NgO}, was also imported into mitochondria in some cases (Figure 3-9), indicating that the signal for mitochondrial targeting of PorB_{NgO} is not exclusively present in the 22 C-terminal amino acid residues, but that, as is the case for Omp85_{NgO}, rather the secondary structure or charge of the protein may play an important role. In contrast to Omp85_{NgO}, the amino acid residues of the last β -barrel strand are not crucial for the import of PorB_{NgO} into mitochondria (Figure 3-11). This shows that the signal which targets β -barrel proteins to mitochondria is not conserved among different proteins, and again suggests a complex internal import signal instead of a short linear signal sequence.

4.3 Two POTRA domains are required for OMM integration and function of Omp85

A study of Bos and colleagues showed that in *N. meningitidis* only the last of the five POTRA domains of Omp85 is required for membrane integration and function (Bos et al., 2007). In contrast to this finding, I could show that in human mitochondria at least two POTRA domains are necessary for Omp85_{NgO} assembly and functionality (Figure 3-13). This difference might be explained by the fact that in *Neisseria*, Omp85 is present together with four accessory lipoproteins that might assist its integration and function. Additionally, Omp85 might be better adapted to the asymmetric outer membrane of gram-negative bacteria, consisting of one phospholipid and one lipopolysaccharide leaflet, than to the phospholipid bilayer membrane of mitochondria.

When only two POTRA domains were present, I could not observe any formation of Omp85_{NgO} protein complexes by BN-PAGE analysis. However, the protein was integrated into the OMM, as there was no loss of membrane potential and therefore no protein accumulation in the IMS (Figure 3-13B), and as it was functional and integrated PorB_{NgO} (Figure 3-13C). Thus, when only two POTRA domains are present, Omp85_{NgO} is probably either present as a monomer or its complex formation is so labile that it is disrupted by digitonin treatment and BN-PAGE analysis. This shows that one more POTRA domain is required for stable oligomerization of the complex, and, in addition, that Omp85 might be functional as a monomer. This finding fits to the study of Bos and colleagues, who could

detect no oligomeric Omp85 when only one POTRA domain was present although the protein was functional, and also suggested that the protein is either not present in a complex or that the complex is instable and falls apart when analyzed by semi-native SDS-PAGE (Bos et al., 2007).

Interestingly, the chimeric protein BamA_{1/2}Omp85, in which all five POTRA domains of Omp85_{NgO} are replaced by those of BamA_{Ecoli}, is functional (Figure 3-4B). This could indicate that the POTRA domains are sufficiently conserved between BamA_{Ecoli} and Omp85_{NgO} to retain their functionality. Alternatively, it might be sufficient that an N-terminal sequence of a specific minimal length is attached to the C-terminal half of Omp85_{NgO} to mediate OMM integration and function. This could be tested in future by adding a random protein sequence to the C-terminal half of Omp85_{NgO}.

4.4 The β -sorting signal is not sufficient for membrane integration of Omp85 and PorB

The fact that two POTRA domains are required for the assembly of Omp85_{NgO} in the OMM additionally demonstrates that the β -signal of the protein is not sufficient membrane integration. This could also be observed when I replaced the β -signal of PorB_{NgO} with the one of Omp85_{NgO}. Expression of this construct, as PorB_{NgO} expression, led to a loss of $\Delta\Psi$ (Figure 3-12), indicating that it could not be integrated into the OMM.

These findings fit to a former study conducted in our group, which demonstrated that the membrane integration of the human β -barrel protein VDAC1 can be impaired by mutating single amino acid residues throughout the protein sequence (Kozjak-Pavlovic et al., 2010). Additionally, a study performed in *N. crassa* showed that removing amino acid residues close to the N-terminus of Tom40 prevents the assembly of this protein (Rapaport et al., 2001).

Thus, both my results and those of previous studies demonstrate that in eukaryotic cells the β -signal is required but not sufficient for OMM integration of β -barrel proteins.

4.5 The MIB complex is a crucial organizer of cristae structure

Previous work in our group has demonstrated that depletion of the central pore-forming component of the SAM complex, Sam50, leads to a complete loss of mitochondrial cristae structure (Ott et al., 2012). Therefore, in my work I aimed to contribute to elucidating in which way Sam50 is linked to the formation and maintenance of cristae structure.

Recently, Xie and co-workers produced an antibody against mitofilin and found that this protein is present in a complex with Sam50, CHCHD3, CHCHD6, DnaJC11, and metaxins 1 and 2 (Xie et al., 2007), but no further investigations into the role of this complex were performed.

Interestingly, mitofilin was shown before to be involved in maintaining cristae structure (John et al., 2005). The phenotype of mitofilin loss, however, differed from the one we observed upon Sam50 knockdown. When mitofilin was depleted, cristae junctions were absent and cristae membranes were present as concentric onion-like rings (John et al., 2005), whereas Sam50 loss resulted in an almost complete absence of cristae (Ott et al., 2012).

In my work and the work performed in our group, we could confirm that the complex described by Xie and co-workers exists and is required for the maintenance of cristae structure (Figure 4-1). We demonstrated by BN-PAGE analysis that mitofilin and CHCHD3 are present in a complex of 700 – 800 kDa and in an additional one of more than 1 MDa, whereas Sam50 is only part of the bigger complex which we termed mitochondrial intermembrane space bridging holo (holo-MIB) complex (Figure 3-15). Furthermore, we could show by BN-PAGE analysis that knockdown of CHCHD3, Sam50 or mitofilin influences the complex formation of each other. The influence of Sam50 and mitofilin on CHCHD3 assembly could additionally be confirmed by *in vitro* import studies (Figure 3-16). We could demonstrate that the connection of mitofilin to the OMM possibly via Sam50 and CHCHD3 is absolutely crucial for cristae maintenance, as the cristae structure is lost upon Sam50 depletion even though the levels of mitofilin are unchanged. Without Sam50 or CHCHD3, mitofilin is present only in the smaller complex (Figure 3-15), which seems alone not to be sufficient for the maintenance of the cristae structure. Likewise, CHCHD3 requires the presence of Sam50 to be integrated into the holo-MIB complex (Ott et al., 2012 and Figures 3-14 and 3-15). In contrast to mitofilin, CHCHD3 levels are reduced upon Sam50 loss (Ott et al., 2012). In addition, the stability of Sam50 seems to depend completely on the presence of mitofilin or CHCHD3. When one of these proteins is depleted, Sam50 protein levels and complex formation are strongly reduced, indicating that Sam50 is present only as a part of the holo-MIB complex. This finding is in contrast to previous studies performed by our group (Kozjak-Pavlovic et al., 2007) and other groups (Humphries et al., 2005), where Sam50 was described to be present in a complex of around 200 kDa, which I could not detect in my work. This difference could be explained by the different methods utilized to detect protein complexes of Sam50. Whereas I used BN-PAGE to study complex formation by Sam50, the previous studies applied BN-PAGE in the first dimension followed by SDS-PAGE in the second dimension. This latter method might be more sensitive for detection of small protein amounts. However, it is possible that the lower Sam50-containing complex is a subcomplex solely appearing upon digitonin solubilization, as a nearly complete loss of Sam50 protein levels upon mitofilin depletion is difficult to explain if Sam50 is present in another stable complex without mitofilin.

Two other components reported by Xie and colleagues to be present in a complex with mitofilin, CHCHD3 and Sam50 are CHCHD6 and DnaJC11 (Xie et al., 2007). CHCHD6 is described to be an IMM-associated protein (An et al., 2012). For DnaJC11, I could show that its largest 64 kDa isoform is soluble, whereas the 57 kDa isoform is membrane-integrated. The 35 kDa isoform is present in the IMS or IMM (Figure 3-17). CHCHD6 is lost upon mitofilin depletion, while DnaJC11 is reduced when Sam50 is depleted and slightly affected by mitofilin loss, probably as a secondary effect of Sam50 reduction (Figure 3-18). CHCHD3 has no effect on CHCHD6 or DnaJC11 levels. When I depleted CHCHD6 or DnaJC11, I could not observe any effect on the levels of other MIB complex components (Figure 3-19) and analysis by TEM showed no pronounced effect on the cristae structure (Figure 3-20). Therefore, these two proteins are probably only peripheral components of the MIB complex.

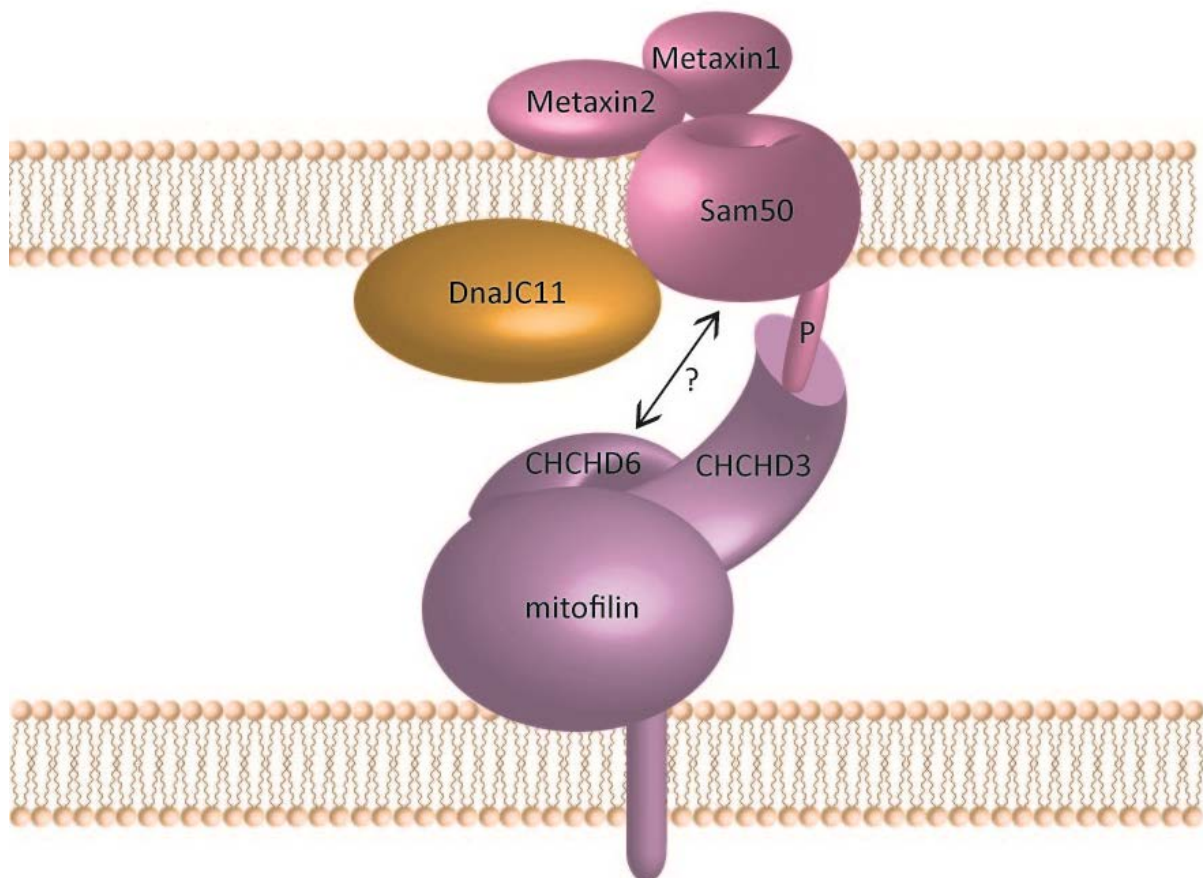


Figure 4-1 The holo-MIB complex spans OMM and IMM. The connection between the OMM protein Sam50 and the IMM protein mitofilin is required for the maintenance of the cristae structure. Both proteins are probably connected by CHCHD3 (Darshi et al., 2011).

Research of other groups confirmed the importance of the MIB complex for the maintenance of the cristae structure. During our investigations, a study was published by Darshi and co-workers which demonstrated CHCHD3 to be crucial as a cristae organizer (Darshi et al., 2011). Upon CHCHD3

reduction, they observed a phenotype similar to the one we see when Sam50 is depleted. They reported an interaction of the N-terminal part of CHCHD3 with Sam50, for which myristoylation at the N-terminal myristoylation site of CHCHD3 is required, and of the C-terminal part with mitofilin. Therefore, they assumed that CHCHD3 connects Sam50 with mitofilin. However, they did not investigate whether Sam50 and mitofilin also directly interact with each other. Besides, they reported that shortening of the C-terminus prevents and shortening of the N-terminus strongly impairs the import of CHCHD3 (Darshi et al., 2011; Darshi et al., 2012); therefore, it is difficult to judge how reliable their results regarding the interaction of mutated CHCHD3 with Sam50 and mitofilin are.

In addition to the interaction of CHCHD3 with Sam50 and mitofilin, Darshi and colleagues observed an interaction with Opa1 and HSP70, and reported a decrease of Opa1 levels upon CHCHD3 depletion (Darshi et al., 2011). Opa1 is a large GTPase with a crucial function in mitochondrial fusion (Cipolat et al., 2004). Besides, it was demonstrated that Opa1 depletion results in an altered cristae morphology and cyt c release (Olichon et al., 2003). Consistently, Darshi and co-workers observed impaired fusion when CHCHD3 levels are reduced. The cristae defect which they and we observe upon CHCHD3 or Sam50 depletion, however, cannot only be attributed to Opa1 decrease, as we did not find reduced Opa1 levels in Sam50-depleted mitochondria (Ott et al., 2012). However, we cannot completely exclude a connection between Sam50 and Opa1. Regarding mitofilin, we could not observe any changes in its levels in Sam50-depleted mitochondria, but only in CHCHD3-depleted mitochondria. Therefore it could be possible that Sam50 depletion accordingly does not alter Opa1 levels but affects the formation of Opa1 complexes, which could subsequently have an influence on cristae formation. Thus, the connection between CHCHD3 and Opa1 observed by Darshi and colleagues would offer an explanation why the loss of both Opa1 and MIB components leads to impaired cristae structure; however, the observed defect cannot solely be attributed to altered Opa1 levels.

An and co-workers described CHCHD6 as a crucial cristae organizer (An et al., 2012). They observed a loss of cristae structure when they downregulated CHCHD6 in RKO and MCF7 cells. Besides, they saw a loss of mitofilin in SK-Mel-103 cells and a reduction in mitofilin levels in RKO cells upon CHCHD6 depletion. On the other hand, when they depleted mitofilin, CHCHD6 was completely lost in RKO cells and reduced in SK-Mel-103 cells. They showed that CHCHD6 interacts with mitofilin via its C-terminus. In addition, they demonstrated an interaction of CHCHD6 with CHCHD3 and DISC1. However, they did not mention the interaction with Sam50. The finding of An and co-workers that CHCHD6 has a role as a cristae organizer is in contrast to my observation that this protein does not

affect the cristae structure. However, they saw a reduction of mitofilin when they depleted CHCHD6, whereas I did not observe any changes in the levels of mitofilin or other MIB components upon CHCHD6 depletion (Figure 3-19). Therefore, the effect they observed upon CHCHD6 loss is probably the consequence of reduced mitofilin levels and not of CHCHD6 reduction alone. This difference might occur due to the different cell types which were used for the investigations. My work was performed in HeLa cells, whereas they used RKO and SK-Mel-103 cells to examine protein levels of CHCHD6 and mitofilin and also observed differences between the cell lines regarding the influence of the two proteins on each other.

Alkhaja and co-workers reported the integral IMM protein MINOS1 as an additional component interacting with mitofilin. Additionally, they confirmed an interaction of MINOS1 with the described mitofilin interaction partners CHCHD3, heat shock 70 kDa protein 9 (HSPA9), Sam50, and metaxins 1 and 2, but did not probe for the interactions with CHCHD6, DnaJC11, DISC1 and Opa1 (Alkhaja et al., 2012). MINOS1 was identified as a homolog of yeast Mio10, which was shown to be one of the crucial proteins involved in cristae formation in that organism (see 4.6). This component was probably overlooked by Xie and co-workers when they first described the interaction partners of mitofilin due to its small size of only 10 kDa. Alkhaja and colleagues, however, only showed that Mio10 strongly affects cristae structure in yeast, but did not demonstrate whether MINOS1 has the same effect in human cells. Therefore, to be able to assess the role and importance of MINOS1 in human mitochondria, it would be necessary to examine the cristae structure and the protein levels of the other MIB components upon MINOS1 depletion.

In conclusion, the research of other groups supports the importance of the MIB complex for the maintenance of cristae structure. However, they all focused on the role of proteins integrated into or associated with the IMM for the cristae structure, but missed the importance of the connection of the mitofilin complex with Sam50 in the OMM, although some of them mentioned this interaction. Our work has established that the connection to Sam50 is crucial for the stability of the MIB complex and subsequent maintenance of the cristae structure.

4.6 Mitofilin complexes as organizers of cristae structure are evolutionary conserved

Homologs of mitofilin exist in both yeast and *C. elegans*. In yeast, the mitofilin homolog was termed Formation of Crista Junction protein 1 (Fcj1), as its loss resulted in decreased crista junction numbers (Rabl et al., 2009). Its function was shown to be antagonized by ATP synthase subunits e and g.

Recently, the mitofilin-containing complex in yeast and its role in cristae organization has been described independently by three groups using different approaches. It was named MINOS (Mitochondrial Inner Membrane Organizing System)/MICOS (Mitochondrial Contact Site complex)/MitOS (Mitochondrial Organizing Structure) (Harner et al., 2011a; Hoppins et al., 2011; von der Malsburg et al., 2011). All groups showed that Fcj1 interacts with the five components Aim5 (Mcs12), Aim13 (Mcs19), Aim37 (Mcs27), Mio10 (Mcs10, Mos1), and Mio27 (Mcs29, Mos2). Aim proteins were first identified in a screen for proteins required for inheritance of mitochondria (Hess et al., 2009), whereas Mio10 and Mio27 are previously uncharacterized proteins. Except for Aim13, which is soluble and located in the IMS, all other MINOS/MICOS/MitOS components are IMM proteins (Harner et al., 2011a; Hoppins et al., 2011; von der Malsburg et al., 2011). All groups demonstrated that Fcj1 and Mio10 affected cristae structure the most, whereas Mio27 deletion had hardly any effect. Harner and colleagues reported that Fcj1 is present in two complexes of about 700 kDa and 1.5 MDa (Harner et al., 2011a), which corresponds to the complex sizes we observe for mitofilin and CHCHD3 in mammalian cells. Von der Malsburg and co-workers found that the size of the MINOS complex is in the MDa range, but reported no smaller Fcj1 containing complex (von der Malsburg et al., 2011).

In addition to this core complex, however, the groups found different interaction partners of Fcj1. Hoppins and co-workers identified the MitOS complex by a genetic interaction map and observed an interaction with the NADH dehydrogenase Nde1, prohibitin subunits, respiratory chain subunits and assembly factors, and mitochondrial carrier proteins. Additionally, they reported interactions with the OMM proteins Por1, Tom70 and OM45. They observed that defects connected to MitOS loss required assembled ATP synthase and suggested that the presence of ATP synthase dimers is necessary for the formation of the normal cristae structure in a MitOS-dependent way (Hoppins et al., 2011).

Harner and colleagues described an interaction of the MICOS complex with the yeast OMM protein Ugo1 and with Sam50 (Harner et al., 2011a). Besides, they saw an interaction of Sam50 not only with Fcj1 but also with Aim37 and Mio27. In contrast to Hoppins and co-workers, they could not detect an interaction of Fcj1 with TOM components or OM45 in co-immunoprecipitation experiments. Interestingly, when they deleted Ugo1, which is required for mitochondrial fusion and interacts with the Opa1 ortholog Mgm1 (Sesaki and Jensen, 2001; Sesaki and Jensen, 2004), they observed an altered mitochondrial structure and a loss of crista junctions. In their later work they also described a cristae defect upon Sam35 depletion and subsequent Sam50 reduction (Körner et al., 2012). They observed that the ratio of IMM to OMM was increased about twofold upon Sam35

down-regulation (Körner et al., 2012), similar to what they found before upon Fcj1 depletion (Rabl et al., 2009). The number of CJs, however, was only moderately reduced after Sam35 downregulation (Körner et al., 2012) Thus, Körner and colleagues, similar to our group, observed the influence of OMM proteins on the cristae structure of the IMM and established a role of the SAM complex in the maintenance of cristae structure in yeast, similar to what we observe in mammalian cells (Ott et al., 2012).

Von der Malsburg and colleagues described an interaction of the MINOS complex with the TOM complex and Mia40, the central component of the MIA import pathway (von der Malsburg et al., 2011). They observed an influence of Fcj1 on the MIA pathway and suggested that the role of mitofilin in the MIA pathway is independent of its function in the MINOS complex, as the other components did not exercise an influence on the protein import via the MIA pathway. In their later work, they could also detect the interaction with Sam50 first described by Harner and colleagues (Zerbes et al., 2012).

The two groups, however, disagree in their findings about the importance of this connection and about the domains of Fcj1 which are required for cristae maintenance and interaction with Sam50. Fcj1 possesses a transmembrane domain behind its N-terminal mitochondrial targeting sequence, followed by a large hydrophilic IMS part, which includes a coiled-coil domain and a conserved mitofilin domain at the C-terminus (Körner et al., 2012; Zerbes et al., 2012). When Zerbes and co-workers dissected the roles of the different Fcj1 domains, they found that the coiled-coil domain interacts with Aim5 and Aim13. Its loss did not result in a complete defect in cristae structure, but led to an intermediate phenotype. The interaction with Sam50 was reduced when this domain was absent. In addition, they reported that the conserved C-terminal mitofilin domain comprising 49 amino acid residues is required for MINOS stability and maintenance of the cristae structure. Its loss, however, did not impair the interaction of MINOS with Sam50 and Tom40 but even enhanced it. Therefore, they concluded that the contact of Fcj1 with the OMM complexes is not sufficient for maintaining cristae structure. However, they could not exclude that this interaction is nevertheless required. Körner and co-workers also reported the importance of the C-terminal domain for the cristae structure (Körner et al., 2012). However, they also found the coiled-coil domain to be required for cristae maintenance. Besides, in contrast to the finding of Zerbes and colleagues, they reported that the C-terminus of Fcj1 interacts with Sam50, and they observed that the loss of the SAM complex disturbed the cristae structure. Interestingly, when they deleted Fcj1, they did not see a reduction in Sam50 levels. Therefore, the connection between Fcj1 and Sam50 does not seem to be required for Sam50 stability in yeast, in contrast to our findings in human cells.

It would, however, be necessary to investigate whether formation of complexes by Sam50 is altered upon Fcj1 depletion in order to evaluate the influence of Fcj1 on Sam50. It is possible that Sam50 in yeast is present in addition in a separate stable complex with Sam37 and Sam35 and therefore Sam50 levels remain unaltered upon Fcj1 depletion.

The two groups also reported contradicting findings regarding the influence of Fcj1 on mitochondrial import of β -barrel proteins. Harner and colleagues claim that the loss of Fcj1 does not significantly influence the import of these proteins, e.g. porin, consistent with their finding that Sam50 levels remain unaltered when Fcj1 is deleted (Harner et al., 2011a). Bohnert and co-workers, on the other hand, observed an effect of Fcj1 on the biogenesis of the β -barrel protein Tom40 (Bohnert et al., 2012). In addition, they found that the defect in Tom40 assembly upon Fcj1 loss is impaired at a stage before the SAM complex. As the two groups investigated the import of different β -barrel proteins, it is possible that the difference they observe can be explained by the fact that depletion of Fcj1 affects the import of some, but not of all β -barrel proteins. We did not investigate the import of β -barrel proteins into human mitochondria of mitofilin-depleted cells, but a defect is probable as Sam50 levels are strongly reduced upon mitofilin depletion in mammalian cells.

Apart from *S. cerevisiae*, mitofilin homologs have also been discovered in *C. elegans*. First, Mun and co-workers described two homologs of mitofilin, IMMT-1 and IMMT-2, which both are IMM proteins. *immt-1* and *immt-2* mutants showed reduced brood size, decreased motility, reduced sensitivity to reactive oxygen species and reduced biogenesis of mitochondria. Their cristae were lengthened, curved and stacked, and had a reduced number of crista junctions. Besides, the *immt-2* mutant and the double mutant had large pores in their OMM (Mun et al., 2010).

Head and colleagues discovered that the mitofilin homolog IMMT-1, the CHCHD3 homolog CHCH3 and the OMM protein MOMA1 all have the same effect on cristae structure. Interestingly, MOMA1 is homologous to yeast Aim37 and Mio27 (Head et al., 2011). They, however, reported that IMMT-1 and IMMT-2 have different effects on mitochondria. *immt-1* mutant cells had mitochondria with localized swellings and thin tubular extensions. *immt-2* mutants, on the other hand, possessed mitochondria that were thinner and more connected. Interestingly, they observed the same effect in Sam50 knockout *C. elegans*. In addition, they found that MOMA-1 and IMMT-1 act in the same pathway and therefore suggested a possible interaction between IMMT-1 and MOMA-1, which they, however, could not confirm with first co-immunoprecipitation experiments. CHCH3 seems to act independently of the other two proteins or have additional functions as its loss in *moma1* or *immt1* mutants resulted in a more severe phenotype (Head et al., 2011)

In conclusion, Head and co-workers also observed a connection between mitofilin and OMM proteins, and demonstrated that these OMM proteins are involved in the maintenance of cristae structure. Together with the work conducted by Harner, Körner and colleagues in yeast, this demonstrates that a mitofilin complex bridging the OMM and IMM did not develop in mammals, but is a conserved structure for maintaining the cristae morphology. Interestingly, Harner and colleagues discovered the complex in an approach to identify the contact site structure between OMM and IMM, and not in search for proteins involved in the maintenance of cristae structure. Likewise, the holo-MIB complex we identified probably represents the contact site structure or one of the contact site structures in mammalian mitochondria, which were described for the first time nearly 50 years ago (Hackenbrock, 1966) but whose components could not be determined before. The work of other groups, on the other hand, highlighted the role of mitofilin complexes in crista junction formation (John et al., 2005; Rabl et al., 2009; von der Malsburg et al., 2011). This suggests that at least mitofilin and CHCHD3 are involved in formation of both contact sites between OMM and IMM and of cristae junctions, and raises again the hypothesis first suggested by van der Klei and co-workers that these two structures are linked (van der Klei et al., 1994). Although electron tomography studies demonstrated a random distribution of both structures (Perkins et al., 1997), our work and that of the other groups raises the possibility that indeed a link between crista junctions and contact sites exists via common protein components.

4.7 The MIB complex influences respiratory complex assembly

After depletion of Sam50, quantitative mass spectrometry indicated a strong reduction in the levels of respiratory complex I, III and IV components. This effect could be confirmed by SDS-PAGE and BN-PAGE analysis (Ott et al., 2012) and, for complex I and IV, by *in vitro* import studies (Figure 3-21). Upon mitofilin loss, complex I and IV assembly and levels were also reduced, although not as strongly as upon Sam50 depletion (Ott et al., 2012). This connection between components of the MIB complex and mitochondrial respiration was also discovered by Darshi and colleagues, who saw a reduction of respiratory complex IV components 2 and 4 when they depleted CHCHD3. They did not see a decrease when they tested the levels of an ATP synthase subunit, a complex III subunit and a complex II subunit (Darshi et al., 2011). However, they did not examine the levels of complex I subunits, on which we observe the strongest effect upon Sam50 or mitofilin depletion.

A link between mitofilin complexes and respiration was also observed in yeast. When Rabl and co-workers first described the effects of Fcj1 loss, they reported a reduced respiratory rate and a slightly reduced membrane potential in Fcj1 mutant cells (Rabl et al., 2009). In their later work, they

demonstrated that deletion of MICOS components resulted in loss or reduction of respiratory capacity, with the strongest effect for Fcj1 and Mio10 and a milder influence of Aim37 and Aim5 (Harner et al., 2011a). Besides, Hoppins and co-workers reported that the MitOS complex interacts with the yeast NADH dehydrogenase Nde1 and several respiratory complex subunits and assembly factors (Hoppins et al., 2011). Interestingly, reduced levels of a respiratory complex IV subunit were also observed in *Trypanosoma brucei* when Tob55/Sam50 was depleted, although the cristae structure was not altered (Sharma et al., 2010).

As we did not find an effect of the SAM complex component metaxin 2 on respiratory complex levels or assembly (Figure 3-22 and Ott et al., 2012), the defect which we observed upon Sam50 depletion is most likely not connected to its function in the SAM complex, but in the MIB complex as a cristae organizer. Interestingly, we observed that Sam50 and mitofilin depletion most strongly affected the respiratory complexes containing the most mtDNA-encoded subunits, namely complexes I (7 mtDNA-encoded subunits) and IV (3 mtDNA-encoded subunits). This suggests that the stability of mtDNA or the ability to repair mtDNA damage could be linked to Sam50 and the MIB complex, and that this structure is therefore crucial for correct respiratory function. Interestingly, two recent studies support a link between mitofilin and the maintenance of intact mtDNA. First, Rossi and colleagues showed that poly(ADP-ribose)polymerase (PARP-1), which has multiple functions including sensing of damaged DNA (D'Amours et al., 1999), is present not only in the nucleus but also in mitochondria. They could demonstrate that the interaction with mitofilin is required for the mitochondrial localization of PARP-1 as without this interaction, mitochondrial location of this protein is reduced. Loss of mitochondrial PARP-1 and also of mitofilin leads to the accumulation of mtDNA damage (Rossi et al., 2009). Recently, it was additionally demonstrated that polynucleotide kinase/phosphatase (PKNP), which repairs DNA strand breaks, is also present in mitochondria and associates with mitofilin (Tahbaz et al., 2012). Interestingly, Tahbaz and colleagues saw a reduction in mitofilin levels when they depleted PKNP.

Another study, which could support the hypothesis that mitofilin is connected to mtDNA stability, demonstrated that Disrupted-in-schizophrenia 1 (DISC1) and mitofilin interact and that this interaction is required for mitofilin stability. (Park et al., 2010). Park and co-workers showed that both depletion of DISC1 and of mitofilin led to reduced complex I activity and decreased cellular ATP levels. As they saw that mitofilin is reduced when DISC1 is depleted, the effect of DISC1 loss on the respiratory chain could be a consequence of mitofilin reduction. The fact that they particularly observed a reduction in complex I activity corresponds to our results of Sam50 and mitofilin

depletion, as we also saw the strongest effect on this respiratory complex. The reduced ATP content which they observed again confirms a link between mitofilin and respiratory complex function.

In conclusion, several studies suggest a connection between the MIB complex component mitofilin and respiratory complex function, and could offer an explanation how the MIB complex and mtDNA stability are linked. However, the finding that mitofilin is required for mitochondrial localization of PARP-1 and PKNP cannot explain the defect in respiratory complex formation which we observe in Sam50-depleted cells, which is even stronger than upon mitofilin loss. As mitofilin levels in these cells are normal, this would mean that PARP-1 or PKNP do not require mitofilin but Sam50 or CHCHD3 for their mitochondrial localization, as these proteins are also reduced upon mitofilin loss. However, PARP-1 and PKNP were shown to directly interact with mitofilin. It is also possible that the presence of mitofilin is not sufficient for mitochondrial import of PARP-1 and PKNP, but that this protein has to be present in the holo-MIB complex together with Sam50. Alternatively, it could be possible that the defect we observed is not linked to PARP-1 or PKNP. To clarify the role of these proteins in the defect in respiratory complex assembly which we observe upon Sam50 or mitofilin depletion, it would be necessary to investigate the influence of Sam50 loss on PARP-1 and PKNP.

Damage or loss of mtDNA could also be not a direct consequence of mitofilin or Sam50 loss, but an indirect consequence due to impaired cristae structure. mtDNA is present together with proteins in nucleoids, which are probably tethered to the IMM (Albring et al., 1977; Iborra et al., 2004). It could be possible that this connection to the IMM is required for nucleoid and therefore mtDNA stability, and that impairment of cristae structure prevents this tethering. An interesting connection between mitochondrial shape and mtDNA stability, for instance, was observed in yeast. The outer membrane proteins Mmm1, Mmm2, Mdm10 and Mdm12 all influence mitochondrial morphology and are required for the maintenance of mtDNA (Berger et al., 1997; Hobbs et al., 2001; Sogo and Yaffe, 1994; Youngman et al., 2004). It was shown that Mmm1, Mdm10 and Mdm12 form a complex which is localized adjacent to mtDNA nucleoids (Boldogh et al., 2003). Interestingly, Mdm10 can also assemble with the SAM core complex and have a function in the biogenesis of β -barrels (Meisinger et al., 2004). In addition to OMM proteins, Mdm31 and Mdm32, two IMM proteins, were identified in a screen for proteins involved in mitochondrial distribution and morphology (Dimmer et al., 2005). Mitochondria of Mdm31 and Mdm32 mutants were nearly immotile and were lacking cristae. Besides, these mutants were respiratory-deficient, and it could be shown that Mdm31 and Mdm32 are required for mtDNA inheritance and the maintenance of the mtDNA organization in nucleoids. Another connection between cristae structure and mtDNA was in addition established in

yeast by Herlan and co-workers. They observed that Mgm1, the yeast ortholog of mammalian Opa1, is required for both maintenance of cristae structure and mtDNA (Herlan et al., 2003). Furthermore, studies with *OPA1* patient cells demonstrated that loss of this protein leads to mtDNA destabilization (Amati-Bonneau et al., 2008; Hudson et al., 2008). Accordingly, the impaired cristae structure which we observe upon Sam50 loss could result in disorganization of nucleoids and destabilization of mtDNA, thereby leading indirectly to defects particularly in respiratory complexes I and IV.

However, damage or loss of mtDNA is only one possible explanation why respiratory complexes are impaired upon Sam50 and mitofilin depletion. It could alternatively be possible that they need the intact cristae structure to be stable, especially for their correct integration into supercomplexes, which are formed by complexes I, III and IV (Schagger and Pfeiffer, 2000). This would also explain why Sam50 and mitofilin loss do not affect complex II as this complex is not part of supercomplexes. However, if impaired supercomplex formation or reduced stability were the cause for the decreased respiratory complex levels upon Sam50 or mitofilin depletion, it would be difficult to explain why we observe a more pronounced effect on respiratory complexes I and IV than on complex III. Alternatively, it is possible that depletion of Sam50 or mitofilin and the subsequent disorganization of cristae structure impair the import of respiratory complex subunits. However, it would remain to be investigated how Sam50 or mitofilin loss could specifically affect solely the import of these proteins.

In conclusion, the work of our group and of other groups highlights the importance of cristae organization for the assembly or stability of respiratory complexes. Interestingly, we observed a stronger effect on both respiratory complex assembly and stability and on cristae structure when Sam50 was depleted than when mitofilin was depleted. The fact that we found complex I to be affected the most, followed by complex IV, strongly suggests a role for the mtDNA in this process.

4.8 The MIB complex influences TTC19

Data of SILAC analyses conducted in our group showed that both Sam50 and mitofilin depletion not only affect the levels of MIB complex and respiratory complex components, but also lead to a reduction in the levels of TTC19 (Ott et al., 2012 and Vera Kozjak-Pavlovic, unpublished data). In my work, I could confirm this connection with western blot (Figure 3-25) and *in vitro* import experiments (Figures 3-27). TTC19 was first described by Ghezzi and co-workers as a complex III assembly factor (Ghezzi et al., 2011). They found TTC19 in two complexes of about 500 kDa and of more than 1 MDa in mouse cells. In human cells, they could only detect the larger complex. Interestingly, they saw that the larger TTC19-containing complex is also present in rho⁰ cells which lack respiratory complexes

containing mtDNA-encoded subunits, and therefore suggested that TTC19 must have an additional function. The observation that assembly of TTC19 into the higher molecular weight complexes was strongly reduced upon Sam50 depletion whereas the smaller complex was detectable earlier (Figure 3-29), raised the interesting hypothesis that TTC19 is present in the large complex together with Sam50. Although this could not be confirmed by co-immunoprecipitation experiments (Figure 3-30), it is possible that the interaction of TTC19 with the MIB complex is occurring but too instable for detection or only transient. Therefore, the exact connection between TTC19 and Sam50 remains to be elucidated in order to be able to explain why Sam50 loss specifically affects TTC19.

4.9 TTC19 plays a role in respiratory complex assembly

TTC19 was first identified as a complex III assembly factor by Ghezzi and co-workers. They demonstrated that cells with mutated TTC19 have a specific reduction in complex III activity, whereas the activities of the other respiratory complexes are unaltered. In addition, they showed that TTC19 interacts with the complex III components Core1 and RISP, and that the smaller TTC19 containing complex migrates at the same size as the complex III dimer, and therefore probably is identical to this respiratory complex (Ghezzi et al., 2011).

This specificity of TTC19 for complex III assembly is in contrast to my investigations into the function of this protein. The SILAC analysis of TTC19-depleted mitochondria showed that TTC19 has an effect on various respiratory complex components, mainly of complex I and IV. Two components of complex III and one of complex V were also affected (Table 3-1). The reduction of these respiratory complex components could partly be confirmed by SDS-PAGE analysis (Figure 3-31). BN-PAGE analysis of TTC19-depleted mitochondria demonstrated that the complex III dimer was absent and a subcomplex of complex IV was reduced (Figure 3-34). When the assembly of complexes I, III and IV was investigated *in vitro*, a clear reduction in respiratory complex assembly could be observed, especially of the respiratory supercomplexes (Figure 3-35). As I could exclude that complex III loss affects NDUF51 and COX2 levels (Figure 3-32), the decrease in the levels of these proteins and the reduced complex IV levels and assembly upon TTC19 depletion cannot be explained by complex III reduction. Therefore, TTC19 seems to play a role also in the assembly of other respiratory complexes. The difference between my results and those of Ghezzi and co-workers might be explained by the different cell types which were used. Ghezzi and co-workers analyzed patient cells with mutations in TTC19 (Ghezzi et al., 2011), whereas my study was conducted in HeLa cells. As these are immortalized cancer cells, their metabolism is altered and they do not depend on energy production via the respiratory chain but can survive by glycolysis. Therefore, there might be changes

in the regulation of respiratory complexes. In addition, we examined different aspects of TTC19 loss. I assessed the levels and assembly of respiratory complexes, whereas Ghezzi and co-workers tested the activity of the respiratory complexes (Ghezzi et al., 2011). I also observed the strongest effect on the levels of complex III subunits and on the complex III dimer, whereas the reduction in complex IV was less pronounced and might not have an effect on respiratory complex activity. For complex I, I observed a reduction in several components in the SILAC analysis and in the levels of the subunit NDUFS1 upon TTC19 depletion, but not in the levels of the complex itself. Therefore, complex I, IV and V activity in *ttc19kd-2* cells would have to be examined to be able to evaluate the functionality of these complexes upon TTC19 depletion. Likewise, the complex assembly and activity of respiratory complexes needs to be examined in *core1kd-1* cells to determine the influence of complex III loss not only on protein levels of subunits of the other respiratory complexes but also on complex assembly and activity.

4.10 Perspectives

In my work, I could demonstrate that neisserial β -barrel proteins are targeted to mitochondria, whereas other work in our lab has shown that this is not the case for all bacterial β -barrel protein (Kozjak-Pavlovic et al., 2011). To gain a deeper insight into the targeting behavior of bacterial β -barrel proteins to mitochondria, it would be necessary to test β -barrel proteins of more bacteria to establish whether really only neisserial ones can be imported. As *E. coli* and *S. enterica* both are Entobacteriaceae, it would especially be interesting to examine proteins of other bacterial families. Testing β -barrel proteins of more neisserial strains would meanwhile help to clarify whether there indeed is a connection between neisserial pathogenicity and targeting of PorB to mitochondria. Besides, it would be interesting to extend the study to yeast β -barrel proteins, in order to understand why there are differences in the behavior between yeast and mammalian import machineries regarding the import of bacterial β -barrel proteins.

In the next part of my work, I could show that β -barrel proteins do not possess a linear mitochondrial targeting sequence but that the secondary structure or charge of the protein seem to play an important role in this process. It would therefore be interesting to compare the sequences and structures of different β -barrel proteins which are known to target or not target mitochondria in order to be able to elucidate which parts contribute to mitochondrial targeting.

Additionally, my own work and the work performed in our group confirmed the connection between the SAM complex and CHCHD3, mitofilin, CHCHD6 and DnaJC11, and demonstrated the role of the MIB complex in the maintenance of cristae structure in mammalian cells. I could show that mitofilin, CHCHD3 and Sam50 are present together in the large > 1 MDa holo-MIB complex, whereas

CHCHD3 and mitofilin are also part of a smaller complex of about 700-800 kDa. However, it is not known exactly which proteins are present in the two different types of mitofilin-containing complexes. Therefore, it would be important to investigate the exact composition of both complexes and to determine which proteins interact directly, especially to be able to explain why the phenotypes upon Sam50 and mitofilin loss differ. In addition, the function of the peripheral components CHCHD6 and DnaJC11 remains to be elucidated.

Furthermore, work by me and our group demonstrated that Sam50 influences the respiratory complexes. However, it needs to be clarified whether reduction of respiratory complex components is a direct effect of Sam50 loss or whether this is a consequence of the altered cristae structure after Sam50 knockdown. Therefore, it would be necessary to impair cristae structure by depleting a protein crucial for cristae formatio which is not connected to the MIB complex and examine whether the same effect on the respiratory chain occurs. In addition, whereas the fact that respiratory complexes with the highest number of mtDNA-encoded subunits are affected the most upon Sam50 depletion points to a connection to mtDNA stability, it is necessary to prove this hypothesis by examining maintenance and repair of mtDNA in Sam50- and mitofilin-depleted cells.

In order to understand the influence of Sam50 and mitofilin on respiratory complex assembly, it would especially be interesting to elucidate the nature of the connection between the MIB complex and the respiratory complex assembly factor TTC19. I could demonstrate that Sam50 and mitofilin influence TTC19 levels and assembly, even though I could not confirm a direct interaction.

Besides, as the work of Ghezzi and co-workers demonstrated TTC19 to be specifically required for complex III assembly, whereas I could additionally see an effect on complex IV, the exact function of TTC19 and its mode of action remains to be elucidated. For that, it would be crucial to determine the components of the TTC19-containing complexes. It would be interesting to investigate this also in rho⁰ cells in order to find more easily other functions of TTC19. Knowing the interaction partners of TTC19 might also help to understand in which way TTC19 is influenced by Sam50 and mitofilin.

5 REFERENCES

- Abrahams, J.P., A.G. Leslie, R. Lutter, and J.E. Walker. 1994. Structure at 2.8 Å resolution of F1-ATPase from bovine heart mitochondria. *Nature*. 370:621-628.
- Acehan, D., Y. Xu, D.L. Stokes, and M. Schlame. 2007. Comparison of lymphoblast mitochondria from normal subjects and patients with Barth syndrome using electron microscopic tomography. *Laboratory Investigation; a Journal of Technical Methods and Pathology*. 87:40-48.
- Adam, A., M. Endres, C. Sirrenberg, F. Lottspeich, W. Neupert, and M. Brunner. 1999. Tim9, a new component of the TIM22.54 translocase in mitochondria. *The EMBO Journal*. 18:313-319.
- Ahting, U., T. Waizenegger, W. Neupert, and D. Rapaport. 2005. Signal-anchored proteins follow a unique insertion pathway into the outer membrane of mitochondria. *The Journal of Biological Chemistry*. 280:48-53.
- Albring, M., J. Griffith, and G. Attardi. 1977. Association of a protein structure of probable membrane derivation with HeLa cell mitochondrial DNA near its origin of replication. *Proceedings of the National Academy of Sciences of the United States of America*. 74:1348-1352.
- Alconada, A., M. Kubrich, M. Moczko, A. Honlinger, and N. Pfanner. 1995. The mitochondrial receptor complex: the small subunit Mom8b/lsp6 supports association of receptors with the general insertion pore and transfer of preproteins. *Molecular and Cellular Biology*. 15:6196-6205.
- Alkhaja, A.K., D.C. Jans, M. Nikolov, M. Vukotic, O. Lytovchenko, F. Ludewig, W. Schliebs, D. Riedel, H. Urlaub, S. Jakobs, and M. Deckers. 2012. MINOS1 is a conserved component of mitofilin complexes and required for mitochondrial function and cristae organization. *Molecular Biology of the Cell*. 23:247-257.
- Allen, S., H. Lu, D. Thornton, and K. Tokatlidis. 2003. Juxtaposition of the two distal CX3C motifs via intrachain disulfide bonding is essential for the folding of Tim10. *The Journal of Biological Chemistry*. 278:38505-38513.
- Alvarez-Dolado, M., M. Gonzalez-Moreno, A. Valencia, M. Zenke, J. Bernal, and A. Munoz. 1999. Identification of a mammalian homologue of the fungal Tom70 mitochondrial precursor protein import receptor as a thyroid hormone-regulated gene in specific brain regions. *Journal of Neurochemistry*. 73:2240-2249.
- Amati-Bonneau, P., M.L. Valentino, P. Reynier, M.E. Gallardo, B. Bornstein, A. Boissiere, Y. Campos, H. Rivera, J.G. de la Aleja, R. Carroccia, L. Iommarini, P. Labauge, D. Figarella-Branger, P. Marcorelles, A. Furby, K. Beauvais, F. Letournel, R. Liguori, C. La Morgia, P. Montagna, M. Liguori, C. Zanna, M. Rugolo, A. Cossarizza, B. Wissinger, C. Verny, R. Schwarzenbacher, M.A. Martin, J. Arenas, C. Ayuso, R. Garesse, G. Lenaers, D. Bonneau, and V. Carelli. 2008. OPA1 mutations induce mitochondrial DNA instability and optic atrophy 'plus' phenotypes. *Brain : a Journal of Neurology*. 131:338-351.
- An, J., J. Shi, Q. He, K. Lui, Y. Liu, Y. Huang, and M.S. Sheikh. 2012. CHCM1/CHCHD6, novel mitochondrial protein linked to regulation of mitofilin and mitochondrial cristae morphology. *The Journal of Biological Chemistry*. 287:7411-7426.
- Anderson, S., A.T. Bankier, B.G. Barrell, M.H. de Bruijn, A.R. Coulson, J. Drouin, I.C. Eperon, D.P. Nierlich, B.A. Roe, F. Sanger, P.H. Schreier, A.J. Smith, R. Staden, and I.G. Young. 1981. Sequence and organization of the human mitochondrial genome. *Nature*. 290:457-465.
- Antonicka, H., S.C. Leary, G.H. Guercin, J.N. Agar, R. Horvath, N.G. Kennaway, C.O. Harding, M. Jaksch, and E.A. Shoubridge. 2003a. Mutations in COX10 result in a defect in mitochondrial heme A biosynthesis and account for multiple, early-onset clinical phenotypes associated with isolated COX deficiency. *Human Molecular Genetics*. 12:2693-2702.
- Antonicka, H., A. Mattman, C.G. Carlson, D.M. Glerum, K.C. Hoffbuhr, S.C. Leary, N.G. Kennaway, and E.A. Shoubridge. 2003b. Mutations in COX15 produce a defect in the mitochondrial heme biosynthetic pathway, causing early-onset fatal hypertrophic cardiomyopathy. *American Journal of Human Genetics*. 72:101-114.

- Armstrong, L.C., T. Komiya, B.E. Bergman, K. Mihara, and P. Bornstein. 1997. Metaxin is a component of a preprotein import complex in the outer membrane of the mammalian mitochondrion. *The Journal of Biological Chemistry*. 272:6510-6518.
- Armstrong, L.C., A.J. Saenz, and P. Bornstein. 1999. Metaxin 1 interacts with metaxin 2, a novel related protein associated with the mammalian mitochondrial outer membrane. *Journal of Cellular Biochemistry*. 74:11-22.
- Arnold, I., K. Pfeiffer, W. Neupert, R.A. Stuart, and H. Schagger. 1998. Yeast mitochondrial F1F0-ATP synthase exists as a dimer: identification of three dimer-specific subunits. *The EMBO Journal*. 17:7170-7178.
- Arnold, S., and B. Kadenbach. 1997. Cell respiration is controlled by ATP, an allosteric inhibitor of cytochrome-c oxidase. *European Journal of Biochemistry / FEBS*. 249:350-354.
- Barghuti, F., K. Elian, J.M. Gomori, A. Shaag, S. Edvardson, A. Saada, and O. Elpeleg. 2008. The unique neuroradiology of complex I deficiency due to NDUFA12L defect. *Molecular Genetics and Metabolism*. 94:78-82.
- Barros, M.H., C.G. Carlson, D.M. Glerum, and A. Tzagoloff. 2001. Involvement of mitochondrial ferredoxin and Cox15p in hydroxylation of heme O. *FEBS Letters*. 492:133-138.
- Baseler, W.A., E.R. Dabkowski, C.L. Williamson, T.L. Croston, D. Thapa, M.J. Powell, T.T. Razunguzwa, and J.M. Hollander. 2011. Proteomic alterations of distinct mitochondrial subpopulations in the type 1 diabetic heart: contribution of protein import dysfunction. *American Journal of Physiology - Regulatory, Integrative and Comparative Physiology*. 300:R186-200.
- Bayrhuber, M., T. Meins, M. Habeck, S. Becker, K. Giller, S. Villinger, C. Vonrhein, C. Griesinger, M. Zweckstetter, and K. Zeth. 2008. Structure of the human voltage-dependent anion channel. *Proceedings of the National Academy of Sciences of the United States of America*. 105:15370-15375.
- Becker, T., S. Pfannschmidt, B. Guiard, D. Stojanovski, D. Milenkovic, S. Kutik, N. Pfanner, C. Meisinger, and N. Wiedemann. 2008. Biogenesis of the mitochondrial TOM complex: Mim1 promotes insertion and assembly of signal-anchored receptors. *The Journal of Biological Chemistry*. 283:120-127.
- Becker, T., L.S. Wenz, V. Kruger, W. Lehmann, J.M. Muller, L. Goroncy, N. Zufall, T. Lithgow, B. Guiard, A. Chacinska, R. Wagner, C. Meisinger, and N. Pfanner. 2011. The mitochondrial import protein Mim1 promotes biogenesis of multispinning outer membrane proteins. *The Journal of Cell Biology*. 194:387-395.
- Beilharz, T., B. Egan, P.A. Silver, K. Hofmann, and T. Lithgow. 2003. Bipartite signals mediate subcellular targeting of tail-anchored membrane proteins in *Saccharomyces cerevisiae*. *The Journal of Biological Chemistry*. 278:8219-8223.
- Berger, K.H., L.F. Sogo, and M.P. Yaffe. 1997. Mdm12p, a component required for mitochondrial inheritance that is conserved between budding and fission yeast. *The Journal of Cell Biology*. 136:545-553.
- Bihlmaier, K., N. Mesecke, N. Terziyska, M. Bien, K. Hell, and J.M. Herrmann. 2007. The disulfide relay system of mitochondria is connected to the respiratory chain. *The Journal of Cell Biology*. 179:389-395.
- Bione, S., P. D'Adamo, E. Maestrini, A.K. Gedeon, P.A. Bolhuis, and D. Toniolo. 1996. A novel X-linked gene, G4.5, is responsible for Barth syndrome. *Nature Genetics*. 12:385-389.
- Bohnert, M., N. Pfanner, and M. van der Laan. 2007. A dynamic machinery for import of mitochondrial precursor proteins. *FEBS Letters*. 581:2802-2810.
- Bohnert, M., L.S. Wenz, R.M. Zerbes, S.E. Horvath, D.A. Stroud, K. von der Malsburg, J.M. Muller, S. Oeljeklaus, I. Perschil, B. Warscheid, A. Chacinska, M. Veenhuis, I.J. van der Klei, G. Daum, N. Wiedemann, T. Becker, N. Pfanner, and M. van der Laan. 2012. Role of mitochondrial inner membrane organizing system in protein biogenesis of the mitochondrial outer membrane. *Molecular Biology of the Cell*. 23:3948-3956.

- Boldogh, I.R., D.W. Nowakowski, H.C. Yang, H. Chung, S. Karmon, P. Royes, and L.A. Pon. 2003. A protein complex containing Mdm10p, Mdm12p, and Mmm1p links mitochondrial membranes and DNA to the cytoskeleton-based segregation machinery. *Molecular biology of the Cell*. 14:4618-4627.
- Bos, M.P., V. Robert, and J. Tommassen. 2007. Functioning of outer membrane protein assembly factor Omp85 requires a single POTRA domain. *EMBO Reports*. 8:1149-1154.
- Böttlinger, L., S.E. Horvath, T. Kleinschroth, C. Hunte, G. Daum, N. Pfanner, and T. Becker. 2012. Phosphatidylethanolamine and cardiolipin differentially affect the stability of mitochondrial respiratory chain supercomplexes. *Journal of Molecular Biology*. 423:677-686.
- Brix, J., S. Rudiger, B. Bukau, J. Schneider-Mergener, and N. Pfanner. 1999. Distribution of binding sequences for the mitochondrial import receptors Tom20, Tom22, and Tom70 in a presequence-carrying preprotein and a non-cleavable preprotein. *The Journal of Biological Chemistry*. 274:16522-16530.
- Carroll, J., I.M. Fearnley, R.J. Shannon, J. Hirst, and J.E. Walker. 2003. Analysis of the subunit composition of complex I from bovine heart mitochondria. *Molecular & Cellular Proteomics : MCP*. 2:117-126.
- Carroll, J., I.M. Fearnley, J.M. Skehel, R.J. Shannon, J. Hirst, and J.E. Walker. 2006. Bovine complex I is a complex of 45 different subunits. *The Journal of Biological Chemistry*. 281:32724-32727.
- Chacinska, A., C.M. Koehler, D. Milenkovic, T. Lithgow, and N. Pfanner. 2009. Importing mitochondrial proteins: machineries and mechanisms. *Cell*. 138:628-644.
- Chacinska, A., M. Lind, A.E. Frazier, J. Dudek, C. Meisinger, A. Geissler, A. Sickmann, H.E. Meyer, K.N. Truscott, B. Guiard, N. Pfanner, and P. Rehling. 2005. Mitochondrial presequence translocase: switching between TOM tethering and motor recruitment involves Tim21 and Tim17. *Cell*. 120:817-829.
- Chacinska, A., S. Pfannschmidt, N. Wiedemann, V. Kozjak, L.K. Sanjuan Szklarz, A. Schulze-Specking, K.N. Truscott, B. Guiard, C. Meisinger, and N. Pfanner. 2004. Essential role of Mia40 in import and assembly of mitochondrial intermembrane space proteins. *The EMBO Journal*. 23:3735-3746.
- Chan, N.C., and T. Lithgow. 2008. The peripheral membrane subunits of the SAM complex function codependently in mitochondrial outer membrane biogenesis. *Molecular Biology of the Cell*. 19:126-136.
- Chen, X.J., and R.A. Butow. 2005. The organization and inheritance of the mitochondrial genome. *Nature Reviews Genetics*. 6:815-825.
- Cipolat, S., O. Martins de Brito, B. Dal Zilio, and L. Scorrano. 2004. OPA1 requires mitofusin 1 to promote mitochondrial fusion. *Proceedings of the National Academy of Sciences of the United States of America*. 101:15927-15932.
- Clarke, S. 1976. A major polypeptide component of rat liver mitochondria: carbamyl phosphate synthetase. *The Journal of Biological Chemistry*. 251:950-961.
- Claros, M.G., and P. Vincens. 1996. Computational method to predict mitochondrially imported proteins and their targeting sequences. *European journal of biochemistry / FEBS*. 241:779-786.
- Collinson, I.R., M.J. Runswick, S.K. Buchanan, I.M. Fearnley, J.M. Skehel, M.J. van Raaij, D.E. Griffiths, and J.E. Walker. 1994. Fo membrane domain of ATP synthase from bovine heart mitochondria: purification, subunit composition, and reconstitution with F1-ATPase. *Biochemistry*. 33:7971-7978.
- Colombini, M. 1979. A candidate for the permeability pathway of the outer mitochondrial membrane. *Nature*. 279:643-645.
- Crompton, M. 2000. Mitochondrial intermembrane junctional complexes and their role in cell death. *The Journal of Physiology*. 529 Pt 1:11-21.

- Cruciat, C.M., S. Brunner, F. Baumann, W. Neupert, and R.A. Stuart. 2000. The cytochrome bc1 and cytochrome c oxidase complexes associate to form a single supracomplex in yeast mitochondria. *The Journal of Biological Chemistry*. 275:18093-18098.
- Cruciat, C.M., K. Hell, H. Folsch, W. Neupert, and R.A. Stuart. 1999. Bcs1p, an AAA-family member, is a chaperone for the assembly of the cytochrome bc(1) complex. *The EMBO Journal*. 18:5226-5233.
- D'Amours, D., S. Desnoyers, I. D'Silva, and G.G. Poirier. 1999. Poly(ADP-ribosyl)ation reactions in the regulation of nuclear functions. *The Biochemical Journal*. 342 (Pt 2):249-268.
- Dabir, D.V., E.P. Leverich, S.K. Kim, F.D. Tsai, M. Hirasawa, D.B. Knaff, and C.M. Koehler. 2007. A role for cytochrome c and cytochrome c peroxidase in electron shuttling from Erv1. *The EMBO Journal*. 26:4801-4811.
- Darshi, M., V.L. Mendiola, M.R. Mackey, A.N. Murphy, A. Koller, G.A. Perkins, M.H. Ellisman, and S.S. Taylor. 2011. ChChd3, an inner mitochondrial membrane protein, is essential for maintaining crista integrity and mitochondrial function. *The Journal of Biological Chemistry*. 286:2918-2932.
- Darshi, M., K.N. Trinh, A.N. Murphy, and S.S. Taylor. 2012. Targeting and import mechanism of coiled-coil helix coiled-coil helix domain-containing protein 3 (ChChd3) into the mitochondrial intermembrane space. *The Journal of Biological Chemistry*. 287:39480-39491.
- de Keyzer, J., C. van der Does, and A.J. Driessen. 2003. The bacterial translocase: a dynamic protein channel complex. *Cellular and Molecular Life Sciences : CMLS*. 60:2034-2052.
- De Meirleir, L., S. Seneca, W. Lissens, I. De Clercq, F. Eyskens, E. Gerlo, J. Smet, and R. Van Coster. 2004. Respiratory chain complex V deficiency due to a mutation in the assembly gene ATP12. *Journal of Medical Genetics*. 41:120-124.
- Dekker, P.J., P. Keil, J. Rassow, A.C. Maarse, N. Pfanner, and M. Meijer. 1993. Identification of MIM23, a putative component of the protein import machinery of the mitochondrial inner membrane. *FEBS Letters*. 330:66-70.
- Derrick, J.P., R. Urwin, J. Suker, I.M. Feavers, and M.C. Maiden. 1999. Structural and evolutionary inference from molecular variation in *Neisseria* porins. *Infection and Immunity*. 67:2406-2413.
- Detmer, S.A., and D.C. Chan. 2007. Functions and dysfunctions of mitochondrial dynamics. *Nature reviews. Molecular Cell Biology*. 8:870-879.
- Deuschle, U., W.K. Meyer, and H.J. Thiesen. 1995. Tetracycline-reversible silencing of eukaryotic promoters. *Molecular and Cellular Biology*. 15:1907-1914.
- Dietmeier, K., A. Honlinger, U. Bomer, P.J. Dekker, C. Eckerskorn, F. Lottspeich, M. Kubrich, and N. Pfanner. 1997. Tom5 functionally links mitochondrial preprotein receptors to the general import pore. *Nature*. 388:195-200.
- Dimmer, K.S., S. Jakobs, F. Vogel, K. Altmann, and B. Westermann. 2005. Mdm31 and Mdm32 are inner membrane proteins required for maintenance of mitochondrial shape and stability of mitochondrial DNA nucleoids in yeast. *The Journal of Cell Biology*. 168:103-115.
- Dolezal, P., V. Likic, J. Tachezy, and T. Lithgow. 2006. Evolution of the molecular machines for protein import into mitochondria. *Science*. 313:314-318.
- Dunning, C.J., M. McKenzie, C. Sugiana, M. Lazarou, J. Silke, A. Connelly, J.M. Fletcher, D.M. Kirby, D.R. Thorburn, and M.T. Ryan. 2007. Human CIA30 is involved in the early assembly of mitochondrial complex I and mutations in its gene cause disease. *The EMBO Journal*. 26:3227-3237.
- Endo, T., H. Yamamoto, and M. Esaki. 2003. Functional cooperation and separation of translocators in protein import into mitochondria, the double-membrane bounded organelles. *Journal of Cell Science*. 116:3259-3267.
- Endres, M., W. Neupert, and M. Brunner. 1999. Transport of the ADP/ATP carrier of mitochondria from the TOM complex to the TIM22.54 complex. *The EMBO Journal*. 18:3214-3221.

- Engelbrecht, S., and W. Junge. 1997. ATP synthase: a tentative structural model. *FEBS Letters*. 414:485-491.
- Eband, R.F., U. Schlattner, T. Wallimann, M.L. Lacombe, and R.M. Eband. 2007. Novel lipid transfer property of two mitochondrial proteins that bridge the inner and outer membranes. *Biophysical Journal*. 92:126-137.
- Fernandez-Vizarra, E., M. Bugiani, P. Goffrini, F. Carrara, L. Farina, E. Procopio, A. Donati, G. Uziel, I. Ferrero, and M. Zeviani. 2007. Impaired complex III assembly associated with BCS1L gene mutations in isolated mitochondrial encephalopathy. *Human Molecular Genetics*. 16:1241-1252.
- Fernandez-Vizarra, E., V. Tiranti, and M. Zeviani. 2009. Assembly of the oxidative phosphorylation system in humans: what we have learned by studying its defects. *Biochimica et Biophysica Acta*. 1793:200-211.
- Frey, T.G., and C.A. Mannella. 2000. The internal structure of mitochondria. *Trends in Biochemical Sciences*. 25:319-324.
- Frezza, C., S. Cipolat, O. Martins de Brito, M. Micaroni, G.V. Beznoussenko, T. Rudka, D. Bartoli, R.S. Polishuck, N.N. Danial, B. De Strooper, and L. Scorrano. 2006. OPA1 controls apoptotic cristae remodeling independently from mitochondrial fusion. *Cell*. 126:177-189.
- Gabaldon, T., and M.A. Huynen. 2003. Reconstruction of the proto-mitochondrial metabolism. *Science*. 301:609.
- Gärtner, F., W. Voos, A. Querol, B.R. Miller, E.A. Craig, M.G. Cumsy, and N. Pfanner. 1995. Mitochondrial import of subunit Va of cytochrome c oxidase characterized with yeast mutants. *The Journal of Biological Chemistry*. 270:3788-3795.
- Geissler, A., A. Chacinska, K.N. Truscott, N. Wiedemann, K. Brandner, A. Sickmann, H.E. Meyer, C. Meisinger, N. Pfanner, and P. Rehling. 2002. The mitochondrial presequence translocase: an essential role of Tim50 in directing preproteins to the import channel. *Cell*. 111:507-518.
- Gentle, I., K. Gabriel, P. Beech, R. Waller, and T. Lithgow. 2004. The Omp85 family of proteins is essential for outer membrane biogenesis in mitochondria and bacteria. *The Journal of Cell Biology*. 164:19-24.
- Gentle, I.E., L. Burri, and T. Lithgow. 2005. Molecular architecture and function of the Omp85 family of proteins. *Molecular Microbiology*. 58:1216-1225.
- Ghezzi, D., P. Arzuffi, M. Zordan, C. Da Re, C. Lamperti, C. Benna, P. D'Adamo, D. Diodato, R. Costa, C. Mariotti, G. Uziel, C. Smiderle, and M. Zeviani. 2011. Mutations in TTC19 cause mitochondrial complex III deficiency and neurological impairment in humans and flies. *Nature Genetics*. 43:259-263.
- Ghezzi, D., P. Goffrini, G. Uziel, R. Horvath, T. Klopstock, H. Lochmuller, P. D'Adamo, P. Gasparini, T.M. Strom, H. Prokisch, F. Invernizzi, I. Ferrero, and M. Zeviani. 2009. SDHAF1, encoding a LYR complex-II specific assembly factor, is mutated in SDH-defective infantile leukoencephalopathy. *Nature Genetics*. 41:654-656.
- Gilkerson, R.W., J.M. Selker, and R.A. Capaldi. 2003. The cristal membrane of mitochondria is the principal site of oxidative phosphorylation. *FEBS Letters*. 546:355-358.
- Giraud, M.F., P. Paumard, V. Soubannier, J. Vaillier, G. Arselin, B. Salin, J. Schaeffer, D. Brethes, J.P. di Rago, and J. Velours. 2002. Is there a relationship between the supramolecular organization of the mitochondrial ATP synthase and the formation of cristae? *Biochimica et Biophysica Acta*. 1555:174-180.
- Glick, B.S., A. Brandt, K. Cunningham, S. Muller, R.L. Hallberg, and G. Schatz. 1992. Cytochromes c1 and b2 are sorted to the intermembrane space of yeast mitochondria by a stop-transfer mechanism. *Cell*. 69:809-822.
- Goping, I.S., D.G. Millar, and G.C. Shore. 1995. Identification of the human mitochondrial protein import receptor, huMas20p. Complementation of delta mas20 in yeast. *FEBS Letters*. 373:45-50.

- Grigorieff, N. 1998. Three-dimensional structure of bovine NADH:ubiquinone oxidoreductase (complex I) at 2.2 Å in ice. *Journal of Molecular Biology*. 277:1033-1046.
- Griparic, L., N.N. van der Wel, I.J. Orozco, P.J. Peters, and A.M. van der Bliek. 2004. Loss of the intermembrane space protein Mgm1/OPA1 induces swelling and localized constrictions along the lengths of mitochondria. *The Journal of Biological Chemistry*. 279:18792-18798.
- Habib, S.J., T. Waizenegger, M. Lech, W. Neupert, and D. Rapaport. 2005. Assembly of the TOB complex of mitochondria. *The Journal of Biological Chemistry*. 280:6434-6440.
- Habib, S.J., T. Waizenegger, A. Niewianda, S.A. Paschen, W. Neupert, and D. Rapaport. 2007. The N-terminal domain of Tob55 has a receptor-like function in the biogenesis of mitochondrial beta-barrel proteins. *The Journal of Cell Biology*. 176:77-88.
- Hackenbrock, C.R. 1966. Ultrastructural bases for metabolically linked mechanical activity in mitochondria. I. Reversible ultrastructural changes with change in metabolic steady state in isolated liver mitochondria. *The Journal of Cell Biology*. 30:269-297.
- Hackenbrock, C.R. 1968. Ultrastructural bases for metabolically linked mechanical activity in mitochondria. II. Electron transport-linked ultrastructural transformations in mitochondria. *The Journal of Cell Biology*. 37:345-369.
- Hägerhäll, C. 1997. Succinate: quinone oxidoreductases. Variations on a conserved theme. *Biochimica et Biophysica Acta*. 1320:107-141.
- Hanahan, D. 1983. Studies on transformation of *Escherichia coli* with plasmids. *Journal of Molecular Biology*. 166:557-580.
- Hao, H.X., O. Khalimonchuk, M. Schraders, N. Dephoure, J.P. Bayley, H. Kunst, P. Devilee, C.W. Cremers, J.D. Schiffman, B.G. Bentz, S.P. Gygi, D.R. Winge, H. Kremer, and J. Rutter. 2009. SDH5, a gene required for flavination of succinate dehydrogenase, is mutated in paraganglioma. *Science*. 325:1139-1142.
- Harner, M., C. Korner, D. Walther, D. Mokranjac, J. Kaesmacher, U. Welsch, J. Griffith, M. Mann, F. Reggiori, and W. Neupert. 2011a. The mitochondrial contact site complex, a determinant of mitochondrial architecture. *The EMBO Journal*. 30:4356-4370.
- Harner, M., W. Neupert, and M. Deponte. 2011b. Lateral release of proteins from the TOM complex into the outer membrane of mitochondria. *The EMBO Journal*. 30:3232-3241.
- Head, B.P., M. Zulaika, S. Ryazantsev, and A.M. van der Bliek. 2011. A novel mitochondrial outer membrane protein, MOMA-1, that affects cristae morphology in *Caenorhabditis elegans*. *Molecular Biology of the Cell*. 22:831-841.
- Herlan, M., F. Vogel, C. Bornhøvd, W. Neupert, and A.S. Reichert. 2003. Processing of Mgm1 by the rhomboid-type protease Pcp1 is required for maintenance of mitochondrial morphology and of mitochondrial DNA. *The Journal of Biological Chemistry*. 278:27781-27788.
- Hess, D.C., C.L. Myers, C. Huttenhower, M.A. Hibbs, A.P. Hayes, J. Paw, J.J. Clore, R.M. Mendoza, B.S. Luis, C. Nislow, G. Giaever, M. Costanzo, O.G. Troyanskaya, and A.A. Caudy. 2009. Computationally driven, quantitative experiments discover genes required for mitochondrial biogenesis. *PLoS Genetics*. 5:e1000407.
- Hill, K., K. Model, M.T. Ryan, K. Dietmeier, F. Martin, R. Wagner, and N. Pfanner. 1998. Tom40 forms the hydrophilic channel of the mitochondrial import pore for preproteins. *Nature*. 395:516-521.
- Hobbs, A.E., M. Srinivasan, J.M. McCaffery, and R.E. Jensen. 2001. Mmm1p, a mitochondrial outer membrane protein, is connected to mitochondrial DNA (mtDNA) nucleoids and required for mtDNA stability. *The Journal of Cell Biology*. 152:401-410.
- Hofmann, S., U. Rothbauer, N. Muhlenbein, K. Baiker, K. Hell, and M.F. Bauer. 2005. Functional and mutational characterization of human MIA40 acting during import into the mitochondrial intermembrane space. *Journal of Molecular Biology*. 353:517-528.
- Honlinger, A., U. Bomer, A. Alconada, C. Eckerskorn, F. Lottspeich, K. Dietmeier, and N. Pfanner. 1996. Tom7 modulates the dynamics of the mitochondrial outer membrane translocase and plays a pathway-related role in protein import. *The EMBO journal*. 15:2125-2137.

- Hoppins, S., S.R. Collins, A. Cassidy-Stone, E. Hummel, R.M. Devay, L.L. Lackner, B. Westermann, M. Schuldiner, J.S. Weissman, and J. Nunnari. 2011. A mitochondrial-focused genetic interaction map reveals a scaffold-like complex required for inner membrane organization in mitochondria. *The Journal of Cell Biology*. 195:323-340.
- Hoppins, S., L. Lackner, and J. Nunnari. 2007. The machines that divide and fuse mitochondria. *Annual Review of Biochemistry*. 76:751-780.
- Hudson, G., P. Amati-Bonneau, E.L. Blakely, J.D. Stewart, L. He, A.M. Schaefer, P.G. Griffiths, K. Ahlqvist, A. Suomalainen, P. Reynier, R. McFarland, D.M. Turnbull, P.F. Chinnery, and R.W. Taylor. 2008. Mutation of OPA1 causes dominant optic atrophy with external ophthalmoplegia, ataxia, deafness and multiple mitochondrial DNA deletions: a novel disorder of mtDNA maintenance. *Brain : a Journal of Neurology*. 131:329-337.
- Hulett, J.M., F. Lueder, N.C. Chan, A.J. Perry, P. Wolynec, V.A. Likic, P.R. Gooley, and T. Lithgow. 2008. The transmembrane segment of Tom20 is recognized by Mim1 for docking to the mitochondrial TOM complex. *Journal of Molecular Biology*. 376:694-704.
- Humphries, A.D., I.C. Streimann, D. Stojanovski, A.J. Johnston, M. Yano, N.J. Hoogenraad, and M.T. Ryan. 2005. Dissection of the mitochondrial import and assembly pathway for human Tom40. *The Journal of Biological Chemistry*. 280:11535-11543.
- Iborra, F.J., H. Kimura, and P.R. Cook. 2004. The functional organization of mitochondrial genomes in human cells. *BMC Biology*. 2:9.
- Ishikawa, D., H. Yamamoto, Y. Tamura, K. Moritoh, and T. Endo. 2004. Two novel proteins in the mitochondrial outer membrane mediate beta-barrel protein assembly. *The Journal of Cell Biology*. 166:621-627.
- Iwata, S., J.W. Lee, K. Okada, J.K. Lee, M. Iwata, B. Rasmussen, T.A. Link, S. Ramaswamy, and B.K. Jap. 1998. Complete structure of the 11-subunit bovine mitochondrial cytochrome bc1 complex. *Science*. 281:64-71.
- Jensen, R.E., and C.D. Dunn. 2002. Protein import into and across the mitochondrial inner membrane: role of the TIM23 and TIM22 translocons. *Biochimica et Biophysica Acta*. 1592:25-34.
- Jiang, F., M.T. Ryan, M. Schlame, M. Zhao, Z. Gu, M. Klingenberg, N. Pfanner, and M.L. Greenberg. 2000. Absence of cardiolipin in the crd1 null mutant results in decreased mitochondrial membrane potential and reduced mitochondrial function. *The Journal of Biological Chemistry*. 275:22387-22394.
- Jiang, J.H., J.K. Davies, T. Lithgow, R.A. Strugnell, and K. Gabriel. 2011. Targeting of Neisserial PorB to the mitochondrial outer membrane: an insight on the evolution of beta-barrel protein assembly machines. *Molecular Microbiology*. 82:976-987.
- John, G.B., Y. Shang, L. Li, C. Renken, C.A. Mannella, J.M. Selker, L. Rangell, M.J. Bennett, and J. Zha. 2005. The mitochondrial inner membrane protein mitofilin controls cristae morphology. *Molecular Biology of the Cell*. 16:1543-1554.
- Johnston, A.J., J. Hoogenraad, D.A. Dougan, K.N. Truscott, M. Yano, M. Mori, N.J. Hoogenraad, and M.T. Ryan. 2002. Insertion and assembly of human tom7 into the preprotein translocase complex of the outer mitochondrial membrane. *The Journal of Biological Chemistry*. 277:42197-42204.
- Kadenbach, B., J. Jarausch, R. Hartmann, and P. Merle. 1983. Separation of mammalian cytochrome c oxidase into 13 polypeptides by a sodium dodecyl sulfate-gel electrophoretic procedure. *Analytical Biochemistry*. 129:517-521.
- Kato, H., and K. Mihara. 2008. Identification of Tom5 and Tom6 in the preprotein translocase complex of human mitochondrial outer membrane. *Biochemical and Biophysical Research Communications*. 369:958-963.
- Kemper, C., S.J. Habib, G. Engl, P. Heckmeyer, K.S. Dimmer, and D. Rapaport. 2008. Integration of tail-anchored proteins into the mitochondrial outer membrane does not require any known import components. *Journal of Cell Science*. 121:1990-1998.

- Kerscher, O., J. Holder, M. Srinivasan, R.S. Leung, and R.E. Jensen. 1997. The Tim54p-Tim22p complex mediates insertion of proteins into the mitochondrial inner membrane. *The Journal of Cell Biology*. 139:1663-1675.
- Kerscher, O., N.B. Sepuri, and R.E. Jensen. 2000. Tim18p is a new component of the Tim54p-Tim22p translocon in the mitochondrial inner membrane. *Molecular Biology of the Cell*. 11:103-116.
- Kim, S., J.C. Malinverni, P. Sliz, T.J. Silhavy, S.C. Harrison, and D. Kahne. 2007. Structure and function of an essential component of the outer membrane protein assembly machine. *Science*. 317:961-964.
- Knowles, T.J., M. Jeeves, S. Bobat, F. Dancea, D. McClelland, T. Palmer, M. Overduin, and I.R. Henderson. 2008. Fold and function of polypeptide transport-associated domains responsible for delivering unfolded proteins to membranes. *Molecular Microbiology*. 68:1216-1227.
- Koebnik, R., K.P. Locher, and P. Van Gelder. 2000. Structure and function of bacterial outer membrane proteins: barrels in a nutshell. *Molecular Microbiology*. 37:239-253.
- Körner, C., M. Barrera, J. Dukanovic, K. Eydt, M. Harner, R. Rabl, F. Vogel, D. Rapaport, W. Neupert, and A.S. Reichert. 2012. The C-terminal domain of Fcj1 is required for formation of crista junctions and interacts with the TOB/SAM complex in mitochondria. *Molecular Biology of the Cell*. 23:2143-2155.
- Kozjak-Pavlovic, V., E.A. Dian-Lothrop, M. Meinecke, O. Kepp, K. Ross, K. Rajalingam, A. Harsman, E. Hauf, V. Brinkmann, D. Gunther, I. Herrmann, R. Hurwitz, J. Rassow, R. Wagner, and T. Rudel. 2009. Bacterial porin disrupts mitochondrial membrane potential and sensitizes host cells to apoptosis. *PLoS Pathogens*. 5:e1000629.
- Kozjak-Pavlovic, V., C. Ott, M. Götz, and T. Rudel. 2011. Neisserial Omp85 protein is selectively recognized and assembled into functional complexes in the outer membrane of human mitochondria. *The Journal of Biological Chemistry*. 286:27019-27026.
- Kozjak-Pavlovic, V., K. Ross, N. Benlasfer, S. Kimmig, A. Karlas, and T. Rudel. 2007. Conserved roles of Sam50 and metaxins in VDAC biogenesis. *EMBO Reports*. 8:576-582.
- Kozjak-Pavlovic, V., K. Ross, M. Götz, C. Goosmann, and T. Rudel. 2010. A tag at the carboxy terminus prevents membrane integration of VDAC1 in mammalian mitochondria. *Journal of molecular Biology*. 397:219-232.
- Kozjak, V., N. Wiedemann, D. Milenkovic, C. Lohaus, H.E. Meyer, B. Guiard, C. Meisinger, and N. Pfanner. 2003. An essential role of Sam50 in the protein sorting and assembly machinery of the mitochondrial outer membrane. *The Journal of Biological Chemistry*. 278:48520-48523.
- Krause, F., N.H. Reifschneider, S. Goto, and N.A. Dencher. 2005. Active oligomeric ATP synthases in mammalian mitochondria. *Biochemical and Biophysical Research Communications*. 329:583-590.
- Krimmer, T., D. Rapaport, M.T. Ryan, C. Meisinger, C.K. Kassenbrock, E. Blachly-Dyson, M. Forte, M.G. Douglas, W. Neupert, F.E. Nargang, and N. Pfanner. 2001. Biogenesis of porin of the outer mitochondrial membrane involves an import pathway via receptors and the general import pore of the TOM complex. *The Journal of Cell Biology*. 152:289-300.
- Kucharczyk, R., M. Zick, M. Bietenhader, M. Rak, E. Couplan, M. Blondel, S.D. Caubet, and J.P. di Rago. 2009. Mitochondrial ATP synthase disorders: molecular mechanisms and the quest for curative therapeutic approaches. *Biochimica et Biophysica Acta*. 1793:186-199.
- Kutik, S., D. Stojanovski, L. Becker, T. Becker, M. Meinecke, V. Kruger, C. Prinz, C. Meisinger, B. Guiard, R. Wagner, N. Pfanner, and N. Wiedemann. 2008. Dissecting membrane insertion of mitochondrial beta-barrel proteins. *Cell*. 132:1011-1024.
- Lazarou, M., M. McKenzie, A. Ohtake, D.R. Thorburn, and M.T. Ryan. 2007. Analysis of the assembly profiles for mitochondrial- and nuclear-DNA-encoded subunits into complex I. *Molecular and Cellular Biology*. 27:4228-4237.
- Leuenberger, D., N.A. Bally, G. Schatz, and C.M. Koehler. 1999. Different import pathways through the mitochondrial intermembrane space for inner membrane proteins. *The EMBO Journal*. 18:4816-4822.

- Lu, H., S. Allen, L. Wardleworth, P. Savory, and K. Tokatlidis. 2004. Functional TIM10 chaperone assembly is redox-regulated in vivo. *The Journal of Biological Chemistry*. 279:18952-18958.
- Lutz, T., W. Neupert, and J.M. Herrmann. 2003. Import of small Tim proteins into the mitochondrial intermembrane space. *The EMBO Journal*. 22:4400-4408.
- Maarse, A.C., J. Blom, P. Keil, N. Pfanner, and M. Meijer. 1994. Identification of the essential yeast protein MIM17, an integral mitochondrial inner membrane protein involved in protein import. *FEBS letters*. 349:215-221.
- Malinverni, J.C., J. Werner, S. Kim, J.G. Sklar, D. Kahne, R. Misra, and T.J. Silhavy. 2006. YfiO stabilizes the YaeT complex and is essential for outer membrane protein assembly in *Escherichia coli*. *Molecular Microbiology*. 61:151-164.
- Mannella, C.A., M. Marko, P. Penczek, D. Barnard, and J. Frank. 1994. The internal compartmentation of rat-liver mitochondria: tomographic study using the high-voltage transmission electron microscope. *Microscopy Research and Technique*. 27:278-283.
- Mannella, C.A., D.R. Pfeiffer, P.C. Bradshaw, Moraru, II, B. Slepchenko, L.M. Loew, C.E. Hsieh, K. Buttle, and M. Marko. 2001. Topology of the mitochondrial inner membrane: dynamics and bioenergetic implications. *IUBMB Life*. 52:93-100.
- Massari, P., Y. Ho, and L.M. Wetzler. 2000. *Neisseria meningitidis* porin PorB interacts with mitochondria and protects cells from apoptosis. *Proceedings of the National Academy of Sciences of the United States of America*. 97:9070-9075.
- Massari, P., C.A. King, A.Y. Ho, and L.M. Wetzler. 2003. Neisserial PorB is translocated to the mitochondria of HeLa cells infected with *Neisseria meningitidis* and protects cells from apoptosis. *Cellular Microbiology*. 5:99-109.
- McKenzie, M., and M.T. Ryan. 2010. Assembly factors of human mitochondrial complex I and their defects in disease. *IUBMB Life*. 62:497-502.
- Meinecke, M., R. Wagner, P. Kovermann, B. Guiard, D.U. Mick, D.P. Hutu, W. Voos, K.N. Truscott, A. Chacinska, N. Pfanner, and P. Rehling. 2006. Tim50 maintains the permeability barrier of the mitochondrial inner membrane. *Science*. 312:1523-1526.
- Meineke, B., G. Engl, C. Kemper, A. Vasiljev-Neumeyer, H. Paulitschke, and D. Rapaport. 2008. The outer membrane form of the mitochondrial protein Mcr1 follows a TOM-independent membrane insertion pathway. *FEBS Letters*. 582:855-860.
- Meisinger, C., M. Rissler, A. Chacinska, L.K. Szklarz, D. Milenkovic, V. Kozjak, B. Schonfisch, C. Lohaus, H.E. Meyer, M.P. Yaffe, B. Guiard, N. Wiedemann, and N. Pfanner. 2004. The mitochondrial morphology protein Mdm10 functions in assembly of the preprotein translocase of the outer membrane. *Developmental Cell*. 7:61-71.
- Meisinger, C., A. Sickmann, and N. Pfanner. 2008. The mitochondrial proteome: from inventory to function. *Cell*. 134:22-24.
- Merkwirth, C., S. Dargazanli, T. Tatsuta, S. Geimer, B. Lower, F.T. Wunderlich, J.C. von Kleist-Retzow, A. Waisman, B. Westermann, and T. Langer. 2008. Prohibitins control cell proliferation and apoptosis by regulating OPA1-dependent cristae morphogenesis in mitochondria. *Genes & Development*. 22:476-488.
- Mesecke, N., N. Terziyska, C. Kozany, F. Baumann, W. Neupert, K. Hell, and J.M. Herrmann. 2005. A disulfide relay system in the intermembrane space of mitochondria that mediates protein import. *Cell*. 121:1059-1069.
- Meyer, B., I. Wittig, E. Trifilieff, M. Karas, and H. Schagger. 2007. Identification of two proteins associated with mammalian ATP synthase. *Molecular & Cellular Proteomics : MCP*. 6:1690-1699.
- Milenkovic, D., K. Gabriel, B. Guiard, A. Schulze-Specking, N. Pfanner, and A. Chacinska. 2007. Biogenesis of the essential Tim9-Tim10 chaperone complex of mitochondria: site-specific recognition of cysteine residues by the intermembrane space receptor Mia40. *The Journal of Biological Chemistry*. 282:22472-22480.

- Milenkovic, D., V. Kozjak, N. Wiedemann, C. Lohaus, H.E. Meyer, B. Guiard, N. Pfanner, and C. Meisinger. 2004. Sam35 of the mitochondrial protein sorting and assembly machinery is a peripheral outer membrane protein essential for cell viability. *The Journal of Biological Chemistry*. 279:22781-22785.
- Milenkovic, D., T. Ramming, J.M. Muller, L.S. Wenz, N. Gebert, A. Schulze-Specking, D. Stojanovski, S. Rospert, and A. Chacinska. 2009. Identification of the signal directing Tim9 and Tim10 into the intermembrane space of mitochondria. *Molecular Biology of the Cell*. 20:2530-2539.
- Minetti, C.A., J.Y. Tai, M.S. Blake, J.K. Pullen, S.M. Liang, and D.P. Remeta. 1997. Structural and functional characterization of a recombinant PorB class 2 protein from *Neisseria meningitidis*. Conformational stability and porin activity. *The Journal of Biological Chemistry*. 272:10710-10720.
- Misaka, T., T. Miyashita, and Y. Kubo. 2002. Primary structure of a dynamin-related mouse mitochondrial GTPase and its distribution in brain, subcellular localization, and effect on mitochondrial morphology. *The Journal of Biological Chemistry*. 277:15834-15842.
- Mitchell, P. 1976. Possible molecular mechanisms of the protonmotive function of cytochrome systems. *Journal of Theoretical Biology*. 62:327-367.
- Model, K., C. Meisinger, T. Prinz, N. Wiedemann, K.N. Truscott, N. Pfanner, and M.T. Ryan. 2001. Multistep assembly of the protein import channel of the mitochondrial outer membrane. *Nature Structural Biology*. 8:361-370.
- Mogensen, J.E., and D.E. Otzen. 2005. Interactions between folding factors and bacterial outer membrane proteins. *Molecular Microbiology*. 57:326-346.
- Müller, A., D. Gunther, V. Brinkmann, R. Hurwitz, T.F. Meyer, and T. Rudel. 2000. Targeting of the pro-apoptotic VDAC-like porin (PorB) of *Neisseria gonorrhoeae* to mitochondria of infected cells. *The EMBO Journal*. 19:5332-5343.
- Müller, A., J. Rassow, J. Grimm, N. Machuy, T.F. Meyer, and T. Rudel. 2002. VDAC and the bacterial porin PorB of *Neisseria gonorrhoeae* share mitochondrial import pathways. *The EMBO Journal*. 21:1916-1929.
- Müller, J.M., D. Milenkovic, B. Guiard, N. Pfanner, and A. Chacinska. 2008. Precursor oxidation by Mia40 and Erv1 promotes vectorial transport of proteins into the mitochondrial intermembrane space. *Molecular Biology of the Cell*. 19:226-236.
- Mun, J.Y., T.H. Lee, J.H. Kim, B.H. Yoo, Y.Y. Bahk, H.S. Koo, and S.S. Han. 2010. Caenorhabditis elegans mitofilin homologs control the morphology of mitochondrial cristae and influence reproduction and physiology. *Journal of Cellular Physiology*. 224:748-756.
- Myung, J., T. Gulesserian, M. Fountoulakis, and G. Lubec. 2003. Deranged hypothetical proteins Rik protein, Nit protein 2 and mitochondrial inner membrane protein, Mitofilin, in fetal Down syndrome brain. *Cell and Molecular Biology*. 49:739-746.
- Naoe, M., Y. Ohwa, D. Ishikawa, C. Ohshima, S. Nishikawa, H. Yamamoto, and T. Endo. 2004. Identification of Tim40 that mediates protein sorting to the mitochondrial intermembrane space. *The Journal of Biological Chemistry*. 279:47815-47821.
- Neupert, W., and J.M. Herrmann. 2007. Translocation of proteins into mitochondria. *Annual Review of Biochemistry*. 76:723-749.
- Nijtmans, L.G., J.W. Taanman, A.O. Muijsers, D. Speijer, and C. Van den Bogert. 1998. Assembly of cytochrome-c oxidase in cultured human cells. *European Journal of Biochemistry / FEBS*. 254:389-394.
- Nunnari, J., T.D. Fox, and P. Walter. 1993. A mitochondrial protease with two catalytic subunits of nonoverlapping specificities. *Science*. 262:1997-2004.
- Ogilvie, I., N.G. Kennaway, and E.A. Shoubbridge. 2005. A molecular chaperone for mitochondrial complex I assembly is mutated in a progressive encephalopathy. *The Journal of Clinical Investigation*. 115:2784-2792.

- Olichon, A., L. Baricault, N. Gas, E. Guillou, A. Valette, P. Belenguer, and G. Lenaers. 2003. Loss of OPA1 perturbs the mitochondrial inner membrane structure and integrity, leading to cytochrome c release and apoptosis. *The Journal of Biological Chemistry*. 278:7743-7746.
- Ott, C., K. Ross, S. Straub, B. Thiede, M. Götz, C. Goosmann, M. Krischke, M.J. Mueller, G. Krohne, T. Rudel, and V. Kozjak-Pavlovic. 2012. Sam50 functions in mitochondrial intermembrane space bridging and biogenesis of respiratory complexes. *Molecular and Cellular Biology*. 32:1173-1188.
- Ott, C., M. Utech, M. Götz, T. Rudel, and V. Kozjak-Pavlovic. 2013. The requirements for the import of neisserial Omp85 into the outer membrane of human mitochondria. *Bioscience Reports*. 33:303-312
- Pagliarini, D.J., S.E. Calvo, B. Chang, S.A. Sheth, S.B. Vafai, S.E. Ong, G.A. Walford, C. Sugiana, A. Boneh, W.K. Chen, D.E. Hill, M. Vidal, J.G. Evans, D.R. Thorburn, S.A. Carr, and V.K. Mootha. 2008. A mitochondrial protein compendium elucidates complex I disease biology. *Cell*. 134:112-123.
- Park, Y.U., J. Jeong, H. Lee, J.Y. Mun, J.H. Kim, J.S. Lee, M.D. Nguyen, S.S. Han, P.G. Suh, and S.K. Park. 2010. Disrupted-in-schizophrenia 1 (DISC1) plays essential roles in mitochondria in collaboration with Mitofilin. *Proceedings of the National Academy of Sciences of the United States of America*. 107:17785-17790.
- Paschen, S.A., W. Neupert, and D. Rapaport. 2005. Biogenesis of beta-barrel membrane proteins of mitochondria. *Trends in Biochemical Sciences*. 30:575-582.
- Paschen, S.A., U. Rothbauer, K. Kaldi, M.F. Bauer, W. Neupert, and M. Brunner. 2000. The role of the TIM8-13 complex in the import of Tim23 into mitochondria. *The EMBO Journal*. 19:6392-6400.
- Paschen, S.A., T. Waizenegger, T. Stan, M. Preuss, M. Cyrklaff, K. Hell, D. Rapaport, and W. Neupert. 2003. Evolutionary conservation of biogenesis of beta-barrel membrane proteins. *Nature*. 426:862-866.
- Paumard, P., J. Vaillier, B. Coulary, J. Schaeffer, V. Soubannier, D.M. Mueller, D. Brethes, J.P. di Rago, and J. Velours. 2002. The ATP synthase is involved in generating mitochondrial cristae morphology. *The EMBO Journal*. 21:221-230.
- Perkins, G., C. Renken, M.E. Martone, S.J. Young, M. Ellisman, and T. Frey. 1997. Electron tomography of neuronal mitochondria: three-dimensional structure and organization of cristae and membrane contacts. *Journal of Structural Biology*. 119:260-272.
- Perkins, G.A., C.W. Renken, I.J. van der Klei, M.H. Ellisman, W. Neupert, and T.G. Frey. 2001. Electron tomography of mitochondria after the arrest of protein import associated with Tom19 depletion. *European Journal of Cell Biology*. 80:139-150.
- Pfanner, N., and M. Meijer. 1995. Protein sorting. Pulling in the proteins. *Current Biology : CB*. 5:132-135.
- Pfeiffer, K., V. Gohil, R.A. Stuart, C. Hunte, U. Brandt, M.L. Greenberg, and H. Schagger. 2003. Cardiolipin stabilizes respiratory chain supercomplexes. *The Journal of Biological Chemistry*. 278:52873-52880.
- Rabl, R., V. Soubannier, R. Scholz, F. Vogel, N. Mendl, A. Vasiljev-Neumeyer, C. Korner, R. Jagasia, T. Keil, W. Baumeister, M. Cyrklaff, W. Neupert, and A.S. Reichert. 2009. Formation of cristae and crista junctions in mitochondria depends on antagonism between Fcj1 and Su e/g. *The Journal of Cell Biology*. 185:1047-1063.
- Rahmani, Z., C. Maunoury, and A. Siddiqui. 1998. Isolation of a novel human voltage-dependent anion channel gene. *European Journal of Human Genetics : EJHG*. 6:337-340.
- Rak, M., E. Tetaud, F. Godard, I. Sagot, B. Salin, S. Duvezin-Caubet, P.P. Slonimski, J. Rytka, and J.P. di Rago. 2007. Yeast cells lacking the mitochondrial gene encoding the ATP synthase subunit 6 exhibit a selective loss of complex IV and unusual mitochondrial morphology. *The Journal of Biological Chemistry*. 282:10853-10864.

- Rapaport, D., R.D. Taylor, M. Kaser, T. Langer, W. Neupert, and F.E. Nargang. 2001. Structural requirements of Tom40 for assembly into preexisting TOM complexes of mitochondria. *Molecular Biology of the Cell*. 12:1189-1198.
- Rehling, P., K. Model, K. Brandner, P. Kovermann, A. Sickmann, H.E. Meyer, W. Kuhlbrandt, R. Wagner, K.N. Truscott, and N. Pfanner. 2003. Protein insertion into the mitochondrial inner membrane by a twin-pore translocase. *Science*. 299:1747-1751.
- Reichert, A.S., and W. Neupert. 2002. Contact sites between the outer and inner membrane of mitochondria-role in protein transport. *Biochimica et Biophysica Acta*. 1592:41-49.
- Reinders, J., R.P. Zahedi, N. Pfanner, C. Meisinger, and A. Sickmann. 2006. Toward the complete yeast mitochondrial proteome: multidimensional separation techniques for mitochondrial proteomics. *Journal of Proteome Research*. 5:1543-1554.
- Rich, P.R., and A. Marechal. 2010. The mitochondrial respiratory chain. *Essays in Biochemistry*. 47:1-23.
- Robert, V., E.B. Volokhina, F. Senf, M.P. Bos, P. Van Gelder, and J. Tommassen. 2006. Assembly factor Omp85 recognizes its outer membrane protein substrates by a species-specific C-terminal motif. *PLoS Biology*. 4:e377.
- Rossi, M.N., M. Carbone, C. Mostocotto, C. Mancone, M. Tripodi, R. Maione, and P. Amati. 2009. Mitochondrial localization of PARP-1 requires interaction with mitofilin and is involved in the maintenance of mitochondrial DNA integrity. *The Journal of Biological Chemistry*. 284:31616-31624.
- Saeki, K., H. Suzuki, M. Tsuneoka, M. Maeda, R. Iwamoto, H. Hasuwa, S. Shida, T. Takahashi, M. Sakaguchi, T. Endo, Y. Miura, E. Mekada, and K. Mihara. 2000. Identification of mammalian TOM22 as a subunit of the preprotein translocase of the mitochondrial outer membrane. *The Journal of Biological Chemistry*. 275:31996-32002.
- Sagona, A.P., I.P. Nezis, N.M. Pedersen, K. Liestol, J. Poulton, T.E. Rusten, R.I. Skotheim, C. Raiborg, and H. Stenmark. 2010. PtdIns(3)P controls cytokinesis through KIF13A-mediated recruitment of FYVE-CENT to the midbody. *Nature Cell Biology*. 12:362-371.
- Sanchez-Pulido, L., D. Devos, S. Genevrois, M. Vicente, and A. Valencia. 2003. POTRA: a conserved domain in the FtsQ family and a class of beta-barrel outer membrane proteins. *Trends in Biochemical Sciences*. 28:523-526.
- Schagger, H., T.A. Link, W.D. Engel, and G. von Jagow. 1986. Isolation of the eleven protein subunits of the bc1 complex from beef heart. *Methods in Enzymology*. 126:224-237.
- Schagger, H., and K. Pfeiffer. 2000. Supercomplexes in the respiratory chains of yeast and mammalian mitochondria. *The EMBO Journal*. 19:1777-1783.
- Schmidt, O., A.B. Harbauer, S. Rao, B. Eyrich, R.P. Zahedi, D. Stojanovski, B. Schonfisch, B. Guiard, A. Sickmann, N. Pfanner, and C. Meisinger. 2011. Regulation of mitochondrial protein import by cytosolic kinases. *Cell*. 144:227-239.
- Schneider, H.C., J. Berthold, M.F. Bauer, K. Dietmeier, B. Guiard, M. Brunner, and W. Neupert. 1994. Mitochondrial Hsp70/MIM44 complex facilitates protein import. *Nature*. 371:768-774.
- Schwall, C.T., V.L. Greenwood, and N.N. Alder. 2012. The stability and activity of respiratory Complex II is cardiolipin-dependent. *Biochimica et Biophysica Acta*. 1817:1588-1596.
- Sesaki, H., and R.E. Jensen. 2001. UGO1 encodes an outer membrane protein required for mitochondrial fusion. *The Journal of Cell Biology*. 152:1123-1134.
- Sesaki, H., and R.E. Jensen. 2004. Ugo1p links the Fzo1p and Mgm1p GTPases for mitochondrial fusion. *The Journal of Biological Chemistry*. 279:28298-28303.
- Setoguchi, K., H. Otera, and K. Mihara. 2006. Cytosolic factor- and TOM-independent import of C-tail-anchored mitochondrial outer membrane proteins. *The EMBO Journal*. 25:5635-5647.
- Sharma, S., U.K. Singha, and M. Chaudhuri. 2010. Role of Tob55 on mitochondrial protein biogenesis in *Trypanosoma brucei*. *Molecular and Biochemical Parasitology*. 174:89-100.

- Sicheritz-Ponten, T., C.G. Kurland, and S.G. Andersson. 1998. A phylogenetic analysis of the cytochrome b and cytochrome c oxidase I genes supports an origin of mitochondria from within the Rickettsiaceae. *Biochimica et Biophysica Acta*. 1365:545-551.
- Sideris, D.P., N. Petrakis, N. Katrakili, D. Mikropoulou, A. Gallo, S. Ciofi-Baffoni, L. Banci, I. Bertini, and K. Tokatlidis. 2009. A novel intermembrane space-targeting signal docks cysteines onto Mia40 during mitochondrial oxidative folding. *The Journal of Cell Biology*. 187:1007-1022.
- Sideris, D.P., and K. Tokatlidis. 2007. Oxidative folding of small Tims is mediated by site-specific docking onto Mia40 in the mitochondrial intermembrane space. *Molecular Microbiology*. 65:1360-1373.
- Sirrenberg, C., M.F. Bauer, B. Guiard, W. Neupert, and M. Brunner. 1996. Import of carrier proteins into the mitochondrial inner membrane mediated by Tim22. *Nature*. 384:582-585.
- Sirrenberg, C., M. Endres, H. Folsch, R.A. Stuart, W. Neupert, and M. Brunner. 1998. Carrier protein import into mitochondria mediated by the intermembrane proteins Tim10/Mrs11 and Tim12/Mrs5. *Nature*. 391:912-915.
- Sklar, J.G., T. Wu, L.S. Gronenberg, J.C. Malinverni, D. Kahne, and T.J. Silhavy. 2007. Lipoprotein SmpA is a component of the YaeT complex that assembles outer membrane proteins in *Escherichia coli*. *Proceedings of the National Academy of Sciences of the United States of America*. 104:6400-6405.
- Sogo, L.F., and M.P. Yaffe. 1994. Regulation of mitochondrial morphology and inheritance by Mdm10p, a protein of the mitochondrial outer membrane. *The Journal of Cell Biology*. 126:1361-1373.
- Stewart, S.A., D.M. Dykxhoorn, D. Palliser, H. Mizuno, E.Y. Yu, D.S. An, D.M. Sabatini, I.S. Chen, W.C. Hahn, P.A. Sharp, R.A. Weinberg, and C.D. Novina. 2003. Lentivirus-delivered stable gene silencing by RNAi in primary cells. *RNA*. 9:493-501.
- Stiburek, L., K. Vesela, H. Hansikova, P. Pecina, M. Tesarova, L. Cerna, J. Houstek, and J. Zeman. 2005. Tissue-specific cytochrome c oxidase assembly defects due to mutations in SCO2 and SURF1. *The Biochemical Journal*. 392:625-632.
- Stiburek, L., and J. Zeman. 2010. Assembly factors and ATP-dependent proteases in cytochrome c oxidase biogenesis. *Biochimica et Biophysica Acta*. 1797:1149-1158.
- Stojanovski, D., B. Guiard, V. Kozjak-Pavlovic, N. Pfanner, and C. Meisinger. 2007. Alternative function for the mitochondrial SAM complex in biogenesis of alpha-helical TOM proteins. *The Journal of Cell Biology*. 179:881-893.
- Stroud, D.A., T. Becker, J. Qiu, D. Stojanovski, S. Pfannschmidt, C. Wirth, C. Hunte, B. Guiard, C. Meisinger, N. Pfanner, and N. Wiedemann. 2011. Biogenesis of mitochondrial beta-barrel proteins: the POTRA domain is involved in precursor release from the SAM complex. *Molecular Biology of the Cell*. 22:2823-2833.
- Struyve, M., M. Moons, and J. Tommassen. 1991. Carboxy-terminal phenylalanine is essential for the correct assembly of a bacterial outer membrane protein. *Journal of Molecular Biology*. 218:141-148.
- Sun, F., X. Huo, Y. Zhai, A. Wang, J. Xu, D. Su, M. Bartlam, and Z. Rao. 2005. Crystal structure of mitochondrial respiratory membrane protein complex II. *Cell*. 121:1043-1057.
- Tahbaz, N., S. Subedi, and M. Weinfeld. 2012. Role of polynucleotide kinase/phosphatase in mitochondrial DNA repair. *Nucleic Acids Research*. 40:3484-3495.
- Tamm, L.K., H. Hong, and B. Liang. 2004. Folding and assembly of beta-barrel membrane proteins. *Biochimica et Biophysica Acta*. 1666:250-263.
- Tanabe, M., and T.M. Iverson. 2009. Expression, purification and preliminary X-ray analysis of the *Neisseria meningitidis* outer membrane protein PorB. *Acta Crystallographica Section F: Structural Biology and Crystallization Communications*. 65:996-1000.
- Tatsuta, T., K. Model, and T. Langer. 2005. Formation of membrane-bound ring complexes by prohibitins in mitochondria. *Molecular Biology of the Cell*. 16:248-259.

- Taylor, A.B., B.S. Smith, S. Kitada, K. Kojima, H. Miyaura, Z. Otwinowski, A. Ito, and J. Deisenhofer. 2001. Crystal structures of mitochondrial processing peptidase reveal the mode for specific cleavage of import signal sequences. *Structure*. 9:615-625.
- Thornton, N., D.A. Stroud, D. Milenkovic, B. Guiard, N. Pfanner, and T. Becker. 2010. Two modular forms of the mitochondrial sorting and assembly machinery are involved in biogenesis of alpha-helical outer membrane proteins. *Journal of Molecular Biology*. 396:540-549.
- Tiranti, V., C. Galimberti, L. Nijtmans, S. Bovolenta, M.P. Perini, and M. Zeviani. 1999. Characterization of SURF-1 expression and Surf-1p function in normal and disease conditions. *Human Molecular Genetics*. 8:2533-2540.
- Tsukihara, T., H. Aoyama, E. Yamashita, T. Tomizaki, H. Yamaguchi, K. Shinzawa-Itoh, R. Nakashima, R. Yaono, and S. Yoshikawa. 1996. The whole structure of the 13-subunit oxidized cytochrome c oxidase at 2.8 Å. *Science*. 272:1136-1144.
- Tuschen, G., U. Sackmann, U. Nehls, H. Haiker, G. Buse, and H. Weiss. 1990. Assembly of NADH: ubiquinone reductase (complex I) in *Neurospora* mitochondria. Independent pathways of nuclear-encoded and mitochondrially-encoded subunits. *Journal of Molecular Biology*. 213:845-857.
- Ujwal, R., D. Cascio, J.P. Colletier, S. Faham, J. Zhang, L. Toro, P. Ping, and J. Abramson. 2008. The crystal structure of mouse VDAC1 at 2.3 Å resolution reveals mechanistic insights into metabolite gating. *Proceedings of the National Academy of Sciences of the United States of America*. 105:17742-17747.
- Ungermann, C., W. Neupert, and D.M. Cyr. 1994. The role of Hsp70 in conferring unidirectionality on protein translocation into mitochondria. *Science*. 266:1250-1253.
- van der Klei, I.J., M. Veenhuis, and W. Neupert. 1994. A morphological view on mitochondrial protein targeting. *Microscopy Research and Technique*. 27:284-293.
- van der Laan, M., N. Wiedemann, D.U. Mick, B. Guiard, P. Rehling, and N. Pfanner. 2006. A role for Tim21 in membrane-potential-dependent preprotein sorting in mitochondria. *Current Biology : CB*. 16:2271-2276.
- Van Laar, V.S., A.A. Dukes, M. Cascio, and T.G. Hastings. 2008. Proteomic analysis of rat brain mitochondria following exposure to dopamine quinone: implications for Parkinson disease. *Neurobiology of Disease*. 29:477-489.
- van Wilpe, S., M.T. Ryan, K. Hill, A.C. Maarse, C. Meisinger, J. Brix, P.J. Dekker, M. Moczko, R. Wagner, M. Meijer, B. Guiard, A. Honlinger, and N. Pfanner. 1999. Tom22 is a multifunctional organizer of the mitochondrial preprotein translocase. *Nature*. 401:485-489.
- Vogel, F., C. Bornhovd, W. Neupert, and A.S. Reichert. 2006. Dynamic subcompartmentalization of the mitochondrial inner membrane. *The Journal of Cell Biology*. 175:237-247.
- Vogel, R.O., R.J. Janssen, C. Ugalde, M. Grovenstein, R.J. Huijbens, H.J. Visch, L.P. van den Heuvel, P.H. Willems, M. Zeviani, J.A. Smeitink, and L.G. Nijtmans. 2005. Human mitochondrial complex I assembly is mediated by NDUFAF1. *The FEBS Journal*. 272:5317-5326.
- Vogel, R.O., J.A. Smeitink, and L.G. Nijtmans. 2007. Human mitochondrial complex I assembly: a dynamic and versatile process. *Biochimica et Biophysica Acta*. 1767:1215-1227.
- Vögtle, F.N., S. Wortelkamp, R.P. Zahedi, D. Becker, C. Leidhold, K. Gevaert, J. Kellermann, W. Voos, A. Sickmann, N. Pfanner, and C. Meisinger. 2009. Global analysis of the mitochondrial N-proteome identifies a processing peptidase critical for protein stability. *Cell*. 139:428-439.
- Volokhina, E.B., F. Beckers, J. Tommassen, and M.P. Bos. 2009. The beta-barrel outer membrane protein assembly complex of *Neisseria meningitidis*. *Journal of Bacteriology*. 191:7074-7085.
- von der Malsburg, K., J.M. Muller, M. Bohnert, S. Oeljeklaus, P. Kwiatkowska, T. Becker, A. Loniewska-Lwowska, S. Wiese, S. Rao, D. Milenkovic, D.P. Hutu, R.M. Zerbes, A. Schulze-Specking, H.E. Meyer, J.C. Martinou, S. Rospert, P. Rehling, C. Meisinger, M. Veenhuis, B. Warscheid, I.J. van der Klei, N. Pfanner, A. Chacinska, and M. van der Laan. 2011. Dual role of mitofilin in mitochondrial membrane organization and protein biogenesis. *Developmental Cell*. 21:694-707.

- Voos, W., B.D. Gambill, B. Guiard, N. Pfanner, and E.A. Craig. 1993. Presequence and mature part of preproteins strongly influence the dependence of mitochondrial protein import on heat shock protein 70 in the matrix. *The Journal of Cell Biology*. 123:119-126.
- Voulhoux, R., M.P. Bos, J. Geurtsen, M. Mols, and J. Tommassen. 2003. Role of a highly conserved bacterial protein in outer membrane protein assembly. *Science*. 299:262-265.
- Waizenegger, T., S.J. Habib, M. Lech, D. Mokranjac, S.A. Paschen, K. Hell, W. Neupert, and D. Rapaport. 2004. Tob38, a novel essential component in the biogenesis of beta-barrel proteins of mitochondria. *EMBO Reports*. 5:704-709.
- Walther, D.M., M.P. Bos, D. Rapaport, and J. Tommassen. 2010. The mitochondrial porin, VDAC, has retained the ability to be assembled in the bacterial outer membrane. *Molecular Biology and Evolution*. 27:887-895.
- Walther, D.M., D. Papic, M.P. Bos, J. Tommassen, and D. Rapaport. 2009a. Signals in bacterial beta-barrel proteins are functional in eukaryotic cells for targeting to and assembly in mitochondria. *Proceedings of the National Academy of Sciences of the United States of America*. 106:2531-2536.
- Walther, D.M., D. Rapaport, and J. Tommassen. 2009b. Biogenesis of beta-barrel membrane proteins in bacteria and eukaryotes: evolutionary conservation and divergence. *Cellular and Molecular Life Sciences : CMLS*. 66:2789-2804.
- Wang, Z.G., P.S. White, and S.H. Ackerman. 2001. Atp11p and Atp12p are assembly factors for the F(1)-ATPase in human mitochondria. *The Journal of biological chemistry*. 276:30773-30778.
- Werner, J., and R. Misra. 2005. YaeT (Omp85) affects the assembly of lipid-dependent and lipid-independent outer membrane proteins of *Escherichia coli*. *Molecular Microbiology*. 57:1450-1459.
- Westermann, B. 2010. Mitochondrial fusion and fission in cell life and death. *Nature Reviews Molecular Cell Biology*. 11:872-884.
- Wiedemann, N., V. Kozjak, A. Chacinska, B. Schonfisch, S. Rospert, M.T. Ryan, N. Pfanner, and C. Meisinger. 2003. Machinery for protein sorting and assembly in the mitochondrial outer membrane. *Nature*. 424:565-571.
- Wiedemann, N., K.N. Truscott, S. Pfannschmidt, B. Guiard, C. Meisinger, and N. Pfanner. 2004. Biogenesis of the protein import channel Tom40 of the mitochondrial outer membrane: intermembrane space components are involved in an early stage of the assembly pathway. *The Journal of Biological Chemistry*. 279:18188-18194.
- Williams, S.L., I. Valnot, P. Rustin, and J.W. Taanman. 2004. Cytochrome c oxidase subassemblies in fibroblast cultures from patients carrying mutations in COX10, SCO1, or SURF1. *The Journal of Biological Chemistry*. 279:7462-7469.
- Wittig, I., B. Meyer, H. Heide, M. Steger, L. Bleier, Z. Wumaier, M. Karas, and H. Schagger. 2010. Assembly and oligomerization of human ATP synthase lacking mitochondrial subunits a and A6L. *Biochimica et Biophysica Acta*. 1797:1004-1011.
- Wiznerowicz, M., J. Szulc, and D. Trono. 2006. Tuning silence: conditional systems for RNA interference. *Nature Methods*. 3:682-688.
- Wiznerowicz, M., and D. Trono. 2003. Conditional suppression of cellular genes: lentivirus vector-mediated drug-inducible RNA interference. *Journal of Virology*. 77:8957-8961.
- Wu, T., J. Malinverni, N. Ruiz, S. Kim, T.J. Silhavy, and D. Kahne. 2005. Identification of a multicomponent complex required for outer membrane biogenesis in *Escherichia coli*. *Cell*. 121:235-245.
- Wurm, C.A., and S. Jakobs. 2006. Differential protein distributions define two sub-compartments of the mitochondrial inner membrane in yeast. *FEBS Letters*. 580:5628-5634.
- Xie, J., M.F. Marusich, P. Souda, J. Whitelegge, and R.A. Capaldi. 2007. The mitochondrial inner membrane protein mitofilin exists as a complex with SAM50, metaxins 1 and 2, coiled-coil-helix coiled-coil-helix domain-containing protein 3 and 6 and DnaJC11. *FEBS Letters*. 581:3545-3549.

- Xu, F., C. Morin, G. Mitchell, C. Ackerley, and B.H. Robinson. 2004. The role of the LRPPRC (leucine-rich pentatricopeptide repeat cassette) gene in cytochrome oxidase assembly: mutation causes lowered levels of COX (cytochrome c oxidase) I and COX III mRNA. *The Biochemical Journal*. 382:331-336.
- Xu, Y., R.I. Kelley, T.J. Blanck, and M. Schlame. 2003. Remodeling of cardiolipin by phospholipid transacylation. *The Journal of Biological Chemistry*. 278:51380-51385.
- Yamamoto, H., M. Esaki, T. Kanamori, Y. Tamura, S. Nishikawa, and T. Endo. 2002. Tim50 is a subunit of the TIM23 complex that links protein translocation across the outer and inner mitochondrial membranes. *Cell*. 111:519-528.
- Young, J.C., N.J. Hoogenraad, and F.U. Hartl. 2003. Molecular chaperones Hsp90 and Hsp70 deliver preproteins to the mitochondrial import receptor Tom70. *Cell*. 112:41-50.
- Youngman, M.J., A.E. Hobbs, S.M. Burgess, M. Srinivasan, and R.E. Jensen. 2004. Mmm2p, a mitochondrial outer membrane protein required for yeast mitochondrial shape and maintenance of mtDNA nucleoids. *The Journal of Cell Biology*. 164:677-688.
- Zara, V., I. Palmisano, L. Conte, and B.L. Trumpower. 2004. Further insights into the assembly of the yeast cytochrome bc1 complex based on analysis of single and double deletion mutants lacking supernumerary subunits and cytochrome b. *European Journal of Biochemistry / FEBS*. 271:1209-1218.
- Zerbes, R.M., M. Bohnert, D.A. Stroud, K. von der Malsburg, A. Kram, S. Oeljeklaus, B. Warscheid, T. Becker, N. Wiedemann, M. Veenhuis, I.J. van der Klei, N. Pfanner, and M. van der Laan. 2012. Role of MINOS in mitochondrial membrane architecture: cristae morphology and outer membrane interactions differentially depend on mitofilin domains. *Journal of Molecular Biology*. 422:183-191.
- Zeth, K. 2010. Structure and evolution of mitochondrial outer membrane proteins of beta-barrel topology. *Biochimica et Biophysica Acta*. 1797:1292-1299.
- Zhang, M., E. Mileykovskaya, and W. Dowhan. 2002. Gluing the respiratory chain together. Cardiolipin is required for supercomplex formation in the inner mitochondrial membrane. *The Journal of Biological Chemistry*. 277:43553-43556.
- Zick, M., R. Rabl, and A.S. Reichert. 2009. Cristae formation-linking ultrastructure and function of mitochondria. *Biochimica et Biophysica Acta*. 1793:5-19.

6 APPENDIX

6.1 List of abbreviations

$\Delta\Psi$	membrane potential
μ	micro
APS	ammonium persulfate
ATP	adenosine triphosphate
BAM	β -barrel assembly machinery
BN	Blue Native
BSA	bovine serum albumin
cDNA	complementary DNA
CHCHD	coiled-coil-helix-coiled-coil-helix domain containing
CJ	crista junction
CM	cristae membrane
C-terminal	carboxy-terminal
cyt c	cytochrome c
dH ₂ O	distilled H ₂ O
DMEM	Dulbecco's modified Eagle medium
DMSO	dimethyl sulfoxide
DNA	deoxyribonucleic acid
dNTP	desoxynucleosid triphosphate
Dox	doxycycline
DTT	dithiothreitol
<i>E. coli</i>	<i>Escherichia coli</i>
ECL	enhanced chemiluminescence
EDTA	ethylenediaminetetraacetic acid
FCS	fetal calf serum
g	gram
GFP	green fluorescent protein
h	hour(s)
HEPES	4-(2-hydroxyethyl)-1-piperazineethanesulfonic acid
Hsp	heat shock protein
IBM	inner boundary membrane
ICS	intracrystal space
IMM	inner mitochondrial membrane
IMS	intermembrane space
k	kilo
kb	kilobase
kDa	kilodalton
l	liter
LB	lysogeny broth
m	milli
M	molar
MDa	Megadalton

MIA	mitochondrial IMS import and assembly
min	minute(s)
MPP	mitochondrial processing peptidase
mRNA	messenger RNA
MT-CYB	cytochrome b
mtDNA	mitochondrial DNA
n	nano
<i>N. cinerea</i>	<i>Neisseria cinerea</i>
<i>N. gonorrhoeae</i>	<i>Neisseria gonorrhoeae</i>
<i>N. lactamica</i>	<i>Neisseria lactamica</i>
<i>N. meningitidis</i>	<i>Neisseria meningitidis</i>
<i>N. sicca</i>	<i>Neisseria sicca</i>
NADH	Nicotinamide adenine dinucleotide
<i>Ngo</i>	<i>Neisseria gonorrhoeae</i>
N-terminal	amino-terminal
OD	optical density
OM	outer membrane
OMM	outer mitochondrial membrane
Omp	outer membrane protein
Opa1	optic atrophy 1
PAGE	polyacrylamide gel electrophoresis
PAM	presequence translocase-associated import motor
PBS	phosphate buffered saline
PCR	polymerase chain reaction
PE	phosphatidylethanolamine
PEI	polyethylenimine
PFA	paraformaldehyde
PK	proteinase K
PMSF	phenylmethanesulfonyl fluoride
POTRA	polypeptide transport-associated
PVDF	polyvinylidene fluoride
RNA	ribonucleic acid
rpm	revolutions per minute
RT	room temperature
s	second(s)
<i>S. enterica</i>	<i>Salmonella enterica</i>
SAM	sorting and assembly machinery
SDS	sodium dodecyl sulphate
shRNA	short hairpin RNA
SILAC	stable isotope labeling with amino acids in cell culture
siRNA	small interfering RNA
TBS	Tris buffered saline
TCA	trichloroacetic acid
TEM	transmission electron microscopy
TEMED	tetramethylethylenediamine
TIM	translocase of the inner membrane

TOB	topogenesis of mitochondrial outer membrane β -barrel proteins
TOM	translocase of the outer membrane
TTC19	tetratricopeptide repeat domain 19
UV	ultra violet
v/v	volume per volume
VDAC	voltage dependent anion-sensitive channel
w/v	weight per volume

6.2 Publications and presentations

Publications

Kozjak-Pavlovic*, V., **C. Ott***, M. Götz, and T. Rudel. 2011. Neisserial Omp85 protein is selectively recognized and assembled into functional complexes in the outer membrane of human mitochondria. *The Journal of Biological Chemistry*. 286:27019-27026.

Ott, C.*, K. Ross*, S. Straub, B. Thiede, M. Götz, C. Goosmann, M. Krischke, M.J. Mueller, G. Krohne, T. Rudel, and V. Kozjak-Pavlovic. 2012. Sam50 functions in mitochondrial intermembrane space bridging and biogenesis of respiratory complexes. *Molecular and Cellular Biology*. 32:1173-1188.

Ott, C., M. Utech, M. Götz, T. Rudel, and V. Kozjak-Pavlovic. 2013. The requirements for the import of neisserial Omp85 into the outer membrane of human mitochondria. *Bioscience reports*. 33:303-312

* both authors contributed equally

Poster presentations

Ott C., V. Kozjak-Pavlovic, M. Götz, and T. Rudel. 2011. Selective import of bacterial β -barrel proteins in human mitochondria. FEMS-Leopoldina Symposium on "Emerging Topics in Microbial Pathogenesis", Würzburg.

Ott C., K. Ross, S. Straub, B. Thiede, T. Rudel, and V. Kozjak-Pavlovic, 2012. The importance of Sam50 in cristae organization and biogenesis of respiratory complexes. Keystone Symposia on Molecular and Cellular Biology "Mitochondrial Dynamics and Function", Banff (Canada).

Ott C., M. Utech, T. Rudel, and V. Kozjak-Pavlovic, 2012. Targeting of neisserial Omp85 to the outer mitochondrial membrane depends on the carboxy-terminus and POTRA domains. XNIIIth International Pathogenic Neisseria Conference (PNC), Würzburg.

6.3 Danksagung

Ich möchte allen sehr herzlich danken, die zum Gelingen meiner Arbeit beigetragen haben.

Zuerst möchte ich mich bei Herrn Prof. Dr. Thomas Rudel für die Möglichkeit bedanken, meine Doktorarbeit am Lehrstuhl für Mikrobiologie verfassen zu können.

Mein ganz besonderer Dank gilt meiner Betreuerin PD Dr. Vera Kozjak-Pavlovic für die exzellente Betreuung, beständige Unterstützung und Begeisterung für meine Arbeit. Vielen Dank, Vera!

Bei Herrn Prof. Dr. Georg Krohne möchte ich mich sehr herzlich für die Übernahme des Zweitgutachtens und für die Unterstützung bei der Elektronenmikroskopie durch seine Arbeitsgruppe bedanken.

Allen Kolleginnen und Kollegen des Instituts danke ich für die nette Arbeitsatmosphäre, die allzeitige Hilfe und die guten Diskussionen. Ein großes Dankeschön vor allem an Christine, Ann-Cathrin, Michaela, Annette, Lisa und Magda!

Besonders danken möchte ich allen, die im Laufe meiner Doktorarbeit mit mir im Labor C237 gearbeitet haben, allen voran Monika für ihre allzeitige Hilfe und Unterstützung sowohl am Anfang beim Einstieg in den Laboralltag als auch während meiner ganzen Arbeit, für ihre zahlreichen hilfreichen Tipps und die gute Stimmung im Labor. Vielen herzlichen Dank auch an Eva, die mich in der „Endphase“ meiner Doktorarbeit durch ihre große Hilfsbereitschaft im Laboralltag sehr unterstützt hat.

Zuletzt möchte ich meinen Eltern, meiner Schwester und ihrer Familie für all ihre Unterstützung, Motivation und Liebe danken.

6.4 Selbständigkeitserklärung

Ich erkläre ehrenwörtlich, dass die vorliegende Arbeit von mir selbständig und nur unter Verwendung der angegebenen Quellen und Hilfsmittel angefertigt wurde.

Diese Dissertation hat weder in gleicher noch in ähnlicher Form in einem anderen Prüfungsverfahren vorgelegen.

Ich habe früher, außer den mit dem Zulassungsgesuch urkundlich vorgelegten Graden, keine weiteren akademischen Grade erworben oder zu erwerben versucht.

Würzburg, den 03.06.2013